TOTAL SYNTHESIS OF DECYTOSPOLIDES A AND B AND PROGRESS TOWARDS THE TOTAL SYNTHESIS OF CARAMBOLAFLAVONE A

by

Hannah Marie Simpson

A Dissertation

Submitted to the Faculty of Purdue University

In Partial Fulfillment of the Requirements for the degree of

Doctor of Philosophy

Department of Chemistry

West Lafayette, Indiana

December 2020

THE PURDUE UNIVERSITY GRADUATE SCHOOL
STATEMENT OF COMMITTEE APPROVAL

Dr. Arun K. Ghosh, Chair
Department of Chemistry

Dr. Paul G. Wenthold
Department of Chemistry

Dr. Christina Li
Department of Chemistry

Dr. Abram Axelrod
Department of Chemistry

Approved by:
Dr. Christine Hyrcyna

To Ripley and Pyrrha, thanks for your love, support and occasional unproductive additions to my graduate career.

ACKNOWLEDGMENTS

First and foremost, I would like to express my gratitude to Professor Arun K. Ghosh - thank you for your guidance, mentorship and the many opportunities you have given me over the years. It was truly an honor to learn from you and work in the lab environment you have cultivated. To my thesis committee members, Professor Paul Wenthold, Professor Christina Li, and Professor Abram Axelrod -a special thanks for your support and advice.

I would like to thank the department staff, Dr. Christine Hyrcyna, Lynn Ryder, Jenalee Converse, and Debra Packer for their guidance throughout my graduate studies. A special thanks to our group operations manager Suzanne Snoeberger for your constant assistance and direction.

To the current and past Ghosh group members -thank you for your advice and support during my time in the Ghosh group, particularly Dr. Joshua Born, Dr. Joseph Bungard, Dr. Emilio Cardenas, Dr. Jacqueline Williams, Dr. Anthony Tomaine, Dr. Anne Veitschegger, Dr. Heather Osswald, Dr. Luke Kassekert, Dr. Margherita Brindisi, Dr. Satish Kovela, Dr. Vasudeva Dodda, Dr. Jinfei Yang, Miranda Belcher, Jennifer Mishevich, Seth Keeling, Megan Johnson, and Rachel Ho.

TABLE OF CONTENTS

LIST OF TABLES

LIST OF FIGURES

LIST OF SCHEMES

LIST OF ABBREVIATIONS

1D	one dimensional
2D	two dimensional
3D	three dimensional
Å	angstrom
Ac	acetate
Bn	benzyl
Bz	benzoyl
Cp	cyclopentadienyl
DBU	1,8-diazabicyclo[5.4.0]undec-7-ene
DDQ	2,3-dichloro-5,6-dicyano-1,4-benzoquinone
DMAP	4-(dimethylamino)pyridine
DMF	*N*,*N*-dimethylformamide
DMP	Dess-Martin periodinane
DMSO	dimethylsulfoxide
DPEN	1,2-diphenyl-1,2-ethylenediamine
dr	diastereomeric ratio
EtOAc	ethyl acetate
ee	enantiomeric excess
Et_2O	diethyl ether
EtOH	ethanol
FDA	food and drug administration
FT-IR	Fourier-Transformed Infrared Spectroscopy
HPLC	High Performance Liquid Chromatography
HRMS	High Resolution Mass Spectrometry
Hz	hertz
IC_{50}	inhibitory concentration at 50%
K_2CO_3	potassium carbonate
LCMS	liquid chromatography mass spectrometry

LDA	lithium diisopropylamide
LRMS	low-resolution mass spectrometry
m-CPBA	3-chloroperbenzoic acid
MeCN	acetonitrile
MeOH	methanol
MOM	methoxymethyl
Ms	methanesulfonyl
MS	molecular sieves
NaH	sodium hydride
NaOH	sodium hydroxide
NBS	N-bromosuccinimide
nM	nanomolar
NMR	Nuclear Magnetic Resonance
Pd/C	palladium on carbon
$Pd(OH)_2/C$	palladium hydroxide on carbon
Ph	phenyl
pH	potential of hydrogen
PhMe	toluene
PivOH	pivalic acid
PMB	para-methoxybenzyl
Py	pyridine
ppm	chemical shift, part per million
R_f	retention factor
TBAB	tetrabutylammonium bromide
TBAF	tetrabutylammonium fluoride
TBHP	*tert*-butylhydrogen peroxide
TBS	*tert*-butyldimethylsilyl
tert	tertiary
TFA	trifluoroacetic acid
THF	tetrahydrofuran
Tf	trifluoromethanesulfonyl

TLC	thin layer chromatography
TMS	trimethylsilyl
TMP	2,2,6,6-tetramethylpiperidine
Ts	para-toluenesulfonyl
UV	ultraviolet
α	alpha
β	beta
μM	micromolar

ABSTRACT

Decytospolides A and B are natural products isolated from *Cytospora* sp. No ZW02 that show mild anticancer properties. The interest in synthesizing these compound lies not in their activities, but rather the simplicity of the structure which could easily be modified to provide more potent derivatives. Previous syntheses of these compounds relied on transition metals to install the tetrahydropyran core or extensive use of protecting groups. Our first generation synthesis made use of the Achmatowicz rearrangement to synthesize the tetrahydropyran moiety. Based on this, a concise, protecting group free synthesis has been accomplished utilizing the Achmatowicz rearrangement of an optically active furanyl alcohol followed by diastereoselective Kishi reduction of the resulting dihydropyranone hemiacetal.

Carambolaflavone A is a natural product isolated from *A. carambola* with antidiabetic properties. Notably, these compound promote both insulin secretion and glucose uptake by muscle cells in hyperglycemic rats. A previous synthesis has been reported by Wang and coworkers, however this synthesis does not offer much potential for the formation of derivatives and relies on a C-glycosylation that requires heating for regio- and diastereoselectivity. Progress towards a concise synthesis has been made featuring a Lewis acid promoted highly diastereoselective substrate controlled C-glycosylation that does not require heating and a one pot oxidation of chroman to chromone utilizing DDQ. Further research is underway to complete the synthesis of this molecule by an oxidative addition to the chromone and subsequent removal of protecting groups.

CHAPTER 1. UTILIZING AN ACHMATOWICZ REARRANGEMENT FOR THE ASYMMETRIC SYNTHESIS OF DECYTOSPOLIDES A AND B

1.1 Introduction

Functionalized and multi-substituted tetrahydropyrans are recurring structural motifs in many biologically active natural products, particularly compounds with anticancer properties[1,2]. There are many methods for the synthesis of these tetrahydropyran rings[3,4,5]. However, there are limitations regarding availability of starting materials, stereo- and regiochemical issues and the number and nature of substituents on the ring. Notably, the incorporation of substitutions at several different positions and certain functional groups are not possible with many existing methods.

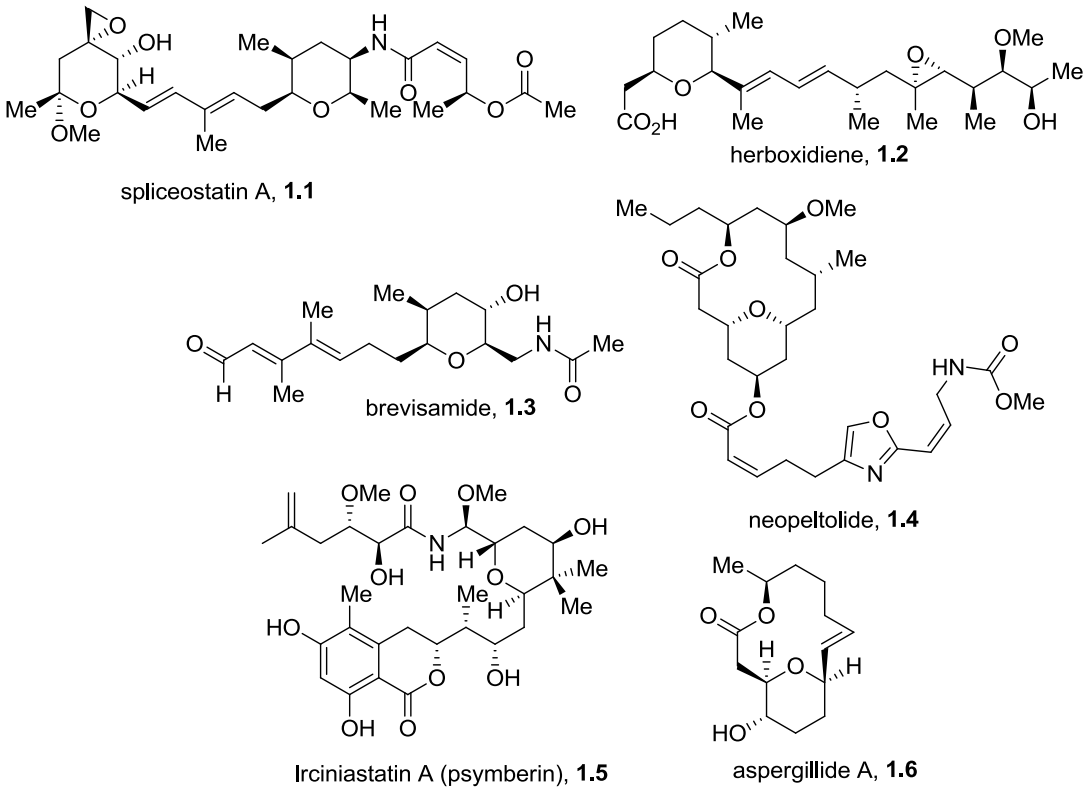

Figure 1.1: Tetrahydropyran Containing Bioactive Natural Products with Anticancer Activtiy

Some of the most notable examples of tetrahydropyran containing natural products are herboxidiene and the spliceostatins, both of which posess strong anticancer properties. This comes from their ability to inhibit the spliceosome and prevent the splicing of pre-mRNA, which is potential target for anticancer medication. Herboxidiene (**1.1**) was isolated from *Streptomyces chromofuscus* A7847 in 1992 by Isaac and coworkers[6]. Herboxidiene is a novel splicing inhibitor that affects the SF3B subunit, of the spliceosome leading to submicromolar anticancer activity across numerous human tumor cell lines[7]. Spliceostatin A (**1.2**), a methylated derivative of natural product FR901464, has been proven to inhibit *in vitro* splicing activity. Similar to Herboxidiene, it also binds to SF3B, specifically on the U2 ribonucleoprotein of the splicesome. This gives the compound both *in vitro* and *in vivo* splicing activity that inhibits tumor growth in multiple human cancer cell lines[8].

Other significant examples of bioactive tetrahydropyran-containing natural products with anticancer properties are shown in Figure 1.1. In 2011, Brevisamide (**1.3**) was isolated from the red tide dinoflagellate *Karenia brevis*. This flagellate produces many fused ring polycyclic ethers known as brevetoxins. One of the most notable of these is the aforementioned brevisamide (**1.3**). It contains a highly conjugated aldehyde, an amide and a tetrahydropyran ring. Brevisamide (**1.3**) is thought to be the simplest compound produced in polycyclic ether biosynthesis and provides a model for polyether formation in other natural products and their bioactive derivatives[9]. In 2007, a 14-membered macrolide known as neopeltolide (**1.4**), was isolated from the deep-water sponge, *Daedalopelta*[10]. It inhibited cell proliferation *in vitro* and had IC_{50} values in the low nanomolar range across numerous human cancer cell lines as well as the P388 murine leukemia cell line[10]. The natural product Irciniastatin A (**1.5**), isolated in 2004 from *Ircinia ramosa*, is another example of a tetrahydropyran containing molecule with anticancer properties. It inhibited the cellular growth of the murine P388 leukemia cell line and six human cancer cell lines with potent GI_{50} values ranging from 0.001 to less than 0.0001 μg/mL[11]. In 2008, aspergillide A (**1.6**), another 14-membered macrolide, was isolated from the *Aspergillus ostianus* strain 01F313. The compound was evaluated in mouse lymphocytic leukemia cells (L1210) and found to have cytotoxic activity[12]. These are a few examples of extremely potent compounds featuring substituted tetrahydropyran rings.

Among the classes of molecules featuring this tetrahydropyran ring are nonanolides and their derivatives. Nonanolides are compounds featuring an interesting 10-membered macrolide

subunit. Nonanolides have been isolated from many plants and marine invertebrates[13]. These natural products have been found to be cytotoxic and phytotoxic[13-17]; and have antimalarial[18], antifungal[13,19,20], antibacterial[13,21-23] and antimicrofilament[24] activities. Research into these tetrahydropyran based molecules is of great in importance because of the diversity in bioactivity and simplicity of their basic scaffold, making them ideal building blocks for future drug development.

1.2 Isolation and Biological Activity

In 2011, Zhang and coworkers isolated a series of nonanolide derivatives, including decytospolides A and B, from the *Cytospora* sp. No ZW02, an endophytic fungus from Ilex canariensis which is an evergreen shrub from the canary islands[25]. To isolate the natural products, the fungus was cultivated on a biomalt agar medium for 4 weeks and the organic residues were extracted with acetone to give 9.87g of crude residue to be purified by column chromatography. Additional purification using semi-preparative reverse-phase HPLC resulted in 1.5 mg of decytospolide B (**1.8**) and 8.1 mg of decytospolide A (**1.7**), both of which were colorless oils Structures of decytospolide A and B were elucidated using HRESIMS and ^{1}H and ^{13}C NMR. For some compounds further data was required and so HMBC and COSY were used for the final determination of bond connectivity and relative stereochemistry. The absolute stereochemistry of these compounds was determined by Mosher ester analysis[26].

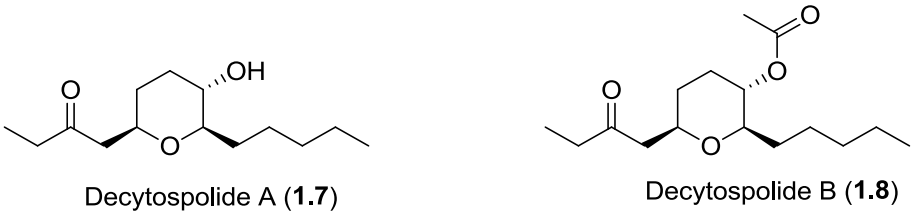

Figure 1.2: Decytospolide A and B

These compounds were evaluated for cytotoxicity against the human tumor cell lines A-549, HCT116, QGY, A375, and U973. Decytospolide B had an IC_{50} of 14.79 µg/mL and 46.79 µg/mL against A-549 and QGY cancer cells, respectively. Decytospolide A had no appreciable biological activity, proving that acylation or other protection of the free alcohol is necessary for

the activity of these compounds. While none of these compounds were as potent as adriamycin, a common chemotherapy medicine, they are still of interest as potential anti-cancer drugs due to the simplicity of their tetrahydropyran scaffold[25].

Table 1.1: Biological Activities (IC_{50}) of Decytospolides in Cancer cell lines

	A-549	HCT116	QGY	A375	U973
Decytospolide A	--	--	--	--	--
Decytospolide B	14.79	--	46.79	--	--
Adriamycin	0.44	0.45	0.28	0.44	0.23

*IC_{50} in μg/mL; -- means IC_{50} > 50 μg/mL

In the isolation paper, Zhang and co-workers proposed a pathway for the biosynthesis of the cytospolide and decytospolide natural products from other compounds isolated from *Cytospora* sp. No ZW02[25]. They suggested that the decytospolides originated from 1,3-diketone **1.9.** Cleavage of the lactone bond would furnish a free alcohol that could undergo an intramolecular oxa-Michael addition to the α,β-unsaturated ketone to synthesize the tetrahydropyran ring. A decarboxylation reaction would then provide decytospolides A and B. No additional evidence has been found to support this conclusion, but it provides the potential for the biomimetic synthetic strategy using a Michael addition.

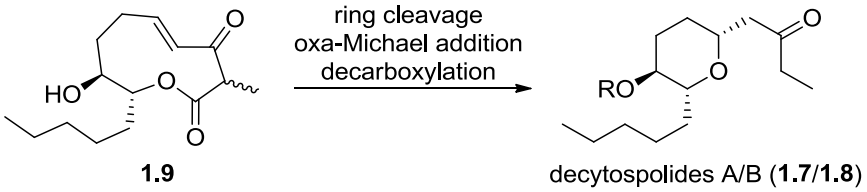

1.9 decytospolides A/B (**1.7**/**1.8**)

Scheme 1.1: Proposed Biosynthesis of the Decytospolides

Based upon the activity of Decytospolide A and B, further investigation into these compounds is needed. While they are not the most potent compounds, the simplicity of the core scaffold provides many opportunities for modification to maximize the anticancer properties of these compounds in human cell lines.

1.3 Previous Syntheses

The core functionalized pyran structure featured in these compounds, is a key moiety featured in many natural products. As such, there are multiple ways to synthesize the pyran core, several of which have been featured in previous syntheses.

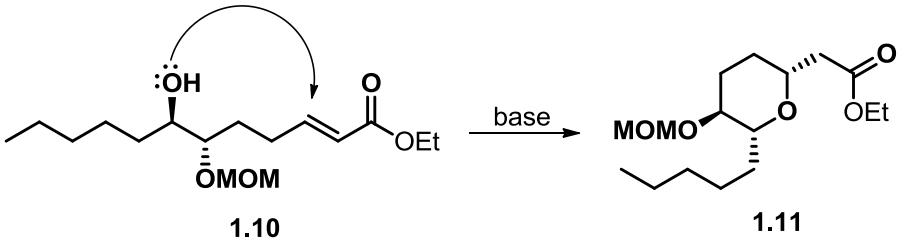

1.10 1.11

Scheme 1.2: Intramolecular Oxa-Michael Addition to Form the Tetrahydropyran Core

Krishna and co-workers present the first stereoselective synthesis of Decytospolides A and B. Similarly to the biogenetic pathway proposed by Zhang and coworkers, they rely on an oxa-Michael addition to install the tetrahydropyran core starting from linear chain **1.10**[27]. While this transition metal free method forms the tetrahydropyran moiety **1.11**, it is obtained as an inseparable mixture of diasteromers (5:1). Additonally, synthesis of the complex linear chain requires a low yielding Sharpless kinetic resolution and extraneous protecting groups to install the desired stereocenters.

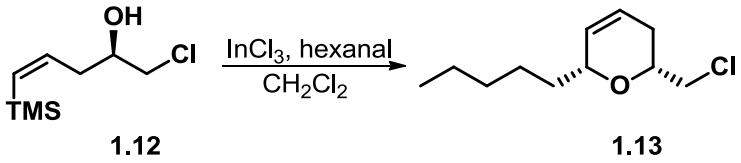

1.12 1.13

Scheme 1.3: Prins Cyclization to Form Tetrahydropyran Core

Another synthesis of the decytospolides was done by Fache and Clarisse, who used a Prins cyclization of **1.12** to form the tetrahydropyran core[28]. While this synthesis provides rapid access to the decytospolides, the construction of the tetrahydropyran core is reliant on activation using transition metals and an unnatural optically active starting material. Thus the ability of this route to be scaled up for pharmaceutical production is limited.

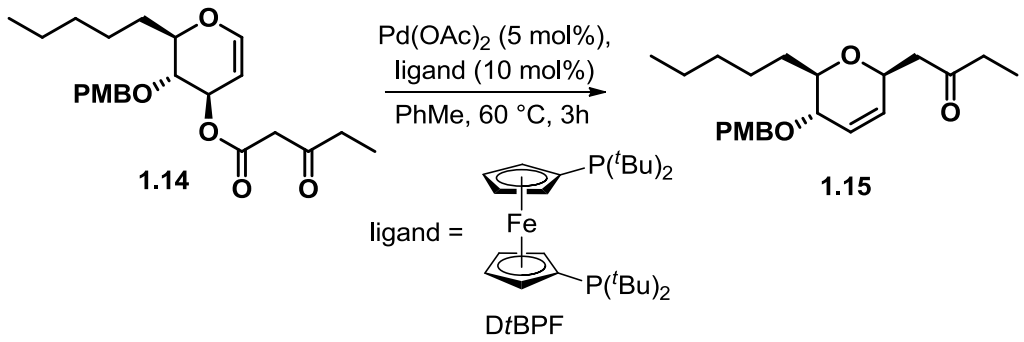

Scheme 1.4: Pd-catalyzed Decarboxylative Allylation to Form Tetrahydropyran Core

Liu and co-workers install the tetrahydropyran core starting from commercially available glucal **1.14**, using a decarboxylative allylation[29]. This methodology was developed by Liu and coworkers for the stereoselective access to cis-tetrahydropyran ring **1.15**. Incorporation in the synthesis of the decytospolides was used to highlight the use of this strategy for stereoselective access to *cis*-tetrahydropyran rings, which can be used for future complex natural product synthesis However, the nature of the ligand and catalyst necessary for this transformation are expensive and not environmentally friendly, and do not present the ideal option for the synthesis of molecules as simple as the decytospolides.

While these syntheses provide routes by which to access the decytospolides, they also rely heavily on transition metal catalyzed reactions and multiple steps to install the tetrahydropyran core. They also demonstrate the utility of these natural products for demonstrating the effectiveness for new methods to synthesize tetrahydropyran rings. Alternatively, a simpler and much greener approach to the synthesis of these natural products was envisioned highlighting the Achmatowicz rearrangement.

1.4 Achmatowicz Rearrangement

A commonly used method to generate substituted tetrahydropyran rings is the Achmatowicz rearrangement, first described in 1971 by Achmatowicz and coworkers[30]. The reaction utilizes furan based compounds as starting materials, which are readily obtained from agricultural byproducts. Starting with a furanyl alcohol, a three-membered ring is formed by oxidation or bromination. Opening of the 3-membered ring via the formation of an oxocarbenium ion followed by ring opening gives the diketone species, which cyclizes to form

the desired tetrahydropyran[31]. The furfuryl alcohol from compound **1.16** is used to attack the ketone and form a 6-membered ring, this also represents the stereocenter in **1.20**. Notably, any chiral centers near the furan are maintained during the reaction and can be used to install other stereocenters. Any other stereocenters about the ring can then be created, usually without the need for a chiral catalyst. This is because of the chair conformation that is dictated by the previously installed chiral center. Because of the ability to install numerous stereocenters around the tetrahydropyran ring without the need for chiral catalysts, the Achmatowicz rearrangement is a versatile transformation for their synthesis.

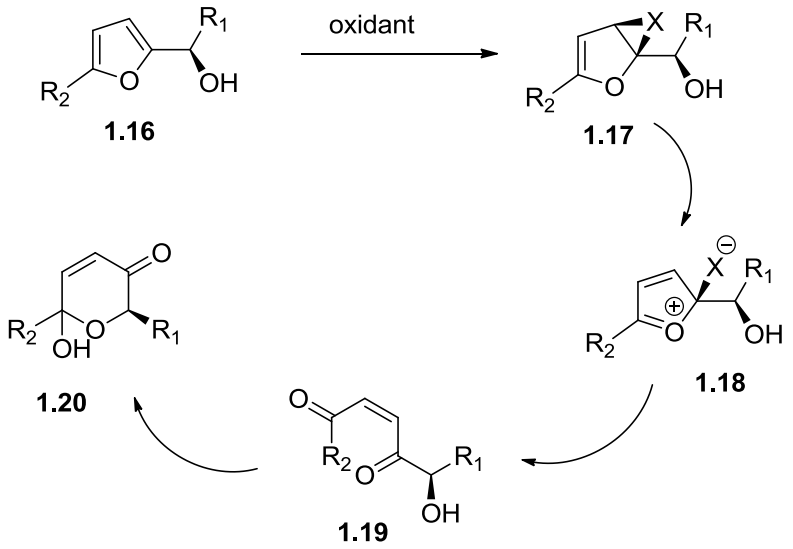

Scheme 1.5: Achmatowicz Rearrangement Mechanism

1.4.1 Common Procedures for the Achmatowicz Rearrangement

A common procedure for this rearrangement utilizes the Sharpless epoxidation system of catalytic $VO(acac)_2$ and *tert*-butylhydrogen peroxide[32]. This uses the furanyl alcohol as a means to coordinate with the vanadium species and direct the installation of the epoxide to one face or another. The epoxidation can also be accomplished with mCPBA rather than the catalytic vanadium system, but this approach is less desirable due to the innate toxicity of mCPBA[33-38]. Another common method utilizes NBS as a brominating with a mixture of $NaHCO_3$ and NaOAc as a buffer system, but this procedure requires the removal of the succinimide byproduct generated by NBS[39-42]. Bromination can also be accomplished using elemental Br_2, but this approach is rarely utilized in modern chemistry. Unfortunately, most of these conditions rely on

transition metals or the use of unstable peroxides, and are not particularly cost effective. They also require purification due to the presence of organic byproducts or excess reagents.

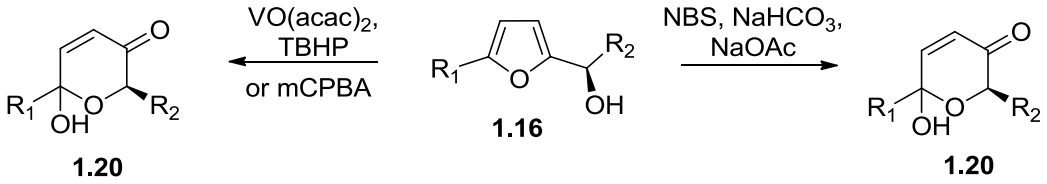

Scheme 1.6: Common Achmatowicz Conditions

Recently, Tong and coworkers developed a greener procedure that utilizes no heavy metal catalysts and avoids the generation of side products[43]. Rather, a combination of inexpensive, non-toxic oxone with a simple inorganic salt, such a KBr, is used to generate a brominating agent in situ with oxone as the terminal oxidant. From there, the reaction follows the general scheme seen with NBS, but without the organic byproducts and need for further purification. All purification for this reaction can be accomplished using an aqueous workup, which is particularly beneficial since the hemiacetal product is often not stable enough for column chromatography.

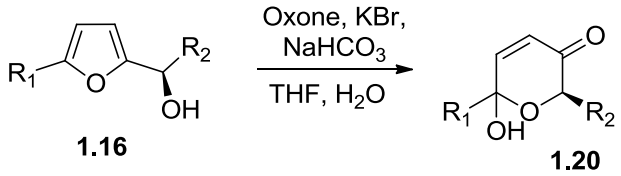

Scheme 1.7: Achmatowicz Rearrangement using Oxone

1.4.2 Using the Achmatowicz Rearrangement to Synthesize Other Tetrahydropyran Containing Natural Products

A total synthesis of herboxidiene utilizing the Achmatowicz rearrangement was reported by Ghosh and Li. Starting from aldehyde **1.21**, addition of allyl Grignard followed by lipase resolution of the racemic alcohol gave optically active alcohol **1.22**. This was subjected to Achmatowicz conditions with catalytic $VO(acac)_2$ and TBHP to give the dihydropyranone hemiacetal rearrangement product. A Kishi reduction of the hemiacetal gave dihydropyranone **1.23** in 65% yield over 2 steps. The vinyl group was then converted to the methyl ester by

ozonolysis quenched by dimethyl sulfide to give the aldehyde, and Pinnick oxidation with aqueous $NaClO_2$ and esterification with EDCI and DMAP in MeOH to give methyl ester **1.24**. The dihydropyranone was then reduced using Luche reduction conditions with $CeCl_3$ and $NaBH_4$ to give the vinyl alcohol. Simmons-Smith cyclopropanation then gave **1.25** as the sole diastereomer. A Barton deoxygenation reaction is used to open the cyclopropane ring and provide the corresponding methyl group to give **1.26**. A series of steps was then used to convert it to vinyl iodide **1.27**. This was subjected to Suzuki coupling conditions with boronate **1.28** followed by a series of steps to complete the synthesis of herboxidiene[44].

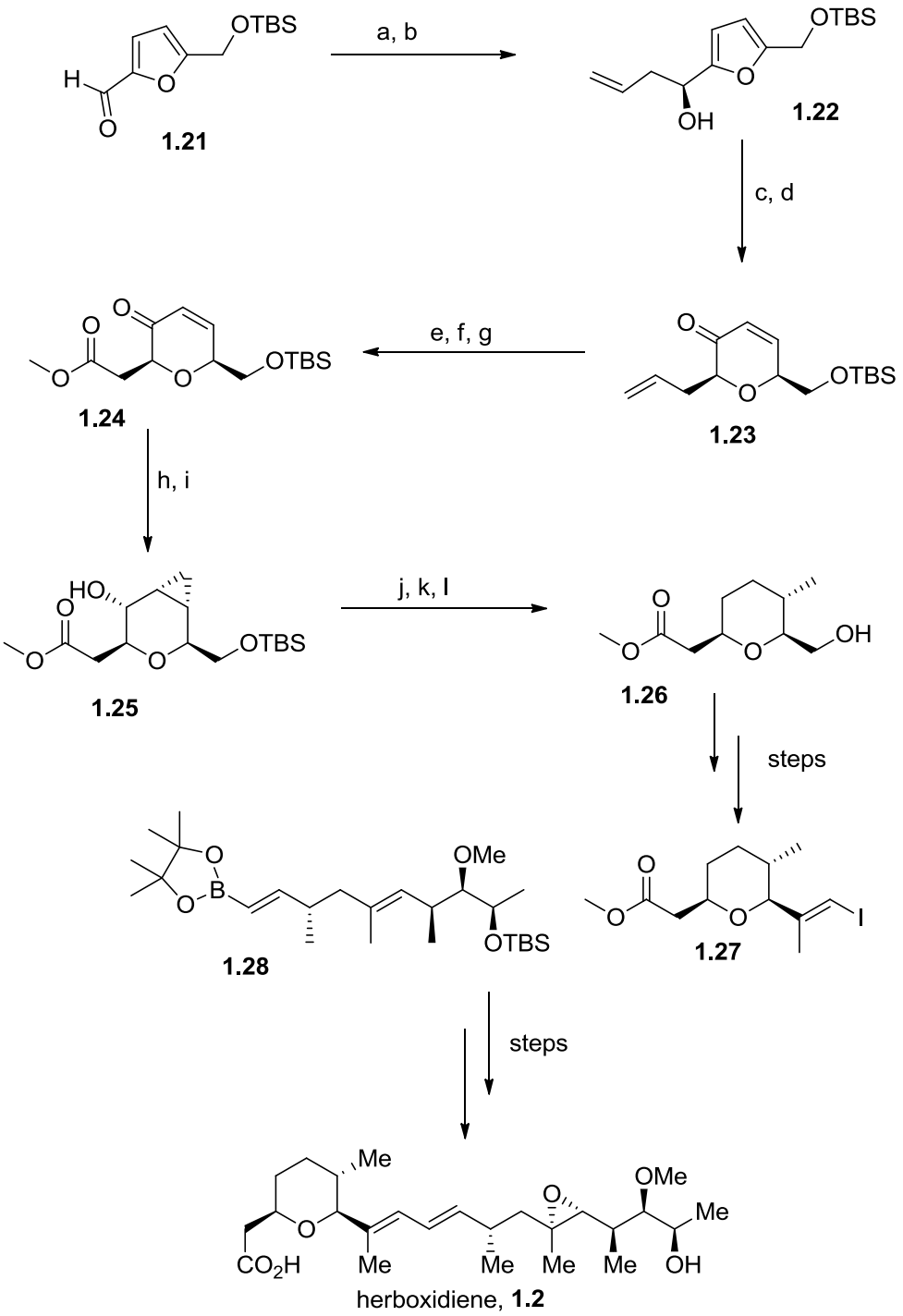

Scheme 1.8: Achmatowicz Based Synthesis of Herboxidiene. Reagents and Conditions: (a) allylMgBr; (b) lipase, vinyl acetate; (c) $VO(acac)_2$, TBHP; (d) Et_3SiH, TFA (65% over 2 steps); (e) O_3, Me_2S; (f) aq. $NaClO_2$; (g) EDCI, DMAP, MeOH; (h) $NaBH_4$, $CeCl_3$; (i) Et_2Zn, CH_2I_2; (j) TCDI, DMAP; (k) $(TMS)_2SiH$, AIBN; (l) H_2, PtO_2, MeOH, HCl.

Ghosh and Chen also utilized the Achmatowicz rearrangement in their synthesis of Spliceostation A. Reduction of commercially available acetyl furan **1.29** is done using CBS catalyst and borane dimethyl sulfide to give optically active alcohol **1.30**. This was subjected to Achmatowicz conditions with catalytic $VO(acac)_2$ and TBHP to give the dihydropyranone hemiacetal rearrangement product. A Kishi reduction of the hemiacetal gave dihydropyranone **1.31** in 63% yield over 2 steps. **1.31** was treated with the Gilman reagent formed from MeLi and CuBr to give the 1,4-addition product **1.32** in high diastereoselectivity. A series of steps converted **1.32** into diene **1.33**. This underwent a cross metathesis with tetrahydropyranyl epoxide **1.34** to give spliceostatin A[45].

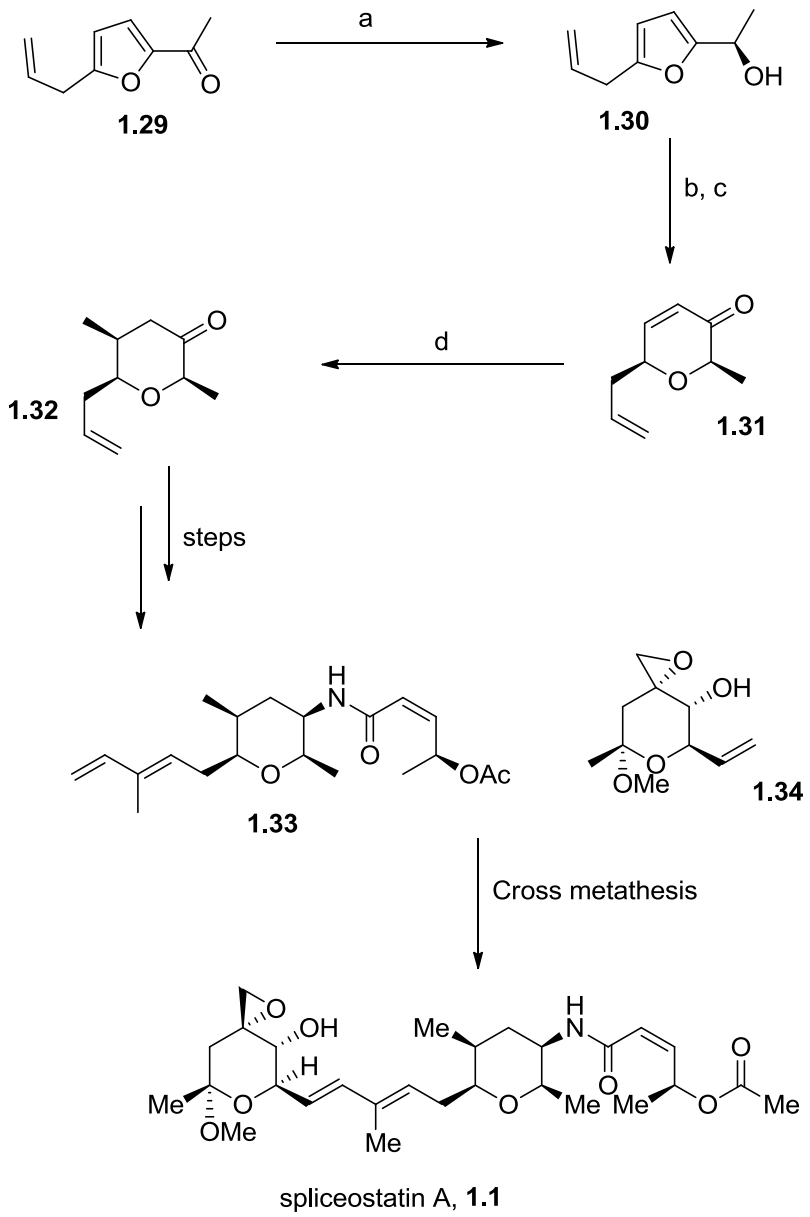

Scheme 1.9: Synthesis of Spliceostatin A Using an Achmatowicz Rearrangement. Reagents and Conditions: (a) (S)-Me-CBS, $BH_3 \cdot SMe$ (b) $VO(acac)_2$, TBHP; (c) Et_3SiH, TFA (63% over 2 steps); (d) MeLi, $CuBr \cdot SMe_2$.

The incorporation of the Achmatowicz rearrangement into the synthesis of decytospolides A and B would lead to a simpler synthesis than those previously reported. Additionally, it can be utilized to develop a greener synthesis since it provides a method to construct the tetrahydropyran ring without organic byproducts or transition metals. This will be accomplished either by the Sharpless procedure or the one using oxone as the terminal oxidant.

1.5 First Achmatowicz based Synthesis

Based on the Achmatowicz rearrangement, an enantioselective synthesis was designed. The final decytospolides A and B were envisioned to come from tetrahydropyranyl derivative **1.35**. This would come from the Achmatowicz rearrangement of furfuryl alcohol **1.36** and reduction of the resulting dihyrdorpyranone hemiacetal by Lewis acid formation of an oxocarbenium ion and quenching with a hydride source. Furanyl alcohol **1.36** can be made from commercially available furan through a series of alkylation and acylation steps.

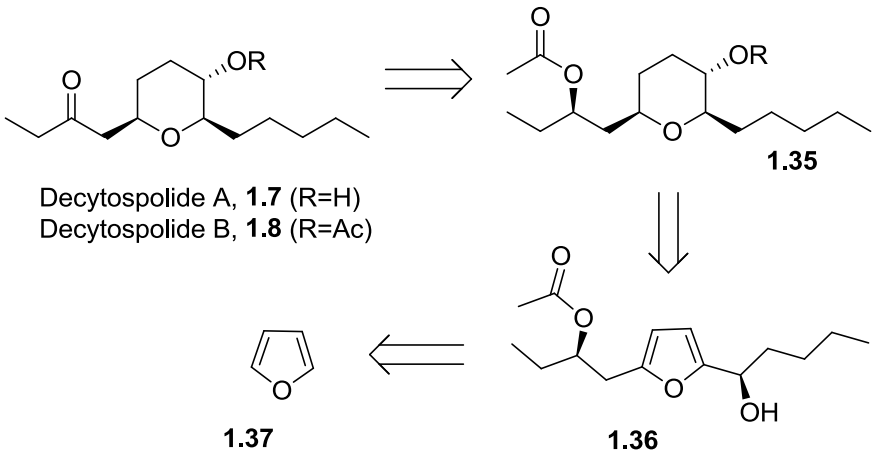

Scheme 1.10: Initial Retrosynthesis of Decytospolides A and B

To synthesize the optically active form of furanyl alcohol **1.36**, furan was deprotonated at the 2-positon with n-BuLi and quenched with (R)-1,2-epoxybutane. The enantiopure epoxide was used to avoid the formation of an inseparable mixture of diastereomers later in the synthesis that made the determination of diastereoselectivity impossible. The corresponding acetate **1.38** was formed by reacting **1.36** with Ac_2O, Et_3N and catalytic DMAP. Friedel-Crafts acylation using hexanoyl chloride, made from hexanoic acid immediately prior to the reaction using heated $SOCl_2$, and $SnCl_4$ at 0 ºC gave ketone **1.39**[46]. The ketone was reduced enantioselectively using a catalytic (1 mol%) amount of Noyori's catalyst, (*R*,*R*) RuCl(mesitylene)-Ts-DPEN, in the presence of H_2, formed in situ by the reaction of Et_3N and formic acid, in DCM at 55 ºC to give **1.36**. The reduction proceeded with high diastereoselectivity (>20:1) and no other diastereomer was observed by ^1H or ^{13}C NMR spectroscopy[45,47]. Noyori's catalyst coordinates with the furan oxygen as it reduces the ketone installed by the Friedel-Crafts acylation. While most Noyori

reductions take place at room temperature, this reaction required heating to progress. This is likely due to the two coordination sites that are possible for the catalyst, one which is the desired coordination between furan and ketone and the other between the furan and the acetate protecting group.

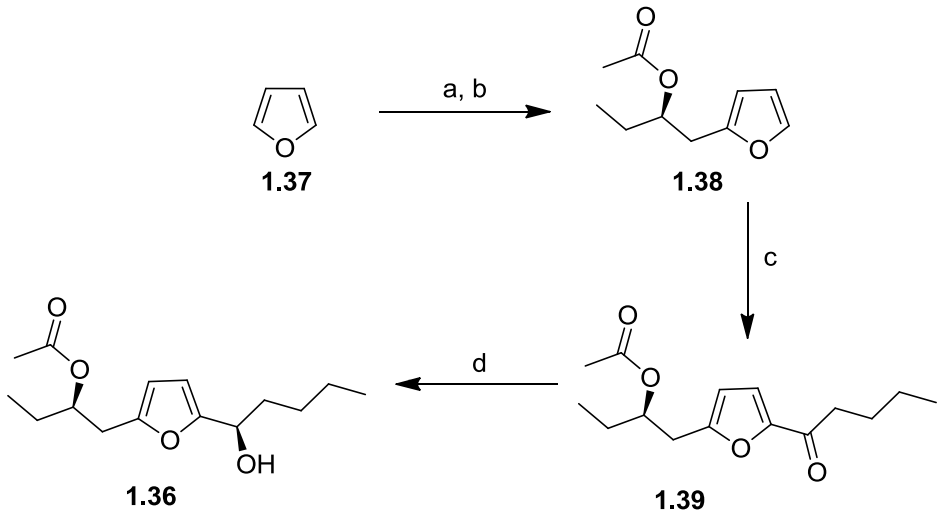

Scheme 1.11: Synthesis of Alcohol **1.36**. Reagents and Conditions: (a) (*R*)-1,2-epoxybutane, *n*-BuLi, THF, 0 °C to 23 °C; (b) Ac_2O, Et_3N, DMAP, CH_2Cl_2, (84%, 2-steps); (c) $C_5H_{11}COCl$, $SnCl_4$, CH_2Cl_2, 0 °C (75%); (d) RuCl(mesitylene), [(*R*,*R*)-Ts-DPEN], (1 mol%), HCO_2H, Et_3N, CH_2Cl_2, 55° C (93%).

Initially, the Achmatowicz reaction was done using the Sharpless conditions of with a catalytic amount of $VO(acac)_2$ and ^tBuOOH to oxidize **1.36**; however, the reaction never went to completion, as indicated by TLC,[48]. The Achmatowicz rearrangement of **1.36** using KBr and oxone, as the terminal oxidant, in the presence of $NaHCO_3$ in a mixture (4:1) of THF and water at 23 °C for 30 min gave the corresponding dihydropyranone hemiacetal (**1.40**)[43]. This reaction was very beneficial for several reasons. Firstly, within 30 minutes complete conversion was observed, as indicated by TLC. Additionally, the reaction works without dry solvents or the need to be under inert atmosphere. Finally, there are no organic impurities so all of them can be removed by aqueous workup. Since **1.40** is unstable and decomposes on silica gel, it is particularly beneficial that the compound can be purified without column chromatography.

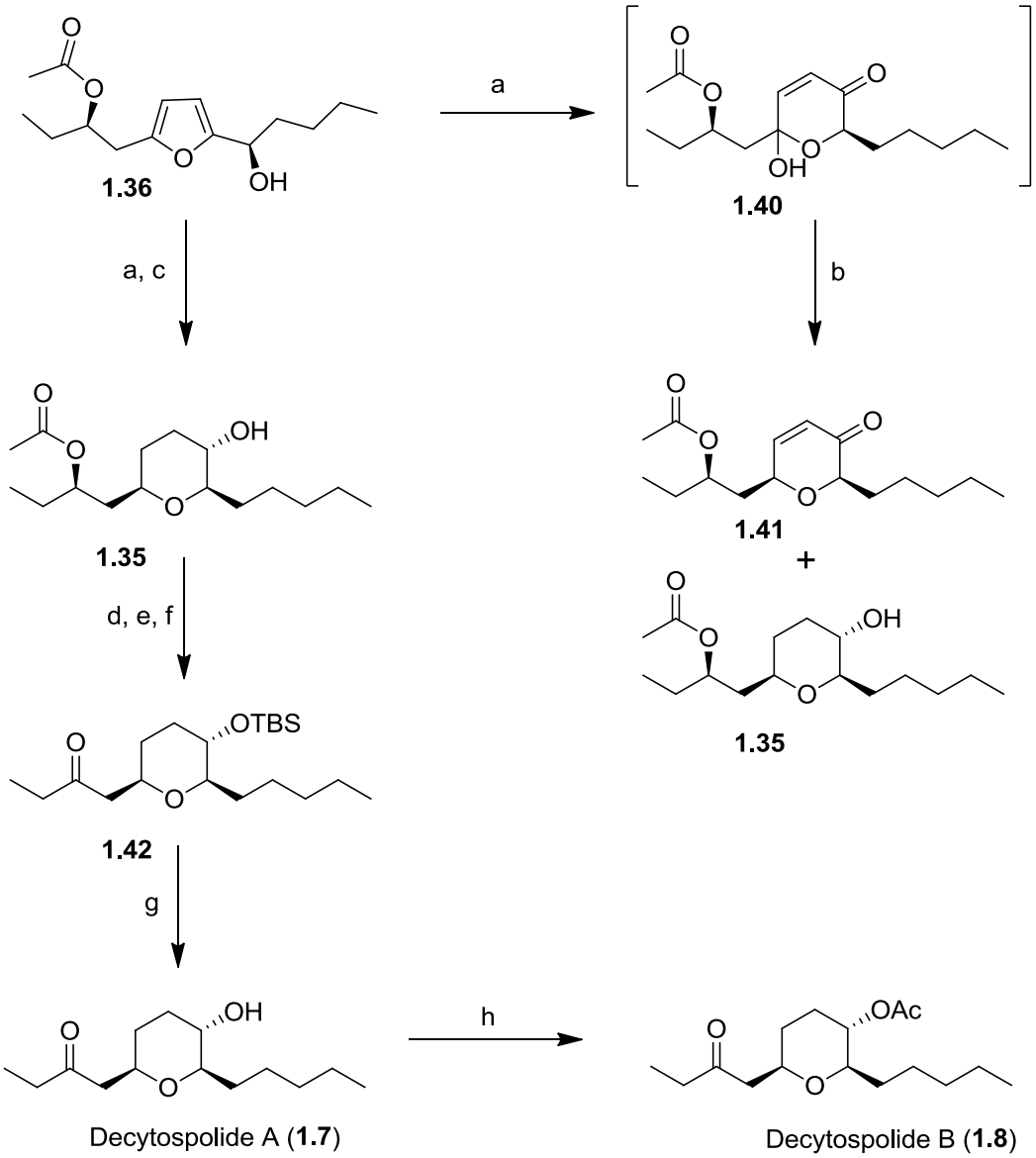

Scheme 1.12: Synthesis of the Decytospolides. Reagents and Conditions: (a) Oxone, KBr, $NaHCO_3$, THF/H_2O (4:1); (b) Et_3SiH, TFA, BF_3•OEt_2, CH_2Cl_2, -45 °C to rt, (47%, 2-steps); (c) Et_3SiH, BF_3•OEt_2, CH_2Cl_2, -45 °C, (56%, 2-steps); (d) TBSOTf, 2,6-lutidine, CH_2Cl_2, 0 °C to 23 °C; (e) K_2CO_3, MeOH; (f) DMP, $NaHCO_3$, CH_2Cl_2, 0 °C to 23 °C, (89%, 3-steps); (g) TBAF, THF, 23 °C (99%); (h) Ac_2O, pyr, DMAP, 23 °C, CH_2Cl_2 (99%).

The resulting dihydropyranone hemiacetal was initially subjected to standard Kishi reduction conditions using Et_3SiH and TFA in DCM at -45 °C for 3 hours. This gave dihydropyranone **1.41** as the major product with a trace amount of alcohol **1.35**. This reduction proceeds through an oxocarbenium ion intermediate formed by the acid promoted loss of water from the dihydropyranone ring. Hydride addition, using Et_3SiH, reduces the oxocarbenium ion

and gives the resulting dihydropyranone. Theoretically, additional equivalents or acid can then coordinate to the enone, prompting addition of the Et_3SiH and diastereoselective reduction of this moiety. This explains the appearance of **1.35** in the reaction. The synthesis of **1.35** was actually more beneficial than that of **1.41**, since it allows for the removal of several steps from the synthesis and so the reaction was modified to selectively form **1.35**. Monitoring the reaction by TLC showed the formation of the spot corresponding to **1.41** prior to the formation of the one for **1.35**. Based on this, it was hypothesized that the formation of **1.35** used **1.41** as an intermediate and that addition of excess acid and hydride would allow for complete conversion of **1.41** to **1.35**. Therefore, it was hypothesized that the addition of more Et_3SiH along with a Lewis acid would be able to increase the yield of **1.35**. The reaction was optimized by adding $BF_3{\bullet}OEt_2$ after complete formation of **1.41** and then stirring for an additional 3 hours at -45 °C, which provided alcohol **1.35** as the sole product in 47% yield over 2 steps.

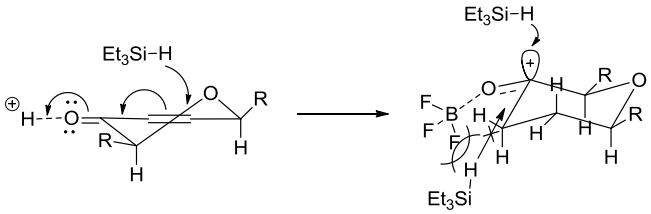

Figure 1.3: Explanation of Kishi Reduction Stereochemistry

The stereochemistry at C8 was determined by analyzing the 1H NMR coupling constants of the proton at C9, which has two J values (2.4 and 9.0 Hz). The J value of 2.4 Hz is for the relationship between the proton at C9 and those on the 5-membered alkyl chain attached to the ring. The J value of 9.0 Hz indicates the relationship between the protons at C8 and C9. In tetrahydropyran ring, a J value as large as 9.0 Hz indicates a trans relationship between the two protons. The configuration of the stereocenter at C9 was set by the Noyori reduction, allowing for the absolute stereochemistry at C8 to be assigned based on that and the trans relationship between the two. By accomplishing the synthesis of **1.35** from **1.36** in a single transformation; an additional two steps in the synthesis that had previously been used to reduce dihydropyranone **1.41** to the tetrahydropyranyl species were removed.

A series of steps were required to then complete the synthesis. First, alcohol **1.35** was protected using TBSOTf and 2,6-lutidine in DCM at 0 °C to 23 °C for 12 hours to give the

corresponding silyl ether. This was to prevent it's oxidation and destruction of the stereocenter in subsequent steps. The acetate was then hydrolyzed with K_2CO_3 in MeOH at 23 °C to provide the corresponding alcohol. This alcohol is then oxidized using Dess-Martin periodinane with $NaHCO_3$ in DCM to give ketone **1.42** in 89% yield over 3 steps. Since this stereocenter from (R)-butylene oxide had to be destroyed to form the natural products, the removal for the need for this stereocenter was a key consideration for the design of subsequent syntheses. Deprotection of the silyl ether was done using tetrabutylammonium fluoride (TBAF) in THF at 23 °C for 12 hours to give access to decytospolide A (**1.7**) in quantitative yield. Reaction of decytospolide A (**1.7**) with Ac_2O, pyridine and a catalytic amount of DMAP in DCM at 23 °C for 1.5 hours gave access to decytospolide B (**1.8**) in quantitative yield.

The NMR spectra of the synthetic decytospolides, both ^{1}H and ^{13}C, are in complete agreement with those reported for both natural decytospolide A {$[\alpha]_D^{20}$+6.1 (*c* 0.08, $CHCl_3$)} and decytospolide B {$[\alpha]_D^{20}$+26.6 (*c* 0.02, $CHCl_3$)} in the isolation paper[25]. The synthetic rotations for decytospolide A {$[\alpha]_D^{23}$+18.4 (*c* 0.45, $CHCl_3$)} and decytospolide B {$[\alpha]_D^{23}$+28.4 (*c* 0.75, $CHCl_3$)} also agreed with those reported for those reported for the natural products within a reasonable margin of error. While the rotation for decytospolide A is not in complete agreement, based on the other data (especially NMR) and the data for decytospolide B being in complete agreement, this discrepancy was viewed as an anomaly. This rotation was taken numerous times across multiple different samples and at various concentrations, including the ones reported in the isolation paper and previous syntheses.

While this synthesis successfully incorporates the Achmatowicz rearrangement, it utilizes the vanadium based procedure and the subsequent Kishi reduction gives a mixture of products, requiring further optimization. The use of a chiral center that has no function in the synthesis other than avoiding the formation of an inseparable mixture of diastereomers is undesirable. However, the ease of incorportating a stereocenter at this position offers benefits in the synthesis of derivatives based around this structural modification. Additionally, there are several protecting groups that add additional steps to the reaction. As such a new route is needed that will use fewer steps and further optimize the Achmatowicz rearrangement and Kishi reduction.

1.6 Optimization of Kishi Reduction

Following completion of the synthesis, it was noted that upon using the traditional Kishi reduction conditions of TFA (15 equivalents) and Et_3SiH (5 equivalents) in CH_2Cl_2 at -45 ºC, trace amounts tetrahydropyranyl alcohol **1.35** was formed and dihydropyranone **1.41** was obtained in 40% yield. Since the Kishi reduction proceeds through the formation of an oxocarbenium intermediate in the tetrahydropyran ring, it was hypothesized that any acidic reagent would be sufficient to form this desired intermediate and initiate the reaction. As such, a number of Lewis acids were considered for the optimization of this reaction. Further attempts were then made to increase the yield of this product, as it would remove several steps from the initial synthesis. All of these attempts had to use the crude hemiacetal **1.35** due to its inability to be purified by column chromatography, resulting in a yield determined over two steps.

Table 1.2: Reduction of the Dihydropyranone Hemiacetal with Various Lewis Acids [a]

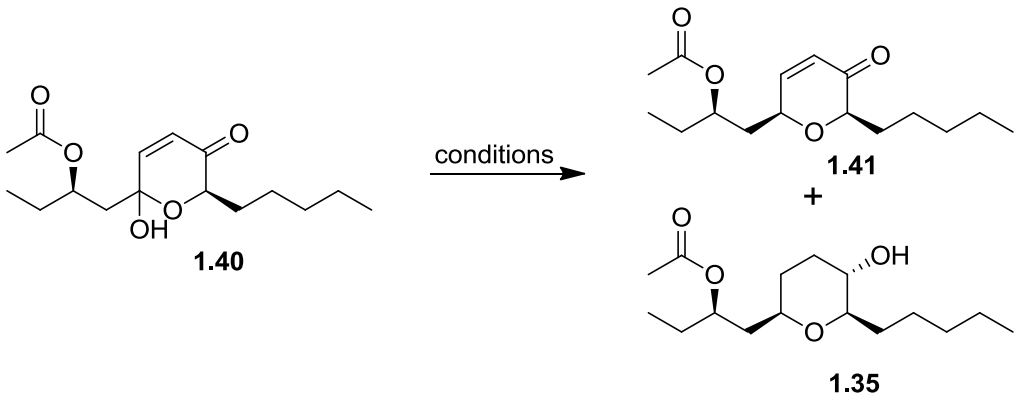

Entry	Lewis Acid (equiv)	Et_3SiH (equiv)	Time	Yield for enone **1.41**	Yield for THP **1.35**
1	TFA [15]	5	24 h	40%	trace
2	TFA [15] BF_3•OEt_2 [3]	5, then 5 more	4 h	none	47%
3	BF_3•OEt_2 [6]	10	6 h	none	56%
4	$SnCl_4$ [6]	10	4 h	none	82%
5	$Cu(OTf)_2$ [6]	10	18 h	trace	none
6	$TiCl_4$ [6]	10	18 h	14%	none
7	$Sc(OTf)_3$ [6]	10	18 h	trace	none

[a]All reactions were carried out in CH_2Cl_2 at -45 ºC

Initially, it was hypothesized that the addition of a Lewis acid would be sufficient to activate the pyranone, allowing for reduction to the corresponding alcohol with Et_3SiH. Following the initial conditions and then adding BF_3•OEt_2 (3 equivalents) after TLC showed complete consumption of starting material resulted in 47% of the tetrahydropyranyl alcohol and no dihydropyranone. Based on these results, the reaction was then carried out in the absence of TFA and with 6 equivalents of BF_3•OEt_2 and 10 equivalents of Et_3SiH giving the desired alcohol in 56% yield with no trace of the dihydropyranone[49]. Based off the positive results with BF_3•OEt_2, additional strong Lewis acids were utilized with $Cu(OTf)_2$ (6 equivalents) and $Sc(OTf)_3$ (6 equivalents) yielding only trace amounts of the dihydropyranone, most of the material remained unreacted dihydropyranone hemiacetal after 18 hours. It is possible that warming the reaction from -45 ºC may have increased yield with these acids, but that was never tested. $SnCl_4$ (6 equivalents) was the most effective Lewis acid, resulting in 82% yield of alcohol **1.35** as the sole product. The use of $TiCl_4$ (6 equivalents) gave 14% of dihydropyranone **1.41**, and the remainder of the dihydropyranone hemiacetal decomposed. This reagent is likely to strong for use at these temperatures, since $TiCl_4$ is most commonly utilized at -78 ºC. Based on these results, the combination of Et_3SiH and either BF_3•OEt_2 or $SnCl_4$ at -45 ºC was the best and would be using the all reductions of the hemiacetal moving forward.

1.7 Completed Optimized Synthesis

An optimized synthesis was envisioned that would remove the need for any protecting groups. The final decytospolides A and B were envisioned to come from the addition of a Grignard to tetrahydropyranyl derivative **1.43** following conversion of the methyl ester to a Weinreb amide. This would be obtained by the Achmatowicz rearrangement of furanyl alcohol **1.44** and subsequent reduction of the resulting hemiacetal all the way to the tetrahydropyranyl alcohol rather than isolating the dihydropyranone. Furanyl alcohol **1.44** is envisioned to come from commercially available furfural using a Jocic reaction, for one carbon homologation, followed by a Friedel-Crafts acylation and Noyori reduction to generate the optically active furfuryl alcohol.

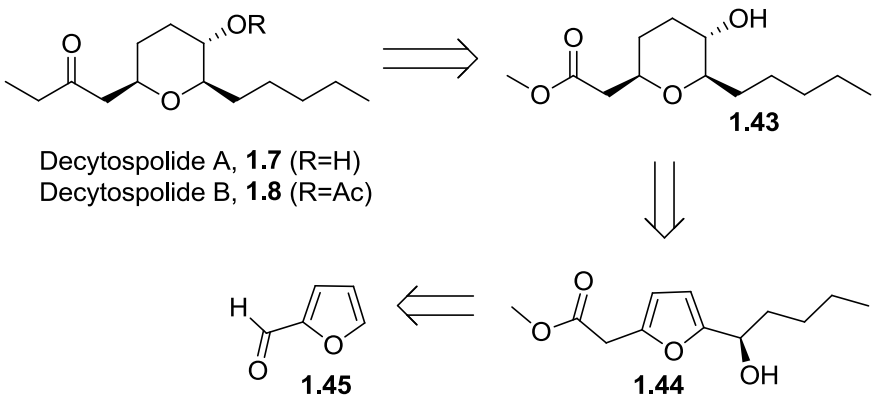

Scheme 1.13: Optimized Retrosynthesis of Decytospolides A and B

From commercially available furural, furan methyl ester **1.46** was synthesized using a one carbon homologation sequence with conditions developed by Snowden and co-workers[50-51]. This proceeded by formation of the trichlorocarbinol from furfural followed by the Jocic reaction forming the furanacetic acid. The acid was then converted to the methyl ester **1.46** using a Fisher esterification. Methyl ester **1.46** is also commercially available. Acylation of methyl ester **1.46** was accomplished using hexanoyl chloride, formed in situ from hexanoic acid and $SOCl_2$, in the presence of $SnCl_4$ to give furanyl ketone **1.47** in 57% yield. This was the same procedure as seen in the initial Achmatowicz-based synthesis. Enantioselective reduction of ketone **1.47** using a very low catalyst loading (1 mol%) of Noyori's catalyst RuCl(mesitylene)[(*R*,*R*)-Ts-DPEN] in the presence of Et_3N and formic acid in DCM at 50 °C for 12 hours gave the optically active furanyl alcohol **1.44** in 83% yield and 99% ee[45,47]. Once more, the reaction required heating to proceed. As was the case with the initial Achmatowicz synthesis, there are two potential coordination sites for the rubidium catalyst. One of these is the desired coordination between the furan and ketone and the other is between the furan and the methyl ester.

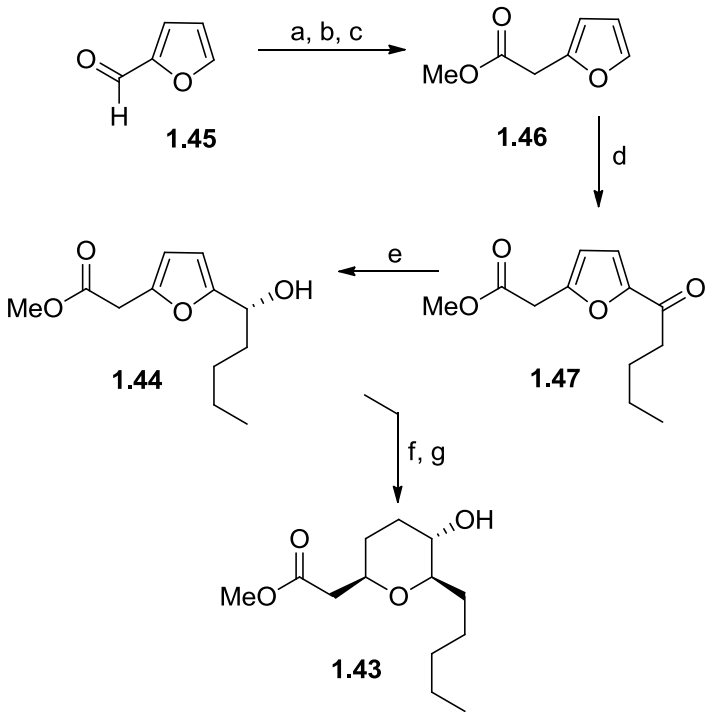

Scheme 1.14: Synthesis of Alcohol **1.43**. Reagents and Conditions: (a) DBU, $CHCl_3$ (78%); (b) Ph_2Se_2, $NaBH_4$, NaOH, EtOH, 30 ºC (92%); (c) cat. H_2SO_4, MeOH, 65 ºC (42%); (d) $C_5H_{11}COCl$, $SnCl_4$, CH_2Cl_2, 0 °C (57%); (e) RuCl(mesitylene)[(*R*,*R*)-Ts-DPEN], (1 mol%), HCO_2H, Et_3N, CH_2Cl_2, 50 °C, 12 h (83%, 99% ee); (f) KBr, $NaHCO_3$, oxone, THF/H_2O (4:1), 0 °C to 23 °C, 3 h; (g) BF_3•OEt_2, Et_3SiH, CH_2Cl_2, -40 °C, 16 h (58%, over 2 steps).

The Achmatowicz rearrangment of **1.44** using the oxone based conditions at 23 °C for 30 min furnished the expected dihydropyranone hemiacetal as the sole product, as determined by TLC and ^{1}H-NMR. The hemiacetal was reacted with excess Et_3SiH in the presence of BF_3•OEt_2 at -40 °C for 16 h to reduce the dihydropyranone hemiacetal all the way to the tetrahydropyranyl alcohol **1.43** as a single product, which was verified by ^{1}H-NMR analysis[49]. Attempts to accomplish this transformation using the TFA and BF_3•OEt_2 combination used in the initial synthesis resulted in the formation of a hyperconjugated product. This is likely due to the conjugate base of TFA that is formed in the system removing one of the acidic protons alpha to the methyl ester in order to remove the reactive oxocarbenium ion. This is done instead of the Et_3SiH quenching the oxocarbenium and is likely faster than this process, as indicated by the lack of dihydropyranone or **1.43** formed using these conditions.

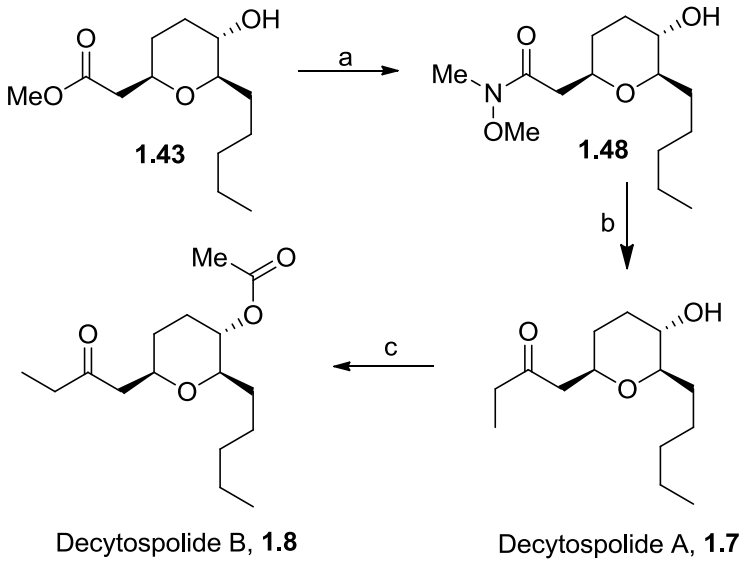

Scheme 1.15: Synthesis of Decytospolides. Reagents and Conditions: (a) NH(OMe)Me•HCl, *i*-PrMgCl, THF, -30 °C, 5 h (93%); (b) EtMgBr, THF, 0 °C to rt, 5 h (97%); (c) Ac_2O, pyridine, DMAP, CH_2Cl_2, 0 °C to 23 °C, 3 h (86%).

Tetrahydropyranyl alcohol **1.43** provided access to the decytospolides via conversion of the methyl ester to an ethyl ketone. The methyl ester was subjected to the species formed by reaction of NH(OMe)Me•HCl with *i*-PrMgCl and the reaction run in THF at -30 °C for 5 hours provided Weinreb amide derivative **1.48** in excellent yield. This bypassed the need for a more traditional formation of the amide by conversion to the acid prior to forming the amide. In an attempt to avoid this step, formation of the corresponding Weinreb amide rather than methyl ester **1.26** was explored, but this compound was not compatible with the Friedel-Crafts acylation. Treatment of Weinreb amide **1.48** with ethyl Grignard in anhydrous THF with the reaction warmed from 0 °C to 23 °C over 5 hours afforded decytospolide A, **1.7** in quantitative yield {$[(\alpha)_D^{23}$+7.8 (*c*, 1.33, $CHCl_3$)]}. Acylation of **1.7** using Ac_2O, pyridine and a catalytic amount of DMAP in DCM gave decytospolide B, **1.8** {$[\alpha]_D^{23}$+22.8 (*c*, 1.96, $CHCl_3$)} in 86% yield. Unlike with the previous synthesis, the rotations of these synthetic products are in complete agreement with the isolated natural products and syntheses reported by other authors. The ^{1}H-NMR and ^{13}C-NMR spectra of synthetic decytospolide A and B are also in complete agreement with the natural product spectra from the isolation paper[25].

1.8 Conclusion

In conclusion, two enantioselective routes for the synthesis of decytospolides A and B. The latter route significantly improves upon the first one by removing the need for protecting groups and avoiding the installation of an extraneous chiral center. Both syntheses feature an Achmatowicz rearrangement of an optically active furfuryl alcohol as the key reaction to install the tetrahydropyran core. This alcohol was obtained from a Friedel-Crafts acylation of a furfural based substrate followed by an enantioselective reduction of the ketone using Noyori's catalyst. The Achmatowicz product is undergoes a diastereoselective reductive from the dihydropyranone hemiacetal to the saturated tetrahydropyran alcohol using $BF_3 \bullet OEt_2$ and Et_3SiH. Presumably, reduction of the enone proceeds via Lewis Acid chelation to the ketone followed by delivery of an axial hydride. This reaction was optimized by investigating the effects of several Lewis acids. The successful synthesis provides access to both natural products in seven steps or fewer from a known intermediate and ten steps total from commercially available starting material. The synthesis also provides many possibilities for the future development of derivatives to maximize the anticancer properties of the tetrahydropyranyl scaffold. The future development of a derivative of decytospolide B containing an acetamide rather than an acetate group is of particular interest to improve the anticancer properties of this scaffold.

1.9 Experimental Section

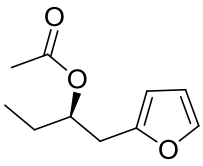

(R)-1-(furan-2-yl)butan-2-yl acetate (**1.38**):

Furan (2.02 mL, 27.74 mmol) was dissolved in THF (23 mL) and cooled to 0 °C. *n*-BuLi (15.6 mL, 24.97 mmol) was added slowly dropwise upon which a bright yellow color developed. After stirring for 1 h at 0 °C, (*R*)-(+)-butylene oxide (1.21 mL, 13.87 mmol) was added and the reaction was slowly warmed to room temperature. After stirring for 12 h, the resulting deep red solution was quenched with sat. NH_4Cl, extracted with EtOAc (3X), washed with brine and dried over Na_2SO_4. It was purified by column chromatography using 10% EtOAc in Hexanes as the eluent to give 1.69g (87% yield) of the resulting furan alcohol as a yellow oil.

(*R*)-furan alcohol (868 mg, 6.19 mmol) was dissolved in CH_2Cl_2 (21 mL) and cooled to 0 °C. Acetic anhydride (1.2 mL, 12.4 mmol), Et_3N (1.3 mL, 9.3 mmol) and a few crystals of DMAP were added and the reaction warmed to room temperature. After 6 h, the reaction was quenched with sat. $NaHCO_3$, extracted with CH_2Cl_2 (3X), washed with brine and dried over Na_2SO_4. It was purified by column chromatography using 5% to 10% EtOAc in Hexanes as the eluent to give 1.1 g (97% yield) of acetate **1.17** as a clear oil $[\alpha]_D^{20}$ +19.6 (*c* 0.73, $CHCl_3$).

^{1}H NMR (500 MHz, $CDCl_3$) δ (ppm): 7.31 (dd, *J* = 1.9, 0.9 Hz, 1H), 6.28 (dd, *J* = 3.2, 1.9 Hz, 1H), 6.05 (dd, *J* = 3.2, 0.9 Hz, 1H), 5.04 (m, 1H), 2.87 (d, *J* = 6.3 Hz, 2H), 2.02 (s, 3H), 1.65-1.55 (m, 2H), 0.92 (t, *J* = 7.5 Hz, 3H);); ^{13}C NMR (125 MHz, $CDCl_3$) δ (ppm): 170.7, 151.9, 141.5, 110.4, 107.0, 73.8, 32.5, 26.7, 21.3, 9.7. FT-IR (neat) ν_{max} = 2965, 2925, 2852, 1738, 1507, 1461, 1436, 1376, 1239, 1012, 739 cm^{-1}

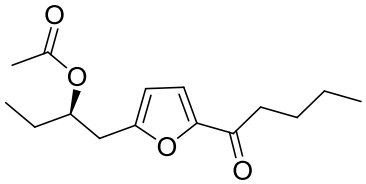

(R)-1-(5-hexanoylfuran-2-yl)butan-2-yl acetate (**1.39**):

Hexanoic acid (604 mg, 5.20 mmol) was refluxed overnight in an excess of thionyl chloride. The excess thionyl chloride was removed by distillation under argon. The hexanoyl chloride was used immediately for the subsequent reaction. Hexanoyl chloride (699 mg, 5.2 mmol) was dissolved in CH_2Cl_2 (15 mL) and cooled to 0 °C. $SnCl_4$ (8.7 mL, 8.7 mmol, 1 M in CH_2Cl_2) was added slowly dropwise. After stirring for 1 h at 0 °C, acetate **1.38** (789 mg, 4.33 mmol) dissolved in CH_2Cl_2 (5 mL) was added to the reaction mixture slowly via cannula. After 30 min at 0 °C, the red-brown solution was quenched with ice, extracted with CH_2Cl_2 (3X), washed with brine and dried over Na_2SO_4. It was purified by column chromatography using 10% to 20% EtOAc in Hexanes as the eluent to give 909 mg (75% yield) of furan derivative **1.39** as a clear oil; $[\alpha]_D^{20}$ +16.2 (*c* 0.86, $CHCl_3$).

^{1}H NMR (500 MHz, $CDCl_3$) δ (ppm): 7.07 (d, *J* = 3.5 Hz, 1H), 6.21 (d, *J* = 3.5 Hz, 1H), 5.07 (quint, *J* = 6.4 Hz, 1H), 2.99-2.91 (m, 2H), 2.74 (t, *J* = 7.9 Hz, 2H), 2.02 (s, 3H), 1.72-1.66 (m, 2H), 1.65-1.59 (m, 2H), 1.34-1.31 (m, 4H), 0.92 (t, *J* = 7.4 Hz, 3H), 0.89 (t, *J* = 6.5 Hz, 3H); ^{13}C NMR (125 MHz, $CDCl_3$) δ (ppm): 189.4, 170.6, 157.0, 152.1, 118.3, 109.9, 73.2, 38.4, 32.8,

31.6, 26.9, 24.3, 22.6, 21.2, 14.0, 9.7. FT-IR (neat) ν_{max} = 2961, 2931, 2866, 1741, 1674, 1588, 1516, 1374, 1238, 1023 cm^{-1}

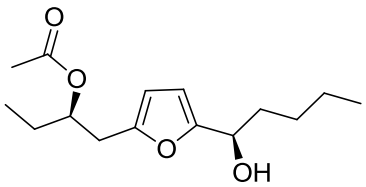

(R)-1-(5-((R)-1-hydroxyhexyl)furan-2-yl)butan-2-yl acetate (**1.36**):

Furan derivative **1.39** (280 mg, 1 mmol) was dissolved in CH_2Cl_2 (5 mL). Et_3N (1.0 mL, 7.5 mmol) was added, followed by formic acid (0.28 mL, 7.5 mmol) and Noyori catalyst, (*R*,*R*) RuCl(mesitylene)-Ts-DPEN (6.2 mg, 0.01 mmol). The reaction was heated to 55 °C. After refluxing for 12 h, the orange solution was diluted with water, extracted with CH_2Cl_2 (3X), washed with brine and dried over Na_2SO_4. It was purified by column chromatography using 10% to 20% EtOAc in Hexanes as the eluent to give 261 mg (93% yield) of alcohol **1.36** as a clear oil. This alcohol was obtained as a single diastereomer as determined by ^{1}H NMR (ratio >20:1) $[\alpha]_D^{20}$ +13.5 (*c* 0.84, $CHCl_3$).

^{1}H NMR (500 MHz, $CDCl_3$) δ (ppm): 6.10 (d, *J* = 3.1 Hz, 1H), 5.97 (d, *J* = 3.1 Hz, 1H), 5.04 (m, 1H), 4.59 (q, *J* = 6.8 Hz, 1H), 2.88-2.80 (m, 2H), 2.01 (s, 3H), 1.92 (d, *J* = 5.2 Hz, 1H), 1.83-1.79 (m, 2H), 1.65-1.55 (m, 2H), 1.42 (m, 1H), 1.31-1.30 (m, 5H), 0.93-0.86 (m, 6H); ^{13}C NMR (125 MHz, $CDCl_3$) δ (ppm): 170.7, 155.9, 151.3, 107.6, 106.7, 73.8, 68.0, 35.6, 32.6, 31.7, 26.8, 25.4, 22.7, 21.3, 14.2, 9.7; FT-IR (neat) ν_{max} = 3447, 2958, 2933, 2859, 1739, 1559, 1464, 1433, 1373, 1242, 1021, 964, 792 cm^{-1}, LRMS-ESI (+) *m/z* 305.1 $[M+Na]^+$.

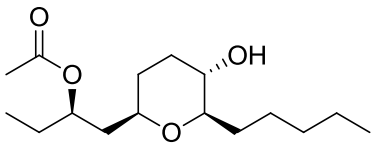

(R)-1-((2R,5S,6R)-5-hydroxy-6-pentyltetrahydro-2H-pyran-2-yl)butan-2-yl acetate (**1.35**):

Furanyl alcohol **1.36** (317 mg, 1.12 mmol) was dissolved in THF (8 mL) and H_2O (2mL) and cooled to 0 °C. KBr (6.7 mg, 0.06 mmol), $NaHCO_3$ (47 mg, 0.56 mmol) and oxone (826 mg, 1.34 mmol) were added after which a light yellow color developed. After stirring at 0 °C for 30 min, the reaction was quenched with sat. $NaHCO_3$, extracted with EtOAc (3X), washed with

brine and dried over Na_2SO_4. The resulting crude hemiacetal **1.40** was used directly for the next reaction with no further purification.

The crude hemiacetal was dissolved in CH_2Cl_2 (10 mL) and cooled to –45 °C. Et_3SiH (0.89 mL, 5.6 mmol) was added followed by and TFA (1.3 mL, 16.8 mmol) being added dropwise, upon which a yellow color developed. The reaction was stirred at –45 °C for 3 h and then warmed to room temperature. After stirring for 30 min at 23 °C, the reaction was cooled to 0 °C and additional Et_3SiH (0.895 mL, 5.6 mmol) was added followed by $BF_3{\cdot}OEt_2$ (0.415 mL, 3.36 mmol). After stirring for 30 min at 0 °C, the reaction was quenched slowly with sat. $NaHCO_3$. The reaction was extracted with CH_2Cl_2 (3X), washed with brine and dried over Na_2SO_4. It was purified by column chromatography using 10% to 30% EtOAc in Hexanes as the eluent to give 151 mg (47% yield over two steps) of tetrahydropyran derivative **1.35** as a clear oil. It was obtained as a single diastereomer as determined by ^{1}H NMR analysis (>20:1) $[\alpha]_D^{20}$ +2.7 (*c* 0.49, $CHCl_3$).

^{1}H NMR (500 MHz, $CDCl_3$) δ (ppm): 5.01 (m, 1H), 3.30-3.22 (m, 2H), 2.95 (td, *J* = 9.0, 2.4 Hz, 1H), 2.06 (m, 1H), 2.03 (s, 3H), 1.79 (m, 1H), 1.65-1.53 (m, 6H), 1.43-1.24 (m, 9H), 0.90-0.85 (m, 6H); ^{13}C NMR (125 MHz, $CDCl_3$) δ (ppm): 170.7, 82.2, 74.1, 72.9, 70.9, 40.0, 33.3, 32.2, 32.1, 32.0, 31.8, 27.8, 25.0, 22.7, 21.3, 14.2, 9.5; FT-IR (neat) ν_{max} = 3451, 2929, 2859, 1739, 1718, 1461, 1436, 1373, 1242, 1080, 1056, 1024, 954 cm^{-1}, LRMS-ESI (+) *m/z* 287.1 $[M+H]^+$.

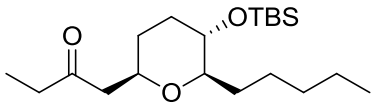

1-((2R,5S,6R)-5-((tert-butyldimethylsilyl)oxy)-6-pentyltetrahydro-2H-pyran-2-yl)butan-2-one (**1.42**):

Tetrahydropyran derivative **1.35** (141 mg, 0.49 mmol) was dissolved in CH_2Cl_2 (5 mL) and cooled to 0 °C. 2,6-lutidine (0.23 mL, 1.97 mmol) and TBSOTf (0.34 mL, 1.48 mmol) were added and the reaction was warmed to 23 °C. After stirring for 12 h, the reaction was quenched with sat. $NaHCO_3$, extracted with CH_2Cl_2 (3X), washed with brine and dried over Na_2SO_4. It was purified by column chromatography using 5% to 10% EtOAc in Hexanes as the eluent to give 200 mg (quantitative) of the resulting silyl ether as a clear oil.

The silyl ether (186 mg, 0.46 mmol) was dissolved in MeOH (3 mL) and cooled to 0 °C. K_2CO_3 (6.4 mg, 0.05 mmol) was added, upon which a yellow color developed. The reaction was

warmed to room temperature. After 12 h, the reaction was diluted with H_2O and EtOAc, extracted with EtOAc (3X), washed with brine and dried over Na_2SO_4. It was purified by column chromatography using 5% to 20% EtOAc in Hexanes as the eluent to give 155 mg (93% yield) of the resulting alcohol as a clear oil.

The resulting alcohol (144 mg, 0.40 mmol) was dissolved in CH_2Cl_2 (4 mL) and cooled to 0 °C. $NaHCO_3$ (202 mg, 2.41 mmol) was added followed by DMP (341 mg, 0.8 mmol) and the reaction was warmed to room temperature. After 12 h, the reaction was quenched with a 1:1 mixture of sat. $Na_2S_2O_3$ and sat. $NaHCO_3$. The mixture was extracted with CH_2Cl_2 (3X), washed with brine and dried over Na_2SO_4. It was purified by column chromatography using 5% to 10% EtOAc in Hexanes as the eluent to give 138 mg (96% yield) of ketone **1.42** as a clear oil $[\alpha]_D^{23}$ +32.0 (*c* 0.58, $CHCl_3$).

^{1}H NMR (500 MHz, $CDCl_3$) δ (ppm): 3.71 (m, 1H), 3.21 (m, 1H), 3.02 (m, 1H), 2.62 (dd, *J* = 14.9, 8.2 Hz, 1H), 2.53-2.41 (m, 2H), 2.36 (dd, *J* = 14.9, 4.7 Hz, 1H), 1.94 (m, 1H), 1.78-1.69 (m, 2H), 1.52-1.22 (m, 9H), 1.03 (t, *J* = 7.3 Hz, 3H), 0.86 (s, 12H), 0.04 (s, 6H); ^{13}C NMR (125 MHz, $CDCl_3$) δ (ppm): 210.3, 82.5, 74.3, 71.4, 48.7, 37.2, 33.6, 32.2, 31.9, 31.5, 25.9, 25.1, 22.7, 18.1, 14.2, 7.6, –3.9, –4.6; FT-IR (neat) νmax = 2954, 2929, 2855, 1721, 1464, 1376, 1253, 1105, 887, 837, 774 cm^{-1}, LRMS-ESI (+) *m/z* 357.3 $[M+H]^+$.

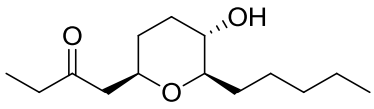

Decytospolide A (**1.7**):

Ketone **1.42** (126 mg, 0.35 mmol) was dissolved in THF (4 mL) and cooled to 0 °C. TBAF (0.71 mL, 0.71 mmol, 1 M in THF) was added and the reaction was warmed to room temperature. After 12 h, the reaction was concentrated and purified by column chromatography using 30% to 50% EtOAc in Hexanes to give 82 mg (96% yield) of decytospolide A (**1.7**) as a clear oil $[\alpha]_D^{23}$ +18.4 (*c* 0.45, $CHCl_3$).

^{1}H NMR (500 MHz, $CDCl_3$) δ (ppm): 3.72 (m, 1H), 3.24 (td, *J* = 9.8, 4.5 Hz, 1H), 3.01 (m, 1H), 2.64 (dd, *J* = 15.0, 8.1 Hz, 1H), 2.53-2.41 (m, 2H), 2.37 (dd, *J* = 15.0, 4.8 Hz, 1H), 2.06 (m, 1H), 1.81-1.69 (m, 2H), 1.54 (brs, 1H), 1.47-1.24 (m, 9H), 1.03 (t, *J* = 7.3 Hz, 3H), 0.86 (t, *J* = 6.7 Hz, 3H); ^{13}C NMR (125 MHz, $CDCl_3$) δ (ppm): 210.2, 82.3, 74.2, 70.6, 48.5, 37.2, 33.1, 32.1, 31.9, 31.4, 25.1, 22.7, 14.2, 7.6; FT-IR (neat) ν_{max} = 3447, 2929, 2859, 1714, 1457, 1376, 1077 cm^{-1};

LRMS-ESI (+) *m/z* 243.1 $[M+H]^+$. HRMS-ESI (+) *m/z* calc'd for $C_{14}H_{27}O_3$ $[M+H]^+$: 243.1955, found 243.1958.

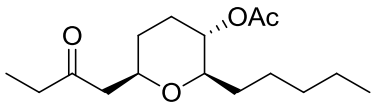

Decytospolide B (**1.8**):

Decytospolide A (**1.7**) (73 mg, 0.30 mmol) was dissolved in CH_2Cl_2 (3 mL) and cooled to 0 °C. Pyridine (73 μL, 0.9 mmol), acetic anhydride (85 μL, 0.9 mmol) and a few crystals of DMAP were added and the reaction was warmed to room temperature. After 90 minutes, the reaction was diluted with H_2O, extracted with CH_2Cl_2 (3X), washed with brine and dried over Na_2SO_4. It was purified by column chromatography using 10% to 20% EtOAc in Hexanes to give 77 mg (89% yield) of decytospolide B (**1.8**) as a clear oil $[\alpha]_D^{20}$ +28.1 (*c* 0.75, $CHCl_3$).

^{1}H NMR (500 MHz, $CDCl_3$) δ (ppm): 4.43 (td, *J* = 10.0, 4.6 Hz, 1H), 3.75 (m, 1H), 3.21 (td, *J* = 9.1, 2.4 Hz, 1H), 2.66 (dd, *J* = 15.2, 8.0 Hz, 1H), 2.52-2.40 (m, 2H), 2.36 (dd, *J* = 15.3, 4.9 Hz, 1H), 2.12 (m, 1H), 2.02 (s, 3H), 1.73 (m, 1H), 1.53-1.35 (m, 4H), 1.29-1.20 (m, 6H), 1.02 (t, *J* = 7.3 Hz, 3H), 0.85 (t, *J* = 6.9 Hz, 3H); ^{13}C NMR (125 MHz, $CDCl_3$) δ (ppm): 209.9, 170.4, 79.4, 74.3, 72.2, 48.3, 37.3, 32.0, 31.8, 30.9, 29.5, 24.9, 22.7, 21.3, 14.1, 7.6; FT-IR (neat) ν_{max} = 2933, 2859, 1739, 1714, 1457, 1373, 1235, 1080, 1042 cm^{-1}; LRMS-ESI (+) *m/z* 285.1 $[M+H]^+$. HRMS-ESI (+) *m/z* calc'd for $C_{16}H_{28}O_4Na$ $[M+Na]^+$: 307.1880, found 307.1884.

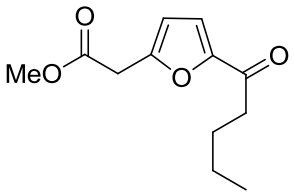

Methyl 2-(5-hexanoylfuran-2-yl)acetate (**1.47**):

Hexanoic acid (94 μL, 0.75 mmol) was dissolved in thionyl chloride (6 mL) and heated to reflux for 3 h. The excess thionyl chloride was removed by distillation under argon to give the resulting acid chloride as a dark yellow oil. It was then dissolved in CH_2Cl_2 (6 mL) and cooled to 0 °C. $SnCl_4$ (1.13 mL, 1 M in CH_2Cl_2, 1.13 mmol) was then added slowly dropwise and the reaction stirred at 0 °C for 45 min. Methyl ester **1.46** (105.3 mg, 0.75 mmol) was dissolved in CH_2Cl_2 (2 mL) before being added slowly to the reaction over the course of 10 minutes. The reaction was

then stirred at 0 °C for 45 min before being quenched with ice. The biphasic mixture was separated and the aqueous layer extracted with CH_2Cl_2 (3X). The combined organic layers were washed with brine, dried over Na_2SO_4 and concentrated under reduced pressure. The crude residue was purified by column chromatography using 10% to 20% EtOAc in hexanes as the eluent to give ketone **1.47** (102 mg, 57%) as a yellow oil.

^{1}H NMR (400 MHz, $CDCl_3$) δ: 7.12 (d, J = 3.5 Hz, 1H), 6.41 (d, J = 3.5 Hz, 1H), 3.77 (s, 2H), 3.74 (s, 3H), 2.84–2.66 (m, 2H), 1.70 (t, J = 7.4 Hz, 2H), 1.34 (h, J = 3.6 Hz, 4H), 0.90 (td, J = 7.1, 5.9, 3.4 Hz, 3H); ^{13}C NMR (100 MHz, $CDCl_3$) δ: 189.3, 168.7, 152.1, 129.0 118.1, 110.7, 77.2, 76.9, 76.6, 52.4, 38.2, 34.0, 31.4, 24.1, 22.3, 13.8; ESI-API MS: [M + H] = 239.1; HRMS-ESI (+) *m*/*z* calc'd for $C_{13}H_{10}O_4$ $[M + H]^+$: 239.1280, found 239.1282.

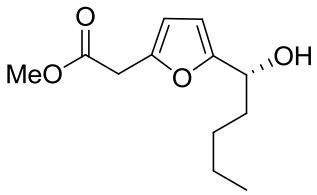

Methyl (R)-2-(5-(1-hydroxyhexyl)furan-2-yl)acetate (**1.44**):

Ketone **1.47** (60.5 mg, 0.25 mmol) was dissolved in CH_2Cl_2 (7 mL) and Et_3N (0.5 mL, 3.81 mmol) was added followed by formic acid (143 μL, 3.81 mmol). RuCl[(*R*,*R*)-TsDPEN](mesitylene) (3.9 mg, 0.006 mmol) was dissolved in a small amount of CH_2Cl_2 (0.5 mL) and then added to the reaction. The reaction was heated to 50 °C for 12 h before being quenched with H_2O. It was then extracted with CH_2Cl_2 (3X) and the combined organic layers washed with brine, dried over Na_2SO_4 and concentrated under reduced pressure. The crude residue was purified by column chromatography using 10% to 30% EtOAc in hexanes as the eluent to give optically active furfuryl alcohol **1.44** (50.3 mg, 83%) as a clear oil. $[\alpha]$ $^{23}_D$ +2.9 (*c* 2.4, $CHCl_3$), $[\alpha]$ $^{23}_D$ +7.9 (*c* 2.97, MeOH).

^{1}H-NMR (400 MHz, $CDCl_3$) δ 6.15 (d, J = 0.9 Hz, 2H), 4.62 (t, J = 6.8 Hz, 1H), 3.71 (s, 3H), 3.66 (s, 2H), 1.98 (s, 1H), 1.88–1.74 (m, 2H), 1.43 (tdd, J = 10.0, 8.1, 7.5, 4.1 Hz, 1H), 1.36–1.22 (m, 5H), 0.88 (q, J = 4.9, 4.1 Hz, 3H); ^{13}C NMR (100 MHz, $CDCl_3$) δ 169.8, 156.5, 146.8, 108.5, 106.6, 67.7, 52.2, 35.3, 33.8, 31.5, 25.1, 22.4, 13.9; ESI-API MS: [M + Na] = 263.1; HRMS-ESI (+) *m*/*z* calc'd for $C_{13}H_{20}O_4Na$ $[M + H]^+$: 263.1254, found 263.1256; 99% ee,

determined by HPLC using Chiralpak IA3 and gradient of 0–10% isopropanol/hexanes (t_{major} = 25.7 min, t_{minor} = 24.8 min).

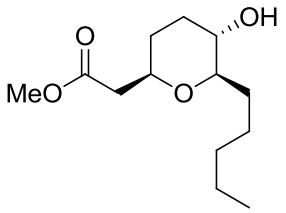

Methyl 2-((2R,5S,6R)-5-hydroxy-6-pentyltetrahydro-2H-pyran-2-yl)acetate (**1.43**):

Furanyl alcohol **1.44** (16.9 mg, 0.07 mmol) was dissolved in THF (2 mL) and H_2O (0.5 mL) and cooled to 0 °C. KBr (0.4 mg, 0.003 mmol), $NaHCO_3$ (2.9 mg, 0.03 mmol) and oxone (51.9 mg, 0.08 mmol) were then added and the reaction slowly warmed to room temperature. After 3 hours, the reaction was quenched with sat. $NaHCO_3$ and the aqueous layer extracted with EtOAc (3X). The combined organic layers were washed with brine, dried over Na_2SO_4 and concentrated under reduced pressure. The crude residue was used immediately for the next reaction without further purification.

The crude oil was dissolved in CH_2Cl_2 (3 mL) and Et_3SiH (112 μL, 0.7 mmol) was added. The reaction was then cooled to −40 °C and $BF_3{\cdot}OEt_2$ (52 μL, 0.42 mmol) was added slowly dropwise. The reaction was then stirred at −40 °C for 16 h before being warmed to 23 °C and stirred for an additional 1 h. It was then quenched with sat. NH_4Cl and the aqueous layer extracted with CH_2Cl_2 (3X). The combined organic layers were washed with brine, dried over Na_2SO_4 and concentrated *in vacuo*. The crude residue was purified by column chromatography using 20% to 30% EtOAc in hexanes as the eluent to give tetrahydropyran alcohol **1.43** (10.0 mg, 58%) as a clear oil. $[\alpha]^{23}_D$ +27.5 (*c* 2.57, $CHCl_3$).

^{1}H NMR (400 MHz, $CDCl_3$) δ: 3.80–3.69 (m, 1H), 3.67 (s, 3H), 3.27 (ddd, *J* = 10.4, 8.9, 4.6 Hz, 1H), 3.04 (td, *J* = 9.0, 2.4 Hz, 1H), 2.53 (dd, *J* = 14.9, 8.0 Hz, 1H), 2.40 (dd, *J* = 14.9, 5.4 Hz, 1H), 2.13–2.01 (m, 1H), 1.85–1.72 (m, 2H), 1.54–1.29 (m, 3H), 1.32–1.22 (m, 6H), 0.87 (t, *J* = 6.8 Hz, 3H); ^{13}C NMR (100 MHz, $CDCl_3$) δ 171.7, 82.1, 73.8, 70.4, 51.5, 40.8, 32.7, 31.7, 31.6, 30.8, 24.8, 22.6, 13.9; ESI-API MS: [M + H] = 245.1, [M + Na] = 267.1; HRMS-ESI (+) *m*/*z* calc'd for $C_{13}H_{25}O_4$ $[M + H]^+$: 245.1747, found 245.1750.

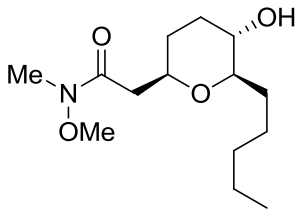

2-((2R,5S,6R)-5-Hydroxy-6-pentyltetrahydro-2H-pyran-2-yl)-N-methoxy-N-methylacetamide (**1.48**):

NH(OMe)Me·HCl (16.0 mg, 0.16 mmol) was dissolved in anhydrous THF (3 mL) and cooled to −30 °C. *i*-PrMgCl (450 μL, 0.45 mmol) was added slowly dropwise and the reaction stirred at −30 °C for 1 hour. Methyl ester **1.43** (10 mg, 0.04 mmol) was dissolved in anhydrous THF and then added slowly, dropwise to the reaction which was stirred at −30 °C for an additional 4 hours before being quenched with sat. NH_4Cl. The aqueous layer was extracted with EtOAc (3X) and the combined organic layers were washed with brine, dried over Na_2SO_4 and concentrated *in vacuo*. The crude residue was purified by column chromatography using 50% to 80% EtOAc in hexanes as the eluent to give Weinreb amide **1.48** (10.4 mg, 93%) as a clear oil. $[\alpha]^{23}_{D}$ +7.8 (*c* 1.33, $CHCl_3$).

^{1}H NMR (800 MHz, $CDCl_3$) δ 3.85–3.80 (m, 1H), 3.71 (d, J = 2.2 Hz, 3H), 3.32–3.27 (m, 1H), 3.20 (s, 3H), 3.09 (ddd, J = 8.9, 6.5, 2.5 Hz, 1H), 2.85 (d, J = 13.4 Hz, 1H), 2.43 (dd, J = 15.1, 6.3 Hz, 1H), 2.13–2.08 (m, 1H), 1.90–1.79 (m, 2H), 1.55–1.44 (m, 2H), 1.46–1.39 (m, 1H), 1.41–1.31 (m, 1H), 1.33–1.27 (m, 5H), 0.90 (td, J = 7.0, 2.3 Hz, 3H); ^{13}C NMR (100 MHz, $CDCl_3$) δ 172.0, 82.2, 74.1, 70.6, 61.3, 37.9, 33.0, 32.0, 31.9, 31.2, 29.7, 25.0, 22.6, 14.1; ESI-API MS: [M + H] = 274.0, [M + Na] = 296.1.

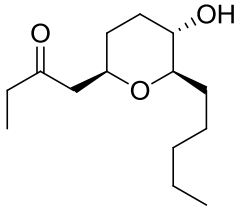

Decytospolide A (**1.7**) via Weinreb amide

Weinreb amide **1.48** (10.4 mg, 0.038 mmol) was dissolved in anhydrous THF (2 mL) and cooled to 0 °C. EtMgBr in a 1M THF solution (305 μL, 0.3 mmol) was added slowly dropwise and the reaction slowly warmed to room temperature. It was stirred for 5 hours, then quenched with sat. NH_4Cl and the aqueous layer extracted with EtOAc (3X). The combined organic layers were

then washed with brine, dried over Na_2SO_4 and concentrated *in vacuo*. The crude residue was purified by column chromatography using 20% to 50% EtOAc in hexanes as the eluent to give decytospolide A, **1.7** (8.9 mg, 97%), as a clear oil. $[\alpha]^{23}_D$ = +7.8 (*c* 1.33, $CHCl_3$).

^{1}H NMR (400 MHz, $CDCl_3$) δ 3.73 (dddd, *J* = 10.2, 8.0, 4.8, 2.0 Hz, 1H), 3.25 (ddd, *J* = 10.6, 9.0, 4.6 Hz, 1H), 3.02 (td, *J* = 8.9, 2.5 Hz, 1H), 2.65 (dd, *J* = 15.0, 8.1 Hz, 1H), 2.58–2.29 (m, 3H), 2.07 (ddd, *J* = 12.0, 5.5, 2.8 Hz, 1H), 1.85–1.70 (m, 2H), 1.53–1.41 (m, 1H), 1.46 (s, 2H), 1.44–1.33 (m, 1H), 1.37–1.24 (m, 5H), 1.03 (t, *J* = 7.3 Hz, 3H), 0.93–0.83 (m, 3H); ^{13}C NMR (100 MHz, $CDCl_3$) δ 209.9, 82.0, 74.0, 70.4, 48.2, 36.9, 32.8, 31.8, 31.7, 31.1, 24.9, 22.5, 13.9, 7.4; ESI-API MS: [M + H] = 243.1, [M + Na] = 265.1; HRMS-ESI (+) *m*/*z* calc'd for $C_{14}H_{27}O_3$ $[M + H]^+$: 243.1955, found 243.1958.

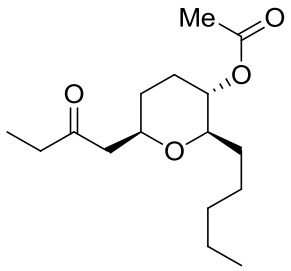

Decytospolide B (**1.8**) via Weinreb amide

Synthetic decytospolide A (9.7 mg, 0.04 mmol), from the Weinreb amide, was dissolved in CH_2Cl_2 (3 mL) and cooled to 0 °C. Pyridine (10 μL, 0.12 mmol), Ac_2O (4 μL, 0.04 mmol) and a few crystals of DMAP were added and the reaction warmed to room temperature. The reaction was stirred for 3 hours before being quenched with water. It was extracted with CH_2Cl_2 (3X) and the combined organic layers washed with brine, dried over Na_2SO_4 and concentrated under reduced pressure. The crude residue was purified by column chromatography using 10 to 30% EtOAc in hexanes as the eluent to give **1.8** (9.8 mg, 86%) as a clear oil. $[\alpha]^{20}_D$ = +22.8 in $CHCl_3$ (*c* 1.96).

^{1}H NMR (400 MHz, $CDCl_3$) δ 4.44 (td, *J* = 10.0, 4.7 Hz, 1H), 3.76 (ddd, *J* = 10.9, 7.8, 4.9 Hz, 1H), 3.22 (td, *J* = 9.0, 2.6 Hz, 1H), 2.67 (dd, *J* = 15.2, 8.0 Hz, 1H), 2.58–2.33 (m, 3H), 2.13 (ddd, *J* = 11.3, 5.6, 3.3 Hz, 1H), 2.03 (s, 3H), 1.79–1.70 (m, 1H), 1.58–1.36 (m, 3H), 1.40–1.17 (m, 7H), 1.03 (t, *J* = 7.3 Hz, 3H), 0.86 (t, *J* = 6.9 Hz, 3H); ^{13}C NMR (100 MHz, $CDCl_3$) δ 209.8, 170.2, 79.2, 74.1, 71.9, 48.1, 37.1, 31.8, 31.6, 30.7, 29.2, 24.7, 22.5, 21.1, 13.9, 7.4; ESI-API MS:

[M + H] = 285.1, [M + Na] = 307.2; HRMS-ESI (+) *m/z* calc'd for $C_{16}H_{28}O_4Na$ $[M + Na]^+$: 307.1880, found 307.1884.

CHAPTER 2. TOTAL SYNTHESIS OF CARAMBOLAFLAVONE A USING A LEWIS ACID PROMOTED DIASTEREOSELECTIVE C-GLYCOSYLATION

2.1 Introduction

Diabetes mellitus is common affliction resulting from the body's inability to regulate blood sugar and insulin, resulting in high blood glucose[52-54]. It is a very common condition, especially in the United States. According to the National Diabetes Statistics Report, 34.2 million people or 10.5% of the population in the United States have diabetes and about 88 million or 34.5% of the population are prediabetic[55]. These numbers have been increasing for the last several decades and diabetes has become one of the most common illnesses in the United States.

There are two types of diabetes. Type 1 diabetes is also referred to as juvenile diabetes and individuals affected by this disease are unable to produce insulin. Scientists believe that this is a result of genes and environmental factors[56,57]. In type 2 or adult-onset diabetes, the body does not make or use insulin well, resulting in high blood glucose. This condition is common in individuals who are overweight or inactive but, there are certain groups that are genetically predisposed[58-60]. Type 2 diabetes typically begins as insulin resistance, where the body requires larger concentrations of insulin to trigger cellular glucose absorption[61]. Type 2 diabetes is also the most common and accounts for the majority of diabetes patients[62].

Traditionally, the body regulates blood glucose through a feedback loop in which as excess of glucose in bloodstream triggers the production of insulin in the pancreas and promotes cellular absorption of glucose. Once inside the cell, glucose undergoes either glycolysis to convert it to energy (ATP) or glycogen synthesis, mostly in the liver, to store the excess glucose for future use. Conversely, low blood sugar prompts the release of glucagon from the pancreas, causing the body to synthesize glucose in the liver. This is done by either breaking down glycogen or gluconeogenesis, in which the body catabolizes amino acids and fatty acids to power glucose synthesis[63,64]. In diabetes, this loop in unbalanced as the body is unable to produce sufficient insulin to stimulate cellular glucose uptake and glycogen synthesis. However, the lack of insulin or response to insulin causes the body to believe that blood glucose is low and so glycogen will be broken down and the body will undergo gluconeogenesis. This results in an unstable hyperglycemic state that the body is unable to regulate on its own[63].

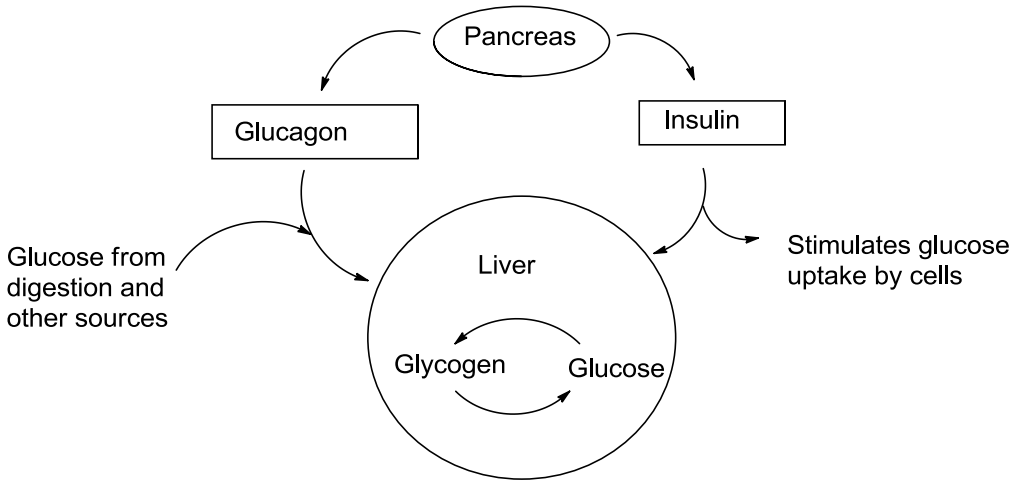

Figure 2.1: The Regulation of Blood Glucose Using Insulin and Glucagon

There are a variety of symptoms that characterize this disease. The most common ones include increased thirst and hunger, fatigue, blurred vision and the presence of ketones in urine. As the disease progresses patients have reported tingling in limbs and sores that do not heal. Severe complications include kidney damage, blindness and an increased risk of heart attack and stroke[65]. Adults with diabetes are also considered high risk when treating other conditions, such as COVID-19 caused by the novel coronavirus[66].

2.1.1 Treatment of Diabetes

Diabetes is traditionally treated by monitoring blood glucose and adjusting diet or making insulin injections as needed, particularly type 1. The patient monitors blood glucose using a glucometer. This device can either be attached to the patient or be external and is used to measure glucose levels in the blood throughout the day[67]. Low glucose is treated with a high sugar snack or drink and high blood glucose typically requires an insulin injection. There are several different types of insulin that are differentiated by onset time and duration. Patients with type 2 diabetes may also see benefits from adjusting diet and increasing levels of physical activity[68].

Other potential treatments seek to turn this from a chronic condition to one that can be managed without the need for constant monitoring. These include methods to increase insulin secretion, stimulate glucose disposal and cellular uptake, inhibiting glucose synthesis in the liver,

and slowing digestion to mediate the rate at which glucose enters the blood stream. Examples of these medications include metformin, which lowers liver glucose production and increases insulin sensitivity; meglintinides and sulfonylureas, which stimulate pancreatic insulin secretion; and thiazolidinediones, which increase insulin sensitivity. Many of these medications cause weight gain, low blood sugar and are linked to an increased risk of more serious conditions such as heart failure and anemia[69,70]. Consequently, research is underway to develop more medications that avoid these unfortunate side effects.

2.1.2 Use of Flavonoid Glycosides

Flavonoids are a large class of phenolic compounds, many of which have promising medicinal properties. They have been shown to scavenge radicals and chelate metals[71] and have the potential to protect the body against free radicals and oxidative compounds[72,73]. It has also been thought that the consumption of flavonoids or flavonoid rich foods can reduce the risk of diabetes[74,75]. These compounds and their derivatives have also been found to treat diabetic neurological retinal and cardiovascular complications[76].

Most notably, glycosylated flavones have been shown to have many benefits. Diosmin, a flavone glycoside from *Scrophularia nodosa* is a nontoxic drug that reduces hyperglycemia in diabetic rats[77]. Rutin, which is a glycosylated form of the glucose homeostatis regulating quercetin, has numerous antidiabetic effects[78]. These include reduction in absorption of glucose from the small intestine into the blood stream, increases in tissue glucose absorption, suppression of tissue gluconeogenesis and increase in insulin secretion[79,80]. Other flavones and flavonoid glycosides have strong antidiabetic properties[81]. Further research in the field is underway to fully explore the properties and activity of these molecules.

2.2 Isolation and Biological Activity of Carambolaflavone A

Carambolaflavone A is a flavonoid glycoside isolated from the leaves of *Averrhoa carambola*, a species of starfruit tree native to southeast Asia, by Araho and coworkers[82]. Carambolaflavone B was also isolated. Notably, these compounds were discovered to have anti-diabetic activity and successfully lower blood glucose in hyperglycemic mice.

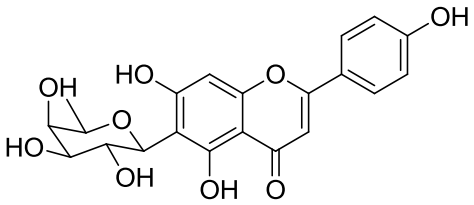

Carambolaflavone A, **2.1**

Figure 2.2: Carambolaflavone A

The crude extract from *A. carambola* is known to reduce levels of blood glucose[83]. A detailed study revealed that a key component of the extract that is responsible for this activity was the flavonoid glycosides, such as Carambolaflavone A.

The biological activity of Carambolaflavone A was further evaluated on its effects in hyperglycemic rats. It was found that the compound significantly lowered blood glucose, comparable to the effects of known anti-diabetic drug glipizide, and was capable of stimulating glucose-induced insulin secretion. Additionally, it increased glucose uptake in normal rat soleus muscle and promoted glycogen synthesis. The application of insulin signal transductor prior to treatment of the muscle nullifies any increases in glycogen synthesis indicating that e MAPK–PP1 and PI3K–GSK3 pathways are key to its glycogen synthesis activity[84,85]. Carambolaflavone A has great potential as an antidiabetic drug due to its ability to treat hyperglycemia as well as increase glycogen synthesis.

2.3 Previous Synthesis

Carambolaflavone A was previously synthesized by Wang and coworkers using a Suzuki C-glycosylation and Baker-Venkataraman rearrangement as the key steps[86]. During the course of this synthesis, they discovered that the stereocenters had been misassigned and the proposed structure was actually the enantiomer of Carambolaflavone A. As a result, both Carambolaflavone A and its enantiomer were synthesized.

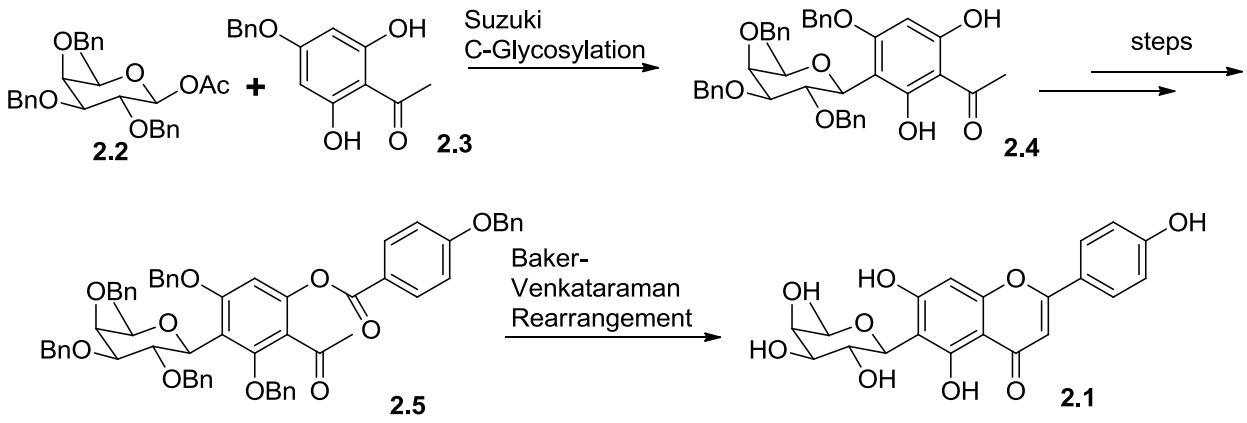

Scheme 2.1: Overview of Carambolaflavone Synthesis by Wang and co-workers

Their synthesis focused on the C-glycosylation of acetophenone derivative **2.3** with fucose derivative **2.2**. This was first attempted using traditional Suzuki glycosylation conditions (Table 2.1, entry 1)[87-90]. However, this resulted in a mixture that was equal portions O-glycoside **2.7** and C-glycosides **2.4** (β anomer) and **2.6** (α anomer). Running the reaction at room temperature in PhMe rather than DCM resulted in a decrease in the yield of the C-glycosides. Heating the reaction to 70 ^{o}C resulted in the desired C-glycoside as the major product in a diastereomeric ratio of 3:1. Most notably, removing the 4A molecular sieves gave the desired C-glycoside as the only product in excellent yield. It is hypothesized that this is due to the slightly basic nature interfering with the acidic conditions of the glycosylation.

Table 2.1: Wang and coworkers optimization of C-glycosylation of acetophenone **2.3**

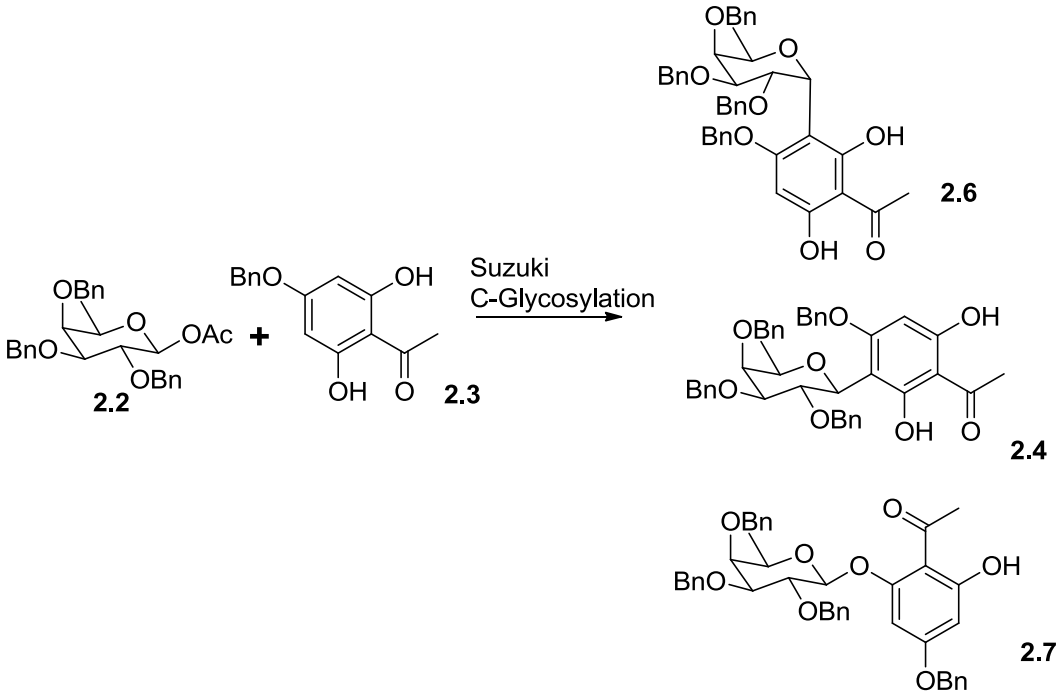

	Conditions	**Yield**
1	$Sc(OTf)_3$, 4A MS, DCM, -30 ^oC to RT	**2.6** (30%), **2.4** (25%), **2.7** (22%)
2	$Sc(OTf)_3$, 4A MS, PhMe	**2.6** (19%), **2.4** (8%), **2.7** (26%)
3	$Sc(OTf)_3$, 4A MS, PhMe, 70 ^oC	**2.6** (20%) **2.4** (64%) **2.7** (trace)
4	$Sc(OTf)_3$, PhMe, 70 ^oC	**2.4** (94%)

While they were able to accomplish the C-glycosylation in excellent yield, it required heating and long reaction times to achieve high diastereoselectivity. Additionally, the synthesis of both starting materials involved the use of multiple protecting groups, drastically increasing the atom economy of this synthesis. Disappointingly, the authors never report a C-glycosylation or C-glycosylation attempts on a flavone moiety, which would have dramatically simplified their synthesis.

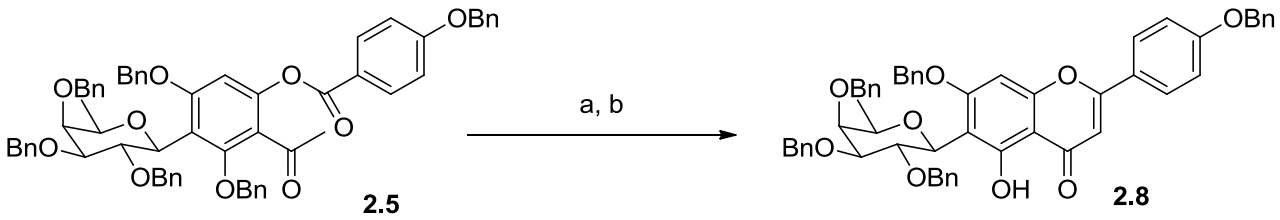

Scheme 2.2: Baker-Venkataraman rearrangement from synthesis by Wang and co-workers. Reagents and Conditions: (a) NaH, THF, reflux; (b) CSA, PhMe, 70 ºC (72% over 2 steps).

Following the successful glycosylation, a series of protection steps along with an acetylation set up the system for a Baker-Venkataraman rearrangement. This rearrangement successfully converted the acetophenone to the corresponding flavone **2.8** in good yield over 2 steps[91,92]. Removal of the benzyl groups then furnished Carambolaflavone A in 12 steps and 11% overall yield. Synthesis of the enantiomer proceeded in 12 steps and 16% overall yield.

2.4 C-Glycosylation of Phenol-based Substrates

In improving the synthesis of Carambolaflavone A, our main goal was to improve the diastereoselectivity of the C-glycosylation reaction. Wang and coworkers rely on the steric hindrance from the benzyl protecting groups to determine the stereochemistry[81]. While this is effective giving them the desired β-anomer, there is still a mixture of diastereomers and regioisomers at the anomeric center when the reaction is run at room temperature or lower. Our goal was to modify the substrates such that higher temperatures were not necessary to achieve high diastereoselectivity, but that the glycosylation could still be done using an electrophilic substitution of a phenol based substrate.

A literature investigation revealed that the conditions that typically give the highest diastereoselectivity at the anomeric center are those that rely upon neighboring group participation. In these instances, a functional group at the C2 position on the sugar acts to control the resulting stereochemistry at the anomeric center. The use of esters, picoyl ethers[93], aryl nitriles[94] and ethers[95] typically leads to the formation of the 1,2-*trans*-glycoside, while thioethers[96-101] and selenoethers[102] result in the 1,2-*cis*-glycoside. Additionally, additives can be used to control the anomeric stereochemistry independent of functionality at the C2 position.

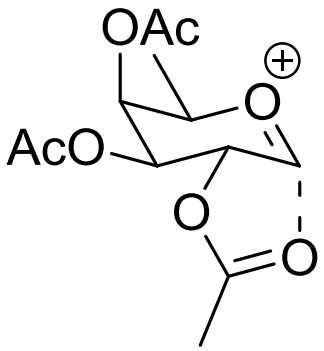

Figure 2.3: Role of C2 Functional Groups in Determining Trans Stereochemistry at the Anomeric Position

For the synthesis of *trans*-glycosides like the one in Carambolaflavone A, the C2 functional group stabilizes the oxocarbenium that forms under acidic conditions to form a dioxolenium or sulfonium ion[103]. This effectively blocks the addition of the nucleophile from one face on the molecule, leading to high diastereoselectivity without the need for a bulky protecting group, such as a benzyl group. The use of one of these functional groups would allow for control of the stereochemical outcome at the anomeric center.

For electrophilic substitution reactions, the most common groups at the C2 position are acetates, which can effectively control the stereochemistry at the anomeric position. Li and coworkers present a diastereoselective C-glycosylation of *para*-methoxyanisole using glycoside **2.9**. Using $SnCl_4$ and AgOTf in dichloromethane at room temperature for 4 to 6 hours, the reaction gives the desired trans-C-glycosides in 69 to 81% yield with no trace of the *cis*-glycoside[104]. In the synthesis of polycarcin V presented by Cai and coworkers, a diastereoselective C-glycosylation of **2.13** with glycoside **2.12** gives the desired trans-glycoside **2.14** in 70% yield and a diastereoselectivity of greater than 95:5. This is done using TMSOTf in dichloromethane at room temperature[105]. Both of these procedures provide the trans-glycoside in high diastereoselectivity using the C2 acetate group to control the stereochemical outcome.

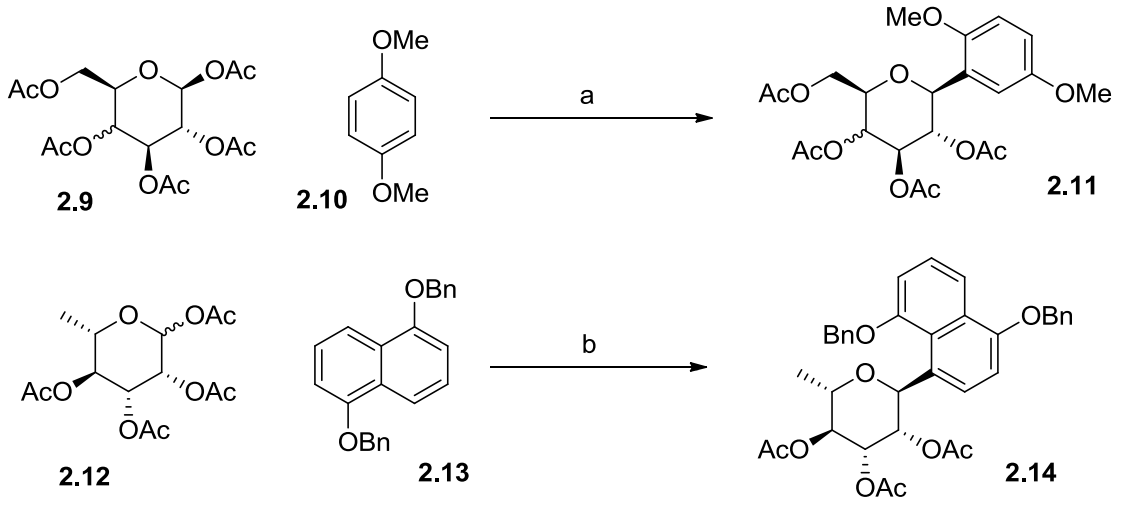

Scheme 2.3: C-glycosylations of Phenol Species using a C2 Acetate for Diastereoselectivity. Reagents and Conditions: (a) $SnCl_4$, AgOTf, DCM, 23 ºC (69-81%); (b) TMSOTf, DCM, 23 ºC (70%).

While the identity of the group at the C2 position is key to the stereochemical outcome of the reaction, the group at the anomeric position controls the overall reactivity of the glycoside. Common options include an acetate, trihaloimidates and halogens[106]. They can all function as leaving groups to form the necessary oxocarbenium under acidic conditions. Of the options, the trihaloimidates are considered the most reactive and are the most commonly used. However, any of these leaving groups are sufficient to form the oxocarbenium ion.

Wang and coworkers report their glycosylation on an acetophenone derivative, which is similar to a flavone in that it possesses a ketone moiety, creating an electron deficient aromatic ring. In this case, the free alcohol acts a directing group for the C-glycosylation. It is proposed that this is because the C-glycosylation proceeds through an O-glycosylate intermediate, explaining the presence of O-glycosylation product[81]. Kumazawa and coworkers report a C-glycosylation of acetophenone **2.15** using $BF_3{\cdot}OEt_2$ and 4A MS in DCM from -78 ºC to room temperature to give the desired C-glycoside **2.17** in 76% yield[107]. This condition uses the molecular sieves to remove any excess water from the reaction. In the original synthesis of Carambolaflavone A, Wang and coworkers use a modified version of Suzuki's $Sc(OTf)_3$ conditions to give glycoside **2.4** in 94% yield.

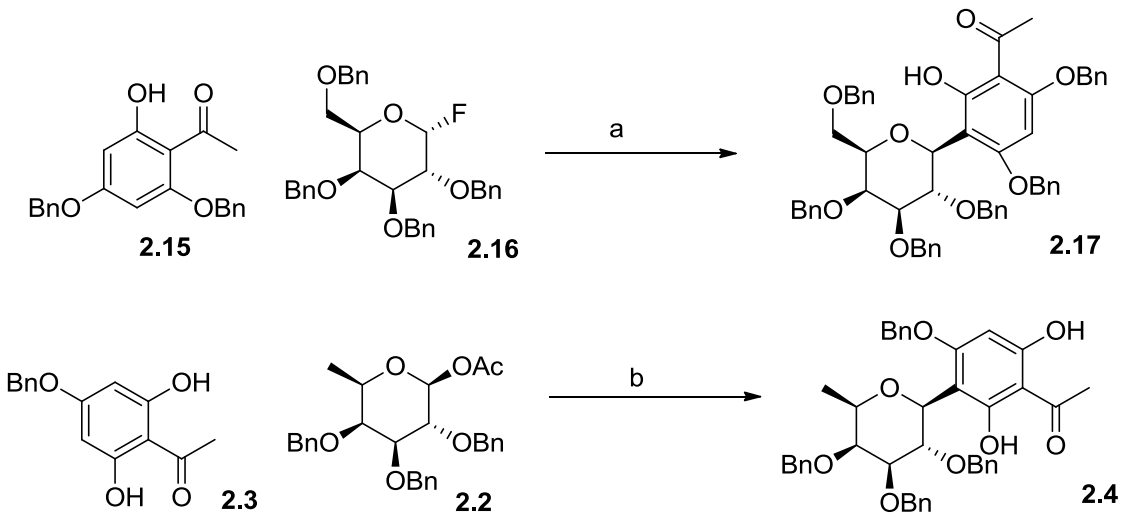

Scheme 2.4: C-glycosylations of Acetophenones. Reagents and Conditions: (a) $BF_3{\cdot}OEt_2$, 4A MS, DCM, -78 ºC to 23 ºC (76%); (b).

Another glycosylation substrate of note is the flavan. While they lack the electron-withdrawing nature of an acetophenone and as a result can be glycosylated under milder conditions, glycosylation of a species like this still provides insight into the C-glycosylation of phenol based species similar to the flavone in Carambolaflavone A.

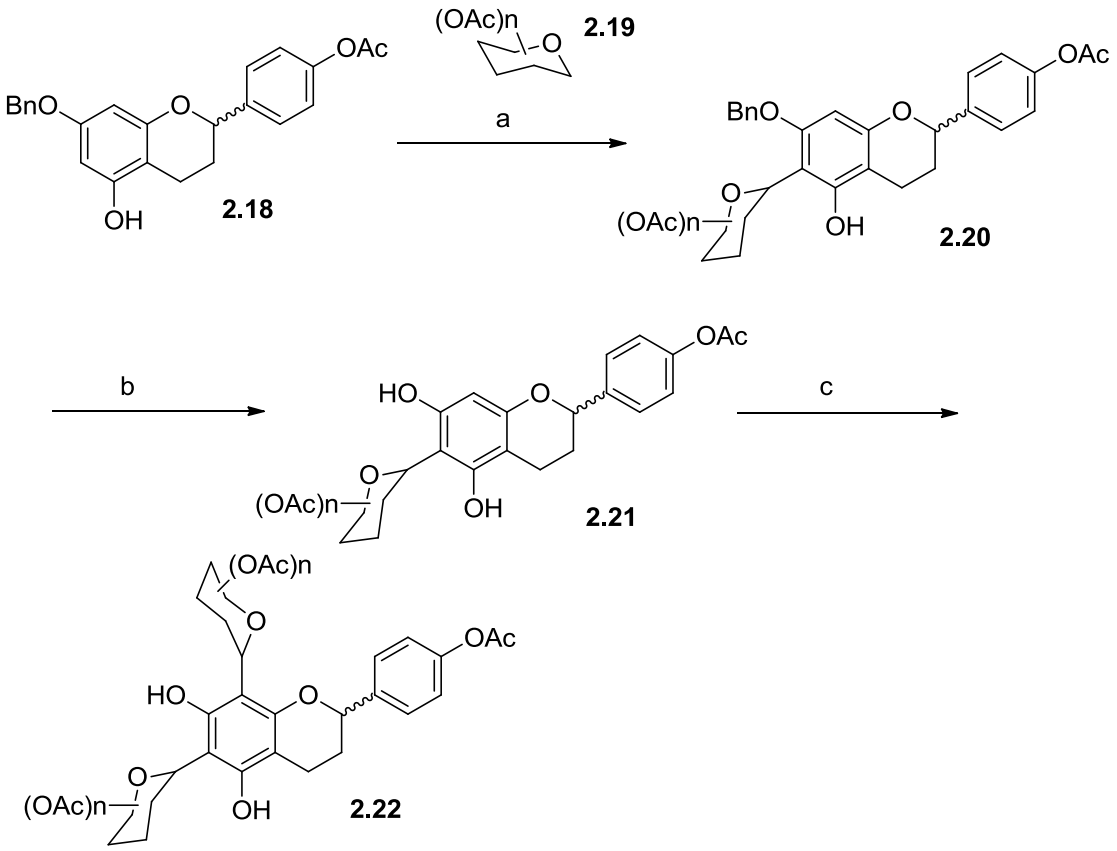

Scheme 2.5: C-Glycosylations of Flavan. Reagents and Conditions: (a) cat. TMSOTf, DCM, -15 ºC to 23 ºC (55-79%); (b) H2, Pd/C, MeOH, EtOAc (83-92%); (c) cat. TMSOTf, DCM, -15 ºC to 23 ºC (55-79%).

Shie and coworkers report a series of C-glycosylations on a flavan compound. This is done using a trichloroacetimidate as the leaving group for glycoside **2.19**. Additionally, the stereochemical outcome of the reaction is controlled using an acetate group at the C2 position. The first glycosylation occurs on monoprotected flavan **2.18** using catalytic TMSOTf in DCM at -15 ºC to room temperature to give C-glycoside **2.20**. Removal of the benzyl group using Pd/C under a hydrogen atmosphere gives flavan **2.21**. This is then subjected to identical glycosylation conditions to give diglycosylated flavan **2.22** in excellent yield[108].

Based on research of previous literature, it was concluded that increasing the natural diastereoselectivity of the reaction reported by Wang and coworkers could be easily accomplished by modifying the substitution at the C2 position of the glycoside. The reactivity of the glycoside can then be tuned by modifying the group at the anomeric position. Previous C-

glycosylations of phenols, acetophenones and flavans offer numerous Lewis acid based conditions for the transformation.

2.5 Initial Synthetic Attempts

Initially, the synthesis focused on improving the number of steps from Wang and coworkers, fewer than 12, and increasing the diastereoselectivity and regioselectivity of the glycosylation under milder conditions. This was to be done by modifying the glycoside to include an acetate at the C2 position and attempting the glycosylation later in the synthesis on a compound much closer in structure to the desired flavone moiety rather than the acetophenone using by Wang and coworkers. C-glycosylation of a flavone using an acetate based glycoside under acidic conditions has not been previously reported in the literature.

2.5.1 Retrosynthesis

It was initially believed that the total synthesis could be accomplished using the Lewis acid C-glycosylation of flavone **2.23** with glycoside **2.25**. This type of C-glycosylation has never been documented without the use of an enzymatic catalyst and would be a new modification on the Suzuki C-glycosylation. Based on review of the literature, the best Lewis acids are TMSOTf, $BF_3{\cdot}OEt_2$, $Sc(OTf)_3$, and the Lewis acid combinations of $HfCp_2Cl_2$ with $AgClO_4$ and $SnCl_4$ with a silver salt.

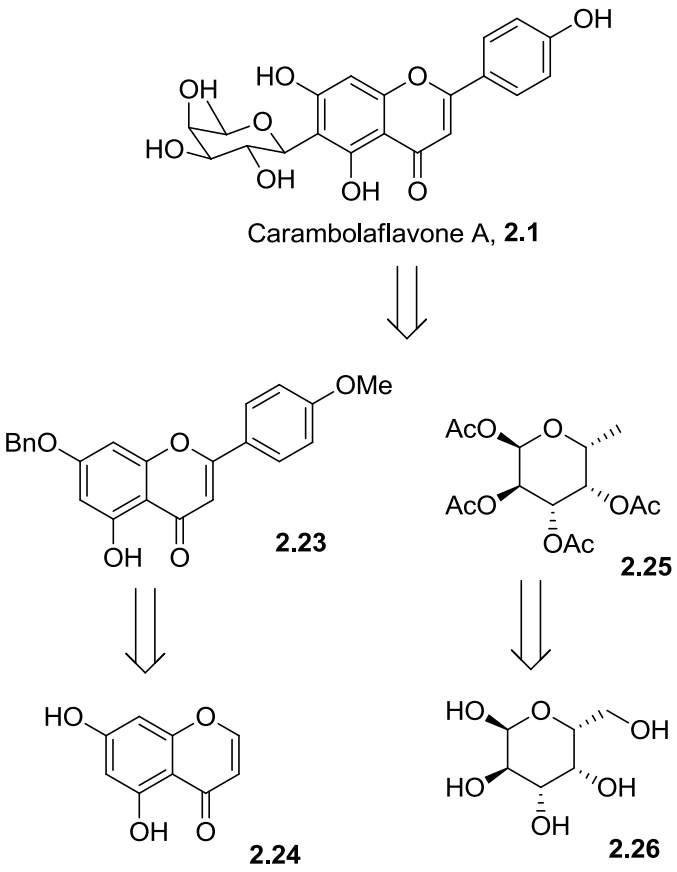

Scheme 2.6: Proposed Retrosynthesis of Carambolaflavone A

Fucose derivative **2.25** can be synthesized from galactose through a series of steps to remove the hydroxyl group at C6. The flavone **2.23** was proposed to come from the regioselective zincation of known chromone **2.24** as developed by Knochel and coworkers, followed by a Negishi coupling. This chromone is commericially available or can be synthesized from the much cheaper 2,4,6-trihydroxyacetophenone monohydrate using a known reaction.

2.5.2 Synthesis of Glycoside Moiety

Preparation of fucose derivative **2.25** is achieved from cheap, commercially available D-galactose using a series of reactions to install the acetate protecting groups and reduce the alcohol at C6 to the methyl group.

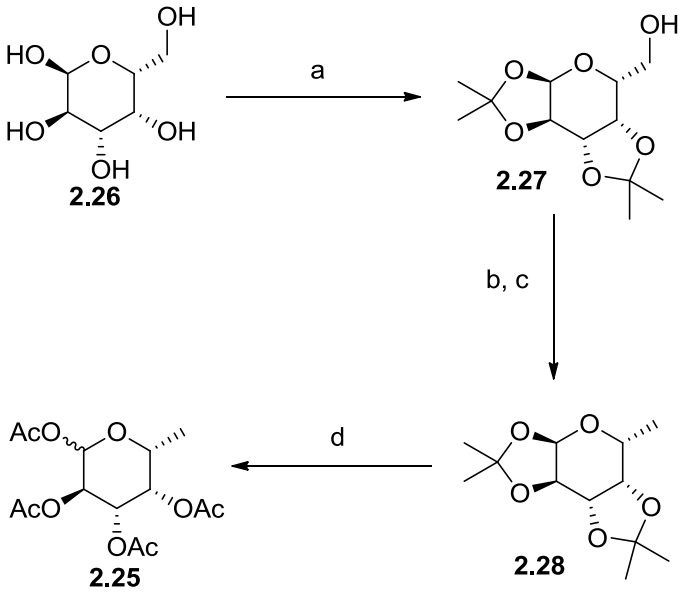

Scheme 2.7: Synthesis of fucose derivative **2.25**. Reagents and Conditions: (a) $ZnCl_2$, H_2SO_4, acetone, 16 h (97%); (b) *p*-TsCl, pyridine, 12 h; (c) $NaBH_4$, DMSO, 87 °C, 24 h (60% over 2-steps); (d) Ac_2O, H_2SO_4, AcOH, 40 °C, 26 h (51%).

Acetylated D-fucose **2.25** is readily prepared from D-galactose **2.26**, which was protected using $ZnCl_2$ and H_2SO_4 in acetone to give diacetonide **2.27**. Alcohol **2.27** was tosylated using p-TsCl in pyridine and subsequently reduced with $NaBH_4$ in DMSO at 87 ^oC to give fucose derivative **2.28** in moderate yield over two steps[109]. The diacetonide was then converted to desired fucose derivative **2.25** in moderate yield using H_2SO_4 and acetic anhydride in acetic acid[110]. This species was then ready to attempt the C-glycosylation.

2.5.3 Flavone Synthesis

To begin the synthesis of the flavone moiety, the first step was the synthesis of several protected chromones. Beginning with 2,4,6-trihydroxyacetophenone, chromone **2.24** was synthesized using a known procedure with BF_3•OEt_2 and MsCl in DMF at 90 ^oC[111]. This gave the chromone in good yield. Several protecting group strategies were then explored including mono and di-benzylation as well as the use of benzoate groups. These were accomplished using either BnBr or BzCl and K_2CO_3 in acetone. If protection of both alcohols was needed, the reaction needed to be heated to reflux regardless of what protecting group was utilized. This was likely due to the strong intramolecular hydrogen bonding interaction between the enone and the

nearest alcohol. These procedures gave three options for the protection of **2.24** to use moving forward: dibenzylchromone **2.16**, monobenzylchromone **2.17** and dibenzoylchromone **2.18**.

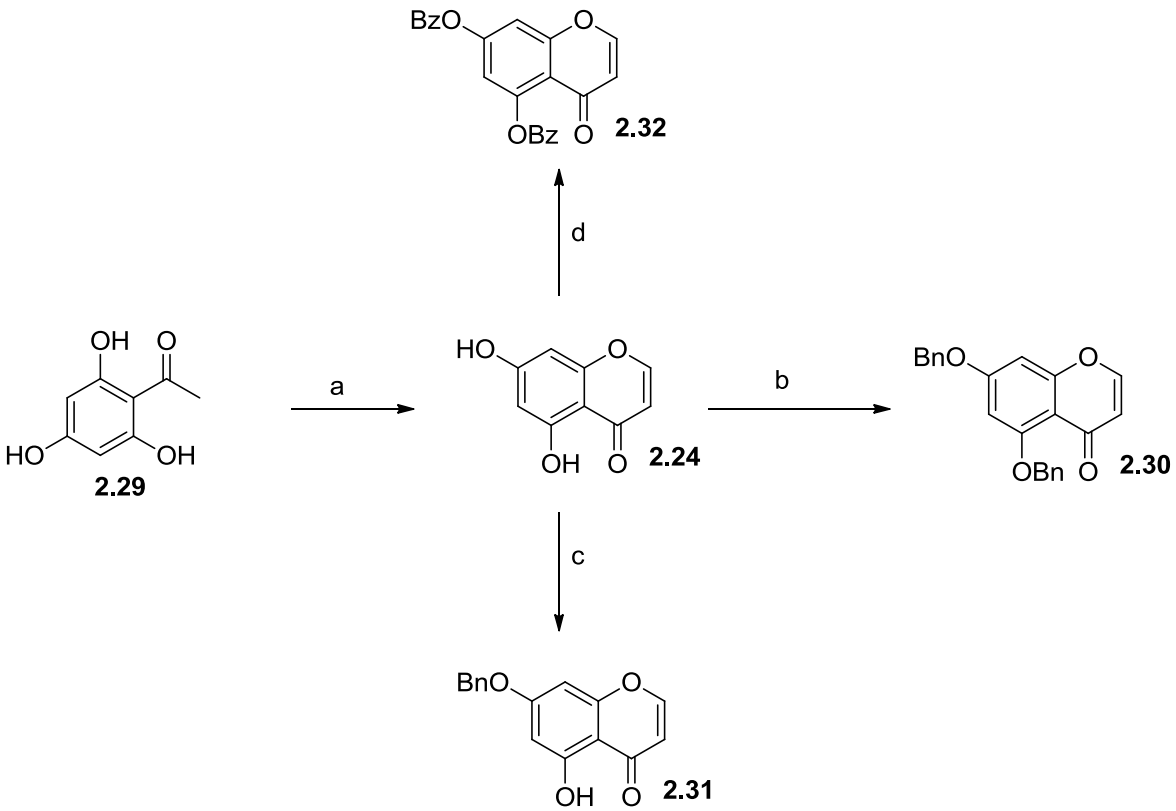

Scheme 2.8: Synthesis of Various Protected Chromones. Reagents and Conditions: (a) BF_3•OEt_2, MsCl, DMF, 90 ^oC (72%); (b) BnBr, K_2CO_3, acetone, 65 ^oC (87%); (c) BnBr, K_2CO_3, acetone (87%); (d) BzCl, K_2CO_3, acetone, 65 ^oC (67%).

Knochel and coworkers described a regioselective zincation followed by Negishi coupling of chromones using TMPZnCl.LiCl to give the flavone (in the presence of $MgCl_2$) or the isoflavone (in the absence of $MgCl_2$)[112,113]. This was applied to chromones **2.30**-**2.32**. Only the dibenzylated compound yielded the desired flavone **2.33** in 61% yield, the other chromones resulted in none of the desired product. In the case of chromone **2.31** this is likely due to the free alcohol disrupting the chelation of the $MgCl_2$ and TMPZn species with the oxygens in the chromone ring. For **2.32**, the TMPZn species is similar to LDA, which does not tolerate benzoate protecting groups; and most likely reacts with the benzoates rather than the chromone.

Table 2.2: Regioselective Zincation and Negishi Coupling

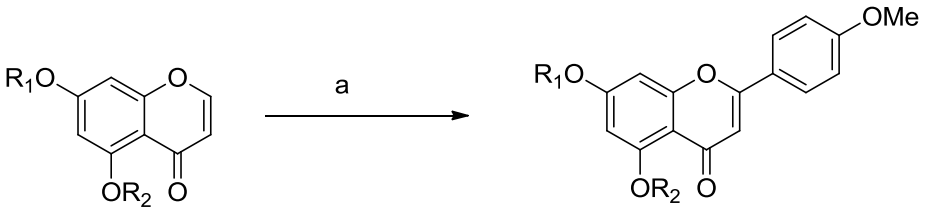

	R1	R2	Yield of 2.33
1	Bz	Bz	0%
2	Bn	Bn	61%
3	Bn	H	0%

Reagents and Conditions: (a) TMPZnCl.LiCl, $MgCl_2$, THF, -5 ^oC, 2 h, then p-iodoanisole, $Pd(dba)_2$, $P(2\text{-furyl})_3$, -5 ^oC, 12 h.

The regioselectivity can be explained by the coordination of the ZnTMP species and $MgCl_2$ to the chromone ring. In the presence of $MgCl_2$, which coordinates to the ketone oxygen attached to C4, the ZnTMP species coordinates to the oxygen at the 1 position. It then deprotonates the C2 position due to proximity. In the absence of $MgCl_2$, the ZnTMP species chelates to the ketone at C4 resulting in deportation at C3. Therefore, in the absence of $MgCl_2$, in the reaction the isoflavone is formed rather than the flavone. For this reason, the presence of extra oxygens in the molecule, particularly alcohols and carbonyls, results in a loss of yield or regioselectivity. This explains the results seen in Table 2.2.

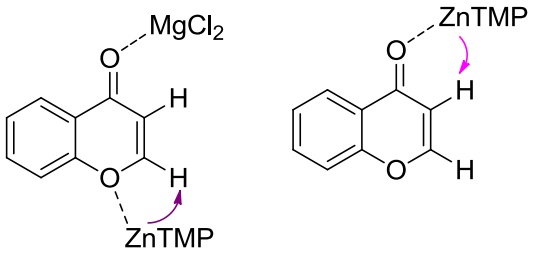

Figure 2.4: Explanation for Zincation Regioselectivity

Flavone **2.33** could be selectively deprotected using AcOH and water at 100 ^oC to give flavone **2.23** in quantitative yield. This selective deprotection is likely due to the compound favoring the strong hydrogen bonding interaction between the alcohol and the ketone. The free alcohol is needed for the C-glycosylation since most C-glycosylations are believed to proceed through an O-glycoside intermediate, allowing the free alcohol to act as a directing group.

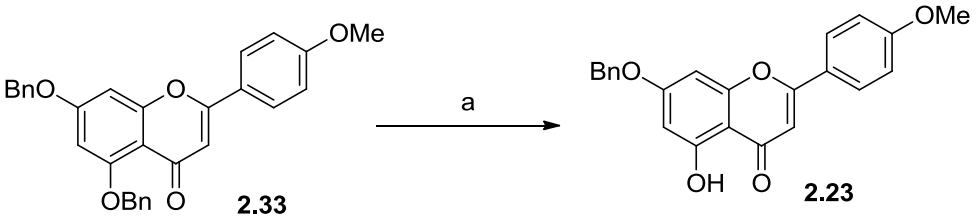

Scheme 2.9: Selective Benzyl Deprotection to Give Flavone **2.23.** Reagents and Conditions: (a) AcOH, H_2O, 100 ^oC (98%).

With **2.23** in hand, focus shifted towards developing a method for C-glycosylation of the flavone moiety using Lewis acids. The Lewis acid promoted C-glycosylation of flavones has not been previously reported in the literature.

2.5.4 Attempted Glycosylations

For the attempted C-glycosylation of flavone **2.23** using fucose derivative **2.25**, multiple Lewis acid based glycosylation conditions were attempted. These were all based on literature conditions for the glycosylation of acetophenone and phenol derivatives. C-glycosylation of flavones and chromones has not been well studied.

Table 2.3: Attempted C-glycosylation of **2.23** with **2.25**

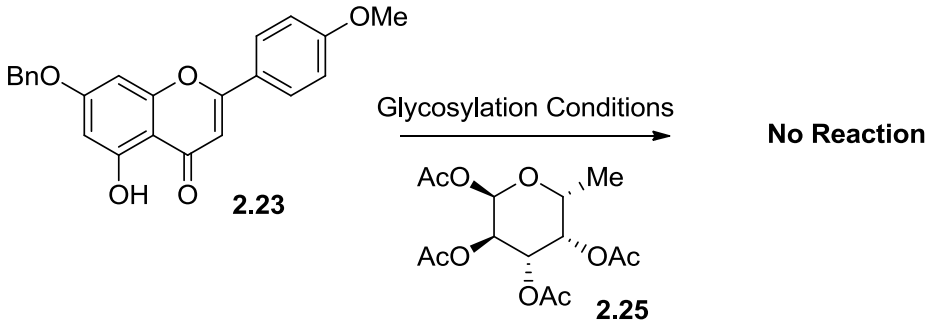

	Lewis Acid	**Solvent**	**Temperature**	**Time**
1	TMSOTf (2 Eq)	DCM	0°C to RT	12 h
2	AgOMs (1.1 Eq) $SnCl_4$ (2.2 Eq)	DCM	0°C to RT	6 h
3	$Sc(OTf)_3$ (2 Eq)	PhMe	70°C	12 h
4	BF_3•OEt_2 (3 Eq)	DCM	0°C to RT	12 h
5	$HfCp_2Cl_2$ (1.1 Eq) $AgClO_4$ (2.2 Eq)	DCM	0°C to RT	12 h

Initially, the glycosylation was attempted using the conditions optimized by Wang and coworkers in the initial synthesis[86]. However, $Sc(OTf)_3$ in PhMe at 70 °C did not lead to coupling of the two components, although glycoside **2.25** was converted into the anomeric hydroxyl glycoside **2.23**. This result was promising as it indicated the formation of an oxocarbenium ion in the reaction that was quenched by water upon workup. Based on this, Lewis acids were chosen with the belief that one of them would prompt the desired glycosylation reaction based on literature precedence[114-117]. However, none of them gave either the C-glycosylation or O-glycosylation product. As such, it was believed that further modification to the substrates was necessary since the aromatic ring of the flavone is electron poor and the electron withdrawing acetates on **2.25** make the glycoside electron deficient as well.

2.5.5 Modification of Glycosides

Based on the failure of the glycosylation attempts, it was hypothesized that the sugar was not reactive enough. Two approaches were envisioned to fix this problem. The first was to replace the anomeric acetate with a better leaving group and the second was to substitute some of the electron withdrawing acetate groups for electron donating benzyl groups to increase the reactivity of the glycoside with the electron poor flavone.

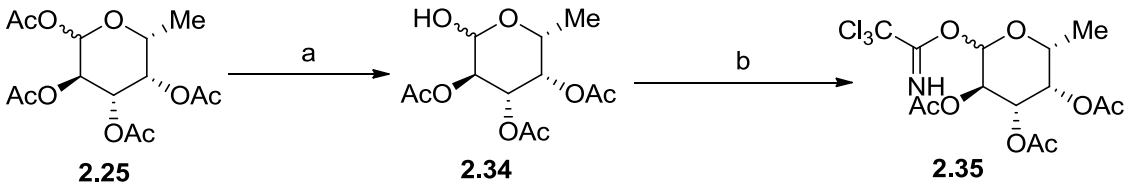

2.25 **2.34** **2.35**

Scheme 2.10: Synthesis of Trichloroacetimidate Glycoside **2.35.** Reagents and Conditions: (a) $BnNH_2$, THF (88%); (b) Cl_3CCN, DBU, DCM (99%).

Synthesis of the trichloroacetimidate glycoside began with previously synthesized fucose derivative **2.25**. The anomeric acetate was selectively removed with benzyl amine to give alcohol **2.34**, as an inseparable mixture of diastereomers at the anomeric center. This was then reacted with trichloroacetonitrle and DBU in DCM to give the desired trichloroimidate **2.35** in quantitative yield[108]. It should be noted that the trichloroacetimidate is such a good leaving group under acidic conditions that column chromatography on silica gel resulted in the recovery of glycoside **2.34** rather than **2.35**. Purification of **2.35** required the deactivation of silica using trace amounts of Et_3N in the eluent.

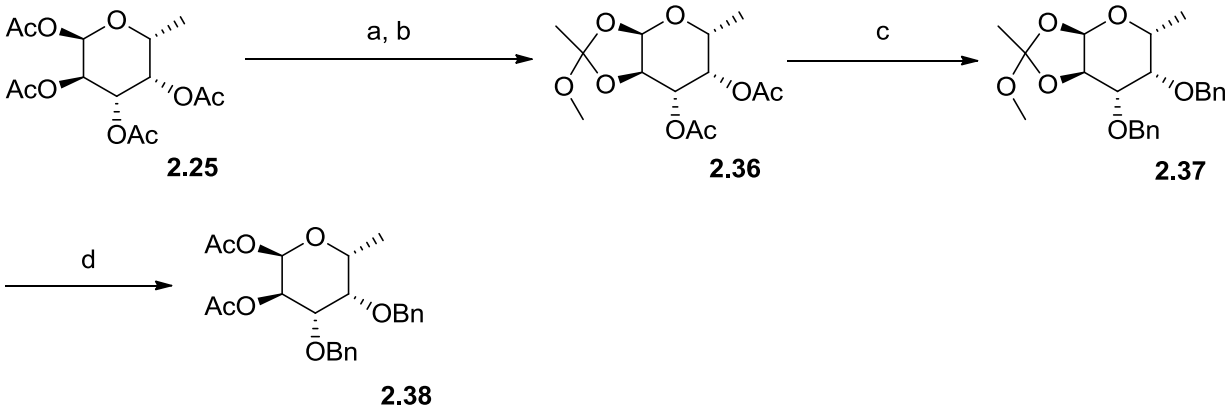

2.25 **2.36** **2.37** **2.38**

Scheme 2.11: Synthesis of dibenzylated glycoside **2.38.** Reagents and Conditions: (a) HBr (33% in AcOH, DCM; (b) 2,6-lutidine, TBAB, DCM, MeOH (24% over 2 steps); (c) KOH, BnBr, PhMe 110 ºC (71%); (d) AcOH (94%)

To make the dibenzylated glycoside **2.38**, previously synthesized glycoside **2.25** was reacted with HBr in AcOH and DCM to give the anomeric bromide and then reacted with 2,6-lutidine and TBAB in a mixture of MeOH and DCM to glycoside **2.36** in low yield[118]. The low yielding nature of this step is due to the formation of an anomeric methoxy glycoside rather than the desired acetal. Unfortunately, this issue could not be fixed with stoichiometric TBAB, no

change in yield, and running the reaction without TBAB resulted in the methoxy glycoside as the sole product. The remaining acetate groups were swapped for benzyl groups using BnBr and KOH in refluxing PhMe to give **2.37** in good yield. The acetal was then cleaved into the corresponding acetate groups to give desired glycoside **2.38** in excellent yield. These modified glycosides were then ready for further glycosylation attempts.

2.5.6 Modification of the Chromone and Flavone

In addition to modifying the glycoside moiety, it was believed that disrupting the conjugation of the flavone would increase its reactivity and increase the electron density in the aromatic ring. This was accomplished by reducing the enone to the ketone to reduce the conjugation and increase the similarity of this species to the acetophenone used by Wang and coworkers[86]. These reactions were carried out on chromone **2.24** with the understanding that they could be applied to the flavone should the glycosylation prove successful.

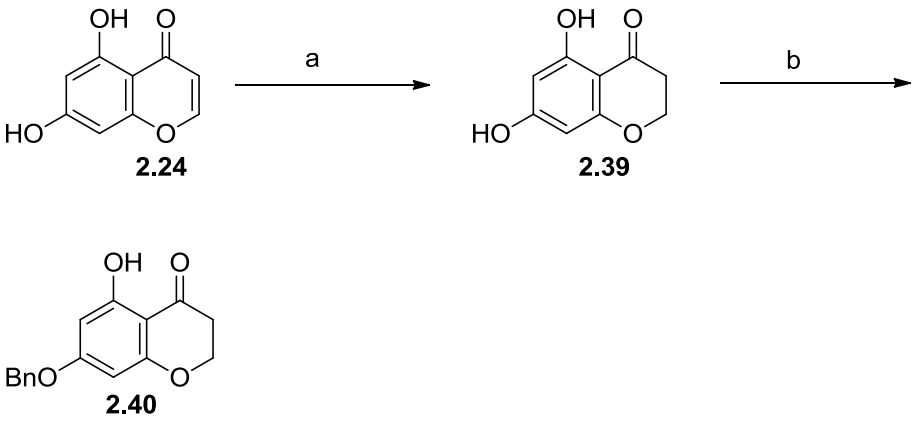

Scheme 2.12: Synthesis of Chromanone **2.40**. Reagents and Conditions: (a) $Pd(OH)_2/C$ (10 mol%), H_2, EtOAc, 23 °C, 18 h (68%); (b) BnBr, K_2CO_3, 23 °C, 12 h (88%).

Initial attempts to reduce the chromone using Pd/C proved unsuccessful, and literature indicated that reduction of this species would need to occur under increased pressure or temperature. In investigating other catalysts, it was discovered that $Pd(OH)_2/C$ had previously been used to reduce chromones in conditions close to room temperature and pressure. Using Pearlman's catalyst, the chromone was reduced to the corresponding chromanone **2.39** in good yield at room temperature and atmospheric pressure. The reaction did not go to completion, but

increasing the time for the reaction did not result in an increase in yield and the remaining chromone could be recovered. A mono-benzyl protection was then accomplished using BnBr and K_2CO_3 in acetone, as was previously used for the chromone, to give chromanone **2.40** in 78% yield. Once more, the monoprotection was accomplished, likely due to the intramolecular hydrogen bonding interaction in the molecule. This modified coupling partner was then used in further glycosylation attempts.

2.5.7 Glycosylation Attempts with Modified Coupling Partners

The modified glycosides marked an increasing in reactivity by either increasing the electron density of the ring or by using the labile trichloroacetimidate as a leaving group. By combining these with the more reactive chromone, we were hopeful that Lewis acid promoted glycosylation would more successful than with **2.23** and **2.25**.

Using the glycosides **2.38** and **2.35**, various Lewis acid glycosylation conditions were attempted. As was seen previously, no glycosylation product was observed. However, if the reaction was quenched with water, hydroxyl glycoside **2.34** was observed. This indicates that the desired oxocarbenium ion was being formed in situ, but was not reacting with the chromone. Based on this, it was hypothesized that the chromone needed to be modified to increase electron density in the aromatic ring.

Table 2.4: Attempted Glycosylations of chromone **2.31** with various glycosides **2.35** and **2.38**

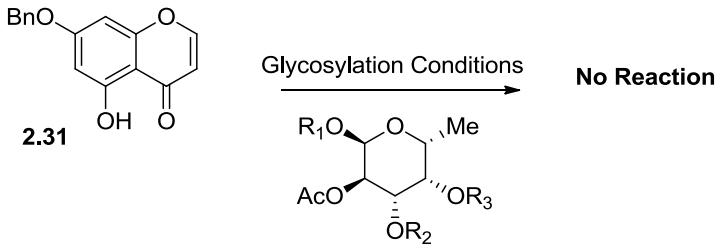

	Lewis Acid	Solvent	Temperature	Time
1	TMSOTf (2 Eq)	DCM	0°C to RT	12 h
2	AgOMs (1.1 Eq) $SnCl_4$ (2.2 Eq)	DCM	0°C to RT	6 h
3	$Sc(OTf)_3$ (2 Eq)	PhMe	70°C	12 h
4	BF_3•OEt_2 (3 Eq)	DCM	0°C to RT	12 h

The chromanone was subjected to the same glycosylation conditions as the chromone using glycosides **2.25**, **2.35** and **2.38**. Unfortunately, none of these gave any noticeable amounts of glycosylation product; most of them resulted in complete decomposition of the glycoside and chromone, especially if warmed to room temperature. The reaction with **2.25** in the presence of AgOMs and $SnCl_4$ gave a trace amount of the glycoside, detected by mass spectrometry. However, this result was not reproducible and was most likely due to a stray peak from a decomposition product, and so this reaction was not pursued further. Once more, if the reaction was quenched with water, hydroxyl glycoside **2.34** was observed using all of the glycosides synthesized. This indicates that the desired oxocarbenium ion was being formed *in situ*, but was not reacting with the chromanone. The prolonged existence of this oxocarbenium ion and interaction with solvent or the Lewis acid likely led to decomposition.

Table 2.5: Attempted Glycosylations of chromanone **2.40** with various glycosides

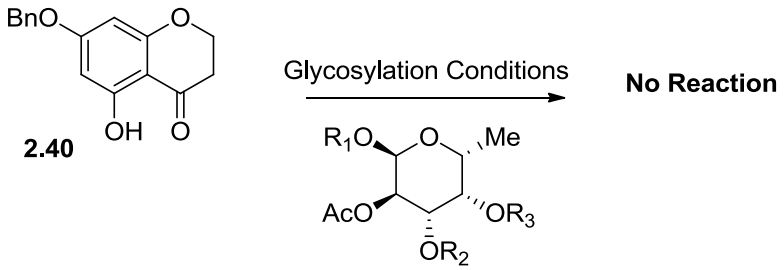

	Lewis Acid	**Solvent**	**Temperature**	**Time**
1	TMSOTf (2 Eq)	DCM	0^oC to RT	12 h
2	AgOMs (1.1 Eq) $SnCl_4$ (2.2 Eq)	DCM	0^oC to RT	6 h
3	$Sc(OTf)_3$ (2 Eq)	PhMe	70^oC	12 h
4	BF_3•OEt_2 (3 Eq)	DCM	0^oC to RT	12 h

Based on these results, more significant modification of the chromone is needed to achieve successful C-glycosylation since the glycosides used, particularly trichloroacetimidate **2.35**, are already extremely reactive. Since the chromanone is likely still too electron deficient, more modifications to increase electron density in the aromatic ring were needed.

2.6 Chroman based synthesis

Based on the failure to glycosylate the flavone/chromone moiety, even with the modified glycosides; it was determined that significant modification to the chromone would need to take place. Since reducing the chromone to the chromanone yielded the same results, it was determined that the problem was not the enone, but rather the presence of any carbonyl species in the ring. As such, further efforts focused on developing a chromone derivative for glycosylation that did not possess a ketone/enone, but could have these easily installed following glycosylation.

2.6.1 Revised Retrosynthesis

Upon revision, it was determined that Carambolaflavone A could come from the oxidation and subsequent coupling reaction of glycosylated chroman derivative **2.41**. This glycosylated moiety would come from the Lewis acid promoted C-glycosylation of chroman **2.42** with previously synthesized fucose derivative **2.25**. While there is no literature precedence for the C-glycosylation of chromans, previous C-glycosylations of flavans indicate that this species is sufficiently reactive for the desired Lewis acid promoted glycosylation reaction.

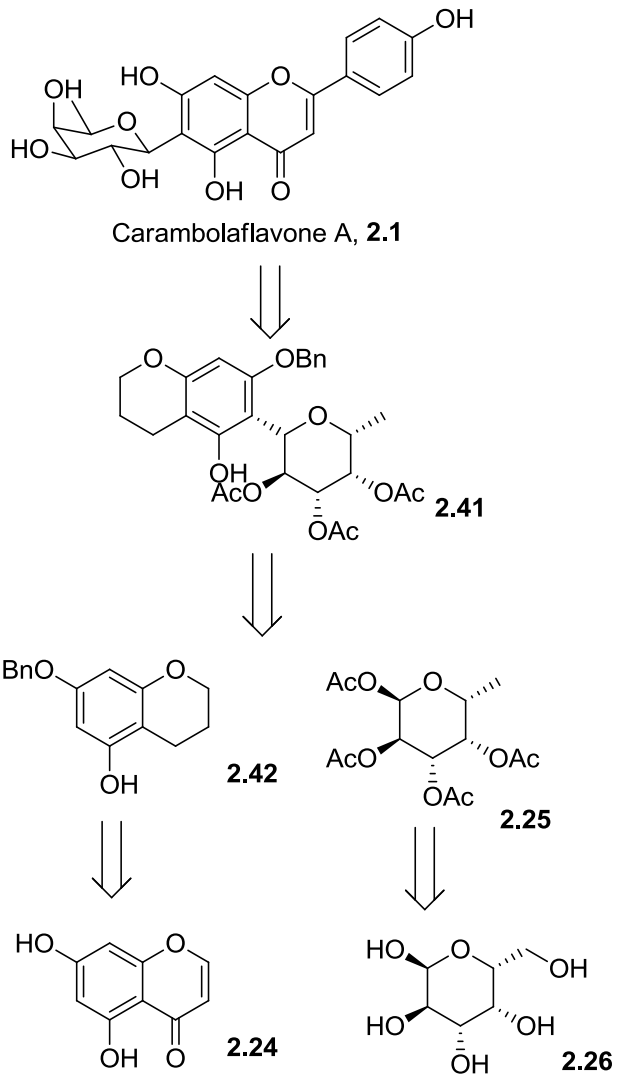

Scheme 2.13: Modified Retrosynthesis of Carambolaflavone A

Chroman **2.42** is proposed to come from the reduction of the enone in previously synthesized chromone **2.24** through a series of steps. This procedure has been previously used to synthesize flavans from the corresponding flavanone.

2.6.2 Synthesis of Chroman

In order to synthesize the needed chroman moiety **2.42**, a method used for the synthesis of a flavan from a flavanone was used[119]. The authors converted the monobenzylated flavanone to the flavan in two steps and it was hypothesized that the same could be done with a chromanone to the chroman.

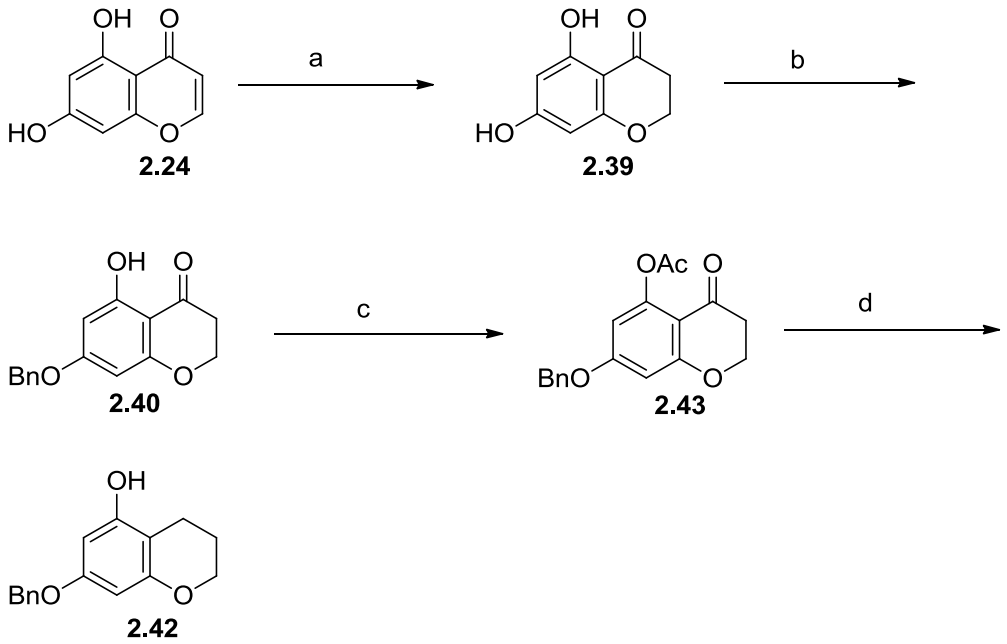

Scheme 2.14: Synthesis of Chroman **2.42**. Reagents and Conditions: (a) $Pd(OH)_2/C$ (10 mol%), H_2, EtOAc, 23 °C, 18 h (68%); (b) BnBr, K_2CO_3, 23 °C, 12 h (88%); (c) Ac_2O, pyridine, DMAP, CH_2Cl_2, 0 °C to 23 °C, 3 h (83%); (d) $NaBH_4$, THF/H_2O (2:1), 0 °C, 1 h (87%).

Starting with known chromone **2.24**, the enone is reduced to a ketone using Pearlman's catalyst to give chromanone **2.39** in good yield. This undergoes selective monobenzylation to give **2.40** in excellent yield. The protection is selective due to the hydrogen bonding interaction between the unreactive alcohol and the enone, requiring higher temperatures to protect that alcohol. Protection of the remaining alcohol as an acetate using Ac_2O, pyridine and DMAP gives **2.43** in excellent yield. Extremely concentrated conditions are required for this reaction, using just enough DCM to dissolve the chromanone. The chromanone is then reduced to chroman **2.42** in excellent yield using $NaBH_4$ in THF/H_2O as described by Arai and coworkers[119]. Following this, the chroman was used for C-glycosylation with the acetate glycoside **2.25** as a coupling partner.

2.6.3 C-Glycosylation of Chroman

With the chroman in hand, glycosylation was attempted using the orginal tetraacetate fucose derivative **2.25** under Lewis acidic conditions. Had these conditions proven unsuccessful,

C-glycosylation would have been attempted using glycosides **2.35** and **2.38** to increase the reactivity of the system.

Table 2.6: Glycosylation of Chroman

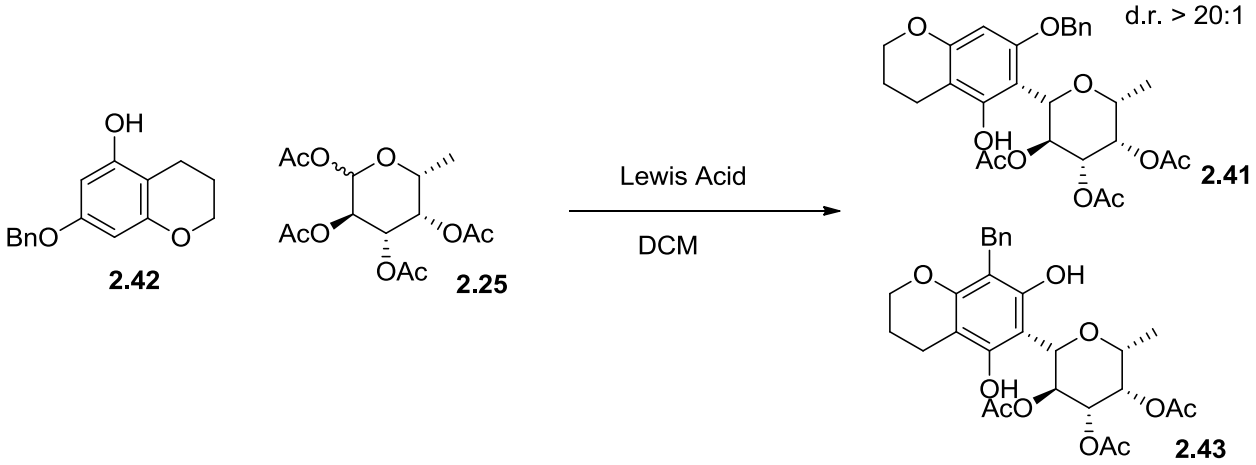

	Lewis Acid	**Temperature**	**Time**	**Yield of 2.41**	**Other products**
1	TMSOTf (2 eq)	0°C to RT	12h	0%	Recover chroman, decomposition of glycoside
2	AgOMs (1.1 eq) $SnCl_4$ (2.2 eq)	0°C to RT	6h	25%	Recover both starting materials
3	AgOTf (1.1 eq) $SnCl_4$ (2.2 eq)	0°C to RT	4h	23%	Recover both starting materials
3	AgOMs (3.5 eq) $SnCl_4$ (7 eq)	0°C to RT	3h	39% (mixture of product and hydroxy glycoside **2.34**)	Recover some chroman and byproduct **2.44** (17%)
4	AgOMs (2.5 eq) $SnCl_4$ (5 eq)	0°C to RT	6h	21% (mixture of product and hydroxy glycoside **2.34**)	Recover some chroman and byproduct **2.44** (17%)
5	AgOMs (1.5 eq) $SnCl_4$ (3 eq)	0°C	2h	28%	Recover some chroman
6	AgOMs (1.1 eq) $SnCl_4$ (2.2 eq) 1.5 eq of **2.25**	0°C	2h	50%	Recover some chroman and glycoside

The use of traditional C-glycosylation conditions with TMSOTf (entry 1) did not yield any product. Changing to the harsher combination of $SnCl_4$ and AgOMs gave the desired C-glycoside in 25% yield as a mixture of rotamers. This is likely due to the rotation around the C-

glycoside linkage being constrained by the rigid nature of the chroman species. The use of AgOTf rather than AgOMs gave the product in 23% yield, so it was concluded that changing the silver salt did not affect reaction yield. It was initially hypothesized that the yield could be increased by increasing the equivalents of Lewis acid since unreacted **2.42** and **2.41**, caused by Lewis acid promoted migration of the benzyl protecting group. To avoid the formation of byproduct, the equivalents were kept at 1.1 equivalents of AgOMs and 2.2 equivalents of $SnCl_4$. Increasing the equivalents of **2.25** from 1 to 1.5 resulted in an increase in yield to 50%, indicating that a higher concentration of **2.25** in the system was beneficial. Excess **2.25** was still able to be recovered following this reaction. These conditions were used moving forward.

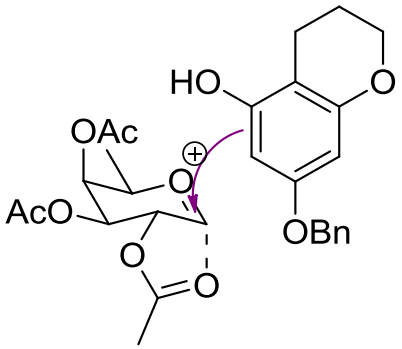

Figure 2.5: Explanation of C-Glycosylation Stereochemistry

The stereochemistry of this reaction was determined by ^{1}H NMR coupling constants. The peak at 5.02 for **2.41** corresponds to the anomeric proton of the glycoside. This doublet has a coupling value of J = 9.9 Hz. In a glycoside ring, a coupling constant that large indicates a *trans* relationship between the protons. Since the configuration of the proton at C2 is determined by the structure of D-galactose, the absolute configuration at the anomeric center can be determined based on this *trans* relationship. As such, it has been determined that the **2.41** is the desired β-anomer. There is no trace of the O-glycoside or α-anomer by ^{1}H NMR, indicating a diastereoselectivity ratio of greater than 20:1.

As was expected based on extensive literature research, the *trans*-C-glycoside was the exclusive product of these glycosylation reactions. This is due to the formation of the oxocarbenium ion being stabilized by the acetate group at the C2 position. This acetate group blocks the addition of the chroman to the top of the glycoside ring. This gives the β-anomer as

the exclusive C-glycoside product with no further reaction optimization necessary to increase diastereoselectivity, unlike in the initial synthesis.

2.6.4 Completion of Synthesis

With the glycosylated chroman in hand, focus shifted to the completion of the synthesis by oxidation to the chromone and a coupling reaction to generate the flavone moiety.

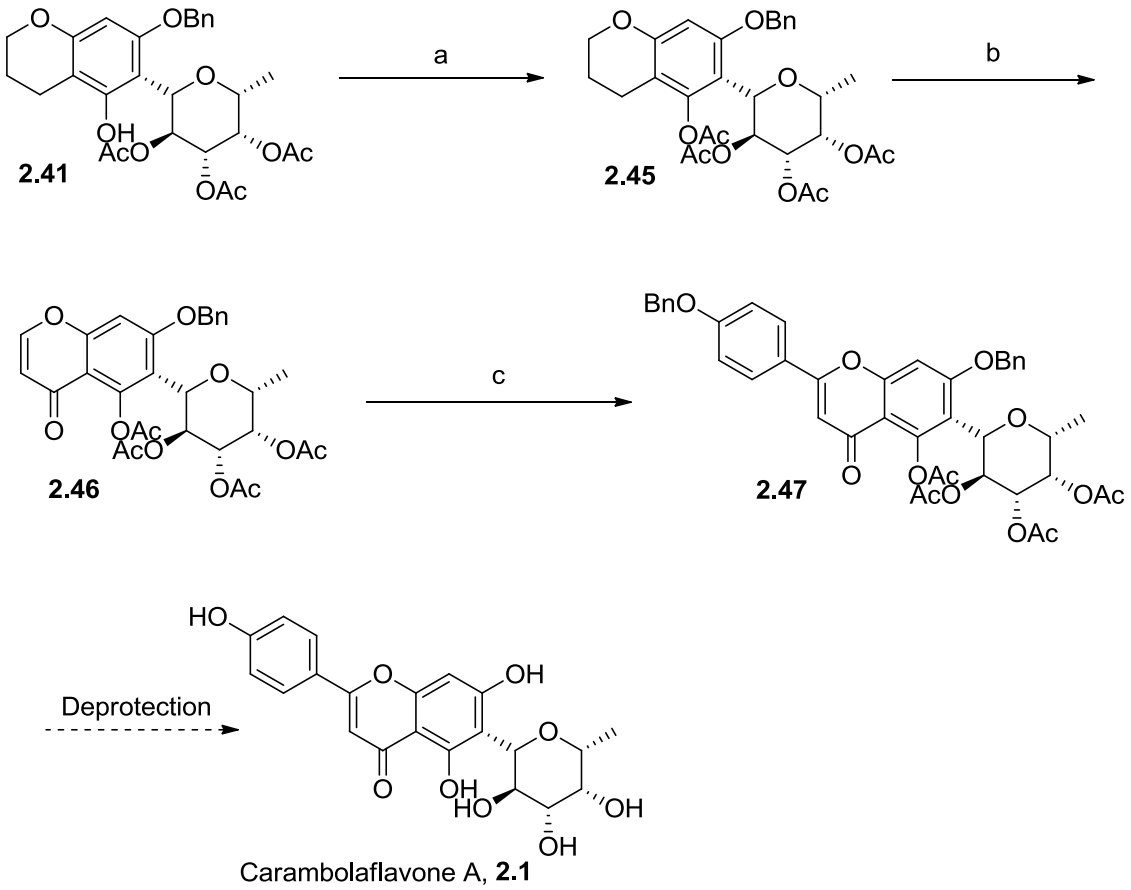

Scheme 2.15: Progess Towards Completing the Synthesis of Carambolaflavone A. Reagents and Conditions: (a) Ac_2O, pyridine, DMAP, CH_2Cl_2, 23 ºC (85%); (b) DDQ, PhMe/H_2O (100:1), 110 ºC (63%); (c) 4-(benzyloxy)phenylboronic acid, $Fe(OTf)_3$, DDQ, KNO_2, $Pd(OAc)_2$, PivOH, 60 ^oC (31%).

Starting with glycoside **2.41**, the free alcohol was acetylated using Ac_2O, pyridine and DMAP in DCM to give **2.45** in excellent yield, although it was still a mixture of rotamers. This was done to prevent the accidental oxidation of the phenol to the corresponding quinone

derivative. The protection also verified the presence of a C-glycoside rather than an O-glycoside, which would not have been acetylated. Oxidation to the chromone was accomplished in one-pot using DDQ in a 100:1 mixture of PhMe and water. This gave the desired chromone **2.46** in good yield as a mixture of rotamers. Remarkably, the benzyl group was not oxidized to a benzoate during this transformation as we had originally hypothesized. This could be due to the glycoside moiety blocking access to this group, making the chroman the more reactive functionality. The flavone moiety was installed using an oxidative addition of 4-(benzyloxy)phenylboronic acid using $Fe(OTf)_3$, DDQ, KNO_2 and $Pd(OAc)_2$ in pivalic acid at 60 ^oC[120]. This gave the flavone **2.47** in 31% yield, with recovery of excess **2.41**. The addition of the boronic acid to the chromone is accomplished using $Fe(OTf)_3$ and $Pd(OAc)_2$ to give the flavanone. This reaction uses the oxygen in air as terminal oxidant for the KNO_2 and DDQ oxidation of the flavanone to the flavone. Further work is underway to optimize this addition and complete the synthesis of Carambolaflavone A by removing the acetate and benzyl protecting groups.

2.7 Conclusion

An enantioselective synthesis of the antidiabetic natural product Carambolaflavone A using a Lewis acid promoted C-glycosylation and oxidative addition of a boronic acid as the key steps. This improves upon the synthesis developed by Wang and coworkers (12 steps longest linear sequence) and allows for more modifications. While initial attempts to glycosylate a flavone, chromone or chromanone using Lewis acid conditions were unsuccessful even those using more reactive glycosides featuring a trichloroacetimidate or benzyl protecting groups. The glycosylation of a chroman proceeded smoothly, and in high diastereoselectivity and moderate yield. The high diastereoselectivity of this process is attributed to the acetate group at the C2 position of the glycoside blocking access to one face of the molecule. Oxidation of the glycosylated product and oxidative addition of a boronic acid to the chromone moiety yielded protected Carambolaflavone A. The synthesis was accomplished in 10 steps (longest linear sequence) and provided many opportunities for the synthesis of derivatives, namely by modifying the glycoside moiety used in glycosylation and changing the boronic acid used for oxidative addition.

2.8 Experimental Section

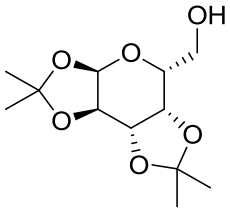

((3aR,5R,5aS,8aS,8bR)-2,2,7,7-tetramethyltetrahydro-3aH-bis([1,3]dioxolo)[4,5-b:4',5'-d]pyran-5-yl)methanol (**2.27**):

To a solution of $ZnCl_2$ (1.21 g, 8,88 mmol) in acetone (12.3 mL) was added concentrated H_2SO_4 dropwise until the solution changed from cloudy white to clear. Then, D-Galactose (1.00g, 5.55 mmol) was added and the reaction stirred for 16 hours before being quenched with sat. $NaHCO_3$. The reaction was filtered through a celite plug and concentrated. The residue was extracted with Et_2O (3X) and the combined organic layers dried over Na_2SO_4. The crude residue was purified by column chromatography using 25-50% EtOAc in hexanes to give **2.27** (1.3948 g, 97%) as a yellow syrup.

^{1}H NMR (400 MHz, Chloroform-*d*) δ 5.57 (d, *J* = 5.0 Hz, 1H), 4.61 (dd, *J* = 7.9, 2.4 Hz, 1H), 4.33 (dd, *J* = 5.0, 2.4 Hz, 1H), 4.27 (dd, *J* = 7.9, 1.5 Hz, 1H), 3.90 – 3.82 (m, 2H), 3.78 – 3.71 (m, 1H), 1.46 (s, 3H), 1.33 (s, 6H). ^{13}C NMR (100 MHz, Chloroform-*d*) δ 109.37, 108.56, 96.19, 71.53, 70.66, 70.47, 67.93, 62.29, 25.93, 25.83, 24.83, 24.19.

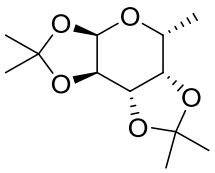

(3aR,5R,5aS,8aS,8bR)-2,2,5,7,7-pentamethyltetrahydro-3aH-bis([1,3]dioxolo)[4,5-b:4',5'-d]pyran (**2.28**):

2.27 (1.3948 g, 5.36 mmol) was dissolved in pyridine (15.3 mL) and *p*-TsCl (1.12 g, 5.89 mmol) was added. The reaction was stirred for 12 hours. It was then concentrated and redissolved in EtOAc before being washed with 1N HCl and sat. $NaHCO_3$. The organic layers were dried over Na_2SO_4 and concentrated in vacuo. The crude was used for the next step.

Crude tosylate was dissolved in DMSO (14.1 mL) and $NaBH_4$ (811 mg, 21.44 mmol) was added. The reaction was heated to 87 ºC and stirred for 24 hours. It was then cooled to 0 ºC and added

slowly to a stirred solution of 1% AcOH in water at 0 ºC. The solution was stirred for 30 minutes and then $CHCl_3$ was added and it stirred for an additional 15 minutes. The layers were separated and the aqueous extracted with $CHCl_3$ (4X). The combined organic layers were washed with water (2X), dried over Na_2SO_4 and concentrated in vacuo. The crude residue was purified by column chromatography using 10-20% EtOAc in hexanes to give **2.28** (0.785 g, 60%) as a clear syrup.

^{1}H NMR (400 MHz, Chloroform-*d*) δ 5.52 (d, *J* = 5.1 Hz, 1H), 4.59 (dd, *J* = 7.9, 2.3 Hz, 1H), 4.29 (dd, *J* = 5.1, 2.3 Hz, 1H), 4.08 (dd, *J* = 7.9, 1.9 Hz, 1H), 3.91 (dd, *J* = 6.5, 2.0 Hz, 1H), 1.58 – 1.52 (m, 2H), 1.49 – 1.42 (m, 3H), 1.38 – 1.30 (m, 6H), 1.25 (d, *J* = 6.6 Hz, 3H). ^{13}C NMR (100 MHz, Chloroform-*d*) δ 108.84, 96.45, 73.43, 70.84, 70.24, 63.37, 25.93, 24.81, 24.32, 15.83.

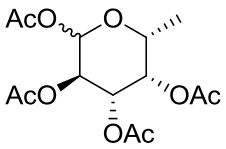

(3R,4S,5S,6R)-6-methyltetrahydro-2H-pyran-2,3,4,5-tetrayl tetraacetate (**2.25**):

2.28 (257.6 mg, 1.05 mmol) was dissolved in AcOH (4.2 mL) and cooled to 0 ºC. In a separate roundbottom flask, Ac_2O (991 µL, 0.0105 mmol) and H_2SO_4 (560 µL, 0.0105 mmol) were mixed and added slowly, dropwise to the glycoside solution. The reaction was warmed to room temperature and then heated at 40 ºC for 26 hours. It was then poured over ice, extracted with EtOAc (3X), washed with sat. $NaHCO_3$ and brine, dried over Na_2SO_4 and concentrated in vacuo. The crude residue was purified by column chromatography using 20-50% EtOAc in hexanes to give **2.25** (176.8 mg, 50.7%) as a white foam.

^{1}H NMR (400 MHz, Chloroform-*d*) δ 6.36 – 6.30 (m, 1H), 5.36 – 5.30 (m, 3H), 4.32 – 4.22 (m, 1H), 2.16 (d, *J* = 13.1 Hz, 7H), 2.00 (d, *J* = 4.8 Hz, 7H), 1.15 (d, *J* = 6.5 Hz, 3H). ^{13}C NMR (100 MHz, Chloroform-d) δ 170.44, 170.10, 169.85, 169.05, 89.86, 70.47, 67.72, 67.18, 66.36, 20.84, 20.59, 20.49, 15.84.

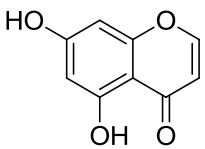

5,7-dihydroxy-4H-chromen-4-one (**2.24**):

2,4,6-trihydroxyacetophenone monohydrate (100 mg, 0.537 mmol) was dried under vacuum and then dissolved in dry DMF (1 mL) and BF_3•OEt_2 (265 µL, 2.15 mmol) was added slowly dropwise followed by MsCl (269 µL, 6M in DMF, 1.61 mmol). The reaction was heated to 90 ºC for 3 hours and then quenched with water. The reaction was filtered through a pad of celite, extracted with EtOAc (3X), dried over Na_2SO_4 and concentrated in vacuo. The crude residue was purified by column chromatography using 10-20% EtOAc in hexanes to give **2.24** (69.2 mg, 72%) as a yellow solid.

^{1}H NMR (400 MHz, Acetone-d_6) δ 8.08 – 8.01 (m, 1H), 6.38 (d, J = 2.1 Hz, 1H), 6.28 – 6.17 (m, 2H).

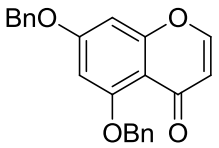

5,7-bis(benzyloxy)-4H-chromen-4-one (**2.30**):

2.24 (74.6 mg, 0.419 mmol) was dissolved in acetone (4.2 mL) and K_2CO_3 (446 mg, 3.23 mmol) and BnBr (135 µL, 1.13 mmol) were added. The reaction was heated to 60 ºC for 12 hours and then concentrated. It was redissoved in EtOAc and quenched with sat. NH_4Cl, extracted with EtOAc (3X), dried over Na_2SO_4 and concentrated in vacuo. The crude residue was purified by column chromatography using 20% EtOAc in hexanes to give **2.30** (130.4 mg, 87%) as an off-white solid.

^{1}H NMR (400 MHz, Chloroform-*d*) δ 7.72 (d, J = 5.9 Hz, 1H), 7.44 – 7.32 (m, 10H), 6.48 – 6.41 (m, 2H), 6.20 (d, J = 6.0 Hz, 1H), 5.11 (s, 2H), 4.70 (s, 2H).

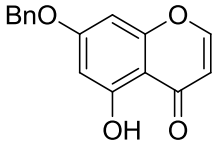

7-(benzyloxy)-5-hydroxy-4H-chromen-4-one (**2.31**):

2.24 (17.1 mg, 0.0960 mmol) was dissolved in acetone (1 mL) and K_2CO_3 (35.8 mg, 0.259 mmol) and BnBr (31 µL, 0.259 mmol) were added. The reaction was stirred at room temperature for 12 hours and then concentrated. It was redissoved in EtOAc and quenched with sat. NH_4Cl, extracted with EtOAc (3X), dried over Na_2SO_4 and concentrated in vacuo. The crude residue was

purified by column chromatography using 20% EtOAc in hexanes to give **2.31** (22.4 mg, 87%) as an off-white solid.

^{1}H NMR (400 MHz, Chloroform-*d*) δ 7.72 (d, *J* = 6.0 Hz, 1H), 7.44 – 7.34 (m, 5H), 6.48 – 6.41 (m, 2H), 6.21 (d, *J* = 6.0 Hz, 1H), 5.11 (s, 2H).

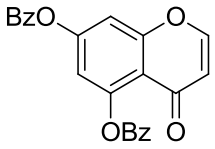

4-oxo-4H-chromene-5,7-diyl dibenzoate (**2.32**):

2.24 (12.8 mg, 0.0719 mmol) was dissolved in acetone (1.4 mL) and K_2CO_3 (70 mg, 0.503 mmol) and BzCl (33 µL, 0.288 mmol) were added. The reaction was heated to 60 ºC for 3 hours and then concentrated. It was redissolved in EtOAc and water, extracted with EtOAc (3X), dried over Na_2SO_4 and concentrated in vacuo. The crude residue was purified by column chromatography using 20% EtOAc in hexanes to give **2.32** (12.5 mg, 67%) as an off-white solid.

^{1}H NMR (400 MHz, Chloroform-*d*) δ 8.23 – 8.15 (m, 2H), 8.15 – 8.07 (m, 2H), 7.83 (d, *J* = 5.9 Hz, 1H), 7.71 – 7.43 (m, 4H), 6.87 (d, *J* = 2.1 Hz, 1H), 6.70 (d, *J* = 2.1 Hz, 1H), 6.31 (d, *J* = 5.9 Hz, 1H), 6.10 (d, *J* = 3.1 Hz, 1H), 5.98 (d, *J* = 3.1 Hz, 1H).

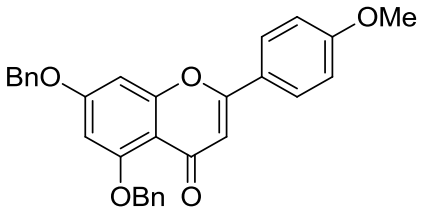

5,7-bis(benzyloxy)-2-(4-methoxyphenyl)-4H-chromen-4-one (**2.33**):

2.30 (245.2 mg, 0.685 mmol) was dissolved in a solution of $MgCl_2$ in dry THF (3.42 mL, 0.4 M) and cooled to 0 ºC. TMPZnCl.LiCl (3.91 mL, 0.21 M in THF) was added slowly dropwise and the reaction stirred at 0 ºC for 2 hours. $Pd(dba)_2$ (7.9 mg, 0.0137 mmol), P(2-furyl)$_3$ (6.4 mg, 0.0274 mmol) and p-iodoanisole (192 mg, 0.822 mmol) were added and the reaction stirred at 0 ºC overnight. It was quenched with sat. NH_4Cl, extracted with EtOAc (3X), dried over Na_2SO_4, and concentrated in vacuo. The crude residue was purified by column chromatography using 20-30-50% EtOAc in hexanes to give **2.33** (192.8 mg, 60.6%) as an off-white solid.

^{1}H NMR (400 MHz, Chloroform-*d*) δ 7.86 – 7.79 (m, 2H), 7.61 (d, *J* = 7.5 Hz, 2H), 7.48 – 7.35 (m, 8H), 7.33 – 7.23 (m, 3H), 7.03 – 6.96 (m, 2H), 6.68 – 6.60 (m, 2H), 6.50 (d, *J* = 2.3 Hz, 1H), 5.23 (s, 2H), 5.12 (s, 2H), 3.90 – 3.85 (m, 3H).

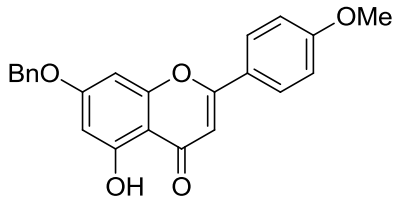

7-(benzyloxy)-5-hydroxy-2-(4-methoxyphenyl)-4H-chromen-4-one (**2.23**):

2.33 (13.5 mg, 0.0291 mmol) was dissolved in AcOH (1.45 mL) and H_2O (0.36 mL) and heated to 100 oC for 6 hours and then stirred at room temperature for 12 hours. The reaction mixture was extracted with EtOAc (3X), dried over Na_2SO_4 and concentrated in vacuo. The crude residue was purified by column chromatography using 30% EtOAc in hexanes to give **2.23** (10.7 mg, 98%) as a white solid.

^{1}H NMR (400 MHz, Chloroform-*d*) δ 7.92 – 7.74 (m, 2H), 7.49 – 7.31 (m, 5H), 7.01 (d, *J* = 8.9 Hz, 2H), 6.63 – 6.49 (m, 2H), 6.44 (d, *J* = 2.2 Hz, 1H), 5.14 (s, 2H), 3.89 (s, 3H).

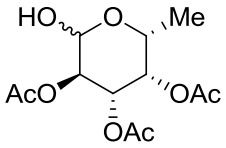

(3R,4S,5S,6R)-2-hydroxy-6-methyltetrahydro-2H-pyran-3,4,5-triyl triacetate (**2.34**):

2.25 (49.1 mg, 0.148 mmol) was dissolved in THF (0.67 mL) and $BnNH_2$ (18 µL, 0.163 mmol) was added. The reaction was stirred for 12 hours then quenched with a few drops of 1N HCl and concentrated. The crude residue was purified by column chromatography using 30-70% EtOAc in hexanes to give **2.34** (37.6 mg, 88%)

^{1}H NMR (400 MHz, Chloroform-*d*) δ 5.44 (dd, *J* = 16.5, 3.5 Hz, 1H), 5.39 (d, *J* = 3.3 Hz, 0.5H), 5.33 – 5.25 (m, 1H), 5.24 (q, *J* = 1.2 Hz, 0.5H), 5.14 (dd, *J* = 10.9, 3.6 Hz, 1H), 5.04 (dd, *J* = 4.7, 2.0 Hz, 1H), 4.44 – 4.34 (m, 1H), 2.16 (d, *J* = 4.5 Hz, 3H), 2.08 (d, *J* = 2.5 Hz, 3H), 1.98 (d, *J* = 1.5 Hz, 3H), 1.14 (d, *J* = 6.6 Hz, 3H).

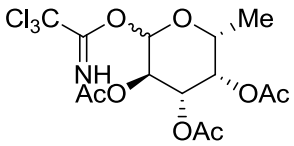

(2R,3S,4S,5R)-2-methyl-6-(2,2,2-trichloro-1-iminoethoxy)tetrahydro-2H-pyran-3,4,5-triyl triacetate (**2.35**):

2.34 (15.0 mg, 0.0517 mmol) was dissolved in DCM (151 µL) and Cl_3CCN (114 µL, 1.137 mmol) was added. The reaction was cooled to 0 ºC and DBU (2 µL, 0.0129 mmol) added slowly. It was warmed to room temperature and stirred for 2 hours, then filtered through celite and concentrated. It was purified by column chromatography using 10% EtOAc in hexanes with 2% Et_3N to give **2.35** (22.5 mg, 99%) as a clear oil.

^{1}H NMR (400 MHz, Chloroform-*d*) δ 8.60 (s, 1H), 6.54 (d, *J* = 3.6 Hz, 1H), 5.41 (dt, *J* = 11.0, 3.3 Hz, 2H), 5.34 (dd, *J* = 10.8, 3.5 Hz, 1H), 4.36 (d, *J* = 6.6 Hz, 1H), 2.18 (s, 3H), 2.01 (d, *J* = 3.4 Hz, 6H), 1.18 (d, *J* = 6.6 Hz, 3H).

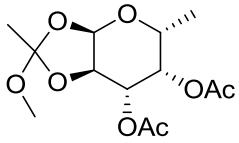

(3aR,5R,6S,7S,7aR)-2-methoxy-2,5-dimethyltetrahydro-3aH-[1,3]dioxolo[4,5-b]pyran-6,7-diyl diacetate (**2.36**):

2.25 (39.5 mg, 0.119 mmol) was dissolved in dry DCM (0.5 mL) and HBr (126 µL, 33% in AcOH) was added slowly. After 2 hours, the reaction was diluted with DCM and poured over ice. It was neutralized with sat. $NaHCO_3$, extracted with DCM (3X), washed with sat. $NaHCO_3$, dried over Na_2SO_4 and concentrated in vacuo. The crude residue was used directly for the next step.

The crude bromide was dissolved in dry DCM (0.5 mL) and TBAB (17.3 mg, 0.0536 mmol) was added followed by dry MeOH (0.5 mL) and 2,6-lutidine (24 µL, 0.202 mmol). The reaction was stirred for 12 hours and then concentrated. The crude residue was purified by column chromatography using 10-20% EtOAc in hexanes to give **2.36** (8.6 mg, 24%) as a clear oil.

^{1}H NMR (400 MHz, Chloroform-*d*) δ 5.80 (d, *J* = 5.0 Hz, 1H), 5.25 (dd, *J* = 3.4, 1.9 Hz, 1H), 5.03 (dd, *J* = 7.1, 3.4 Hz, 1H), 4.31 – 4.23 (m, 2H), 4.23 – 4.13 (m, 1H), 3.30 (s, 3H), 2.14 (d, *J* = 0.7 Hz, 3H), 2.06 (s, 3H), 1.20 (d, *J* = 6.6 Hz, 3H).

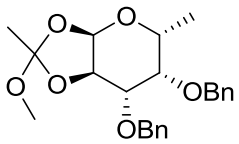

(3aR,5R,6S,7S,7aR)-6,7-bis(benzyloxy)-2-methoxy-2,5-dimethyltetrahydro-3aH-[1,3]dioxolo[4,5-b]pyran (**2.37**):

2.36 (9.9 mg, 0.0325 mmol) was dissolved in PhMe (1 mL) and KOH (5.5 mg, 0.0976 mmol) and BnBr (12 µL, 0.0976 mmol) were added. The reaction was heated to 110 ºC for 4 hours. It was then concentrated and the crude residue purified by column chromatography using 10-20% EtOAc in hexanes to give **2.37** (9.2 mg, 71%) as a white foam.

^{1}H NMR (400 MHz, Chloroform-*d*) δ 5.76 (d, *J* = 4.6 Hz, 1H), 4.99 – 4.90 (m, 1H), 4.84 (dd, *J* = 12.1, 2.6 Hz, 1H), 4.68 (dd, *J* = 12.0, 5.7 Hz, 2H), 4.47 (dd, *J* = 6.4, 4.6 Hz, 1H), 3.96 (ddd, *J* = 16.1, 6.4, 2.5 Hz, 1H), 3.74 – 3.61 (m, 2H), 3.28 (d, *J* = 3.9 Hz, 3H), 1.57 (d, *J* = 6.5 Hz, 3H), 1.23 (d, *J* = 6.6 Hz, 3H).

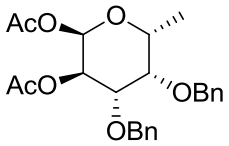

(2R,3R,4S,5S,6R)-4,5-bis(benzyloxy)-6-methyltetrahydro-2H-pyran-2,3-diyl diacetate (**2.38**):

2.37 (9.9 mg, 0.0247 mmol) was dissolved in AcOH (0.7 mL) and stirred for 12 hours. It was diluted with DCM and quenched with sat. $NaHCO_3$. It was extracted with DCM (3X), washed with sat. $NaHCO_3$, dried over Na_2SO_4 and concentrated in vacuo. The crude residue was purified by column chromatography using 10-20-30% EtOAc in hexanes to give **2.38** (10.0 mg, 94%) as a white foam.

^{1}H NMR (400 MHz, Chloroform-*d*) δ 7.39 – 7.23 (m, 11H), 5.56 (d, *J* = 8.3 Hz, 1H), 5.49 (d, *J* = 9.9 Hz, 1H), 5.30 (s, 1H), 4.98 (d, *J* = 11.7 Hz, 1H), 4.68 (dd, *J* = 12.0, 6.7 Hz, 2H), 4.56 (d, *J* = 12.2 Hz, 1H), 3.67 – 3.54 (m, 3H), 2.01 (s, 3H), 1.22 (d, *J* = 6.4 Hz, 3H).

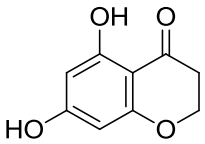

5,7-dihydroxychroman-4-one (**2.39**):

2.25 (72.0 mg, 0.404 mmol) was dissolved in EtOAc (4.0 mL) and $Pd(OH)_2/C$ (29.2 mg, 20 wt%) was added. The reaction was stirred under H_2 atmosphere for 24 hours and then filtered through celite and concentrated. The crude residue was purified by column chromatography using 20-30% EtOAc in hexanes to give **2.39** (49.4 mg, 68%) as a white solid.

^{1}H NMR (400 MHz, Acetone-d_6) δ 12.19 (s, 1H), 5.93 – 5.87 (m, 2H), 4.51 – 4.43 (m, 2H), 2.80 – 2.72 (m, 2H). ^{13}C NMR (100 MHz, Acetone-d_6) δ 196.09, 166.14, 164.41, 95.71, 94.59, 66.45, 35.92.

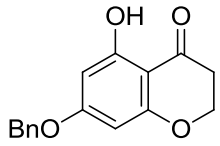

7-(benzyloxy)-5-hydroxychroman-4-one (**2.40**):

2.39 (18.1 mg, 0.100 mmol) was dissolved in acetone (3 mL) and K_2CO_3 (37.5 mg, 0.271 mmol) and BnBr (32 µL, 0.271 mmol) were added. The reaction was stirred at room temperature for 12 hours and then concentrated. It was redissoved in EtOAc and quenched with sat. NH_4Cl, extracted with EtOAc (3X), dried over Na_2SO_4 and concentrated in vacuo. The crude residue was purified by column chromatography using 20% EtOAc in hexanes to give **2.40** (23.9 mg, 88%) as an off-white solid.

^{1}H NMR (400 MHz, Chloroform-*d*) δ 12.05 (s, 1H), 7.42 – 7.31 (m, 5H), 6.12 (d, *J* = 2.3 Hz, 1H), 6.05 (d, *J* = 2.3 Hz, 1H), 5.06 (s, 2H), 4.45 (t, *J* = 6.4 Hz, 2H), 2.77 (t, *J* = 6.4 Hz, 2H).

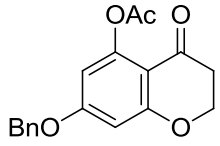

7-(benzyloxy)-4-oxochroman-5-yl acetate (**2.43**):

2.40 (28.7 mg, 0.106 mmol) was dissolved in DCM (0.25 mL) and pyridine (0.2 mL), Ac_2O (77 µL), and a few crystals of DMAP were added. The reaction was stirred at room temperature for 6 hours and then diluted with DCM. It was washed with 1N HCl and sat. $NaHCO_3$, dried over Na_2SO_4 and concentrated in vacuo. The crude residue was purified by column chromatography using 20% EtOAc in hexanes to give **2.43** (27.4 mg, 83%) as a white solid.

^{1}H NMR (500 MHz, Chloroform-*d*) δ 7.49 – 7.38 (m, 5H), 6.47 (dd, *J* = 2.5, 1.3 Hz, 1H), 6.38 (dd, *J* = 2.5, 1.3 Hz, 1H), 5.12 (d, *J* = 1.3 Hz, 2H), 4.57 – 4.50 (m, 2H), 2.78 – 2.71 (m, 2H), 2.43 (s, 3H).

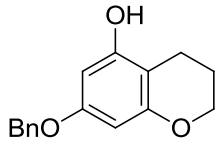

7-(benzyloxy)chroman-5-ol (**2.42**):

2.43 (27.4 mg, 0.0872 mmol) was dissolved in THF (0.5 mL) and water (0.25 mL) and cooled to 0 ºC. $NaBH_4$ (6.6 mg, 0.175 mmol) was added and the reaction stirred at 0 ºC for 30 minutes before being quenched with sat. NH_4Cl. It was extracted with EtOAc (3X), dried over Na_2SO_4 and concentrated in vacuo. The crude residue was purified by column chromatography using 20% EtOAc in hexanes to give **2.42** (19.6 mg, 88%) as a pale yellow solid.

^{1}H NMR (400 MHz, Chloroform-*d*) δ 7.43 – 7.28 (m, 5H), 6.07 (dd, *J* = 16.0, 2.4 Hz, 1H), 4.97 (s, 1H), 2.59 (t, *J* = 6.6 Hz, 2H), 2.01 – 1.94 (m, 2H).

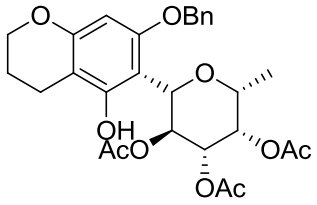

(2S,3S,4S,5S,6R)-2-(7-(benzyloxy)-5-hydroxychroman-6-yl)-6-methyltetrahydro-2H-pyran-3,4,5-triyl triacetate (**2.41**):

2.42 (0.184 mmol) and **2.25** (91.7 mg, 0.276 mmol) were dissolved in dry DCM (1.80 mL). The reaction was cooled to 0^{o}C and AgOMs (41.1 mg, 0.202 mmol) was added followed by $SnCl_4$ (400 µL, 1 M in DCM). The reaction was stirred at 0^{o}C for 2 hours and then diluted with DCM and quenched with sat. $NaHCO_3$. It was extracted with DCM (3X) and dried over Na_2SO_4. The crude residue was purified by column chromatography using 30-40-50% EtOAc in hexanes to give the **2.41** (48.1 mg, 49.5%) as an off-white foam.

^{1}H NMR (500 MHz, Chloroform-*d*) δ 7.66 – 7.53 (m, 1H), 7.45 – 7.33 (m, 4H), 6.22 (t, *J* = 10.0 Hz, 0.5H), 6.15 (t, *J* = 9.9 Hz, 0.5H), 6.00 (d, *J* = 6.7 Hz, 1H), 5.69 (s, 1H), 5.34 (dd, *J* = 3.4, 1.0 Hz, 0.5H), 5.30 (dd, *J* = 3.6, 1.1 Hz, 0.5H), 5.17 (dd, *J* = 9.9, 3.5 Hz, 1H), 5.02 (d, *J* = 9.9 Hz,

1H), 4.95 (d, *J* = 3.8 Hz, 0.5H), 4.92 (d, *J* = 6.1 Hz, 0.5H), 4.37 – 4.26 (m, 0.5H), 4.23 – 4.08 (m, 3H), 3.92 (dd, *J* = 6.4, 1.2 Hz, 0.5H), 3.82 – 3.73 (m, 1H), 2.63 – 2.48 (m, 2H), 2.27 (s, 1.5H), 2.09 (s, 1.5H), 2.01 (s, 1.5H), 1.85 (s, 1.5H), 1.81 (s, 1.5H), 1.69 (s, 1.5H), 1.21 (dd, *J* = 12.1, 6.4 Hz, 3H). ^{13}C NMR (201 MHz, Chloroform-*d*) δ 171.13, 170.88, 170.52, 170.38, 169.77, 169.55, 157.87, 156.41, 156.31, 155.05, 155.00, 154.72, 137.66, 137.10, 128.49, 128.14, 127.80, 127.68, 127.41, 126.94, 104.27, 103.99, 103.11, 101.78, 93.78, 92.86, 73.69, 73.46, 73.14, 73.01, 72.23, 72.07, 71.28, 71.06, 70.58, 70.37, 67.99, 67.24, 66.45, 65.84, 21.65, 21.04, 20.77, 20.72, 20.70, 20.66, 20.10, 18.81, 18.36, 16.54, 16.48. LRMS-ESI (+) *m/z* 551.1 $[M+Na]^+$.

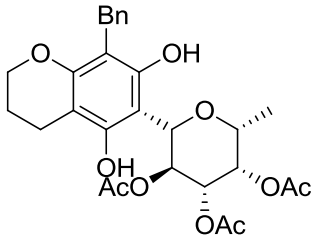

(2S,3S,4S,5S,6R)-2-(8-benzyl-5,7-dihydroxychroman-6-yl)-6-methyltetrahydro-2H-pyran-3,4,5-triyl triacetate (**2.44**):

2.44 was prepared using the same procedure as **2.41**. It appears as a byproduct.

^{1}H NMR (500 MHz, Chloroform-*d*) δ 7.75 (s, 1H), 7.37 – 7.30 (m, 6H), 5.68 (t, *J* = 10.0 Hz, 1H), 5.43 (d, *J* = 3.3 Hz, 1H), 5.25 (dd, *J* = 10.1, 3.2 Hz, 1H), 5.12 (d, *J* = 9.9 Hz, 1H), 4.71 (s, 1H), 4.22 – 4.00 (m, 7H), 2.60 – 2.54 (m, 2H), 2.28 (s, 3H), 2.10 (s, 3H), 2.04 (s, 3H), 1.31 (d, *J* = 6.7 Hz, 3H).

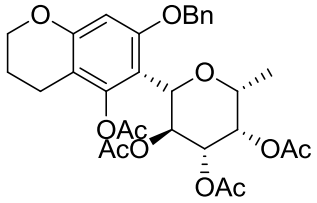

(2S,3S,4S,5S,6R)-2-(5-acetoxy-7-(benzyloxy)chroman-6-yl)-6-methyltetrahydro-2H-pyran-3,4,5-triyl triacetate (**2.45**):

2.41 (90.1 mg, 0.170 mmol) was dissolved in DCM (1.7 mL). Pyridine (34 µL, 0.425 mmol), Ac_2O (36 µL, 0.375 mmol) and a few crystals of DMAP were added. The reaction was stirred at room temperature for 3 hours and then concentrated. The crude residue was purified by column

chromatography using 30% EtOAc in hexanes to give the **2.45** (82.1 mg, 84.6%) as an off-white foam.

^{1}H NMR (500 MHz, Chloroform-*d*) δ 7.65 (d, *J* = 7.5 Hz, 1H), 7.49 – 7.32 (m, 4H), 6.34 (d, *J* = 19.2 Hz, 1H), 6.23 (t, *J* = 10.0 Hz, 0.5H), 6.13 (t, *J* = 10.0 Hz, 0.5H), 5.37 – 5.25 (m, 2H), 5.22 – 4.97 (m, 4H), 4.36 (ddd, *J* = 10.1, 6.1, 3.4 Hz, 0.5H), 4.27 – 4.12 (m, 1.5H), 4.01 – 3.89 (m, 0.5H), 3.87 (t, *J* = 6.4 Hz, 0.5H), 2.55 (dd, *J* = 8.8, 5.9 Hz, 2H), 2.31 (s, 3H), 2.28 – 2.24 (m, 1H), 2.05 (d, *J* = 0.8 Hz, 1.5H), 2.00 (d, *J* = 0.8 Hz, 1.5H), 1.83 (d, *J* = 0.8 Hz, 1.5H), 1.82 – 1.79 (m, 1.5H), 1.69 – 1.65 (m, 1.5H), 1.25 (dd, *J* = 6.4, 3.7 Hz, 3H). ^{13}C NMR (201 MHz, Chloroform-*d*) δ 171.04, 170.77, 170.43, 170.32, 169.49, 169.42, 168.43, 168.38, 157.77, 156.23, 156.19, 154.54, 150.04, 150.00, 137.32, 136.75, 128.55, 128.20, 127.92, 127.71, 127.67, 127.50, 127.08, 109.77, 109.70, 109.23, 107.83, 99.89, 98.89, 73.64, 73.38, 73.22, 73.01, 72.04, 71.93, 71.26, 71.04, 70.92, 70.84, 67.57, 66.98, 66.52, 66.03, 21.33, 20.88, 20.76, 20.75, 20.73, 20.70, 20.60, 20.57, 20.12, 19.35, 19.04, 16.69, 16.55. LRMS-ESI (+) *m/z* 571.2 [M+H], 588.2 $[M+NH_4]^+$.

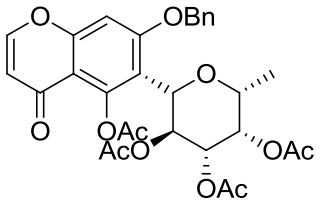

(2S,3S,4S,5S,6R)-2-(5-acetoxy-7-(benzyloxy)-4-oxo-4H-chromen-6-yl)-6-methyltetrahydro-2H-pyran-3,4,5-triyl triacetate (**2.46**):

2.45 (82.1 mg, 0.144 mmol) was dissolved in PhMe (14.4 mL), and H_2O (0.14 mL) and DDQ (196 mg, 0.863 mmol) were added. The reaction was heated to 110 ºC for 6 hours and then concentrated. It was redissolved in EtOAc and quenched with sat. $NaHCO_3$. The layers were separated and the organic layer dried over Na_2SO_4 and concentrated in vacuo. The crude residue was purified by column chromatography using 40-60% EtOAc in hexanes to give **2.46** (52.4 mg, 63%) as a red solid.

^{1}H NMR (400 MHz, Chloroform-*d*) δ 7.71 – 7.55 (m, 2H), 7.45 – 7.31 (m, 5H), 6.81 (d, *J* = 19.0 Hz, 1H), 6.29 – 6.06 (m, 2H), 2.37 (d, *J* = 3.3 Hz, 3H), 2.02 (d, *J* = 11.9 Hz, 3H), 1.96 (s, 1.5H), 1.73 (d, *J* = 2.9 Hz, 3H), 1.63 (s, 1.5H), 1.23 (dt, *J* = 17.7, 7.2 Hz, 3H). ^{13}C NMR (125 MHz, Chloroform-*d*) δ 169.74, 167.99, 148.33, 137.54, 135.43, 128.80, 128.49, 128.17, 127.86,

127.14, 114.13, 113.11, 112.17, 108.32, 105.99, 103.92, 102.59, 73.96, 73.35, 73.10, 73.04, 71.90, 71.48, 71.31, 71.16, 71.00, 70.79, 70.56, 67.47, 67.05, 29.63, 20.88, 20.77, 20.63, 20.55, 20.51, 20.42, 20.08, 16.69, 16.45. LRMS-ESI (+) *m/z* 605.1 $[M+Na]^+$.

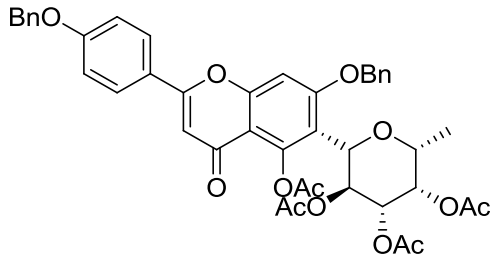

(2S,3S,4S,5S,6R)-2-(5-acetoxy-7-(benzyloxy)-2-(4-(benzyloxy)phenyl)-4-oxo-4H-chromen-6-yl)-6-methyltetrahydro-2H-pyran-3,4,5-triyl triacetate (**2.47**):

2.46 (14.8 mg, 0.0254 mmol) was dissolved in PivOH (0.25 mL) heated to 60^{o}C. 4-(benzyloxy)phenylboronic acid (17.4 mg, 0.0762 mmol), DDQ (1.1 mg, 0.00508 mmol), KNO_2 (0.4 mg, 0.00508 mmol), $Pd(OAc)_2$ (1.1 mg, 0.00508 mmol) and $Fe(OTf)_3$ (1.3 mg, 0.00254 mmol) were added and the reaction stirred at 60^{o}C for 18 hours. It was diluted with DCM, washed with sat. $NaHCO_3$ and dried over Na_2SO_4. The crude residue was purified by column chromatography using 30-40-50% EtOAc in hexanes as an eluent to give **2.47** (6.1 mg, 31%) as a yellow oil.

^{1}H NMR (400 MHz, Chloroform-*d*) δ 7.99 – 7.80 (m, 1H), 7.68 – 7.51 (m, 2H), 7.38 (dq, *J* = 15.7, 8.6, 7.4 Hz, 5H), 6.81 (d, *J* = 18.9 Hz, 1H), 6.25 (d, *J* = 10.2 Hz, 2H), 6.19 – 6.05 (m, 1H), 5.38 – 4.96 (m, 6H), 4.01 (t, *J* = 6.4 Hz, 1H), 3.89 (d, *J* = 6.4 Hz, 1H), 2.63 (s, 1H), 2.44 – 2.30 (m, 2H), 2.18 (s, 2H), 2.04 – 1.92 (m, 3H), 1.75 (d, *J* = 10.9 Hz, 3H), 1.71 – 1.60 (m, 3H), 1.22 – 1.13 (m, 3H).

CHAPTER 3. BIOLOGICAL EVALUATION OF HIV-1 PROTEASE INHIBITORS

3.1 Introduction

In the early 1980s, a new virus that would later be known as Human Immunodeficiency Virus (HIV) was discovered. This retrovirus primarily targets the immune system of patients, but is also known to affect the central nervous system (CNS). Over time, patients that are affected by the virus suffer from acquired immunodeficiency syndrome (AIDS) that is most often characterized by recurrent, opportunistic infections[121]. As of 2018, it is estimated that there are 37.9 million people living with AIDS and approximately 770,000 AIDS related deaths that year [122]. The development of several treatment methods have led to longer life expectancies in patients affected by this disease.

3.1.1 HIV Classification

The first HIV particle was discovered by Montagnier and Gallo, which was designated as HIV-1. Soon after this initial discovery, Montagnier discovered a second strain that was designated as HIV-2. While the two viruses posess similar structure and properties, HIV-2 is less infectious and progresses to AIDS much slower than HIV-1. As a result, it has not greatly affected areas outside of western Africa[123]. Both HIV-1 and HIV-2 are classified as part of the *Retroviridae* family, which require their genomes to be transcribed from RNA to DNA upon entering cells. Additionally, they are members of the *Lentivirus* genus, members of whom are known for being progressive diseases with long incubation periods[124].

Both HIV-1 and HIV-2 are believed to have originated from the cross species transmission of SIV (simian immunodeficiency virus) from primates. Initial theories attributed potential cross species transmission to the exposure to infected blood during hunting, processing of infected non-human primate for bushmeat, bites, and injuries from non-human primates[125]. Studies have indicated, HIV-1 originated from cross-species transmission of chimpanzees infected with SIV_{cpz} and gorillas infected with SIV_{gor}[126]. HIV-2 cross-species transmission occurred from sooty mangabeys, monkeys who harbored the SIV_{smm} infection. The difference in origin also explains the difference in virulence between these two strains.

3.1.2 HIV Virion Structure

Both strains of the virus have similar virion structure. HIV virions are approximately 100-120 nm icosahedrons shaped spheres with an outer membrane, inner protein matrix and an internal nucleocapsid that houses the viral genome and essential enzymes. The outer lipid membrane contains the protruding glycoproteins gp120 and gp41. The matrix, located just under the membrane, is made of the matrix protein p17. The nucleocapsid is underneath the matrix and is comprised of the protein p24. Inside the nucleocapsid is (+)-single stranded RNA genome along with the integrase (p32), protease (p10) and reverse transcriptase (p64)[124].

Additionally, the accessory proteins Vpu, Vif, Vpr, Tat, Rev and Nef are contained in the nucleocapsid and play a role in virus-host interactions[127]. Nef and Vpu both downregulate the expression of CD4 and Vpu enhances the release of new virions. Vpr is associated with increasing the infectivity factor of HIV. Vif is required for the replication of HIV in lymphocytes and macrophages, as well as certain cell lines. Tat and Rev are both involved in the regulation of viral gene expression. Tat serves as a *trans*-activator of transcription of full length HIV transcripts. Rev facilitates the export of unspliced and partially spliced viral RNA to the cytoplasm for translation[124].

3.1.3 HIV Lifecycle

The process by which HIV infects and destroys the host's immune system is known as the HIV life cycle. The virus primarily targets CD4 cells, which is the classification given to numerous immune cells including T-helper cells and macrophages that possess the CD4 glycoprotein on their membrane surface[124]. HIV virions interact with these glycoproteins using the membrane protein gp120. This causes a conformational change that exposes new binding regions on gp120 and gp41. The virus is then able to embed itself in the membrane of the host cell and the gp41 protein changes into a coiled shape that facilitates fusion with the membrane of the host cell via interactions with the co-receptors CCR5 and CXCR4[128-130].

Following fusion, the virus enters the cell and uncoats to reveal the viral genome and essential proteins within the capsid[131]. The single stranded RNA genome is converted using the reverse transcriptase enzyme into double stranded DNA containing long terminal repeats (LTRs). The viral DNA is transported to the nucleus of the cell where it can be integrated into the host

cell's genome using the viral integrase. The proviral DNA is transcribed using the host cell machinery from a single promoter in the 5' LTR into a 9kb primary viral RNA transcript. The accessory proteins Tat and Rev are involved in the regulation of viral gene expression. The resulting viral RNA is transported to the cytoplasm where the ribosomes of the host cell translate the mRNA into a large polyprotein. The viral polyprotein is cleaved by the viral protease, with the exception of the viral envelope section of the polyprotein which is transported to the Golgi apparatus. There it is glycosylated and cleaved by a cellular protease into gp41 and gp120[124].

The key components of the HIV virion are concentrated at budding sites in the host cell for the creation of new virions. Two copies of the viral RNA genome are packed into the new particle along with the necessary proteins, cleaved by HIV protease. The mature virion then exits the host cell by a pinching of the cellular membrane known as budding to release more mature HIV virions into the host[124,132,133]. The process of HIV replication and creation of new virions will continue for the entire lifespan of the host cell.

An HIV infection progresses through three significant stages: acute, latent and AIDS. An acute HIV infection manifests two to four weeks after infection, when an individual will begin experiencing flu-like symptoms. The initial attack of the virus on the host's immune system triggers an inflammatory response as more white blood cells are infected. There is also an increase HIV particles in the bloodstream as replication begins. The virus progresses to tissue cells to continue its replication process as HIV targets differentiated tissue macrophage mimic cells[134]. Once the levels of virus in blood have dropped again, the infection is classified as progressing to latency in which viral replication proceeds primarily in tissue cells. Without treatment, the virus continues to suppress the immune system and destroys the host's ability to fight off opportunistic infections as the patient progresses to AIDS, at which point the patient has no quantifiable immune response. Known opportunistic infections for HIV positive patients include *Pneumocystis carinii*, *cytomegalovirus*, *mycobacterial*, *herpesvirus*, and other common bacteria and viruses[135-139]. These decrease the lifespan of the patient and increase the risk of severe symptoms and death. Most patients with AIDS do not live more than a few years following diagnosis.

3.1.4 Treatment of HIV

The current method of treatment, combined antiretroviral therapy (cART), relies upon the combination of these HIV inhibitors. Access to this method of treatment has greatly improved HIV/AIDS treatment and the United Nations estimates that 23.3 million people are reliant on antiretroviral therapy. The development of cART allows current HIV/AIDS patients to manage this chronic condition and achieve a near normal life expectancy by reducing the rate of replication and lowering the risk of transmission[122,140,141].

cART typically consists of a combination of numerous inhibitors of key stages of the HIV lifecycle. The most common are integrase, protease and reverse transcriptase inhibitors. Additionally, some inhibitors have been found to inhibit entry into CD4 cells by blocking the necessary glycoprotein receptors. The combination of two or more different classes of inhibitor led to the advent of highly active antiretroviral therapy (HAART).

Unfortunately, there are many problems associated with both the short and long-term use of cART. Many of the compounds used are toxic and there are complications associated with long term use including increased risk of cancer, immune reconstitution inflammatory syndrome (IRIS) and CNS complications[142-144]. Following treatment, many patients fail to re-establish normal immunological function. Additionally, the complex drug regimen is difficult for many patients to adhere to and due to the nature of the virus, drug resistance is common. This necessitates the continued development of new compounds to treat this disease.

3.1.5 Entry and Fusion Inhibitors

The first significant class of inhibitors target the entry and fusion of HIV virions into the cell. Inhibitors that target entry and fusion are effective against highly resistant HIV strains, lower the number of latent HIV reservoirs, decrease the cytopathic immune response, and increase the immune responses[145,146]. Entry and fusion inhibitors primarily target the gp120/CD4 interaction, gp120 interaction with co-receptor, gp41 following conformational change, and fusion.

Enfuvirtide received FDA approval in 2003 and is currently the only FDA approved fusion inhibitor[147]. It functions by binding to gp41, preventing the HIV and host membranes

from interacting and thus completing the embedding and fusion process. However, its highly peptidic nature presents some problems with metabolic stability and dosage.

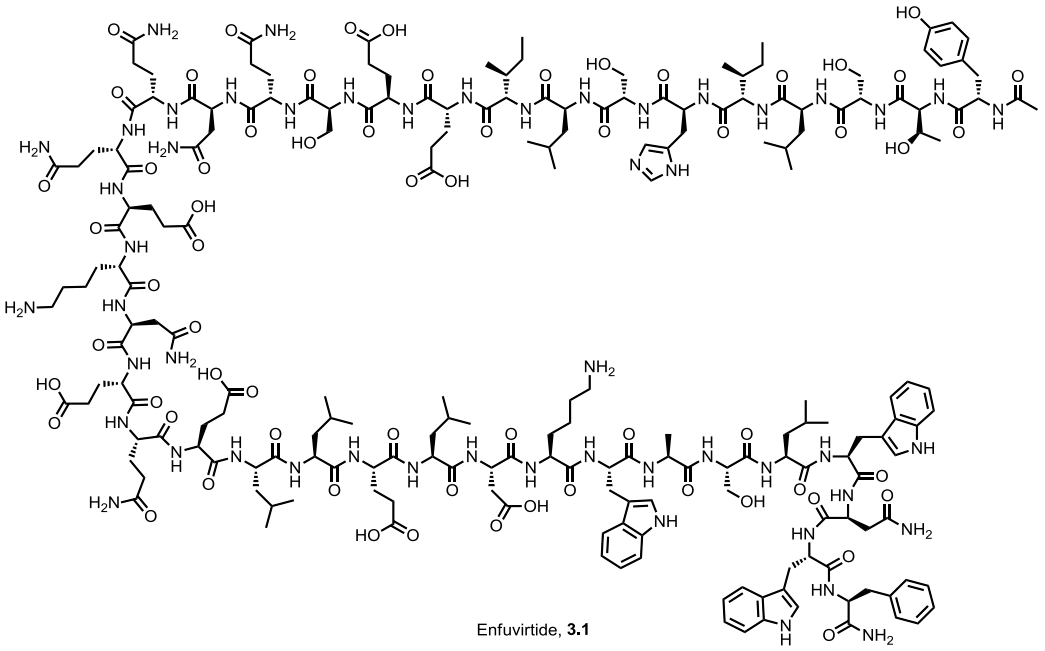

Figure 3.1: The HIV Entry Inhibitor Enfurvitide

Inhibitors of HIV entry into cells focus on the inhibition of the CCR5 and CXCR4 co-receptors that interact with gp120 and gp41 and facilitate entry into the cell. TAK-779 was the first potent antagonist that blocked HIV-1 from binding to CCR5, but the bioavailability profile was poor and so further development was stopped[148]. AMD3100 was the first potent CXCR4 antagonist but development was halted due to its low oral bioavailability, similar to TAK-779[149]. However, these compounds did provide the framework for the development of more CCR5 and CXCR4 receptor antagonists. In 2007, the FDA approved Maraviroc (MRV), the only successful CCR5 inhibitor. Unfortunately, prior to treatment, the patient must be identified as having a CCR5 dependent strain of HIV. The only other instance of an entry/fusion inhibitor is the monoclonal antibody Ibalizumab, which was approved by the FDA in 2018 as a post attachment inhibitor. It prevents the HIV-1 gp120/gp41 conformational change following virion attachment to the cell by binding to the CD4 receptor and in doing so prevents the secondary binding to co-receptors CCR5 and CXCR4 and entry into the cell[150].

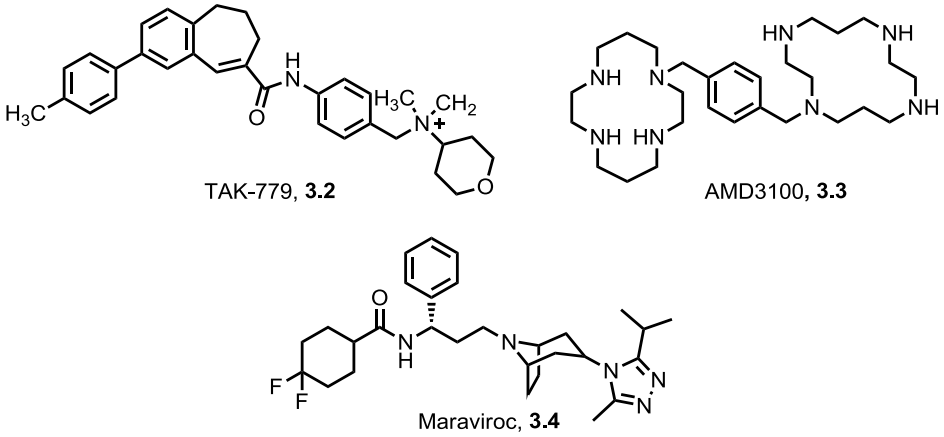

Figure 3.2: Structures of CCR5 and CXCR4 Inhibitors

3.1.6 Integrase Inhibitors

Another key method for the treatment of HIV-1 infection is targeting the irreversible integration of the viral genome into the host DNA using viral integrase. Directly following reverse transcription, integras interacts with new viral DNA and cellular cofactors to form the pre-integration complex (PIC). Removal of the terminal nucleotides on each viral DNA by integrase exposes the desired 3' hydroxyl group. The PIC enters the host nucleus and DNA strand transfer begins. Integrase binds to the host cell DNA and slices both strands to expose the 5'phosphate groups. PIC then covalently binds the host cell 5' phosphate groups to the viral DNA 3' hydroxyl groups, integrating the viral genome. Completion of the strand transfer triggers the host cell enzymes to close any of the gaps between the viral and host cell DNA using native DNA repair machinery, such as polymerases[124].

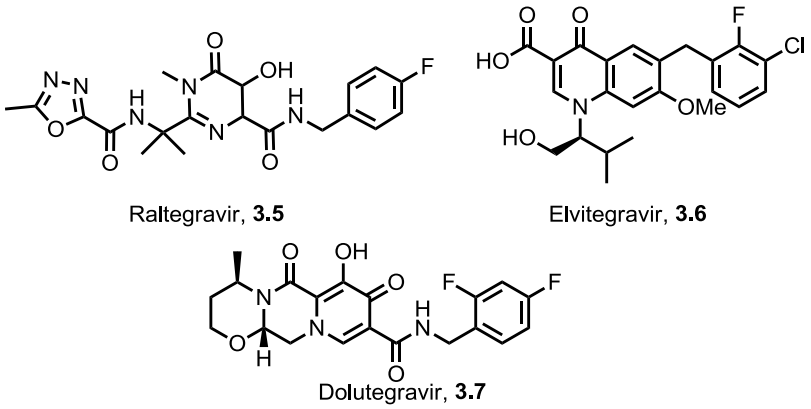

Figure 3.3: Integrase Inhibitors

Current integrase inhibitors prevent the PIC from binding to the host cell DNA and halt integration based replication[151]. Integrase inhibitors Raltegravir, Elvitegravir, and Dolutegravir bind with high affinity to the PIC only when it is complexed with the host cell DNA. The inhibitors then work by stopping strand transfer[152].

3.1.7 Reverse Transcriptase Inhibitors

Reverse transcriptase was the first HIV enzyme targeted by inhibitors and most FDA approved HIV medications are reverse transcriptase inhibitors. There are two main classes of reverse transcriptase inhibitors, nucleoside (NRTIs) and non-nucleoside (NNRTIs). Nucleoside based inhibitors contain a purine or pyrimidine based moiety as the key functionality. Azidothymidine is a derivative of thymidine; and Emtricitabine, Lamivudine are derivatives of cytidine; and Abacavir from deoxyguanosine. When initially dosed, these inhibitors are inactive, they require metabolic modification prior to exhibiting any activity. NRTIs are converted to their active phosphorylated nucleoside analogs by cellular kinases through three different phosphorylation stages. The first phosphorylation occurs by deoxynucleoside kinases and often is the rate-limiting step. The second phosphorylation is carried out by nucleoside monophosphate (NMP) kinases. A variety of cellular kinases can catalyze the final phosphorylation step[153]. These NRTI triphosphates act as reverse transcriptase inhibitors by competing with natural nucleosides for their incorporation into viral DNA. Each inhibitor lacks a key 3'-hydroxyl group that is needed for the natural binding of the next nucleotide, thus, halting the viral DNA

replication and elongation[154,155]. Because this process occurs in the cytoplasm, these inhibitors do not interfere in the natural replication of host cell DNA which occurs in the nucleus.

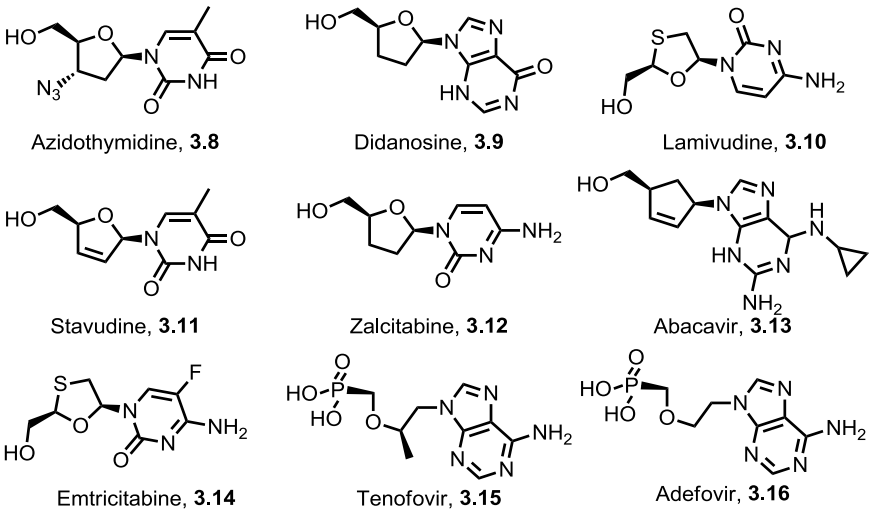

Figure 3.4: HIV-1 Nucleoside Reverse Transcriptase Inhibitors

The other class of reverse transcriptase inhibitors is non-nucleoside reverse transcriptase inhibitors (NNRTIs). These compounds avoid the need for a nucleoside based compound by binding to an allosteric site of reverse transcriptase and induce the formation of a hydrophobic pocket that is approximately 10 Å from the polymerase active site[156]. This pocket is known as the NNRTI-binding pocket (NNIBP) and has been shown to not interfere with the RT active site directly. Binding induces a slight conformational change in the active site that reduces polymerase activity and viral DNA synthesis. However, this is not a dramatic change, allowing NNRTIs to be used in combination with NRTIs for more effective cART treatments.

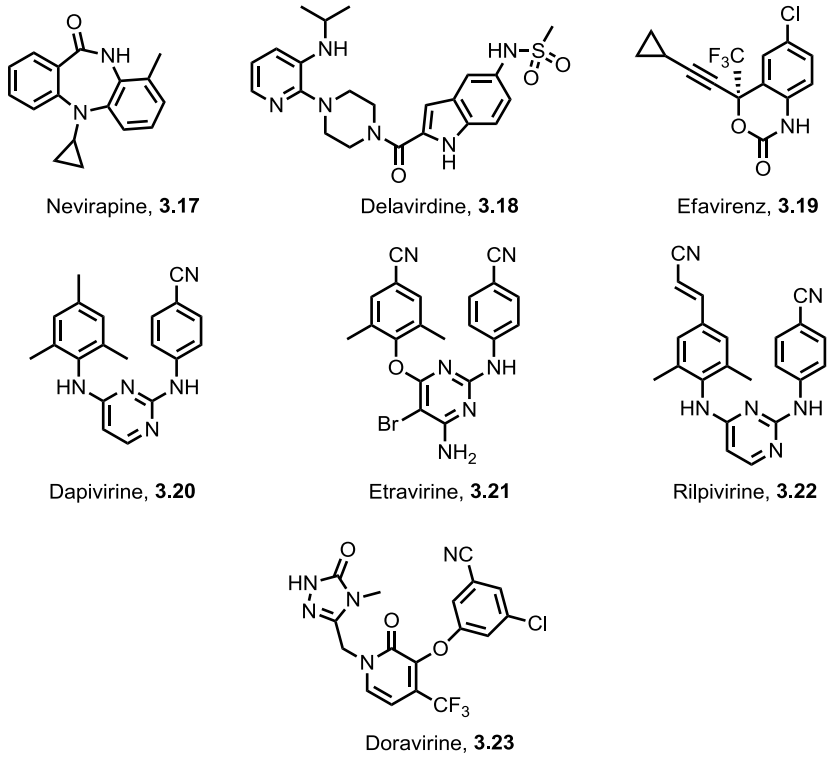

Figure 3.5: Non-nucleoside Reverse Transcriptase Inhibitors

The first generation of inhibitors were Nevirapine, Delavirdine, and Efavirenz. They all contain a butterfly-like binding motif with the two conjugated portions acting similar to the wings to reach different pockets of the binding site. HIV reverse transcriptase is a very error-prone enzyme and does not possess the DNA proofreading enzymes that regulate cellular DNA replication. Therefore, mutations that occur in or near the NNIBP led to major resistance towards the first generation of NNRTIs. This low-genetic barrier was observed because of the structural rigidity of initial drugs which could not bind to the NNIBP successfully[157]. The second generation consists of Etravirine and Rilpivirine. They are more accommodating to mutations that occur in the NNIBP by increasing structural flexibility by through an increased number of rotatable bonds and their ability to adopt a horseshoe-like confirmation, rather than the more rigid butterfly[158]. This allowed an additional interaction with residue W229 which is not subject to frequent mutations. The third generation inhibitor Doravirine was recently discovered and incorporates a vital, new hydrogen bond to the enzymatic backbone carbonyl of K101[159]. This increases the potential for this compound to be effective against multidrug resistant strains of HIV.

3.2 HIV-1 Protease Inhibitors

Inhibition of the HIV-1 protease prevents the formation and budding of mature virions by preventing the cleavage of the viral polyprotein. This constructs the virus's specific enzymes: reverse transcriptase, integrase, and the numerous structural proteins. Completion of this process alters the outer capsid structure and yields fully mature, infectious virions[160]. The removal of functional HIV protease prevents mature, infectious virions from being formed and leaving the cell to infect others. The HIV-1 protease is a retroviral aspartic acid protease and that is structurally very similar to human and other eukaryotic aspartic proteases: pepsin, renin, and others[161]. This presents the challenge of creating a drug that in no way interferes with any of the host proteases. Fortunately, the HIV-1 exists as a dimer while most human proteases are monomeric, bilobal and much larger.

X-ray crystal structures of the HIV-1 protease dimer show that each monomer contains 99 amino acids[162]. All aspartic proteases, including HIV, share common catalytic active sites within a conserved Asp-Thr-Gly sequence. The two catalytic aspartic acid residues interact with a water molecule that binds to the flap region of the protease. Specifically, the HIV protease active site is at the juncture of monomers binding, creating a symmetrical active site. Structurally, one beta strand from each monomer forms a glycine-rich, flexible loop to serve as the entrance into the active site known as the flap region, which is key to the development of inhibitors. The flap exists in an open conformation in the absence of a substrate and closes in the presence of a substrate. The catalytic active site consists of Asp25-Thr26-Gly27 and Asp25'-Thr26'-Gly27' resdiues from each subunit. This catalytic Asp-Thr-Gly triad interacts via extensive hydrogen bonding in the absence of a substrate. The catalytic aspartic acid residues Asp25 and Asp25' mediate the cleavage of the peptide bond by activating a water molecule to add to the carbonyl of the native peptide substrate. A stabilized germinal diol tetrahedral intermediate results and undergoes a hydrolysis step to complete the cleavage of the peptide bond to yield two new peptides[163].

3.2.1 First Generation

Development of the first generation of HIV-1 protease inhibitors focused on the development of peptidic compounds that mimic the diol tetrahedral immediate observed in the

hydrolysis of the native substrate. They were also designed to be competitive inhibitors of the natural substrate.

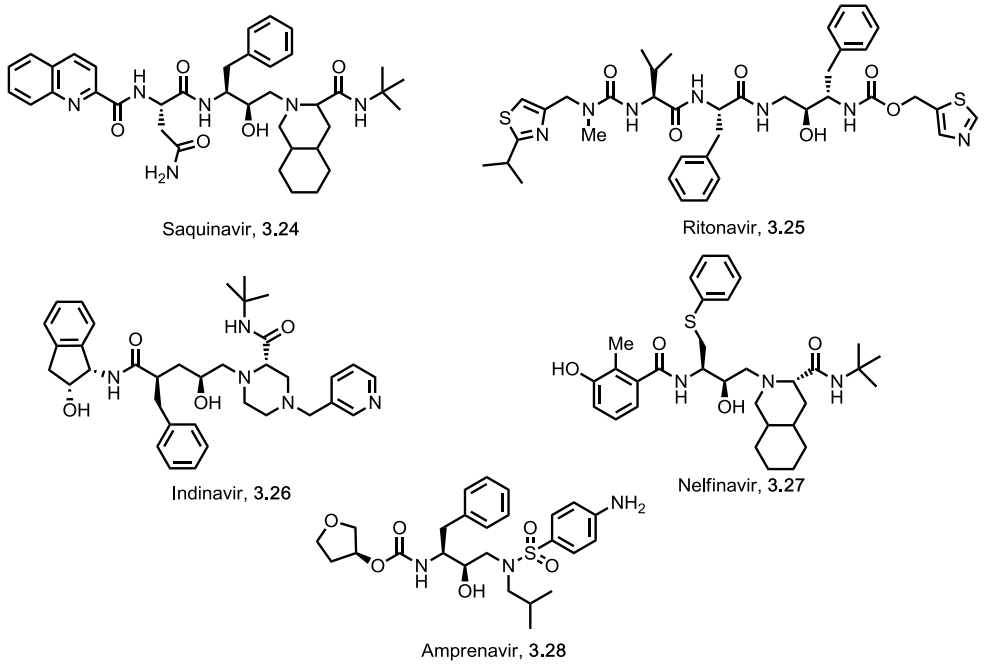

Figure 3.6: First Generation HIV-1 Protease Inhibitors

The first HIV-1 protease inhibitor, saquinavir, was approved by the FDA in 1995. This is a highly potent compound featuring a non-cleavable hydroxyethylamine isostere that binds to the viral protease in an extended fashion. The hydroxyl group binds to the aspartic acid residues and mimics the intermediate found in the intermediate of the hydrolysis of the native substrate. Saquinavir is a competitive inhibitor with an enzyme inhibitory activity K_i of 0.12 nM[164,165]. The effectiveness of this hydroxyethylamine isotere led to the development of Ritonavir, Indinavir, Nelfinavir and Amprenavir. Ritonavir was developed by Abbott Laboratories (Abbvie) and approved for the treatment of HIV by the FDA in 1996. It exhibits a K_i of 0.015 nM and is commonly used today in combination with other protease inhibitors in a cART regimen[166]. Ritonavir is known for deactivating cytochrome P450, leading to an increase in its pharmacokinetic properties[167]. Indinavir, featuring a larger hydroxyethyleneamine isotere that increases oral bioavailability, was developed by Merck and was also approved in 1996, but it is currently not recommended for use due to its toxicity. It has an enzyme inhibitory activity K_i of 0.36 nM[168]. Nelfinavir is a modified version of saquinavir with a K_i of 2.0 nM. Its unique phenyl

thioether moiety interacts with the S1 subsite and branches into the S3 subsite to acquire more favorable interactions within the active site[169]. Amprenavir, FDA approved in 1999, was developed by GlaxoSmithKline and features an aminobenzenesulfonamide group that interacts closely with the flap region of the protease via water-mediated hydrogen bonds. Unfortunately, production of Amprenavir was discontinued in 2004, although a prodrug version (fosamprenavir) is still available[170].

The first generation of HIV-1 protease inhibitors features compounds with highly peptidic structures. This led to a low half-life, poor oral bioavailability and numerous undesirable side effects. However, the most significant issue was the ease with which drug resistant strains emerged, rendering most of this generation useless. The development of new inhibitors with less peptidic structures, lower toxicity, improved bioavailability and increased activity against drug resistant strains became the next focus.

3.2.2 Second Generation

Based on the limitations of the first generation of protease inhibitors, a second generation was developed including: lopinavir, fosamprenavir, atazanavir, tipranavir and darunavir. These compounds show a remarkable decrease in peptidic nature compared to the first generation, and as a result show increased activity. Lopinavir was developed to overcome ritonavir resistant HIV-1 strains, by simplifying the the structure, with a K_i of 1.3 pM[171]. Atazanavir had an impressive antiviral activity profile towards HIV resistant strains with a K_i of 2.66 nM[172]. Additionally, atazanavir has very impressive bioavailability properties and is the first protease inhibitor to only require a single dose per day. Tipranavir is a non-peptidic PI with an impressive antiviral profile and a K_i of 8 pM. However, tipranavir is highly cytotoxic and is typically used as a treatment of last resort against multidrug resistant strains due to the extreme risk to the patient[173].

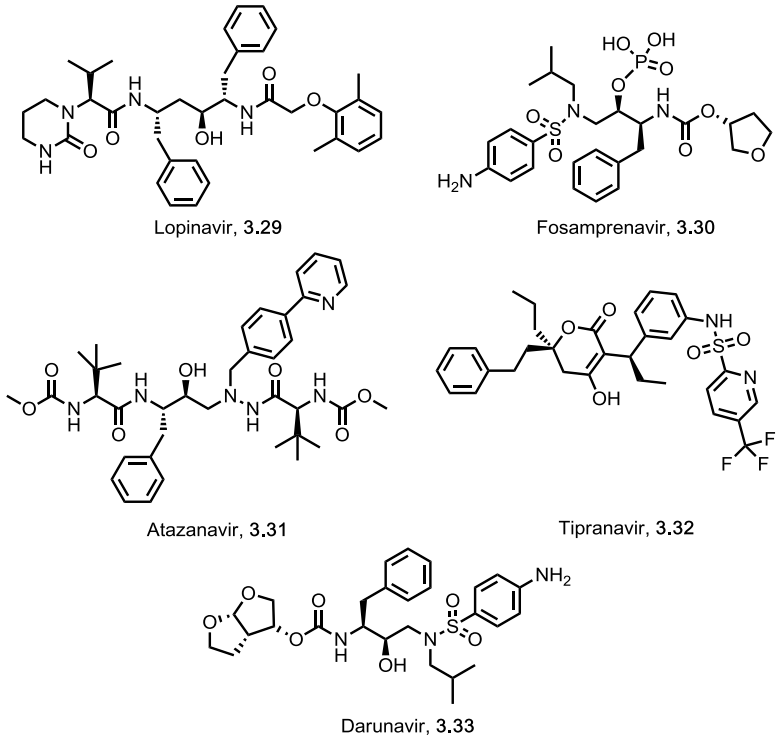

Figure 3.7: Second Generation HIV-1 Protease Inhibitors

Darunavir, FDA approved in 2006, displayed the greatest antiviral activity profile of this generation, minimal cytotoxicity and a high genetic barrier towards multidrug-resistant HIV-1 strains[174]. Darunavir resistant strains have begun to emerge, marking the need for the development of a third generation of HIV-1 protease inhibitors.

3.2.3 Darunavir

The use of protein X-ray structure-based design led to the discovery of many highly potent non-peptidic protease inhibitors[174,175]. Due to the design philosophy, these molecules feature moieties that interact with not only the catalytic residues in the active site, but also fill the hydrophobic pockets utilized by the native substrate. One key feature of these ligands are cyclic ethers in which the oxygens are used to mimic the carbonyls of peptide bonds. Towards this goal, work was done to maximize inhibitor interactions with the backbone of the HIV-1 protease active site, especially those of drug resistant strains of HIV[176-179]. This work culminated in the discovery of many potent PIs, particularly FDA-approved darunavir (DRV), which contains a key 3(R),3a(S),6a(R)-bistetrahydrofuranylurethane (*bis*-THF)[172,174,180].

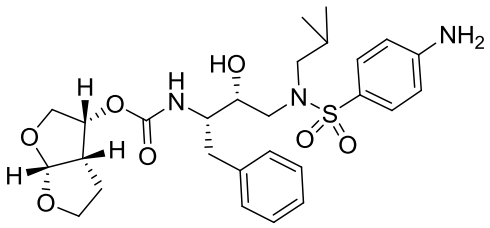

Darunavir, **3.33**

Figure 3.8: FDA approved Protease Inhibitor Darunavir

The main goal in the development of darunavir was to develop an HIV-1 protease inhibitor that would be effective against multidrug resistant strains of HIV. To this end, the concept of backbone binding was developed. While mutations in the viral genome change the specific amino acid sequence of the viral protease, the 3D structure of the protein remains similar. As such, the design of the structure of darunavir is based entirely on the backbone of HIV-1 protease, rather than the individual residues[178]. This creates a higher genetic barrier towards multidrug resistant HIV-1 strains.

To further validate the backbone binding based design theory, the activity of darunavir is attributed to the number of hydrogen-bonds that it forms with the HIV-1 protease backbone, primarily in the S2 and S2' subsites. The X-ray crystal structure illustrates many of these essential interactions (Figure 3.9)[179]. Both oxygens on the bis-THF ligand form hydrogen bonds to the backbone residues, Asp30 and Asp29. The P2' portion of DRV hydrogen bonds to the backbone of the active site and interacts with a water molecule to further access additional hydrogen bond interactions with Gly27, Asp25, Asp25', and water-mediated hydrogen bonds with Ile50' and Ile50. These interactions have been used as the basis for the design of new HIV-1 protease inhibitors, as future inhibitors seek to further explore the active site and create additional hydrogen bonding and hydrophobic interactions. Darunavir is also capable of preventing the formation of the HIV protease dimer. Work is focused on developing a new generation of protease inhibitors based on improvements to the structure of darunavir, particularly for targeting darunavir resistant strains.

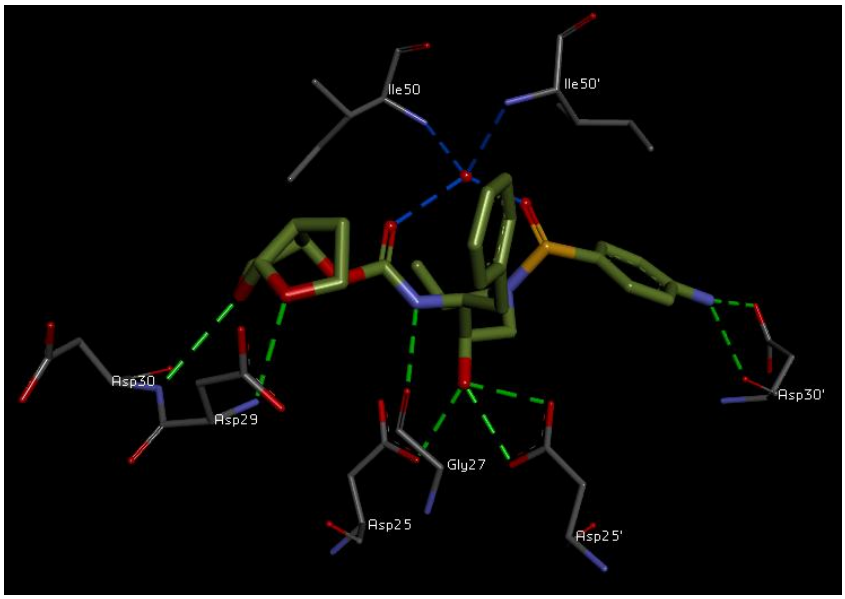

Figure 3.9: X-ray crystal structure of Darunavir bound HIV-1 protease. Inhibitor carbons are in olive and important hydrogen bonding interactions are shown with dotted lines. (PDB: 2IEN)

3.3 Biological Evaluation of HIV-1 Protease Inhibitors

We envisioned a series of HIV-1 protease inhibitors incorporating aminothiochromane and aminotetrahydronaphthalene carboxamide derivatives as the P2 ligands to promote additional hydrogen bonding and van der Waals interactions. The lead compound **3.34** showed promising results with a K_i of 26.7 nM, but no detectable cellular activity. Further investigation determined that the opposite diastereomer **3.35** was more active and oxidation of the thiane to the sulfone derivative further improved potency through an increase in hydrogen bonding interactions. In fact, inhibitor **3.36** had an IC_{50} of 47 nM which was only 10-fold greater than the IC_{50} of Darunavir, 3 nM, indicating that this is a great candidate for further biological evaluation.

Table 3.1: Biological Data of Selected Aminothiochromane and Aminotetrahydronaphthalene Carboxamide Inhibitors

Entry	Compound	K_i (nM)	IC_{50} (nM)
1	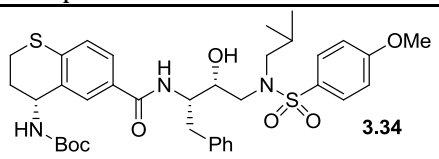 **3.34**	26.7	>1000
2	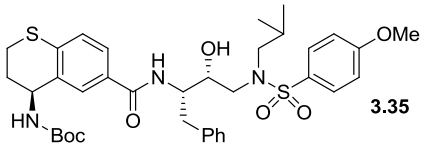 **3.35**	0.38	>1000
3	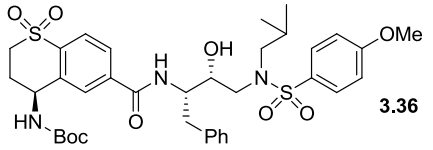 **3.36**	0.008	47
4	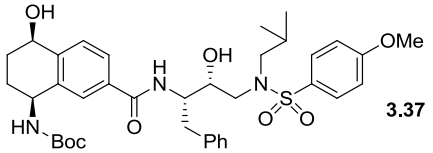 **3.37**	0.3	>1000
5	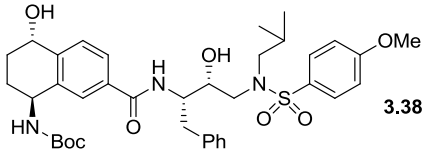 **3.38**	0.14	254
6	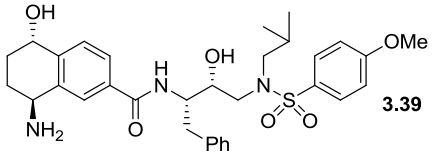 **3.39**	0.06	232

Following the discovery of the potency of the sulfone inhibitor, aminotetrahydronaphthalene inhibitors were developed. It was believed that the free hydroxyl group would be able to mimic the additional hydrogen bonding interactions that were displayed by the sulfone oxygens. However, while all of these compounds had good enzyme inhibitory activity, their cellular potency was worse than the aminothiochromane inhibitors, which the lowest being compound **3.39** with an IC_{50} of 232 nM. This is likely due to the instability of the free hydroxyl group, which can be readily be modified by numerous enzymatic processes. Based on these results, further optimization of compounds bearing these P2 ligands, particularly the aminothiochromane, are underway in our laboratory.

Another series of HIV-1 protease inhibitors was designed using a bicyclic oxazolidinone scaffold as the P2 ligand. These compounds proved to be extremely potent the lead compound

3.40, which was the active diastereomer, having a K_i of 1.2 pM and IC_{50} of 48.3 nM. Methylation of the amine leads to inhibitor **3.42**, which was more potent in cells with an IC_{50} of 36 nM. Incorporation of an isobutyl or isobutylene group at that position also leads to inhibitors with comparable IC_{50}'s to that of **3.42**. Replacement of the anisole P2' ligand with cyclopropylaminobenzylthiazole moiety led to inhibitor **3.45** with an IC_{50} of 28 nM, making it the most potent of this series.

Table 3.2: Biological Data of Selected Bicyclic Oxazolidinone Inhibitors

Entry	Compound	K_i (nM)	IC_{50} (nM)
1	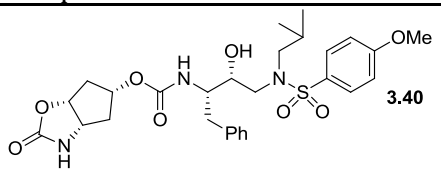 **3.40**	0.0012	48.3
2	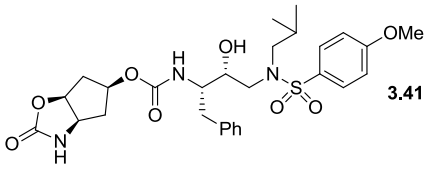 **3.41**	1.33	>1000
3	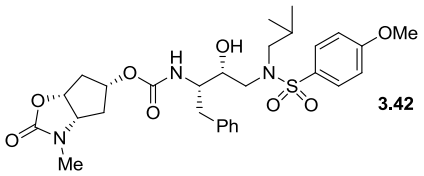 **3.42**	0.03	36
4	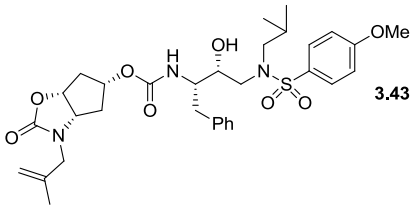 **3.43**	0.04	31
5	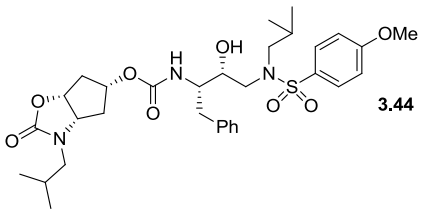 **3.44**	0.16	41
6	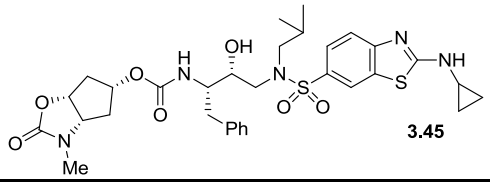 **3.45**	0.19	28

Based upon this data, further development of compounds containing a bicyclic oxazolidinone or related moiety as the P2 ligand is in development in our laboratory. Of particular interest are those that also incorporate cyclopropylaminobenzylthiazole as the P2' ligand.

3.4 Experimental Section

The enzyme inhibitory activity of these compounds was evaluated using an improved version of the procedure developed by Toth and Marshall[181]. In this, the concentrations of enzyme, substrate and inhibitor are kept low so that Michaelis-Menten kinetics applies. This allows for the calculation of K_i using the changes in v_{max} across different concentrations of inhibitor.

For our modified assay, the inhibitor (1-2 mg) is dissolved in BioPure DMSO. The inhibitor is then further diluted out in NaOAc buffer (pH = 5.5) with DTT to give four different submicromolar concentrations of inhibitor. 10 µL of HIV protease (0.025 mg/mL) was added to separate tubes of 480 µL of DTT buffer. To these were added either 5 µL of inhibitor solution or an additional 5 µL of buffer (for blanks). These were incubated at 37 ºC for 15 minutes and then 5 µL of substrate (BACHEM 4048265), which is a mimic of the natural peptide substrate with a quenched fluorophore, was added. The fluorescence of the samples was monitored in a spectrometer with a heated sample holder, to keep them at 37 ºC. Once all four samples of inhibitor had been run, the slopes these curves were divided by the average slope of the blank runs. The program GraFit was then used to calculate the K_i for the inhibitor with this data.

APPENDIX. NMR SPECTRA

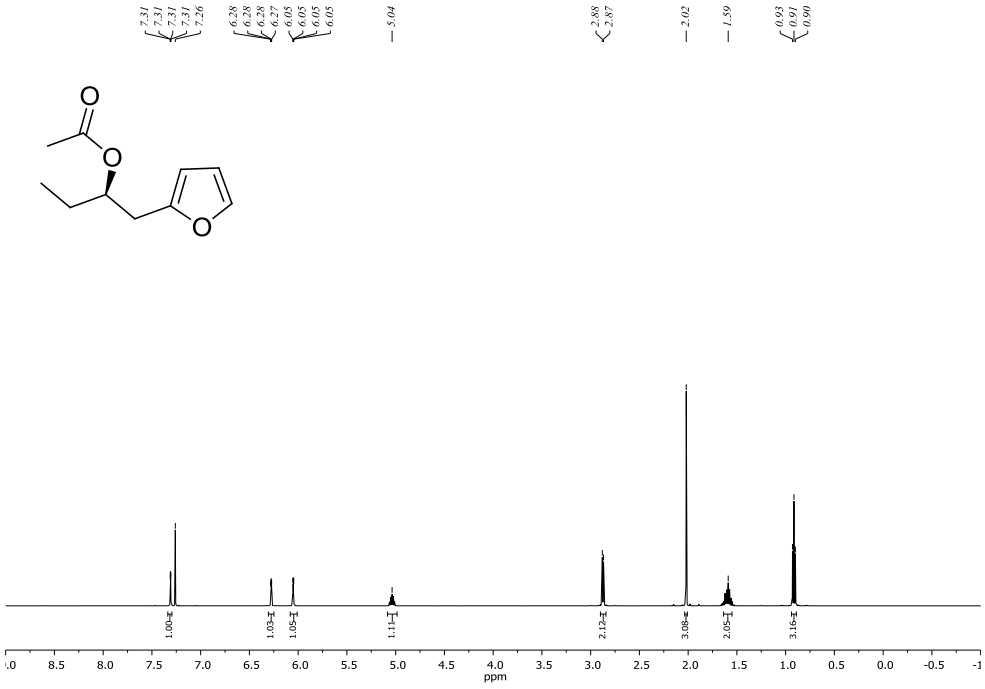

^{1}H NMR (500 MHz, $CDCl_3$) of Acetate **1.38**

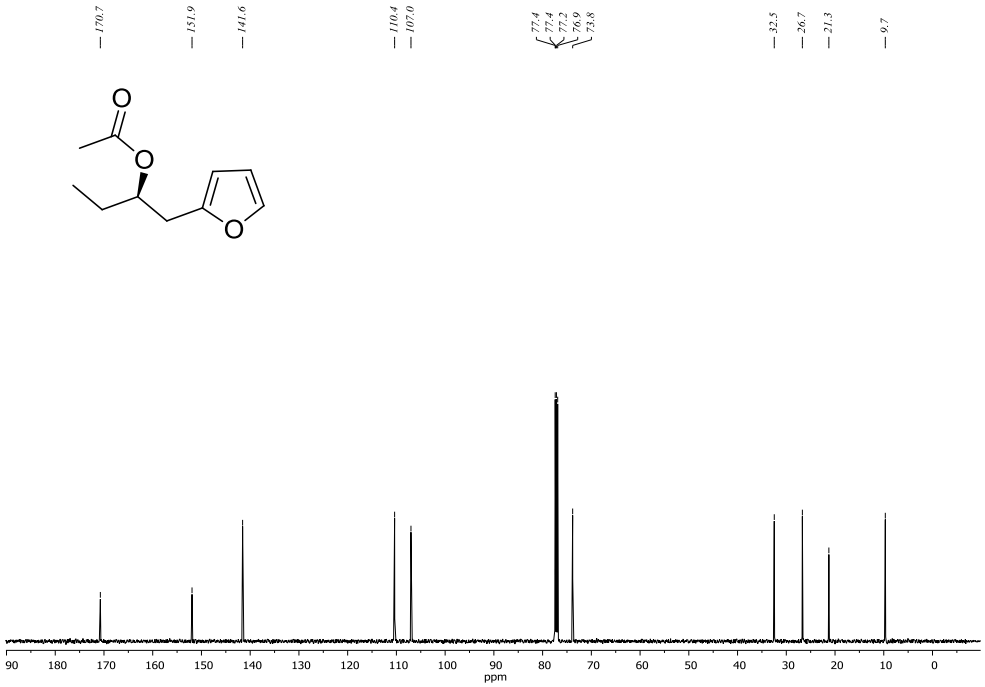

^{13}C NMR (125 MHz, $CDCl_3$) of Acetate **1.38**

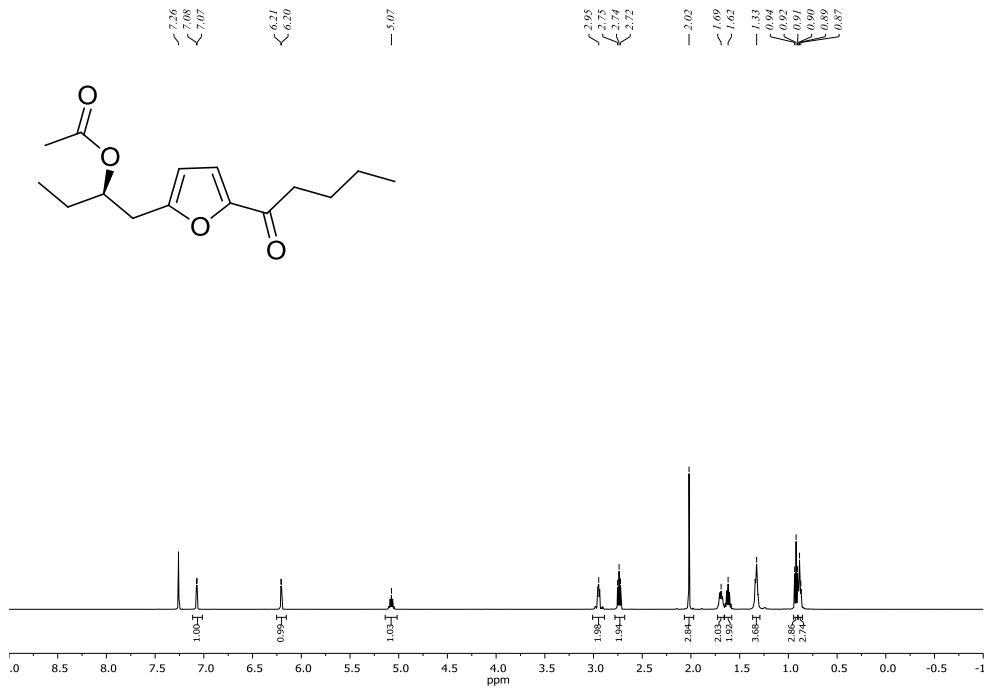

^{1}H NMR (500 MHz, $CDCl_3$) of Furanyl ketone **1.39**

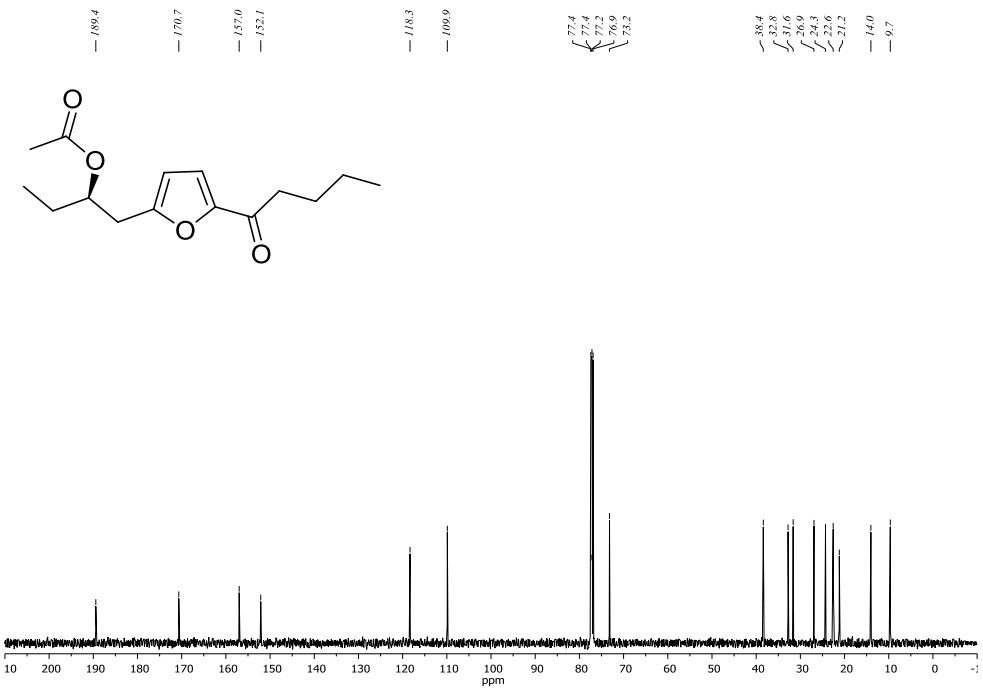

^{13}C NMR (125 MHz, $CDCl_3$) of Furanyl ketone **1.39**

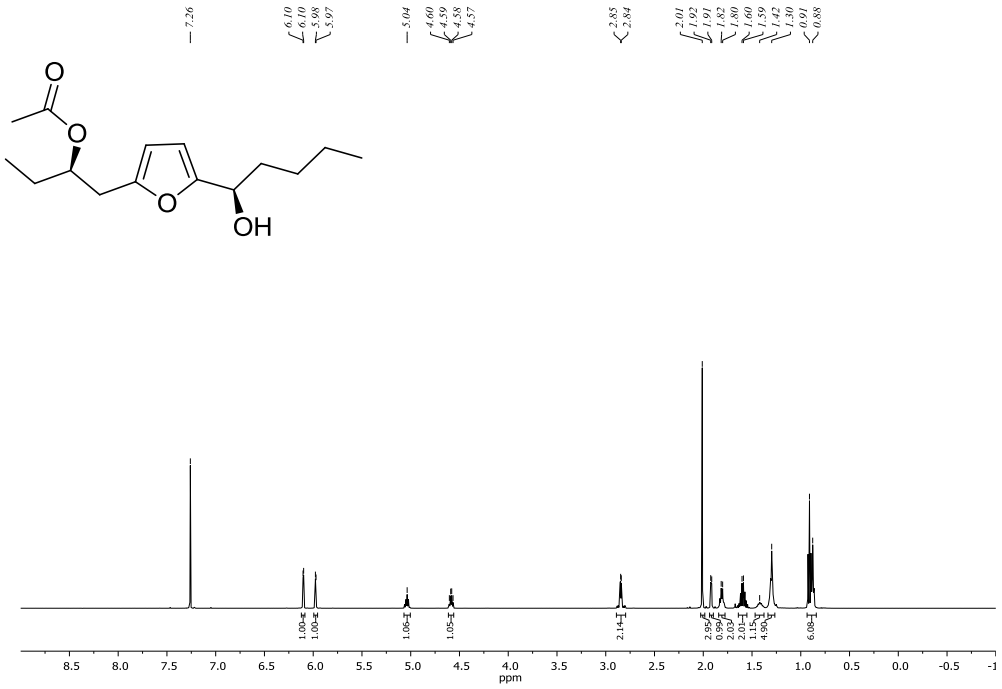

^{1}H NMR (500 MHz, $CDCl_3$) of Alcohol **1.36**

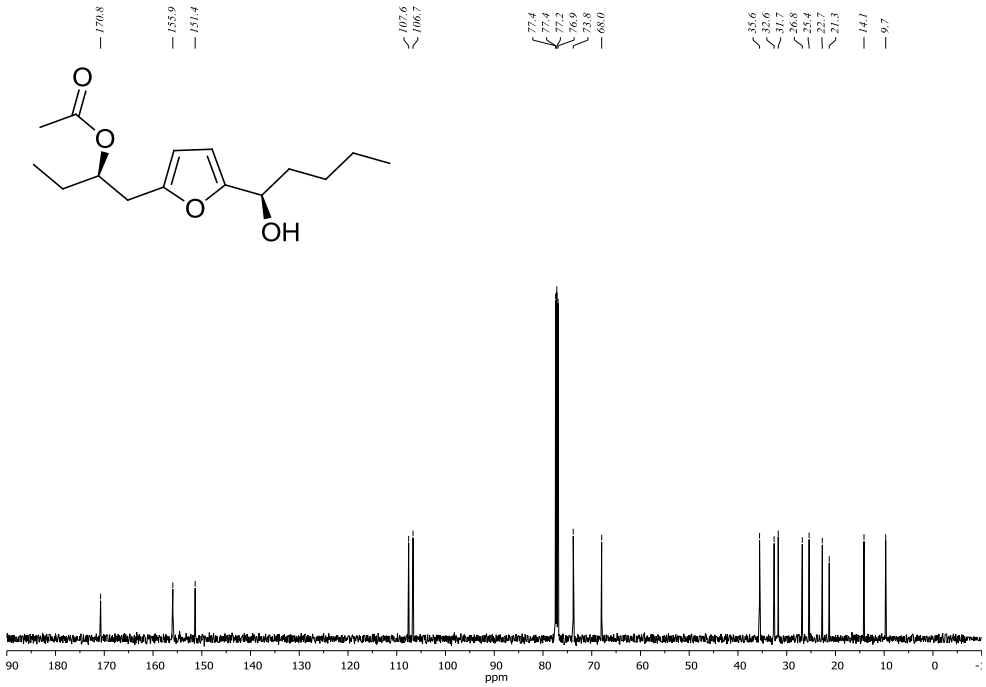

^{13}C NMR (125 MHz, $CDCl_3$) of Alcohol **1.36**

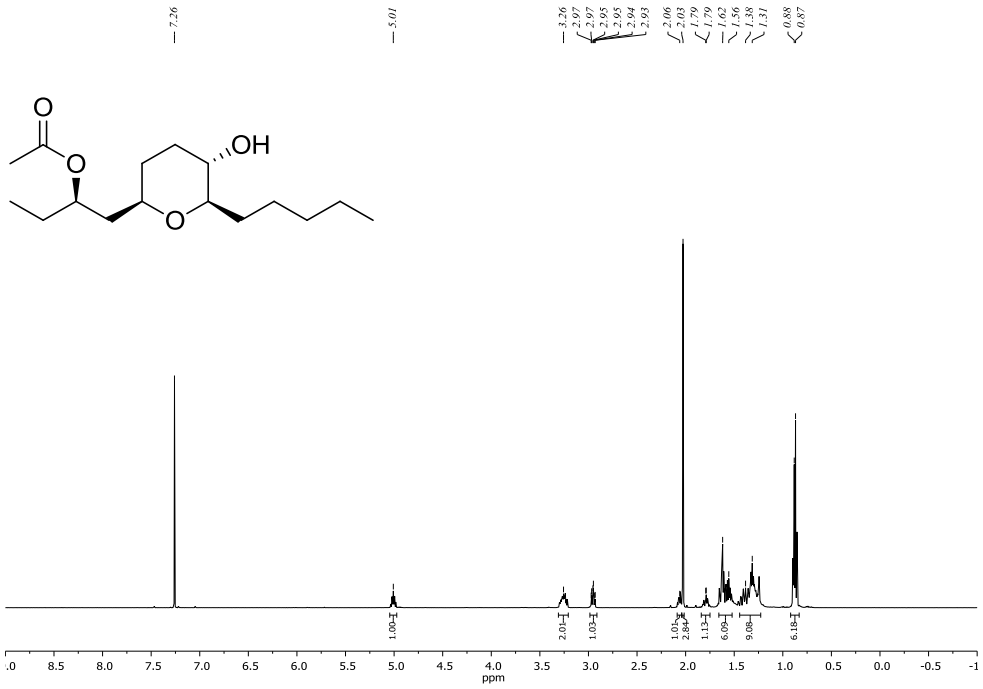

^{1}H NMR (500 MHz, $CDCl_3$) of tetrahydrpyran **1.35**

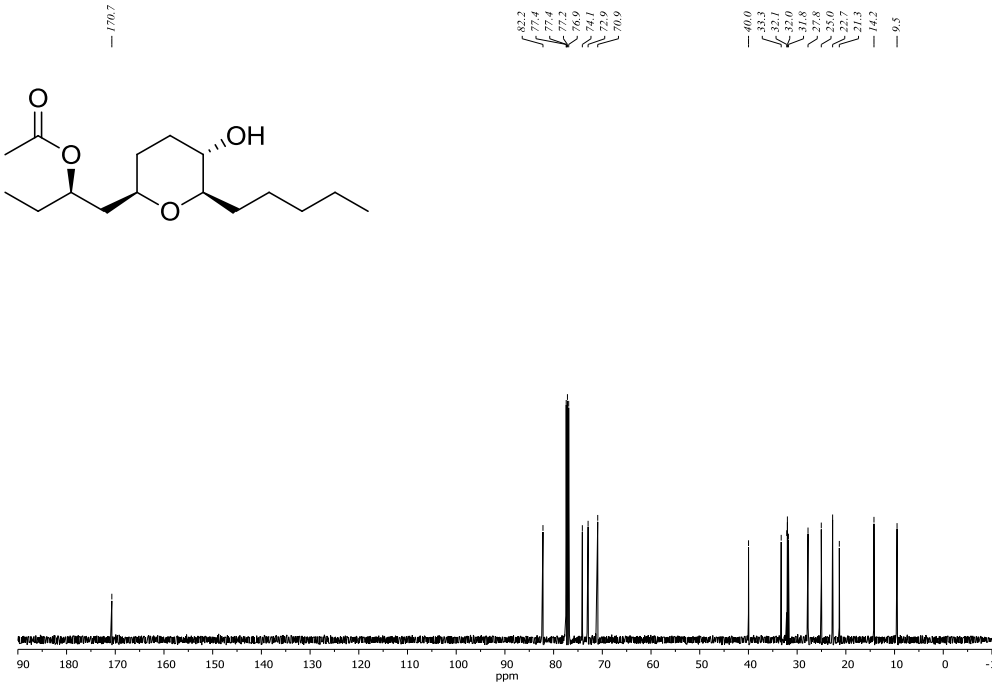

^{13}C NMR (125 MHz, $CDCl_3$) of tetrahydropyran **1.35**

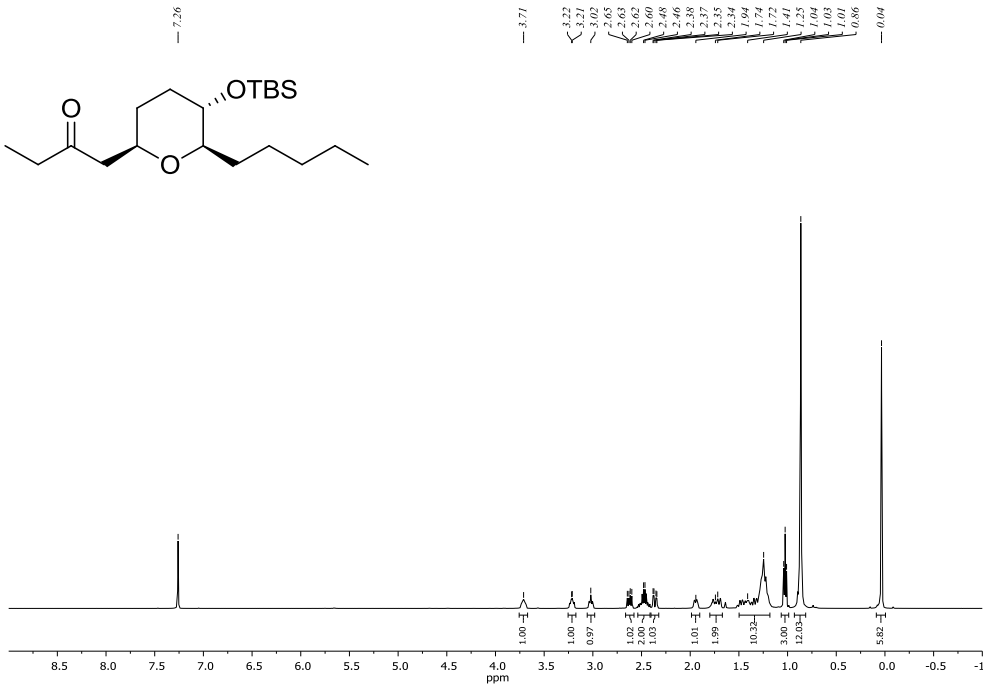

^{1}H NMR (500 MHz, $CDCl_3$) of Ketone **1.42**

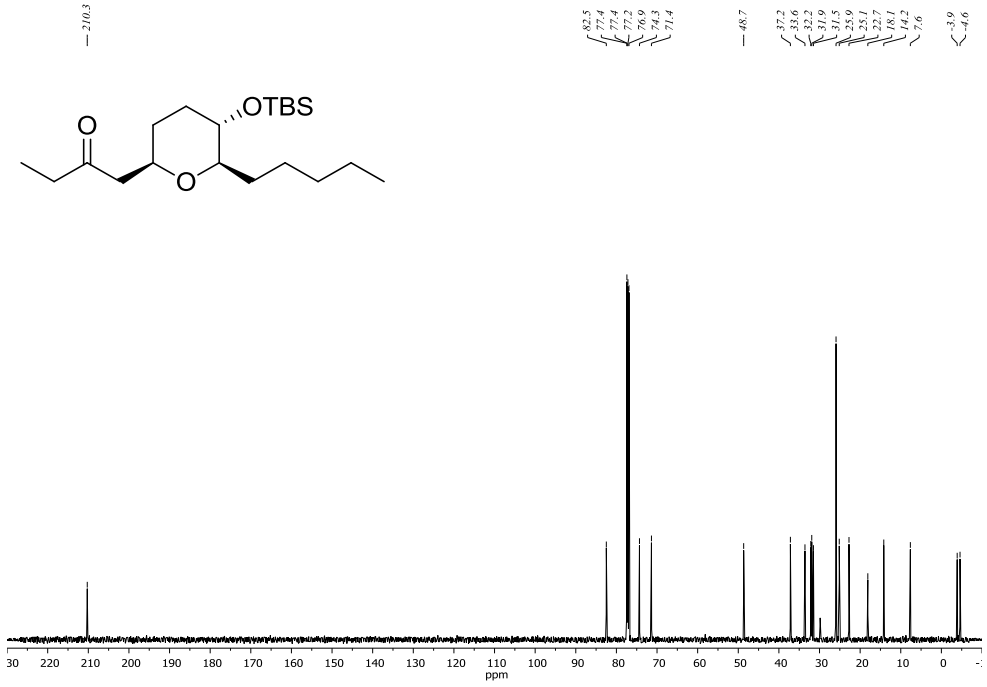

^{13}C NMR (125 MHz, $CDCl_3$) of Ketone **1.42**

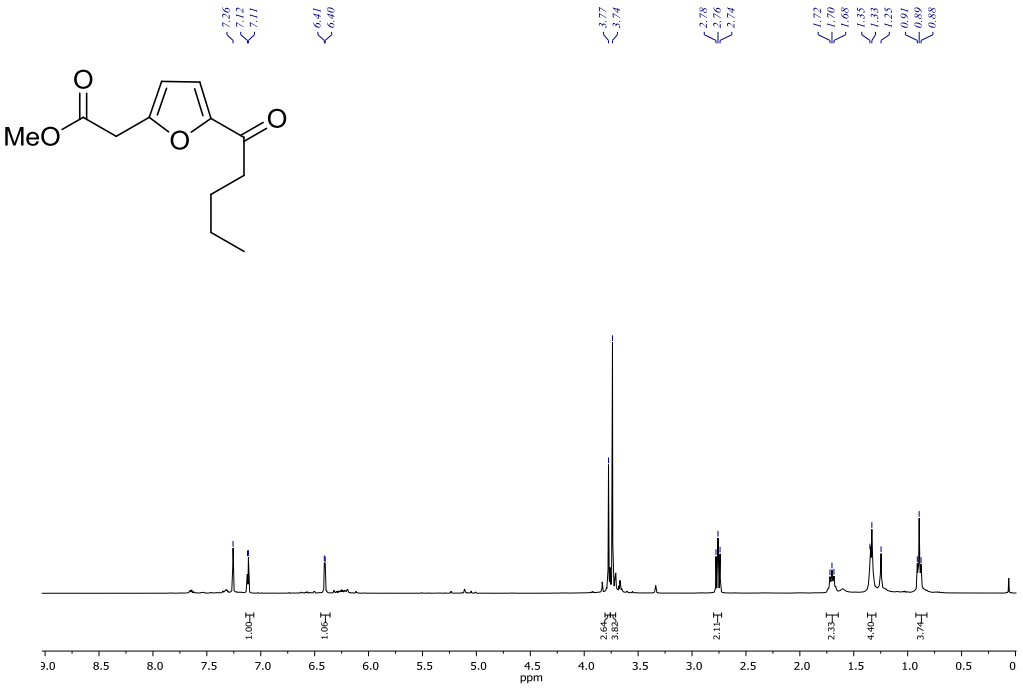

^{1}H NMR (400 MHz, $CDCl_3$) of Ketone **1.47**

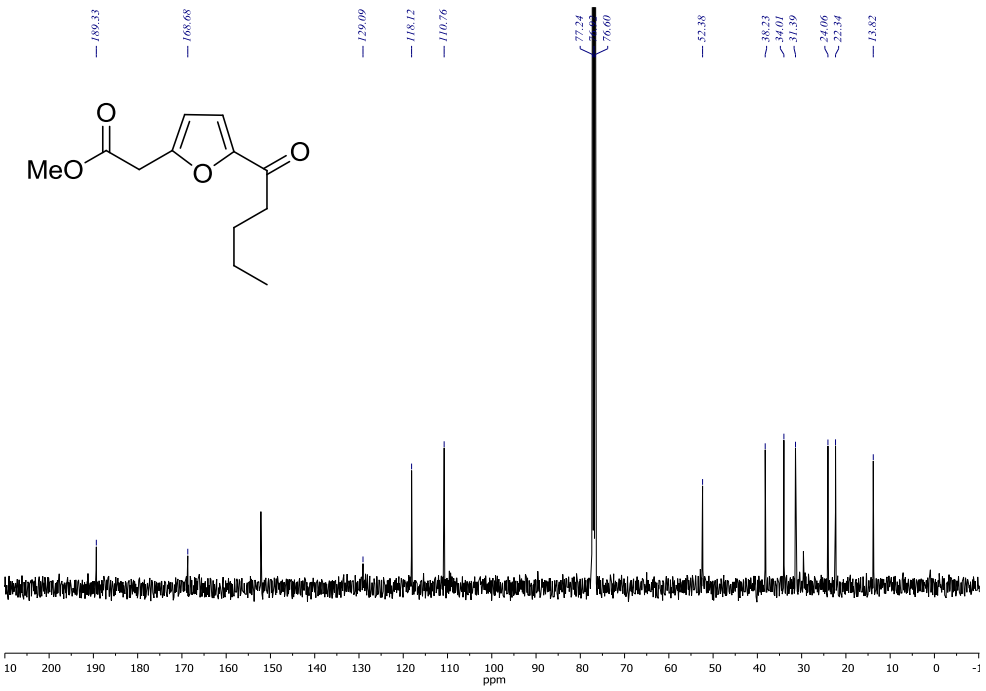

^{13}C NMR (100 MHz, $CDCl_3$) of Ketone **1.47**

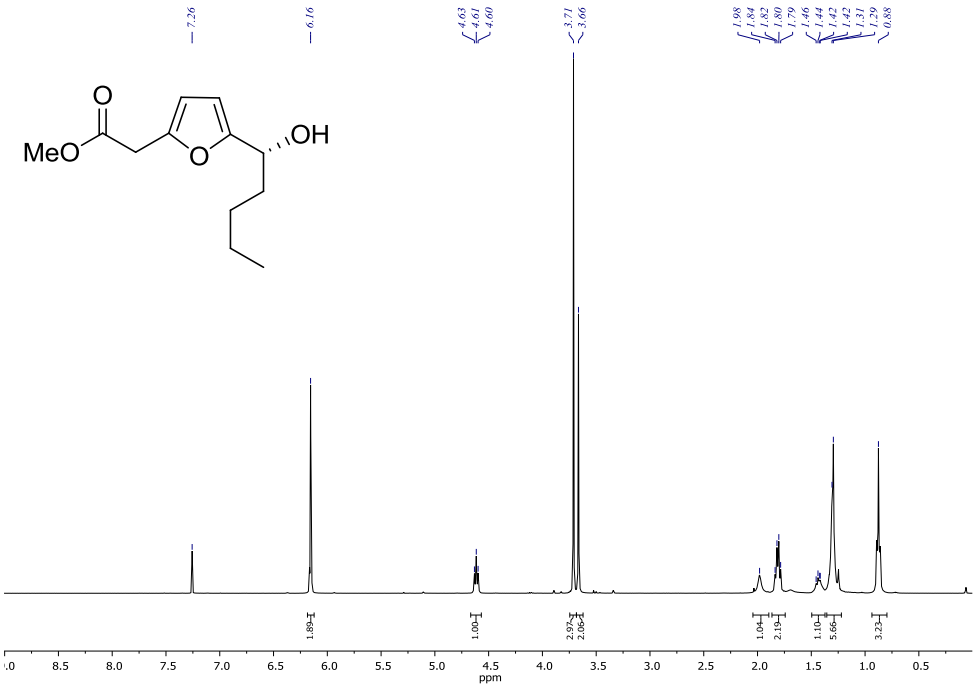

^{1}H NMR (400 MHz, $CDCl_3$) of Alcohol **1.44**

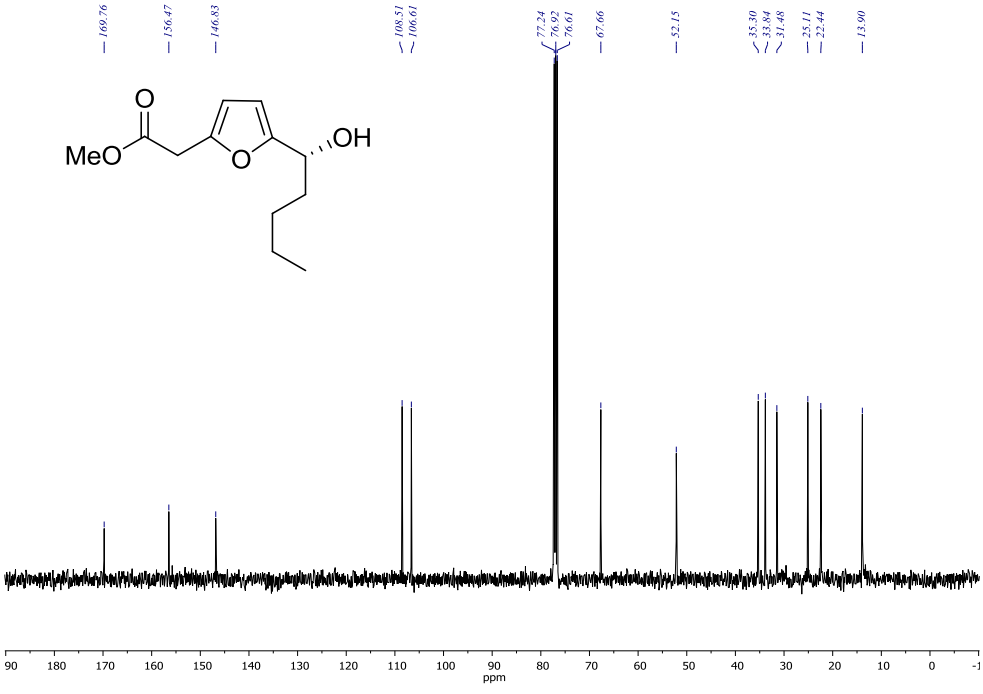

^{13}C NMR (100 MHz, $CDCl_3$) of Alcohol **1.44**

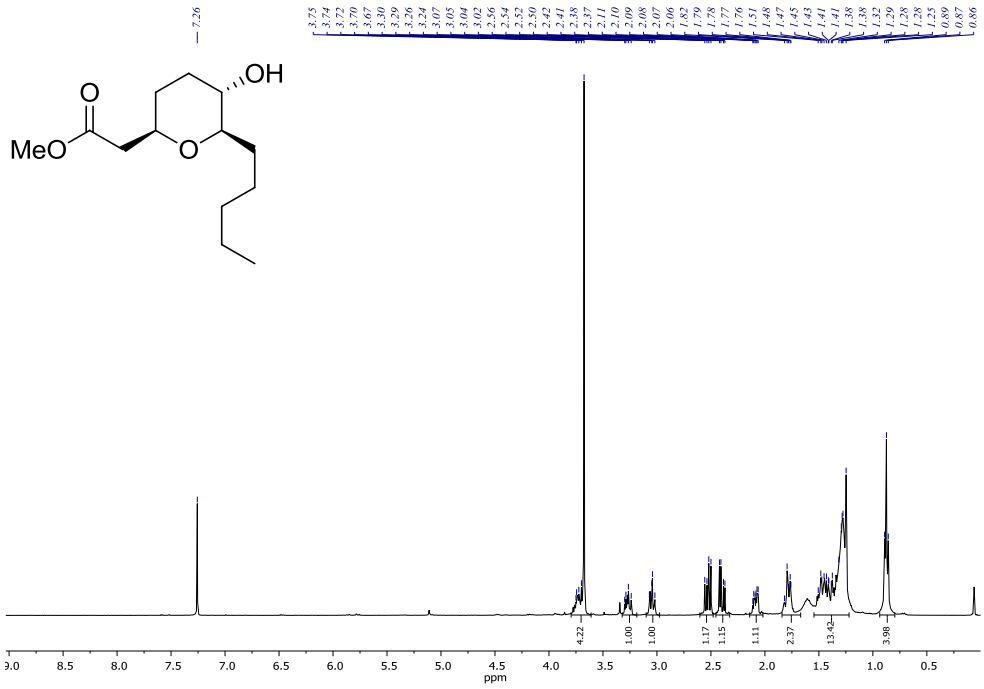

^{1}H NMR (400 MHz, $CDCl_3$) of Alcohol **1.43**

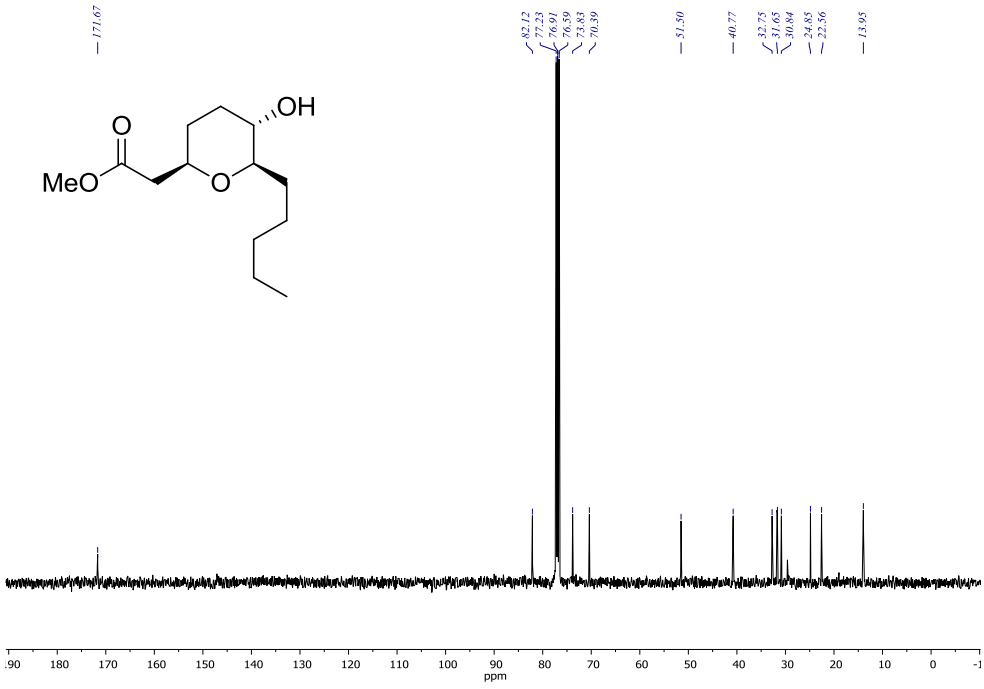

^{13}C NMR (100 MHz, $CDCl_3$) of Alcohol **1.43**

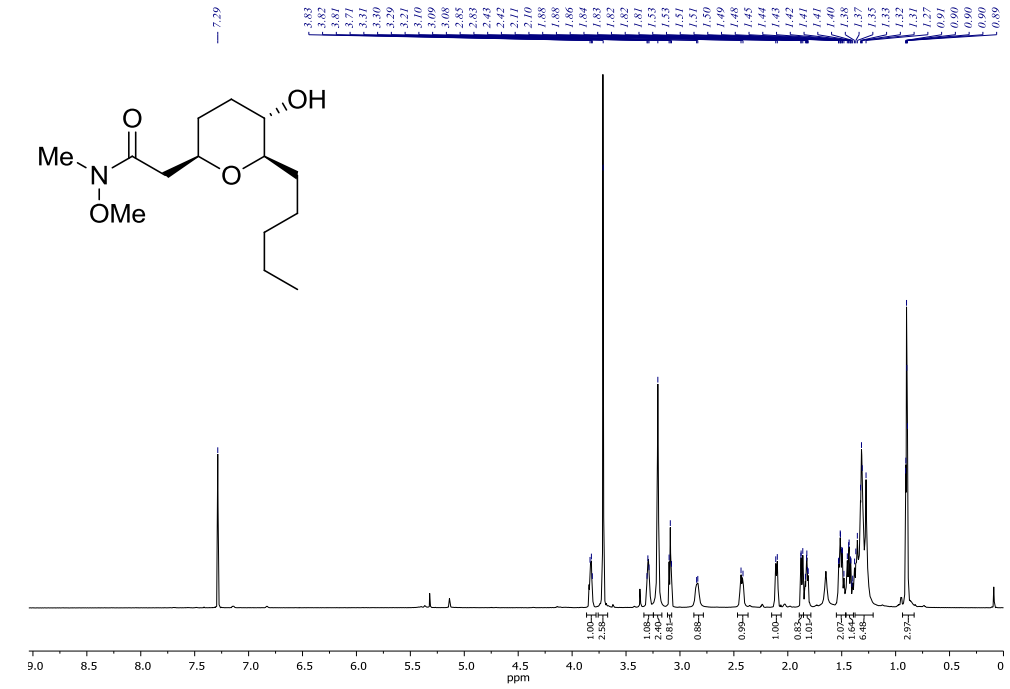

^{1}H NMR (800 MHz, $CDCl_3$) of Amide **1.48**

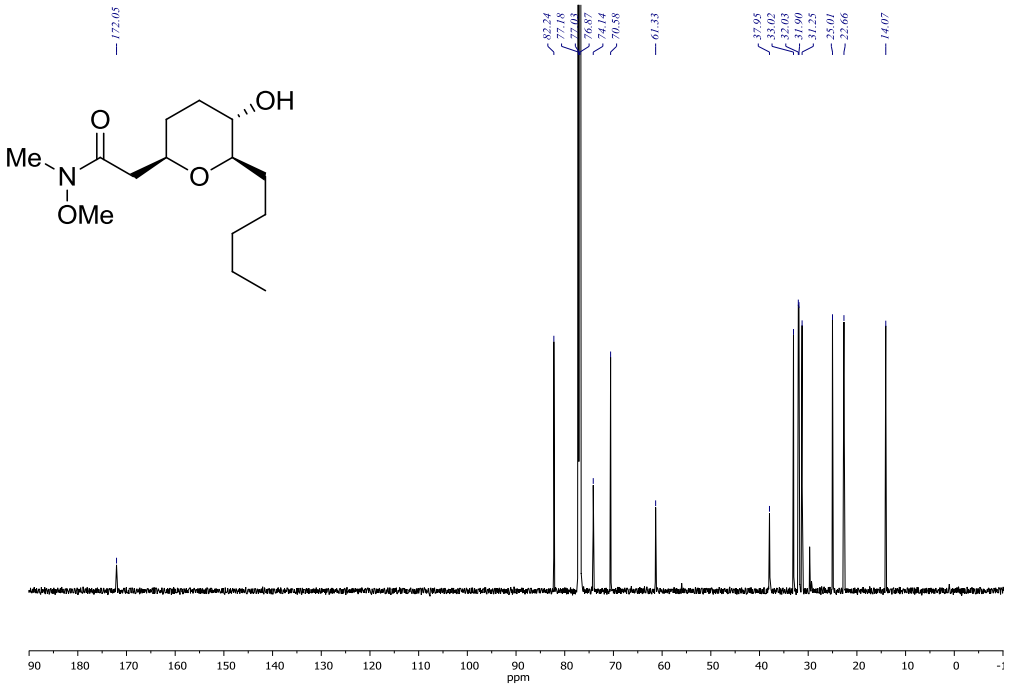

^{13}C NMR (200 MHz, $CDCl_3$) of Amide **1.48**

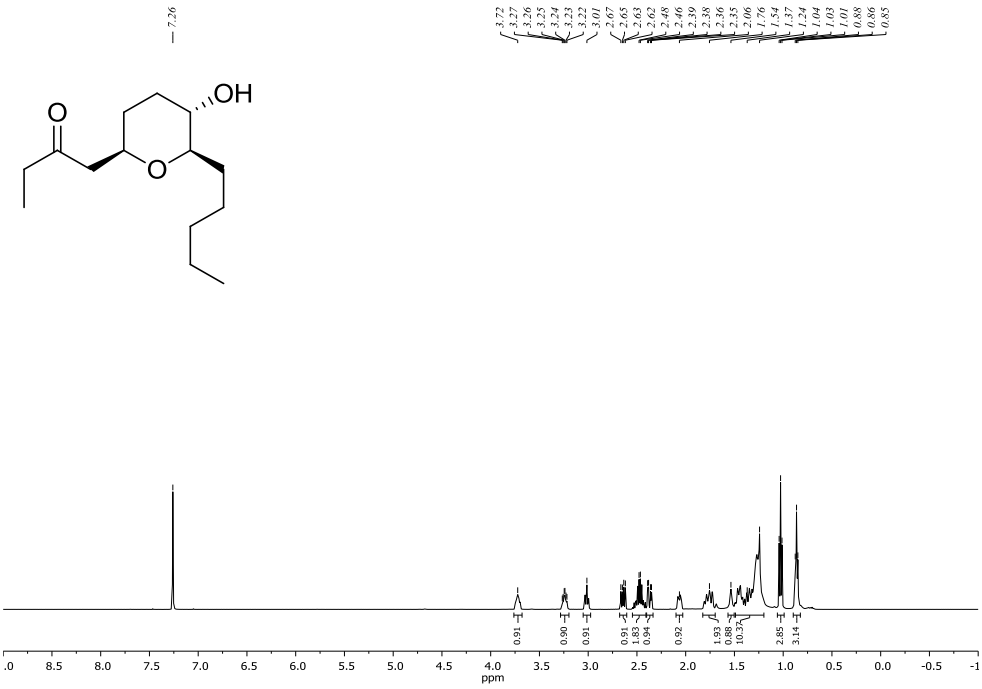

^{1}H NMR (500 MHz, $CDCl_3$) of Decytospolide A, **1.7**

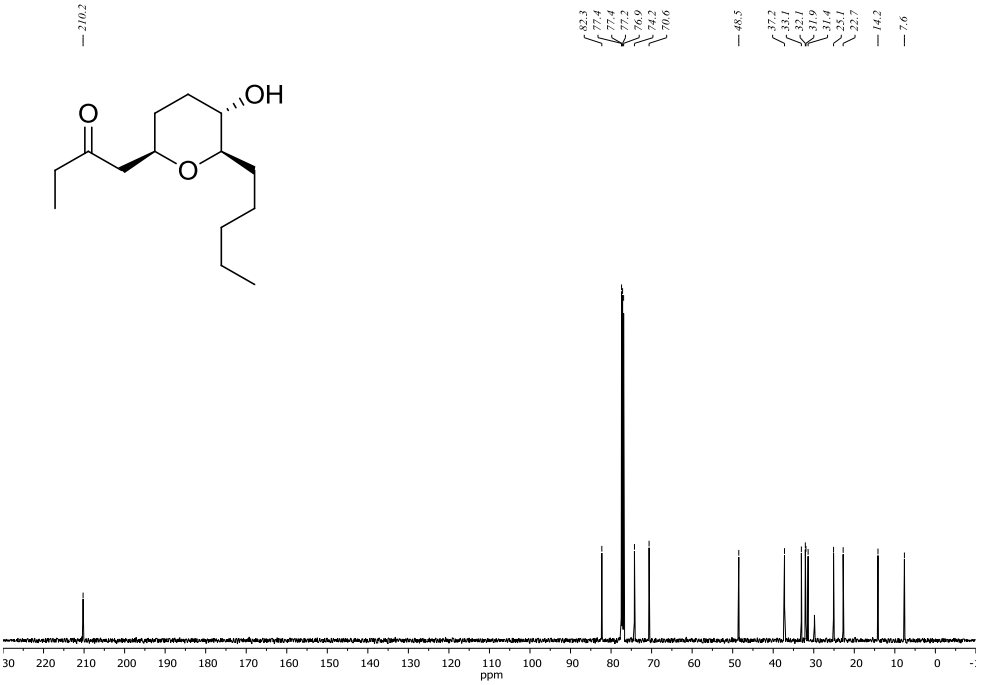

^{13}C NMR (125 MHz, $CDCl_3$) of Decytospolide A, **1.7**

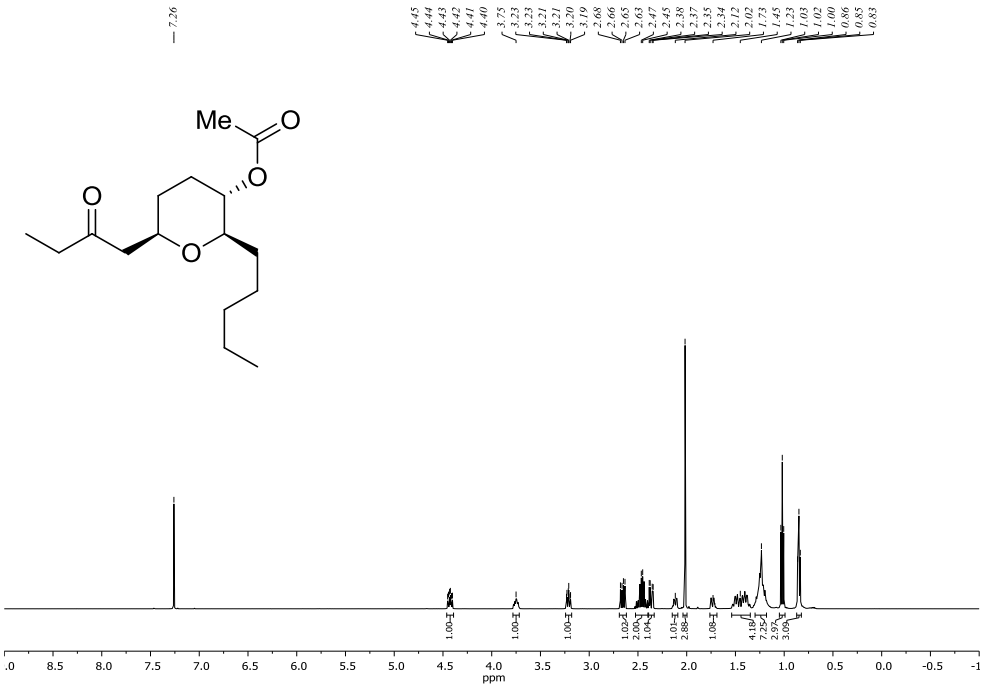

^{1}H NMR (500 MHz, $CDCl_3$) of Decytospolide B, **1.8**

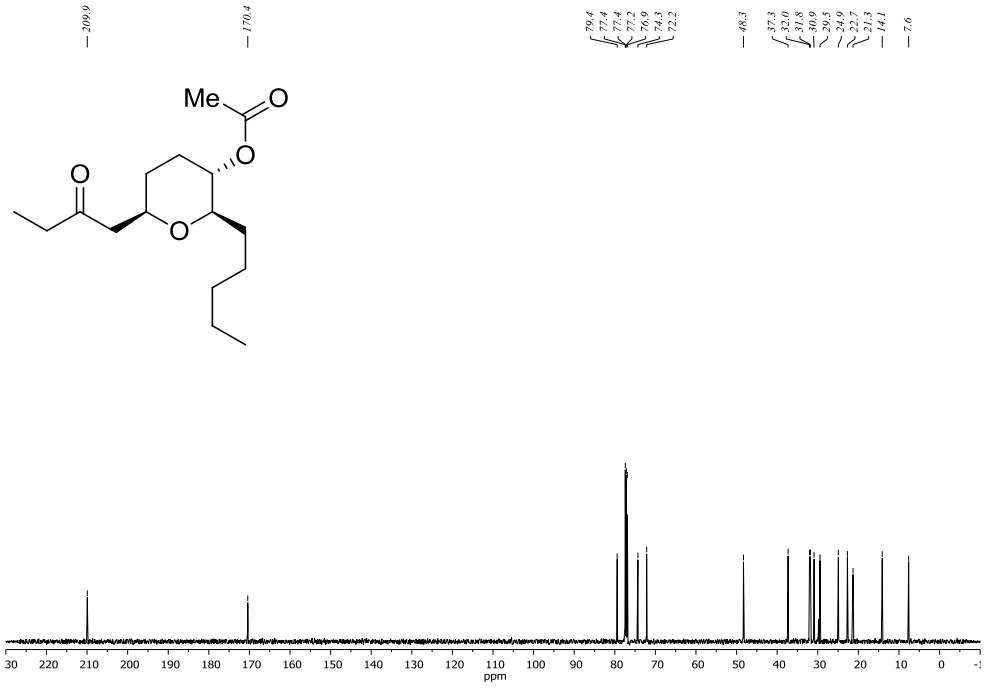

^{13}C NMR (125 MHz, $CDCl_3$) of Decytospolide B, **1.8**

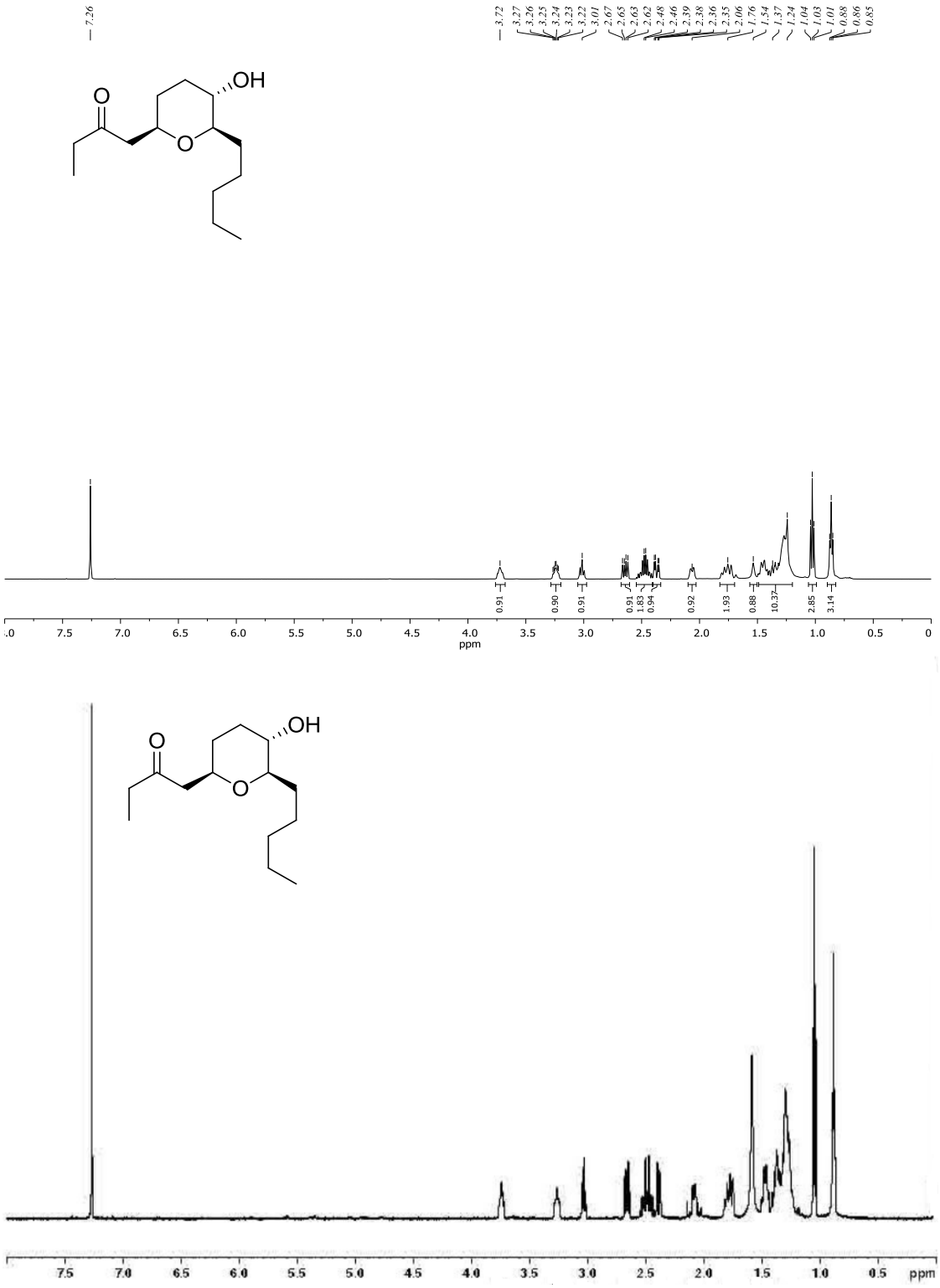

^{1}H NMR (500 MHz, $CDCl_3$) of Synthetic (top) and Natural (bottom) Decytospolide A, **1.7**

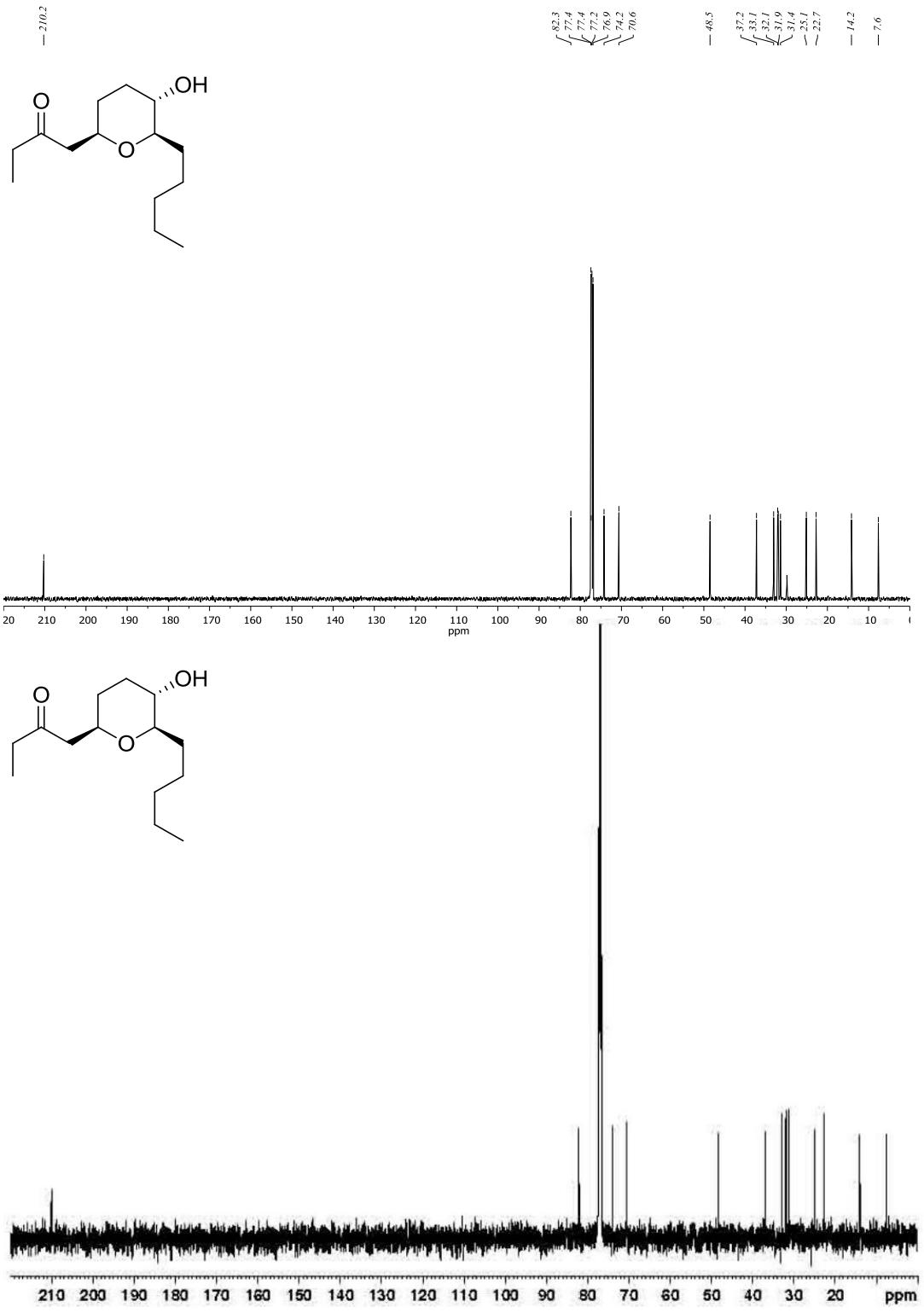

^{13}C NMR (125 MHz, $CDCl_3$) of Synthetic (top) and Natural (bottom) Decytospolide A, **1.7**

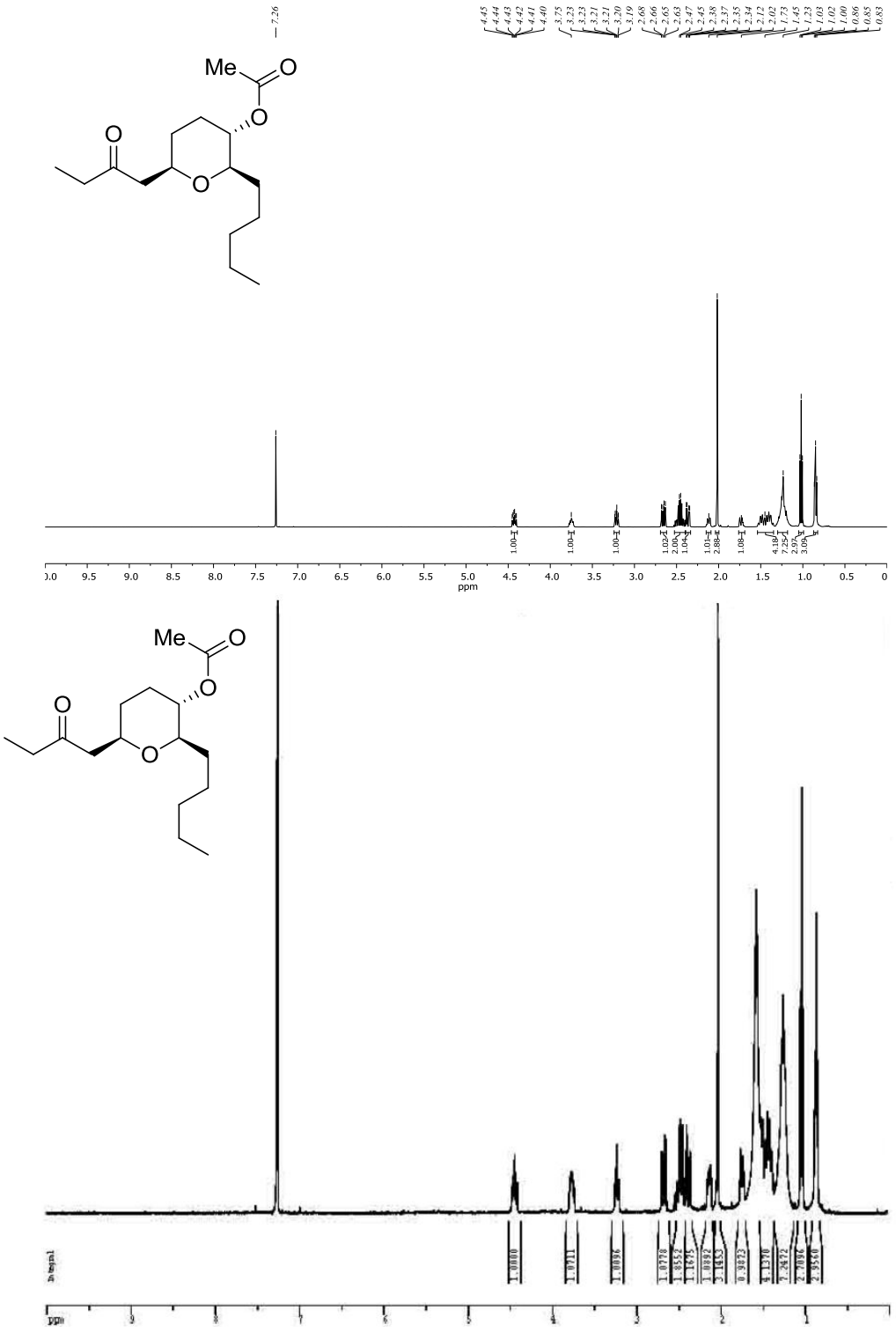

^{1}H NMR (500 MHz, $CDCl_3$) of Synthetic (top) and Natural (bottom) Decytospolide B, **1.8**

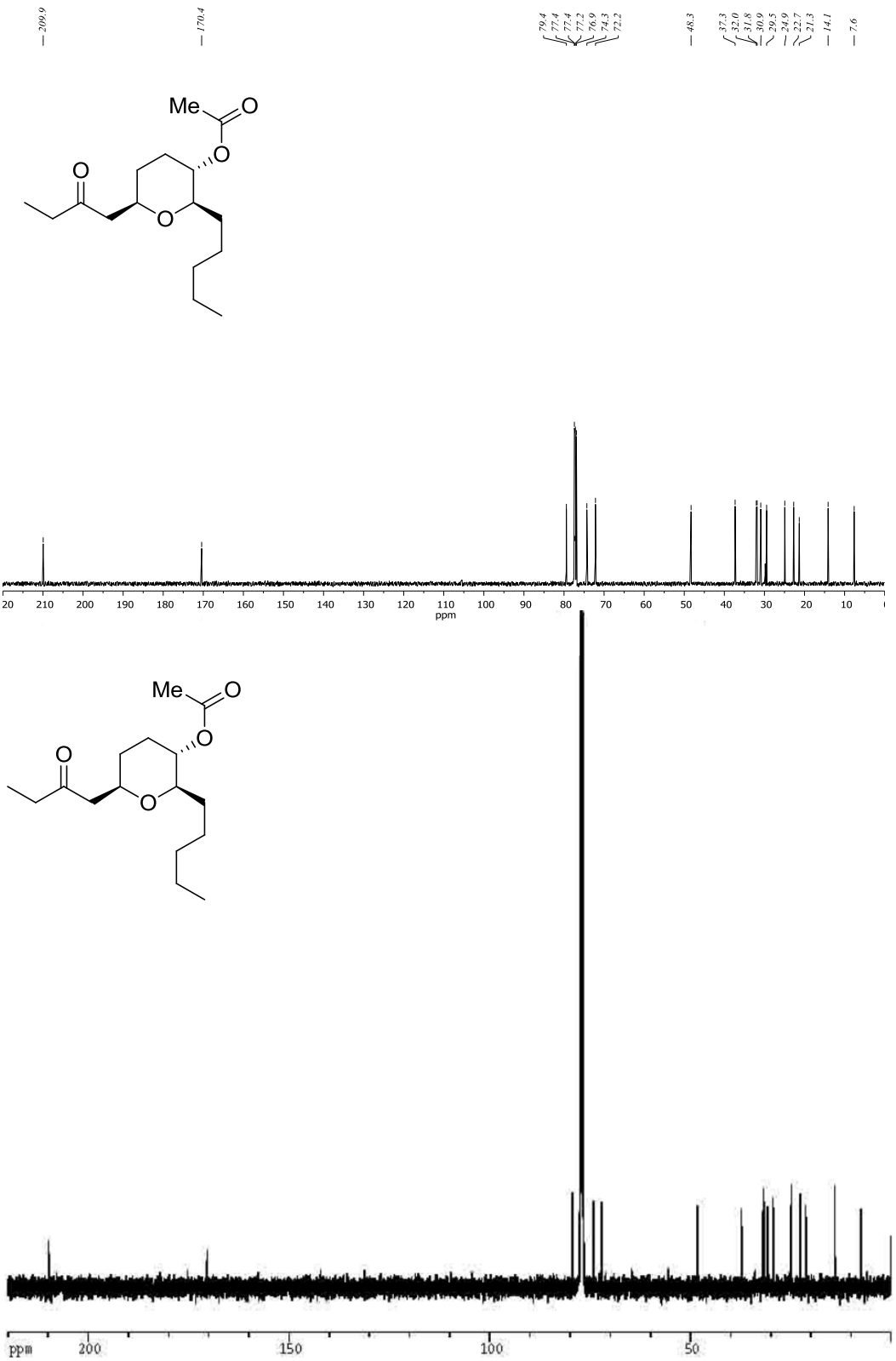

^{13}C NMR (125 MHz, $CDCl_3$) of Synthetic (top) and Natural (bottom) Decytospolide B, **1.8**

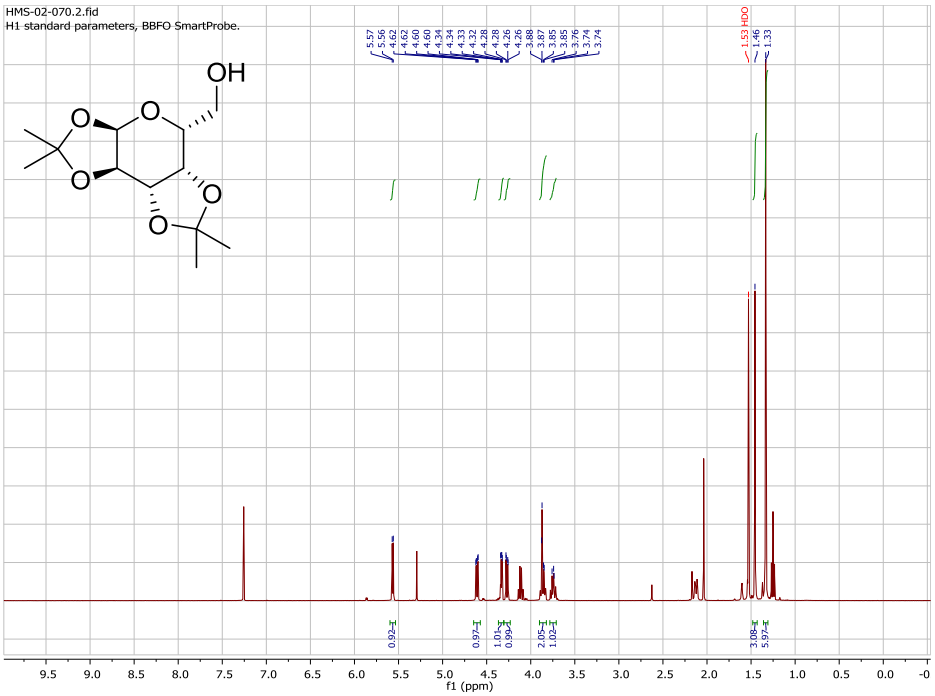

^{1}H NMR (400 MHz, $CDCl_3$) of Glycoside **2.27**

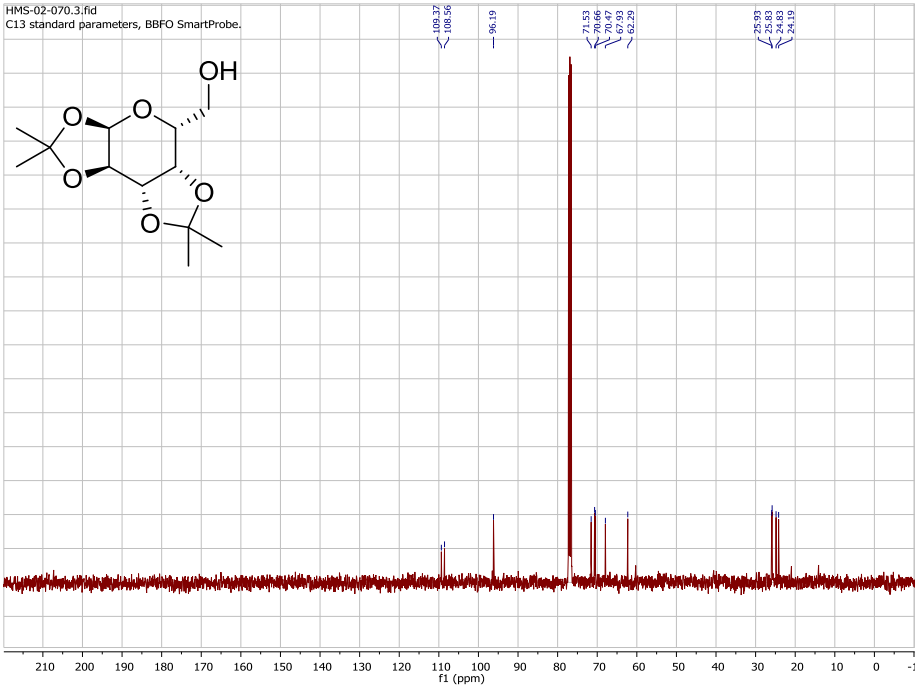

^{13}C NMR (100 MHz, $CDCl_3$) of Glycoside **2.27**

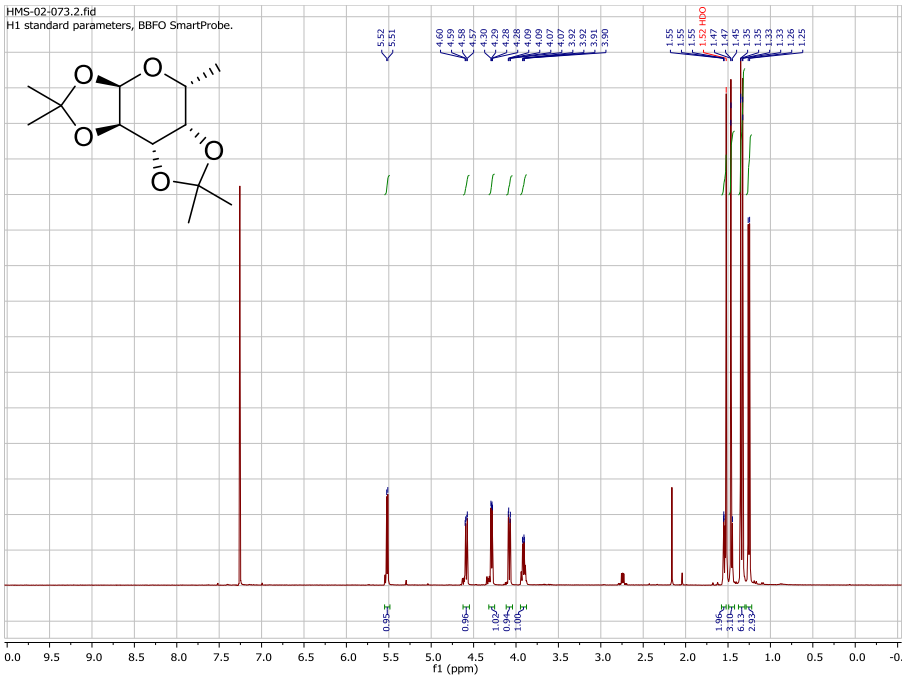

^{1}H NMR (400 MHz, $CDCl_3$) of Glycoside **2.28**

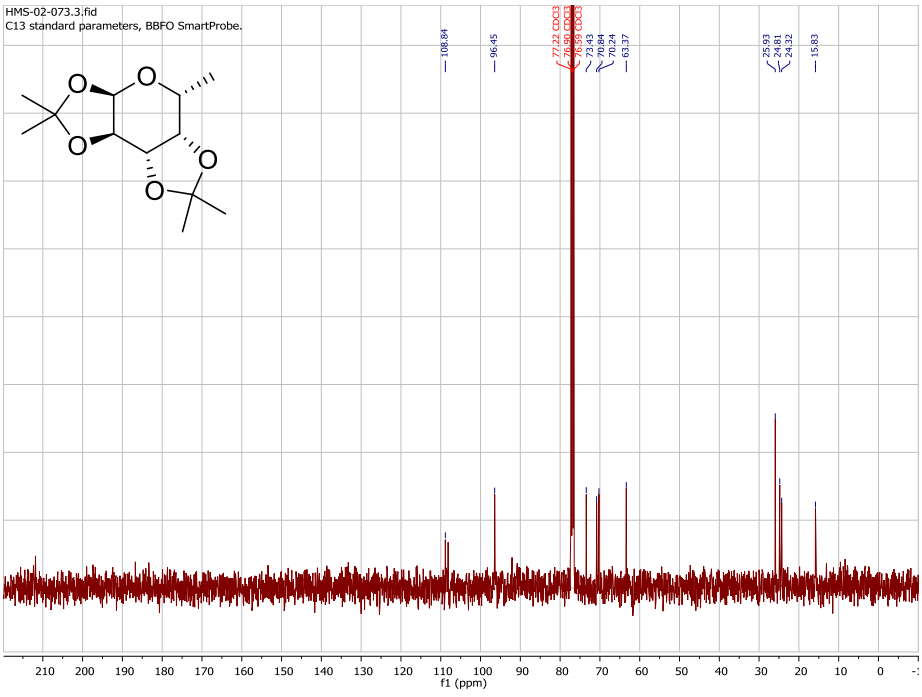

^{13}C NMR (100 MHz, $CDCl_3$) of Glycoside **2.28**

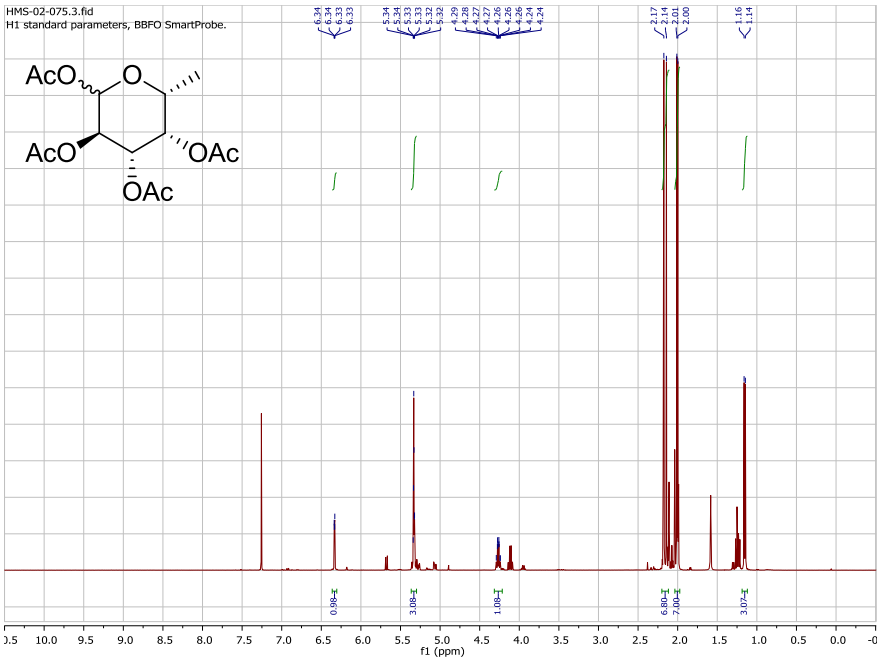

^{1}H NMR (400 MHz, $CDCl_3$) of Glycoside **2.25**

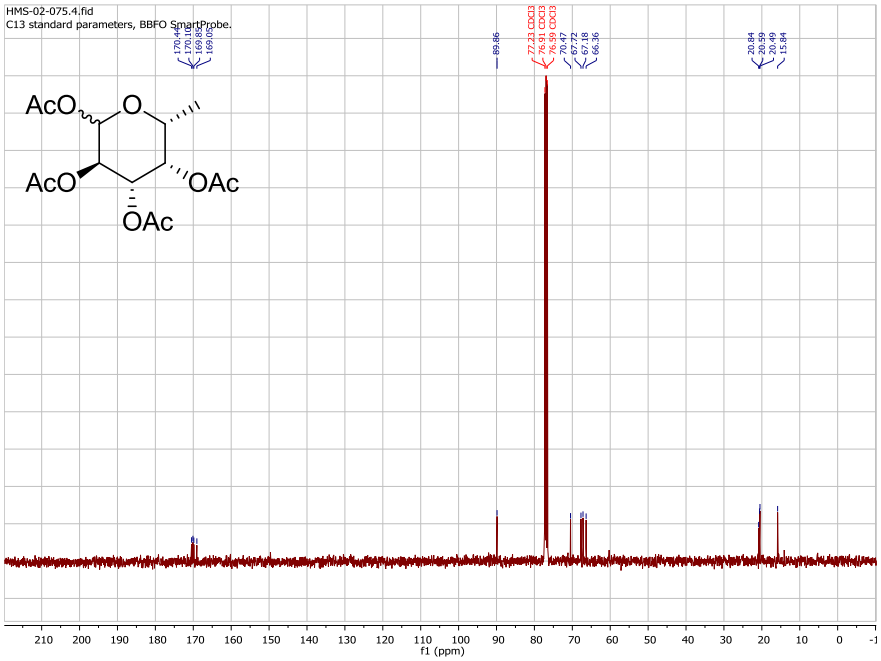

^{13}C NMR (100 MHz, $CDCl_3$) of Glycoside **2.25**

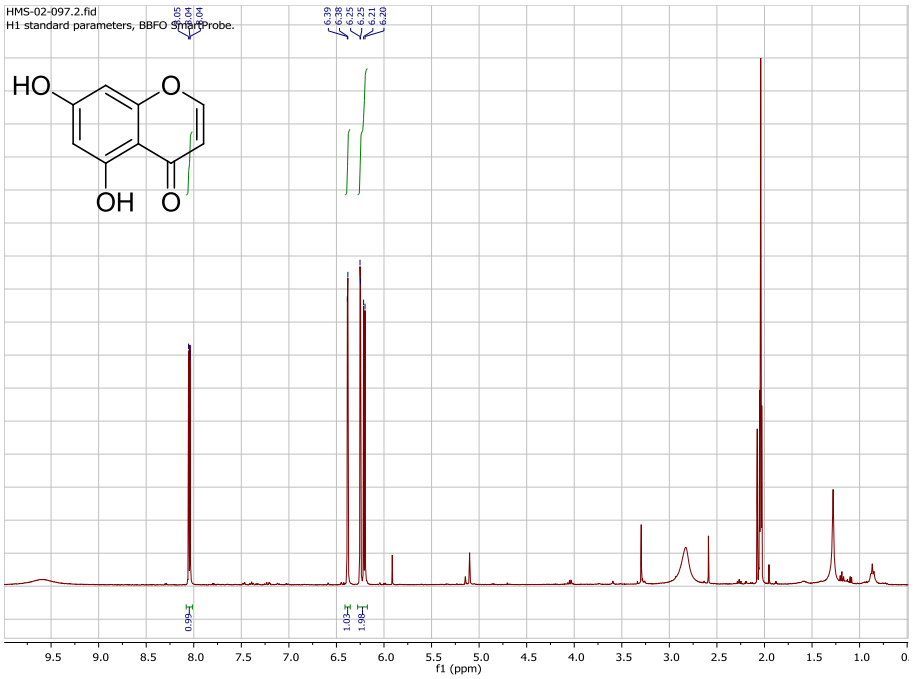

^{1}H NMR (400 MHz, acetone-d^6) of Chromone **2.24**

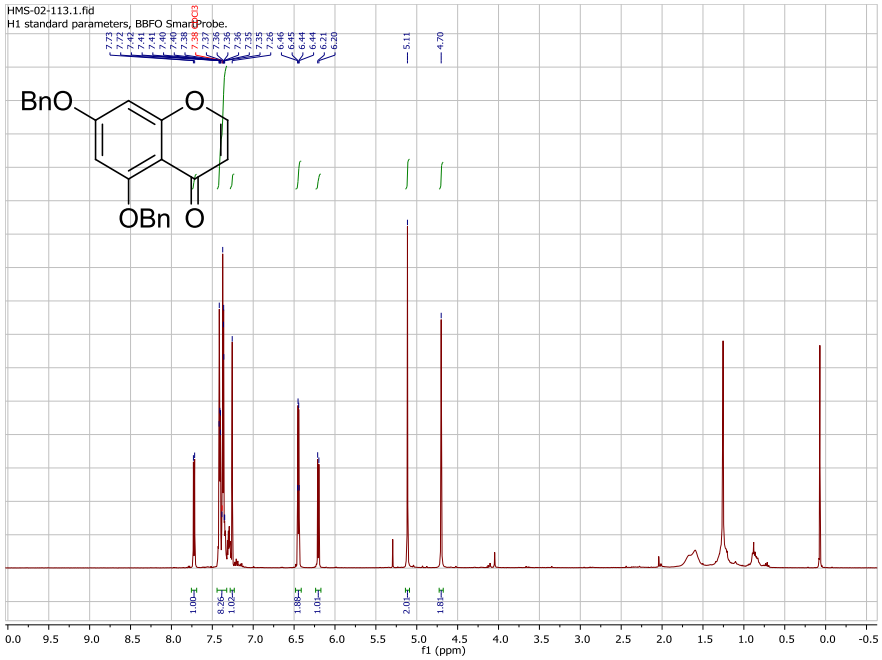

^{1}H NMR (400 MHz, $CDCl_3$) of Chromone **2.30**

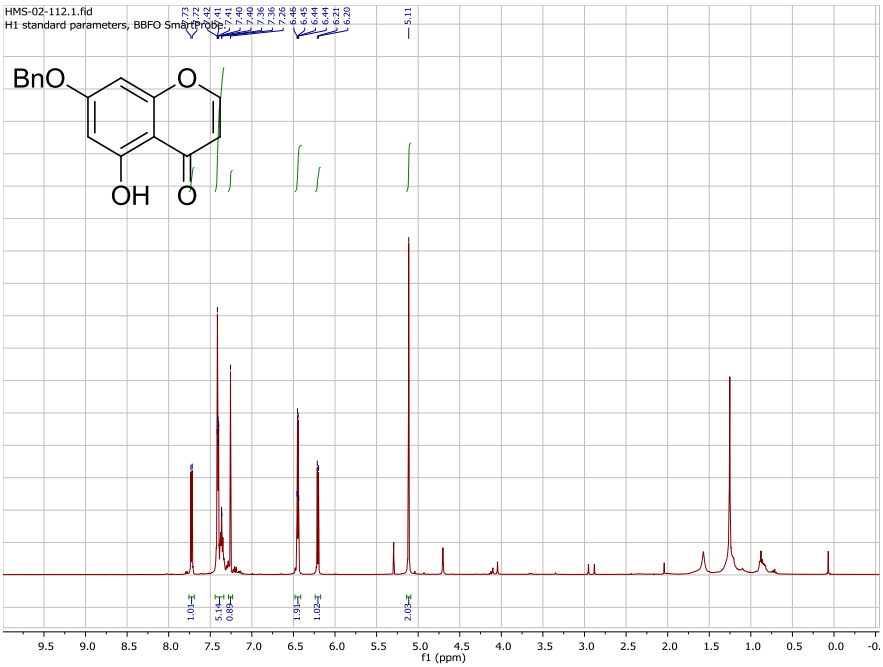

^{1}H NMR (400 MHz, $CDCl_3$) of Chromone **2.31**

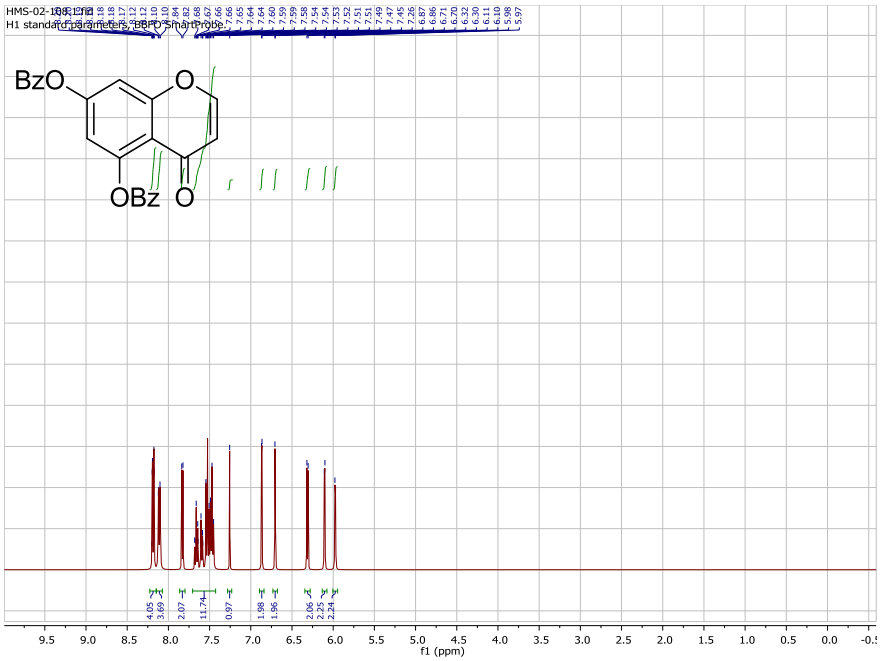

^{1}H NMR (400 MHz, $CDCl_3$) of Chromone **2.32**

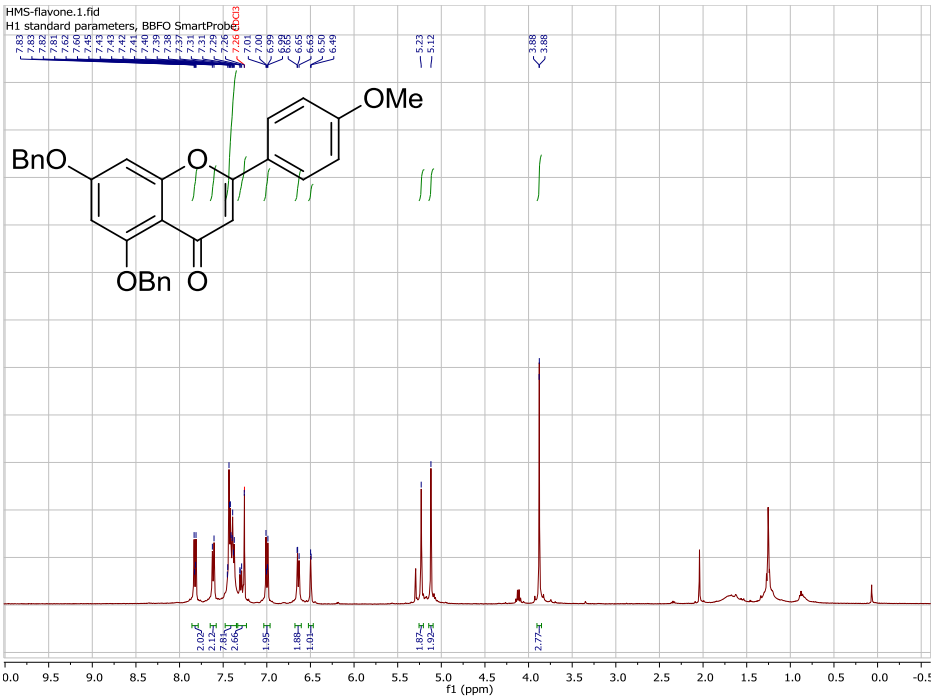

^{1}H NMR (400 MHz, $CDCl_3$) of Flavone **2.33**

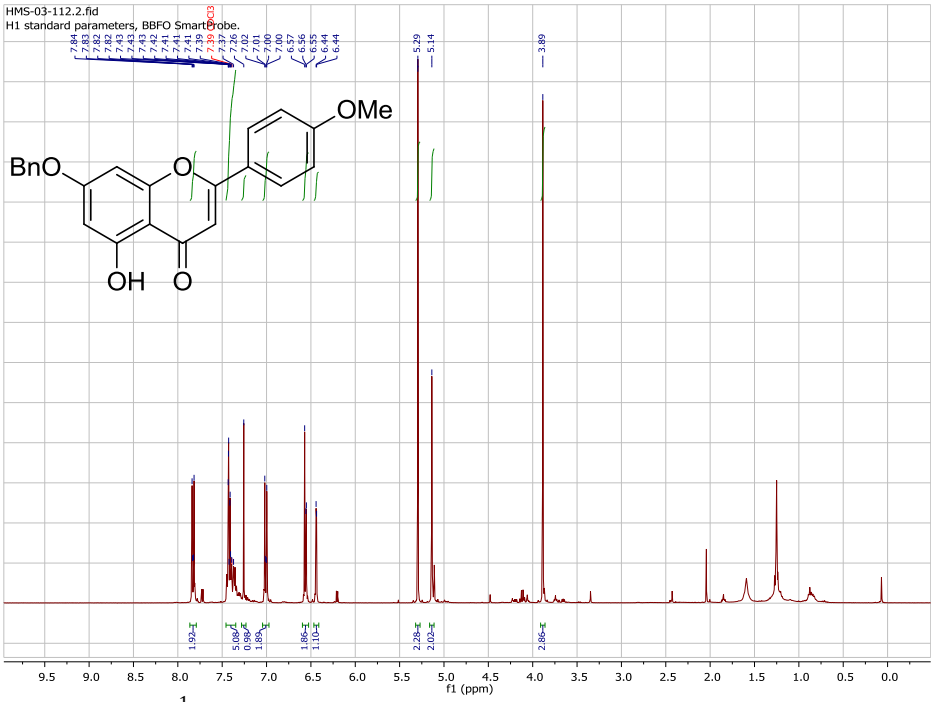

^{1}H NMR (400 MHz, $CDCl_3$) of Flavone **2.23**

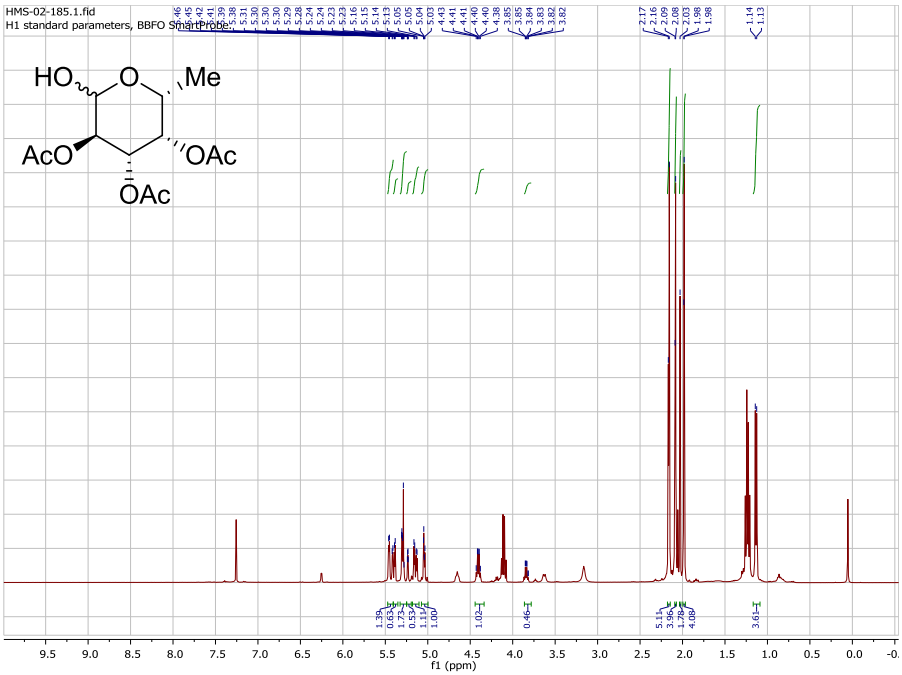

^{1}H NMR (400 MHz, $CDCl_3$) of Glycoside **2.34**

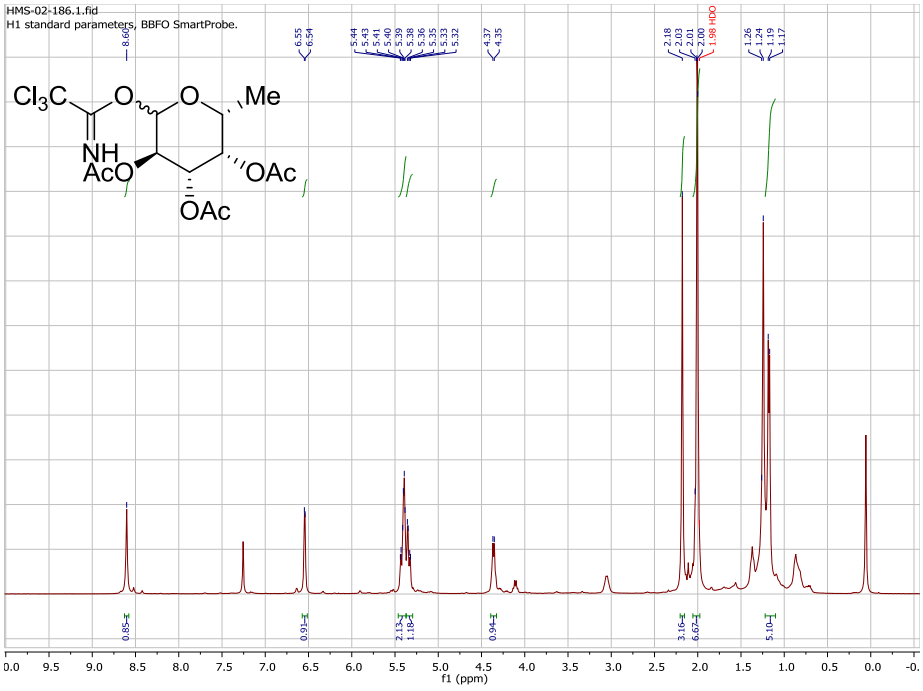

^{1}H NMR (400 MHz, $CDCl_3$) of Glycoside **2.35**

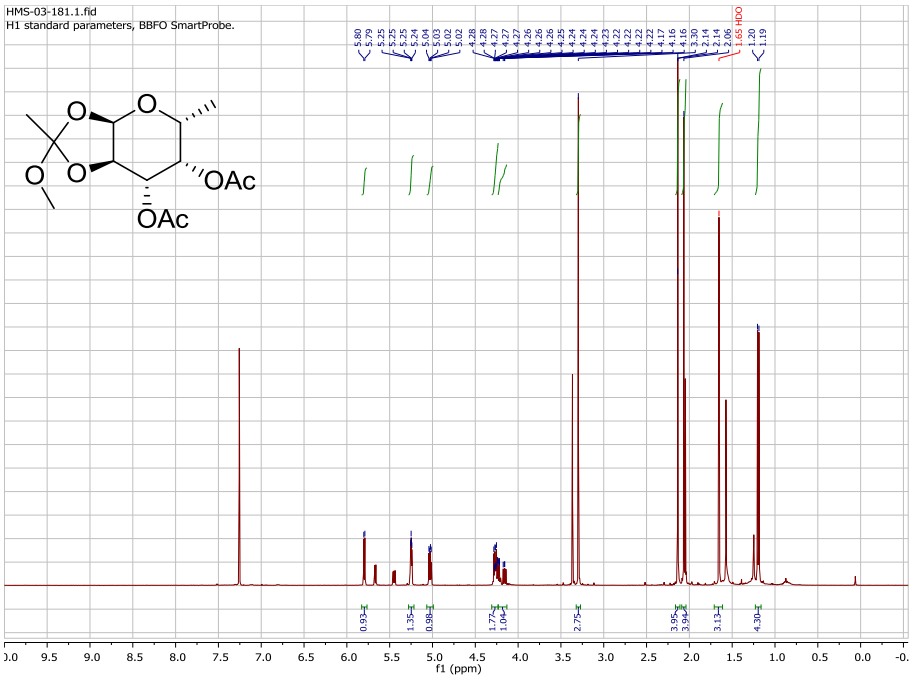

^{1}H NMR (400 MHz, $CDCl_3$) of Glycoside **2.36**

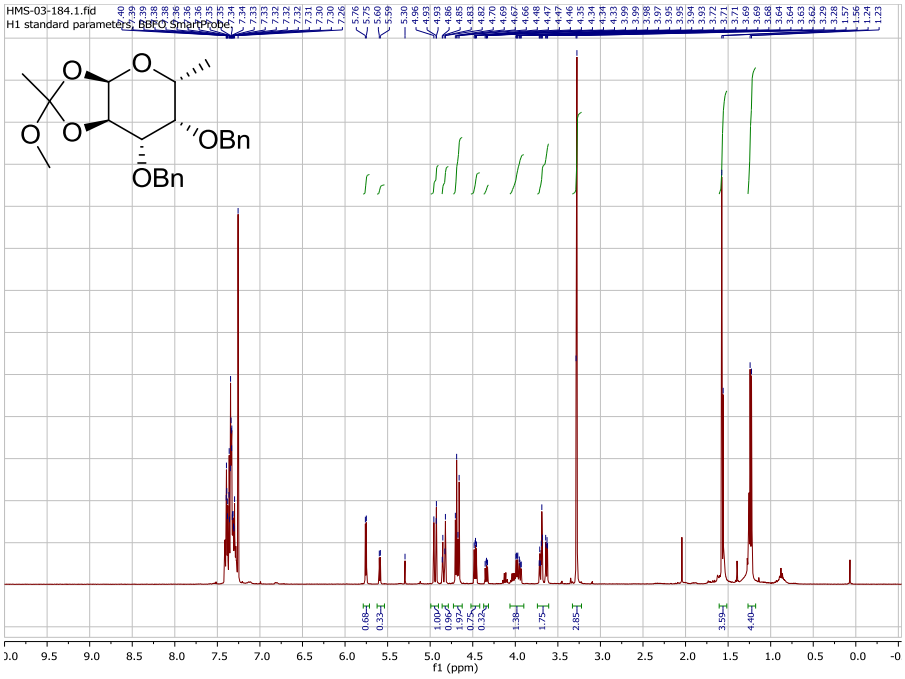

^{1}H NMR (400 MHz, $CDCl_3$) of Glycoside **2.37**

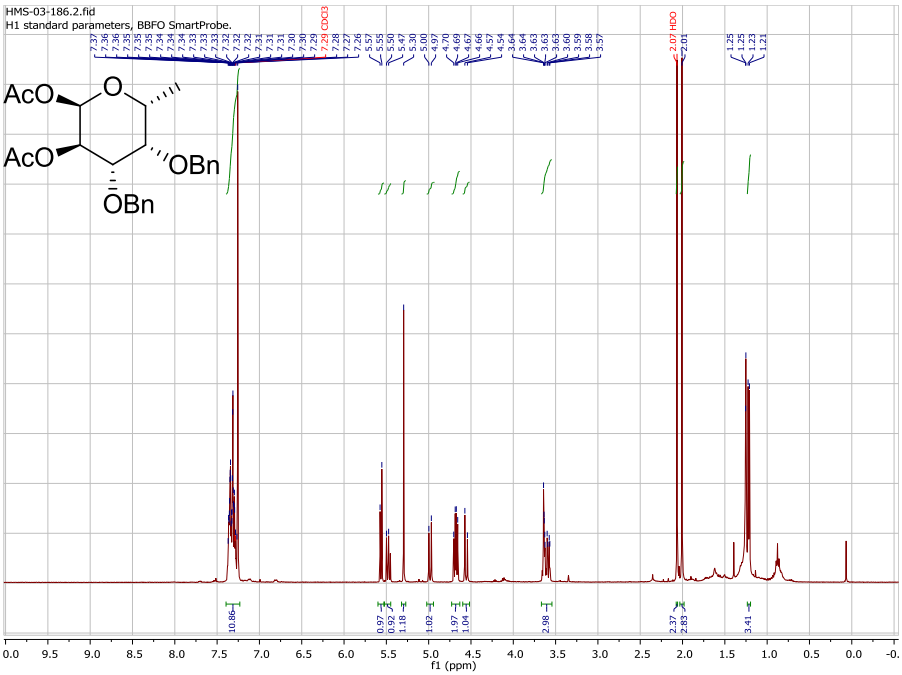

^{1}H NMR (400 MHz, $CDCl_3$) of Glycoside **2.38**

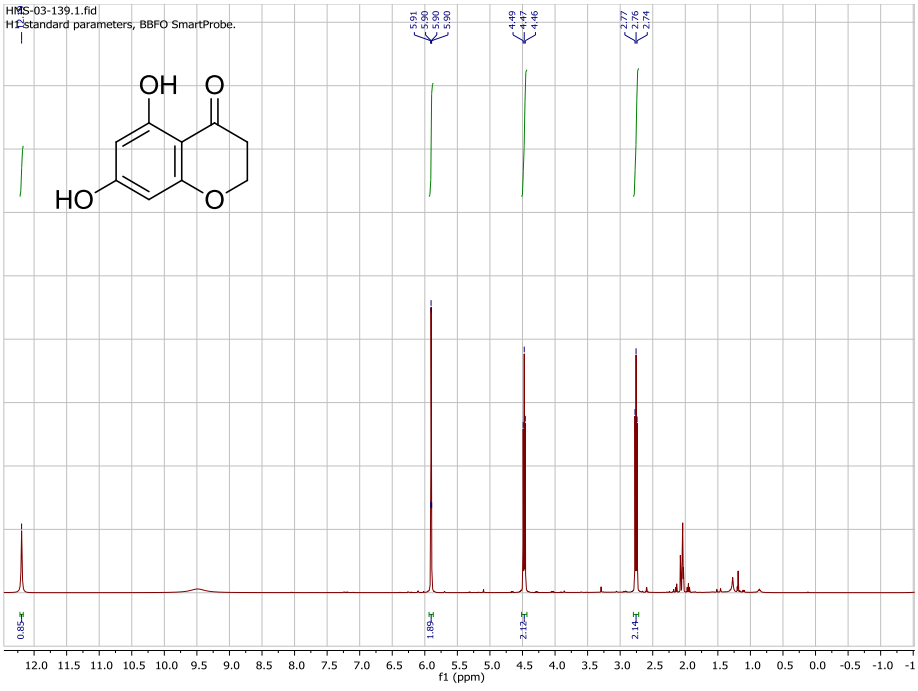

^{1}H NMR (400 MHz, (acetone-d^6) of Chromanone **2.39**

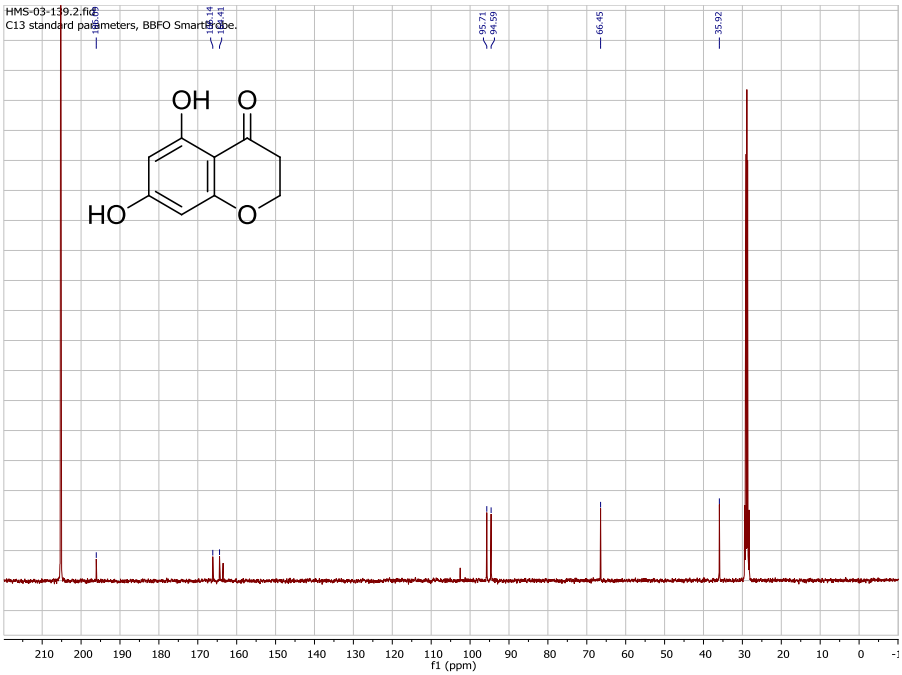

^{13}C NMR (100 MHz, (acetone-d^6) of Chromanone **2.39**

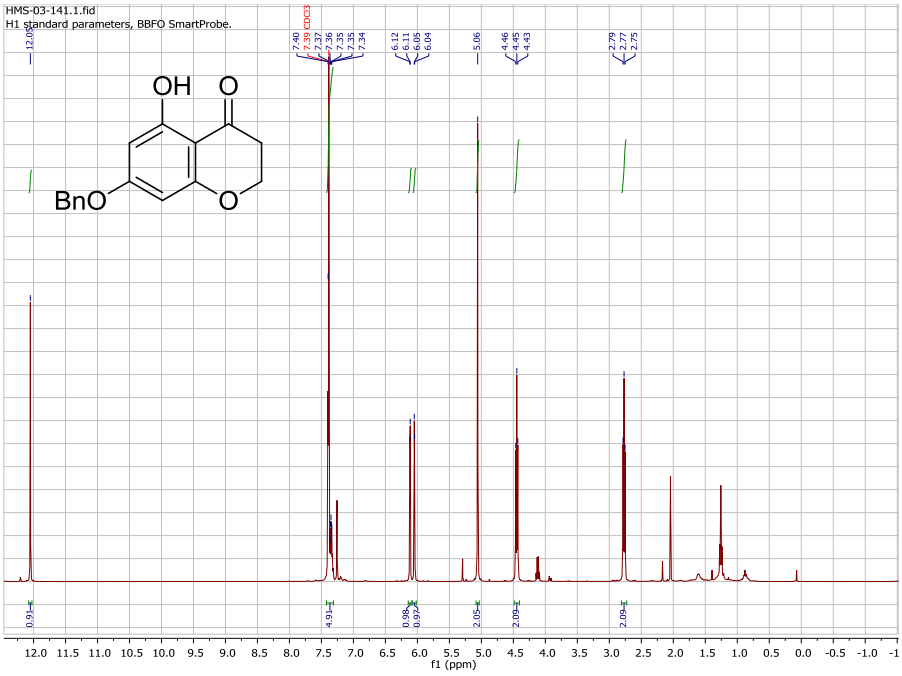

^{1}H NMR (400 MHz, $CDCl_3$) of Chromanone **2.40**

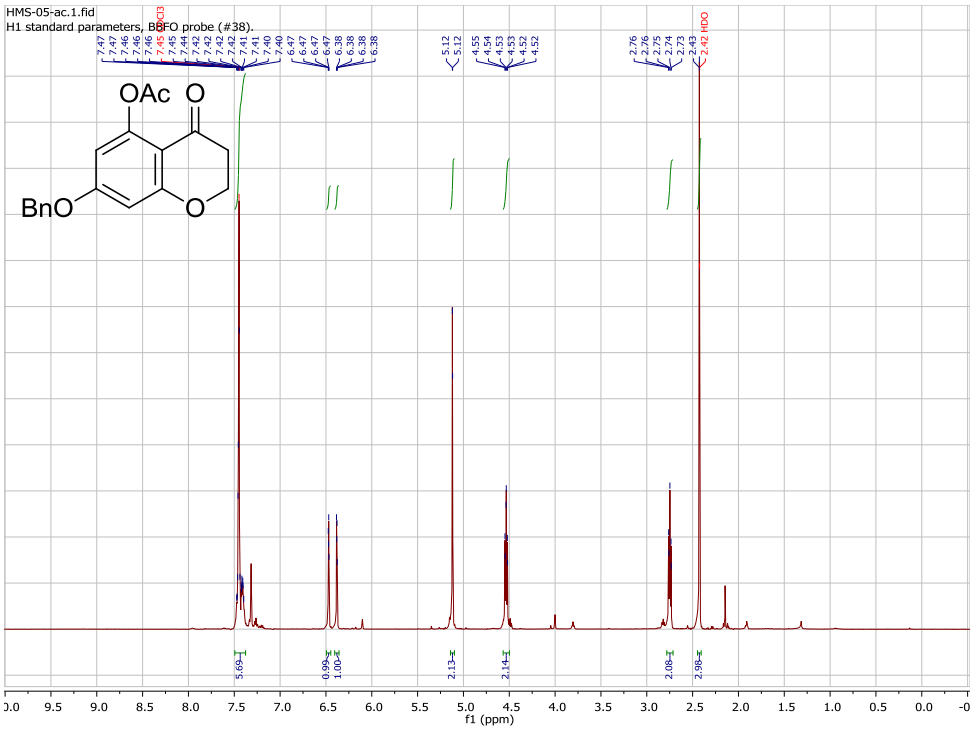

^{1}H NMR (500 MHz, $CDCl_3$) of Chromanone **2.43**

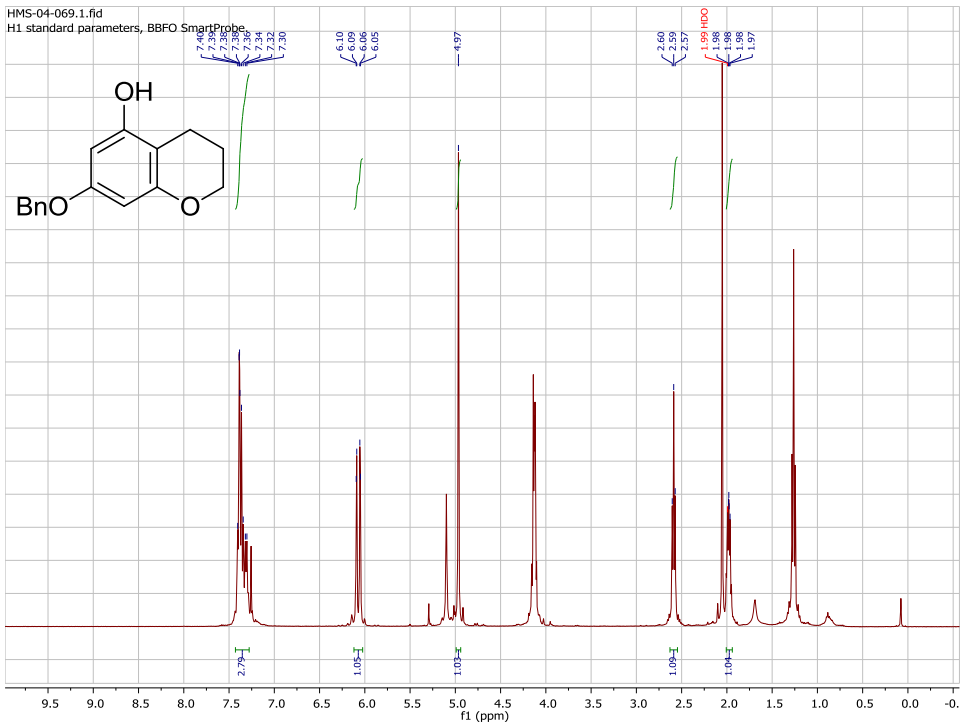

^{1}H NMR (400 MHz, $CDCl_3$) of Chroman **2.42**

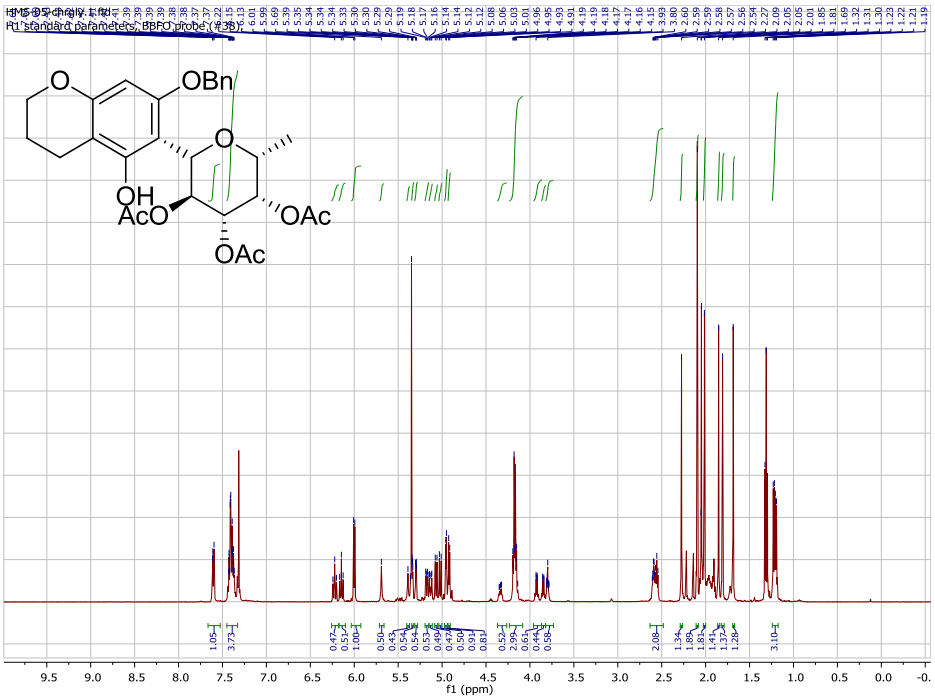

^{1}H NMR (500 MHz, $CDCl_3$) of Chroman **2.41**

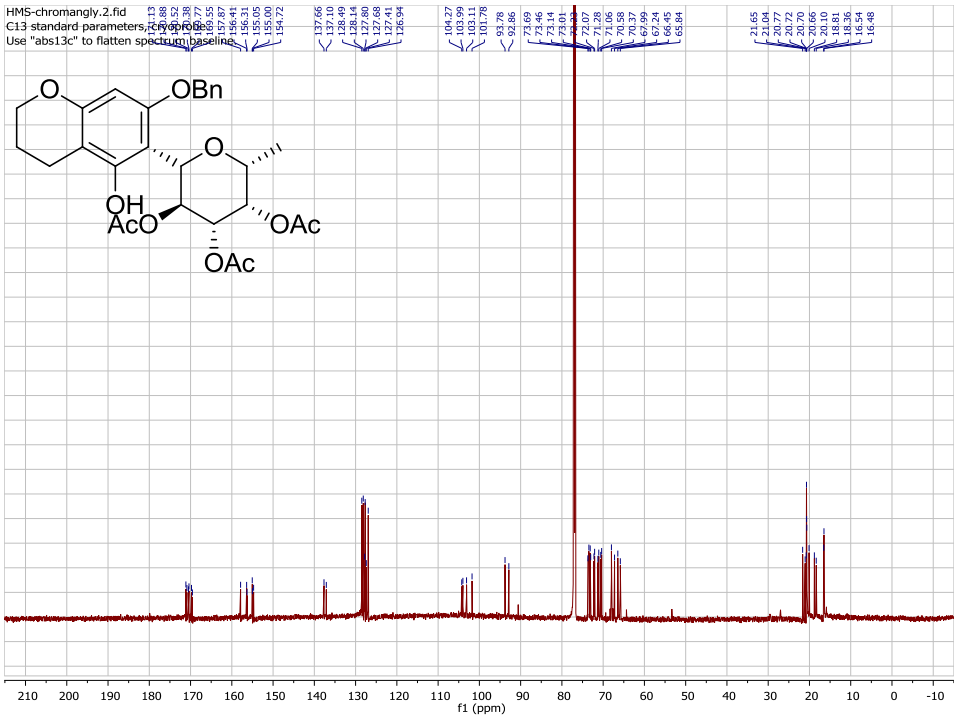

^{13}C NMR (200 MHz, $CDCl_3$) of Chroman **2.41**

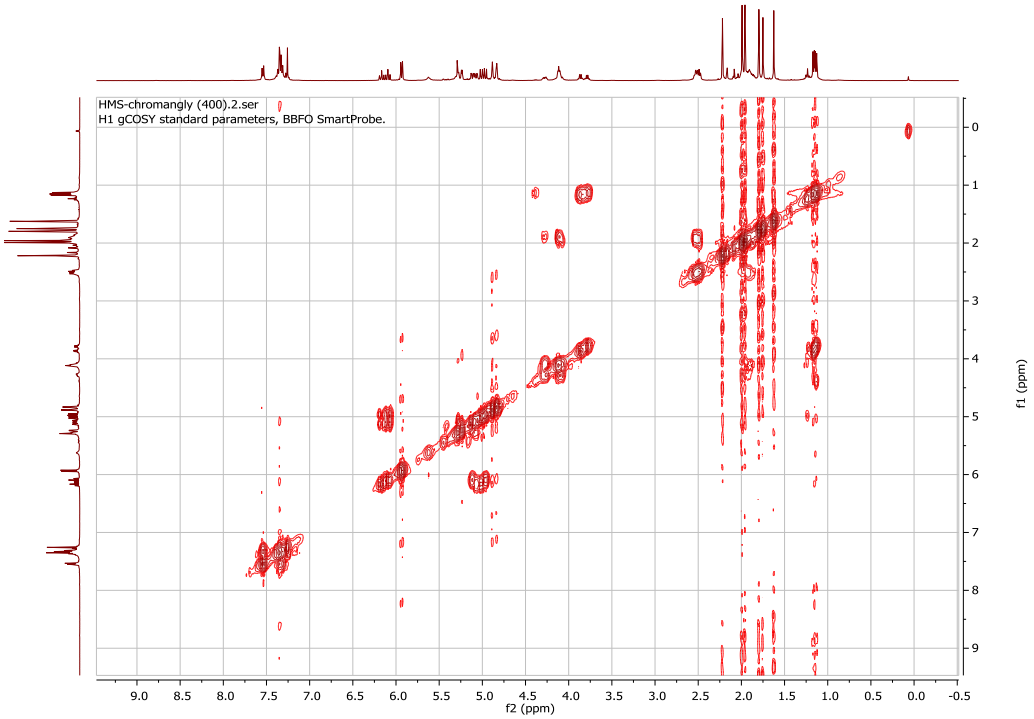

COSY NMR (400 MHz, $CDCl_3$) of Chroman **2.41**

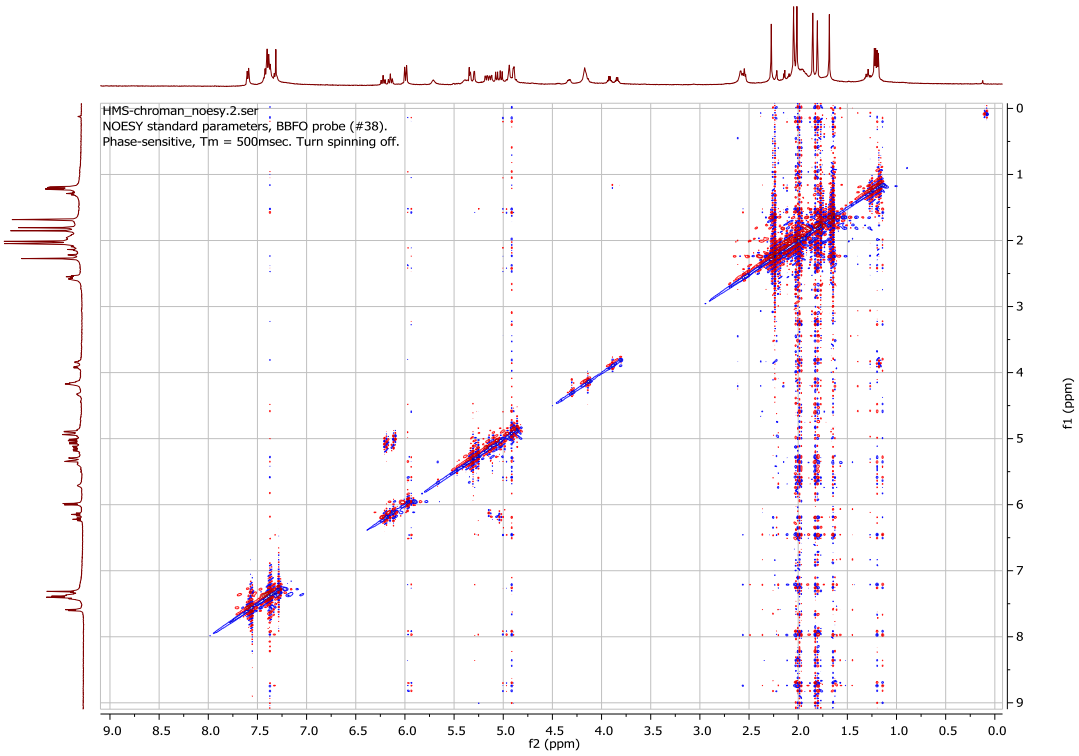

NOESY NMR (500 MHz, $CDCl_3$) of Chroman **2.41**

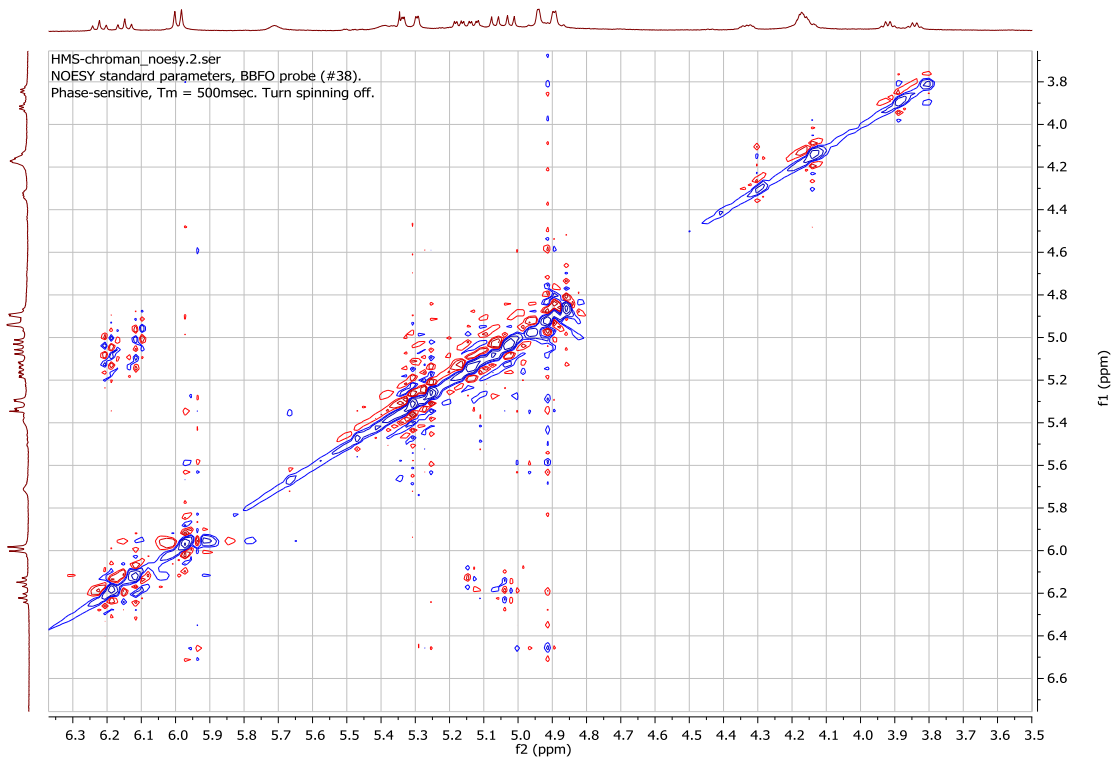

NOESY NMR (500 MHz, $CDCl_3$) of Chroman **2.41** (zoomed in on glycoside region)

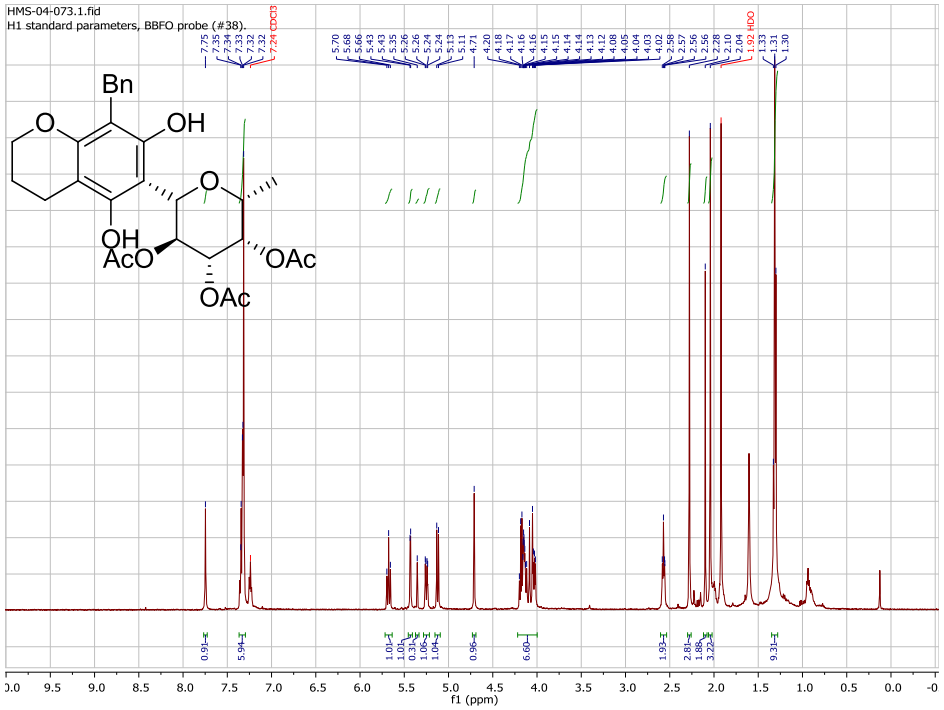

^{1}H NMR (500 MHz, $CDCl_3$) of Chroman **2.44**

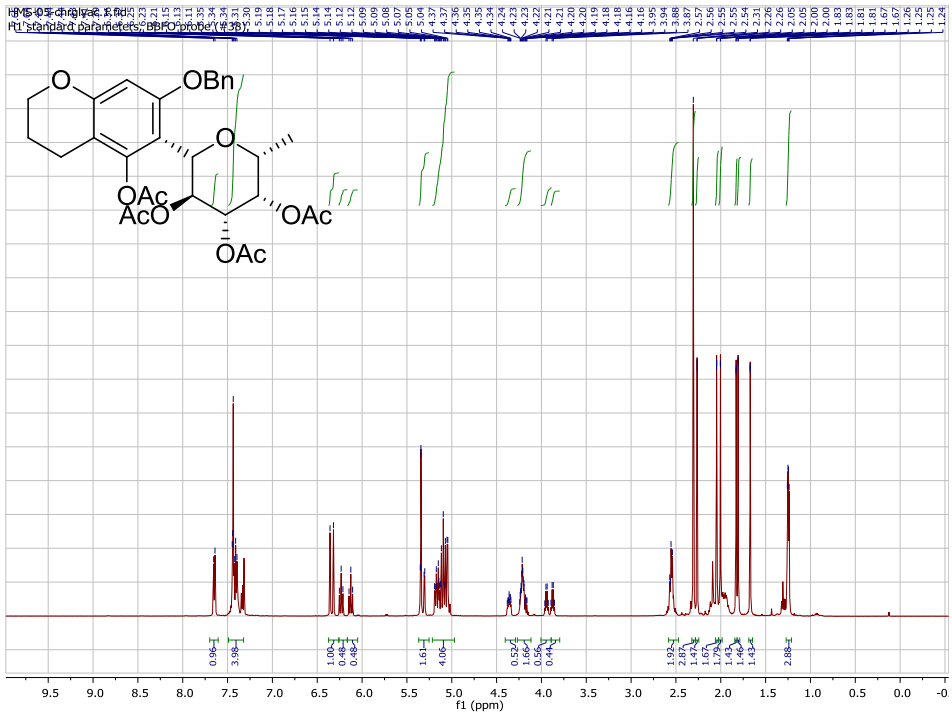

^{1}H NMR (500 MHz, $CDCl_3$) of Chroman **2.45**

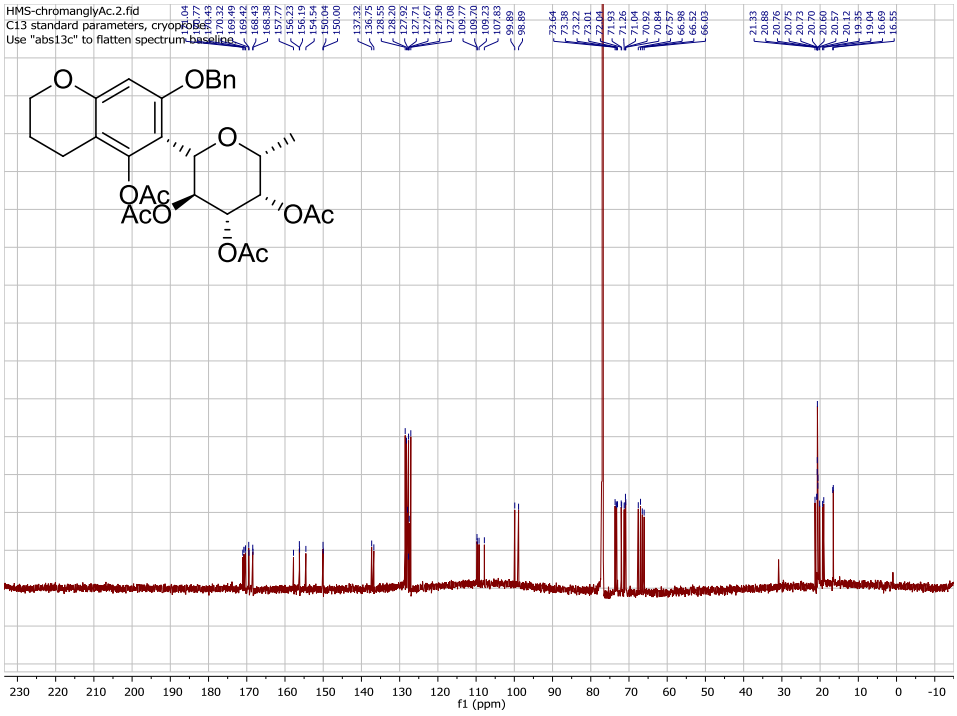

^{13}C NMR (200 MHz, $CDCl_3$) of Chroman **2.45**

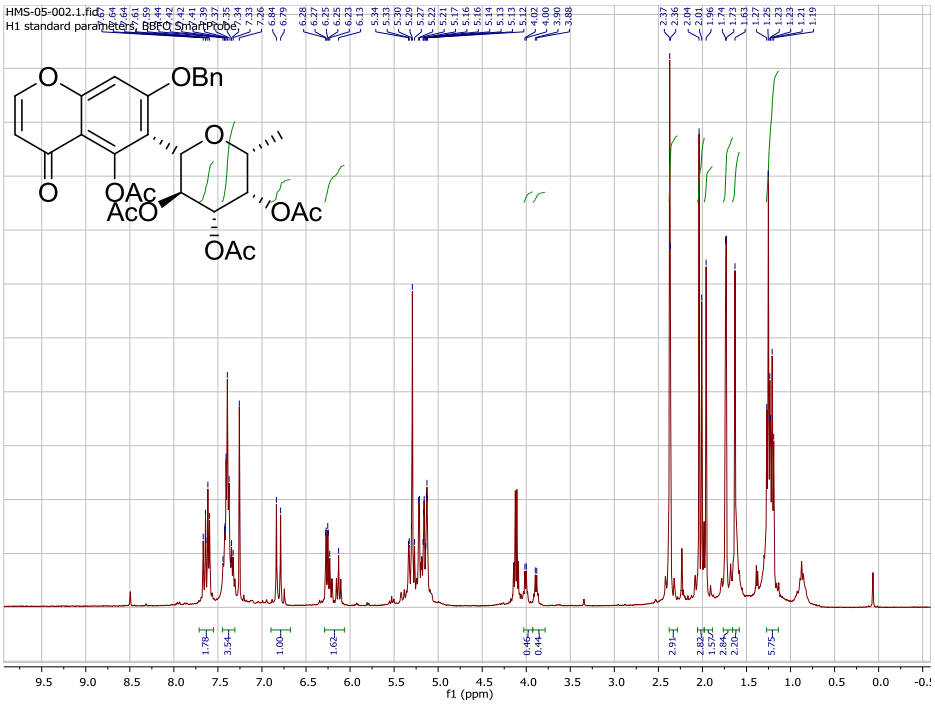

^{1}H NMR (400 MHz, $CDCl_3$) of Chromone **2.46**

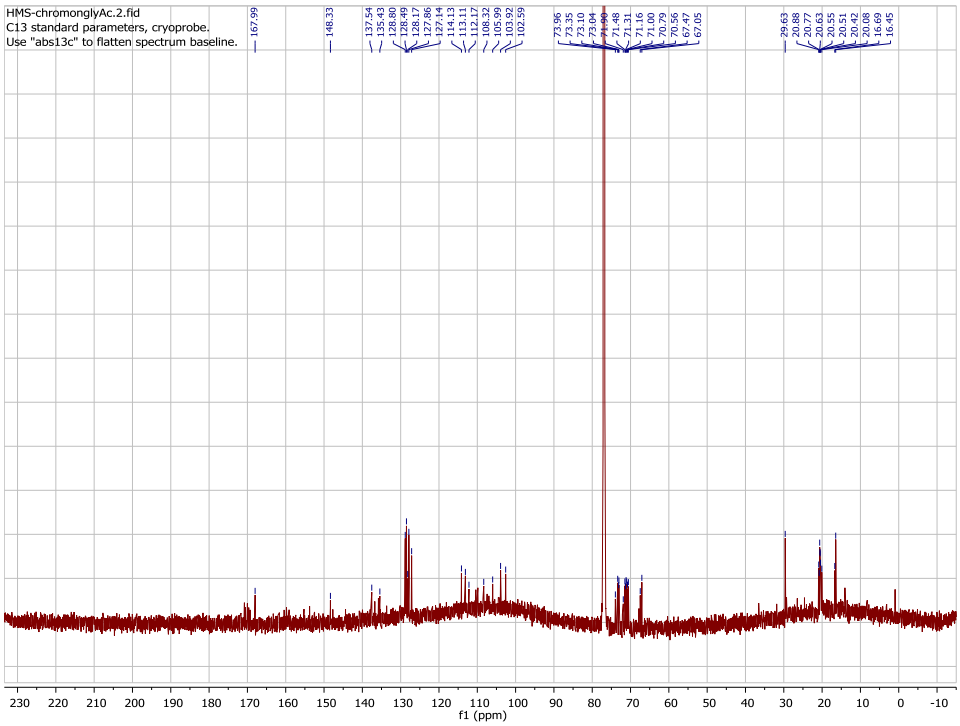

^{13}C NMR (125 MHz, $CDCl_3$) of Chroman **2.46**

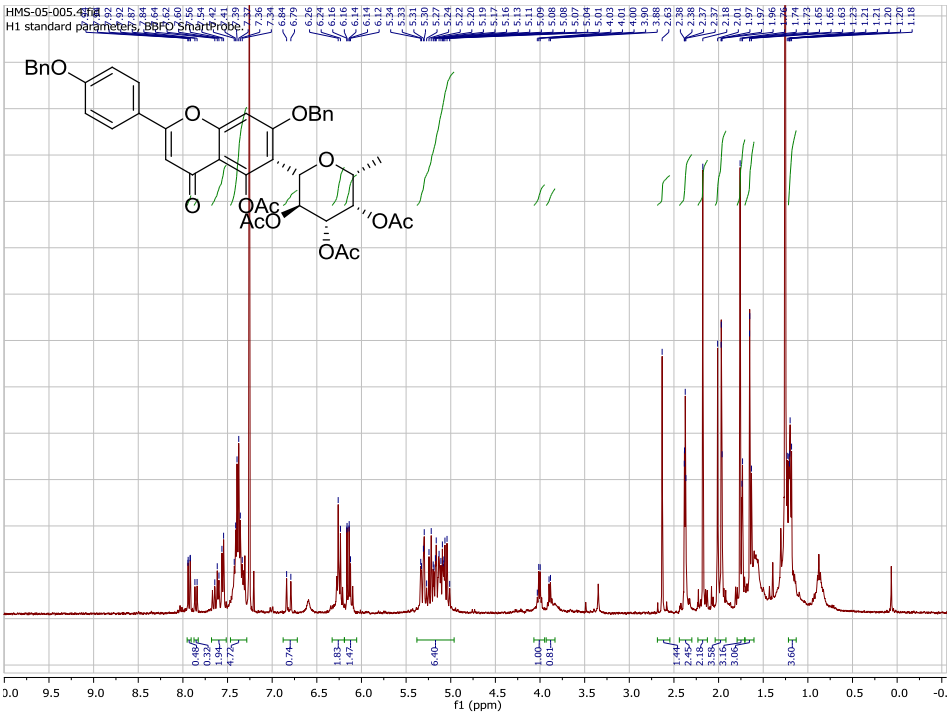

^{1}H NMR (400 MHz, $CDCl_3$) of Flavone **2.47**

REFERENCES

[1] E. J. Kang and E. Lee, *Chem. Rev.*, 2005, **105**, 4348-4378.

[2] K. S. Yeung and I. Paterson, *Chem. Rev.*, 2005, **105**, 4237-4313.

[3] H. Fuwa *Mar. Drugs*, 2016, **14**, 65.

[4] N. M. Nasir, K. Ermanis and P. A. Clarke *Org. Biomol. Chem.* 2014, **12**, 3323-3335.

[5] M. A. Brimble, K. P. Kaliappan, A. J. Moreno-Vargas, K. Palanichamy, M. A. Perry, J. D. Rainier, S. D.Rychnovsky, N. Sizemore, L. A. Stubbing, P. Vogel, *Synthesis of saturated oxygenated heterocycles. I, 5- and 6-membered rings*, Springer Berlin 2014.

[6] B. G. Isaac, S. W. Ayer, R. C. Elliott, R. J. Stonard, *J. Org. Chem.* 1992**, 57** 7220-7226.

[7] B. Thirupathi, M. K. Zilla, *ChemistrySelect* 2019, **4**, 11944-11958.

[8] D. Kaida, H. Motoyoshi, E. Tashiro, T. Nojima, M. Hagiwara, K. Ishigami, H. Watanabe, T. Kitahara, T. Yoshida, H. Nakajima, T. Tani, S. Horinouchi, M. Yoshida, *Nat. Chem. Biol.* 2007, **3,** 576–583.

[9] T. Kuranaga, T. Shirai, D. G. Baden, J. L. Wright, M. Satake, K. Tachibana, *Org Lett*. 2009, **11**, 217-220.

[10] A. E. Wright, J. C. Botelho, E. Guzman, D. Harmody, P. Linley, P. J. McCarthy, T. P. Pitts, S. A. Pomponi, J. K. Reed, *J. Nat. Prod*. 2007, **70**, 412.

[11] R. H. Cichewicz, F. A. Valeriote, P. Crews, *Org. Lett.* 2004, **6**, 1951-1954.

[12] K. Kito, R. Ookura, S. Yoshida, M. Namikoshi, T. Ooi, Y. Kusumi, *Org. Lett.* 2008, **10**, 225– 228.

[13] G. Dräger, A. Kirschning, R. Thierickeb, M. Zerlin., M. *Nat. Prod. Rep*. 1996, **13**, 365– 375.

[14] A. Evidente, A. Cimmino, A. Berestetskiy, A. Andolfi, A. J. Motta, *Nat. Prod*. 2008, **71**, 1897– 1901.

[15] O. Yuzikhin, G. Mitina, A. Berestetskiy, *J. Agric. Food Chem*. 2007, **55**, 7707– 7711.

[16] J. F. Rivero-Cruz, G. García-Aguirre, C. Cerda-García-Rojas, R. Mata, *Tetrahedron* 2000, **56**, 5337– 5344.

[17] A. Evidente, R. Capasso, A. Andolfi, M. Vurro, M. C. Zonno, *Phytochemistry* 1998, **48**, 941– 945.

[18] V. Rukachaisirikul, S. Pramjit, C. Pakawatchai, M. Isaka, S. Supothina, *J. Nat. Prod.* 2004, **67**, 1953– 1955.

[19] S. Boonphong, P. Kittakoop, M. Isaka, D. Pittayakhajonwut, M. Tanticharoen, Y. Thebtaranonth, *J. Nat. Prod.* 2001, **64**, 965– 967.

[20] S. Wu, Y. W. Chen, S. C. Shao, L. D. Wang, Z. Y. Li, L. Y. Yang, S. L. Li, R. Huang, *J. Nat. Prod.* 2008, **71**, 731– 734.

[21] M. Tsuda, T. Mugishima, K. Komatsu, T. Sone, M. Tanaka, Y. Mikami, J. Kobayashi, *J. Nat. Prod.* 2003, **66**, 412– 415.

[22] M. Chu, R. Mierzwa, L. Xu, L. He, J. Terracciano, M. Patel, V. Gullo, T. Black, W. Zhao, T. Chan, A. T. McPhail, *J. Nat. Prod*. 2003, **66**, 1527– 1530.

[23] T. S. Bugni, J. E. Janso, R. T. Williamson, X. Feng, V. S. Bernan, M. Greenstein, G. T. Carter, W. M. Maiese, C. M. Ireland, *J. Nat. Prod.* 2004, **67**, 1396– 1399.

[24] A. S. Ratnayake, W. Y. Yoshida, S. L. Mooberry, T. Hemscheidt, *Org. Lett*. 2001, **3**, 3479–3481.

[25] S. Lu, P. Sun, T. Li, T. Kurtán, A. Mándi, S. Antus, K. Krohn,S. Draeger, B. Schulz, Y. Yi, L. Li and W. Zhang, *J. Org.Chem*., 2011,**76**, 9699–9710.

[26] J. A. Dale and H. S. Mosher, *J. Am. Chem. Soc*., 1973, **95**,512–519.

[27] P. Radha Krishna, R. Nomula, D. Venkata Ramana, D, *Tetrahedron Lett.* 2012, **53**, 3612.

[28] D. Clarisse and F. Fache, Tetrahedron Lett. *2012*, **55**, 2221–2222.

[29] J. Zeng, Y. J. Tan, J. Ma, M. L. Leow, D. Tirtorahardjo, X.-W. Liu, *Chem. Eur. J*. 2014, **20**, 405.

[30] O. Achmatowicz , P. Bukowski , B. Szechner , Z. Zwierzchowska and A. Zamojski, *Tetrahedron*, 1971, **27** , 1973 -1996.

[31] F. van der Pijl , F. L. van Delft and F. P. J. T. Rutjes , *Eur. J. Org. Chem.* 2015, 4811 —4829.

[32] T. L. Ho and S. G. Sapp , *Synth. Commun.* 1983, **13** , 207 —211.

[33] J. Ren and R. Tong , *J. Org. Chem.* 2014, **79** , 6987 —6995.

[34] Z. Li , T. F. Leung and R. Tong , *Chem. Commun.* 2014, **50** , 10990 —10993.

[35] J. A. Gazaille , J. A. Abramite and T. Sammakia , *Org. Lett.* 2012, **14** , 178 —181.

[36] T. H. Al-Tel , M. H. Semreen and W. Voelter , *Org. Biomol. Chem.* 2010, **8** , 5375 —5382.

[37] J. Bi and V. K. Aggarwal , *Chem. Commun.* 2008, 120 —122.

[38] C. A. Leverett , M. P. Cassidy and A. Padwa , *J. Org. Chem.* 2006, **71** , 8591 —8601.

[39] Y. Sridhar and P. Srihari , *Org. Biomol. Chem.* 2014, **12** , 2950 —2959.

[40] Y. Sridhar and P. Srihari , *Org. Biomol. Chem.* 2013, **11** , 4640 —4645.

[41] M. H. Haukaas and G. A. O'Doherty , *Org. Lett.* 2001, **3** , 3899 —3902.

[42] M. Li , J. Scott and G. A. O'Doherty , *Tetrahedron Lett.* 2004, **45** , 1005 —1009

[43] Z. L. Li and R. B. Tong , *J. Org. Chem.*, 2016, **81** , 4847 -4855.

[44] A. K. Ghosh, J. Li, *Org. Lett.* 2011, **13**, 66-69.

[45] A. K. Ghosh, Z.-H. Chen, *Org. Lett*. 2013, **15**, 5088-5091.

[46] M. Tofi, K. Koltsida and G. Vassilikogiannakis *Org. Lett.* 2009, **11**, 313-316.

[47] M.-P. Georgiadis, K. F. Albizati and T. M. Georgiadis, *Org. Prep. Proc. Int.* 1992, **24**, 95-118.

[48] P.-F. Koh and T.-P. Loh, *Green Chem.* 2015, **17**, 3746-3450.

[49] L. R. Cafiero and T. S. Snowden, *Org. Lett*. 2008, **10**, 3853-3856.

[50] J. L. Shamshina and T. S. Snowden, *Org. Lett*. 2006, **8**, 5881-5884.

[51] P. H. Gore, *Chem. Rev.* 1955, **55**, 229-281.

[52] American Diabetes Association, *Diabetes Care.* 2014, **37**, Suppl 1:S81–S90.

[53] M. E. Craig, A. Hattersley, K. C. Donaghue, *Pediatr Diabetes*. 2009, **10**, Suppl 12:3–12.

[54] F. Galtier, *Diabetes Metab.* 2010, **36**, 628–651.

[55] Centers for Disease Control and Prevention. National Diabetes Statistics Report, 2020. Atlanta, GA: Centers for Disease Control and Prevention, U.S. Dept of Health and Human Services; 2020.

[56] S. Canivell, R. Gomis, *Autoimmun Rev.* 2014, **13**, 403-407.

[57] J. Couper, K. C. Donaghue, *Pediatr Diabetes.* 2009, **10**, Suppl 12: 13-16.

[58] H. Ginsberg, G. Kimmerling, J. M. Olefsky, G. M. Reaven, *J Clin Invest.* 1975, **55**, 454–461.

[59] J. Olefsky, J. W. Farquhar, G. Reaven, *Diabetes.* 1973, **22**, 507–513.

[60] F. B. Kraemer, H. N. Ginsberg, G. M. Reaven, *Diabetes Care.* 2014, **37**, 1178–1181.

[61] A.M. Gharravi, A. Jafar, M. Ebrahimi, A. Mahmodi, E. Pourhashemi, N. Haseli, *Diabetes Metab Syndr Clin Res Rev*, 2018, 12, 1133-1139.

[62] D. Dabelea, E. J. Mayer-Davis, S. Saydah, G. Imperatore, B. Linder, J. Divers, R. Bell, A. Badaru, J. W. Talton, T. Crume, A. D. Liese, A. T. Merchant, J. M. Lawrence, K. Reynolds, L. Dolan, L. L. Liu, R. F. Hamman, *J. Am. Med. Assoc.* 2014, **311**, 1778-1786.

[63] A. Ojha, U. Ojha, R. Mohammed, A. Chandrashekar, H. Ojha, *Clinical pharmacology : advances and applications*. 2019, **11**, 57–65.

[64] G. Karp, *Cell and Molecular Biology: Concepts and Experiments.* 2013, **7**, 644-645.

[65] Centers for Disease Control and Prevention, *Diabetes Symptoms*. 2020, https://www.cdc.gov/diabetes/basics/symptoms.html.

[66] A. Abdi, M. Jalilian, P. A. Sarbarzeh, Z. Vlaisavljevic, *Diabetes research and clinical practice*. 2020, **166**, 108347.

[67] WebMD, *Diabetes Treatments and How it is Diagnosed*. 2020, https://www.webmd.com/diabetes/guide/understanding-diabetes-detection-treatment.

[68] National Institute of Diabetes and Digestive and Kidney Diseases, *Insulin, Medicines & Other Diabetes Treatments*. 2020, https://www.niddk.nih.gov/health-information/diabetes/overview/insulin-medicines-treatments.

[69] Mayo Clinic, *Type 2 diabetes – Diagnosis and treatment.* 2020, https://www.mayoclinic.org/diseases-conditions/type-2-diabetes/diagnosis-treatment/drc-20351199.

[70] S. Y. Tan, J. L. M. Wong, Y. J. Sim, S. S. Wong, S. A. M. Elhassan, S. H. Tan, G. P. L. Lim, N. W. R. Tay, N. C. Annan, S. K. Bhattamisra, M. Candasamy, *Diabetes & Metabolic Syndrome: Clinical Research & Reviews* 2019, **13**, 364-372.

[71] I. C. Arts, P. C. Hollman, *Am. J. Clin. Nutr.* 2005, **81**, 317S–325S.

[72] C. A. Rice-Evans, N. J. Miller, G. Paganga, *Free Radic. Biol. Med.* 1996, **20**, 933–956.

[73] C. Kandaswami, E. Middleton Jr., *Adv. Exp. Med. Biol.* 1994, **366**, 351–376.

[74] K. B. Pandey, S. I. Rizvi, *Oxid. Med. Cell Longev*. 2009, **2**, 270–278.

[75] Z. Bahadoran, P. Mirmiran, F. Azizi, *J. Diabetes Metab. Disord.* 2013, **12**, 43.

[76] R. Testa, A. R. Bonfigli, S. Genovese, V. De Nigris, A. Ceriello,A. *Nutrients*. 2016, **8**, 310.

[77] S. Srinivasan, V. Vinothkumar, R. Murali, *Bioactive Food as Dietary Interventions for Diabetes.* 2019, **2**, 335-346.

[78] H. M. Eid, P. S. Haddad, *Curr. Med. Chem*. 2017, **24**, 355-364.

[79] W. Y. Huang, H. C. Zhang, W. X. Liu, C. Y. Li, *Nanjing. J. Zhejiang Univ. Sci. B.* 2012, **13**, 94–102.

[80] A. Ghorbani, *Biomed. Pharmacother.* 2017, **96**, 305–312.

[81] R. K. Al-Ishaq, M. Abotaleb, P. Kubatka, K. Kajo, D. Büsselberg, *Biomolecules*. 2019, **9**, 430.

[82] D. Araho, M. Miyakoshi, W-H. Chou, T. Kambara, K. Mizutani, T. Ikeda, *Nat. Med.* 2005, **59**, 113−116.

[83] M. Provasi, C. E. Oliveira, M. C. Martino, L. G. Pessini, R. B. Bazotte, D. A. G. Cortez, *Acta Sci — Health Sci*. 2001, **23**, 665-669.

[84] L. H. Cazarolli, P. Folador, H. H. Moresco, I. M. C. Brighente, M. G. Pizzolatti, F. R. M. B. Silva, Eur. *J. Med. Chem.* 2009, **44**, 4668−4673.

[85] L. H. Cazarolli, P. Folador, H. H. Moresco, I. M. C. Brighente, M. G. Pizzolatti, F. R. M. B. Silva, *Chem.-Biol. Interact.* 2009, **179**, 407−412.

[86] Y. Wang, M. Liu, L. Liu, J-H. Xia, Y-G. Du, J-S. Song, *J. Org. Chem*. 2018, **83**, 4111−4118.

[87] T. Matsumoto, M. Katsuki, K. Suzuki, *Tetrahedron Lett.* 1988, **29**, 6935−6938.

[88] T. Matsumoto, T. Hosoya, K. Suzuki, *Tetrahedron Lett.* 1990, **31**, 4629−4632.

[89] T. Yamauchi, Y. Watanabe, K. Suzuki, T. Matsumoto, *Synthesis*. 2006, 2818−2824.

[90] K. Kitamura, Y. Ando, T. Matsumoto, K. Suzuki, *Angew. Chem.,Int. Ed.* 2014, **53**, 1258−1261.

[91] H. S. Mahal, K. Venkataraman, *J. Chem. Soc.* 1934, **0**, 1767-1769.

[92] W. Baker, *J. Chem. Soc.*, 1933, 0, 1381-1389.

[93] J. T. Smoot, A. V. Demchenko, *J. Org. Chem.* 2008, **73** , 8838 —8850.

[94] K. Le Mai Hoang, X. Liu, *Nat. Commun.*, 2014, **5** , 5051.

[95] M. Karak , Y. Joh , M. Suenaga , T. Oishi and K. Torikai, *Org. Lett.*, 2019, **21** , 1221 — 1225.

[96] R. A. Mensink , H. Elferink , P. B. White , N. Pers , F. P. J. T. Rutjes, T. J. Boltje, *Eur. J. Org. Chem.*, 2016, **2016** , 4656 —4667.

[97] M. A. Fascione , C. A. Kilner , A. G. Leach, W. B. Turnbull, *Chemistry* 2012, **18** , 321 — 333.

[98] T. Fang , Y. Gu , W. Huang, G. J. Boons, *J. Am. Chem. Soc.* 2016, **138** , 3002 —3011.

[99] J.-H. Kim , H. Yang , J. Park, G.-J. Boons, *J. Am. Chem. Soc.* 2005, **127** , 12090 —12097.

[100] T. J. Boltje , J.-H. Kim , J. Park, G.-J. Boons, *Org. Lett.* 2010, **13** , 284 —287.

[101] S. J. Moons , R. A. Mensink , J. P. J. Bruekers , M. L. A. Vercammen , L. M. Jansen, T. J. Boltje , *J. Org. Chem.* 2019, **84** , 4486 —4500.

[102] D. J. Cox , G. P. Singh , A. J. A. Watson, A. J. Fairbanks, *Eur. J. Org. Chem.* 2014, **2014** , 4624 —4642.

[103] F. F. J. de Kleijne, S. J. Moons, P. B. White, T. J. Boltje, *Org. Biomol. Chem.* 2020, **18**, 1165-1184.

[104] L. He, Y. Z. Zhang, M. Tanoh, G.-R. Chen, J.-P. Praly, E. D. Chrysina, C. Tiraidis, M. Kosmopoulou, D. D. Leonidas, N. G. Oikonomakos, *Eur. J. Org. Chem*. 2007, 596-606.

[105] X. Cai, K. Ng, H. Panesar, S.-J. Moon, M. Paredes, K. Ishida, K. Hertweck, T. G. Minehan, *Org. Lett.* 2014, **16**, 2962–2965.

[106] H. Liao, J. Ma, H. Yao, X-Wei Liu, *Org. Biomol. Chem.* 2018, **16**, 1791-1806.

[107] T. Kumazawa, M. Chiba, S. Matsuba, S. Sato, J. Onodera, *Carbohydrate Research.*2000, **328**, 599-603.

[108] G. Zong, E. Barber, H. Aljewari, J. Zhou, Z. Hu, Y. Du, W. Q. Shi, *J. Org. Chem*. 2015, **80**, 9279-9291.

[109] L. M. Lerner, *Carbohydrate Res*. 1993, **241**, 291-294.

[110] J. Zeng, G. Sun, W. Yao, Y. Zhu, R. Wang, L. Cai, K. Liu, Q. Zhang, X. Liu, Q. Wan. *Ang. Chem. Int. Ed*. 2017, **56**, 5227-5231.

[111] S-Y. Li, X-B. Wang, S-S. Xie, N. Jiang, K. D. G. Wang, H-Q. Yao, H-B. Sun, L-Y. Kong, *Eur. J. Med. Chem.* 2013, **69**, 632-646.

[112] L. Klier, D. S. Ziegler, R. Rahimoff, M. Mosrin, P. Knochel, *Organic Process Research & Development.* 2017 **21,** 660-663.

[113] L. Klier, Tomke Bresser, Tobias A. Nigst, Konstantin Karaghiosoff, and Paul Knochel, *Journal of the American Chemical Society.* 2012, **134**, 13584-13587.

[114] J-J. Shie, C-A.Chen, C-C. Lin, A. F. Ku, T-J. R. Cheng, J-M. Fang, C-H. Wong, *Org. Biomol. Chem.* 2010,**8**, 4451-4462

[115] T. Kumazawa, M. Chiba, S. Matsuba, S. Sato, J. Onodera, *Carbohydrate Research*. 2000, **328**, 599-603.

[116] T. Hayashi, K. Ohmori, K. Suzuki, *Synlett.* 2016, **27**, 2345-2351.

[117] G. E. Morton, A. G. M. Barrett, *Org. Lett.* 2006, **8**, 2859-2861.

[118] J. B. Son, M. Wang, W. Lee, D-H. Lee, *Org. Lett.* 2007, **9**, 3897-3900.

[119] M. A. Arai, Y. Yamaguchi, M. Ishibashi, *Org. Biomol. Chem.* 2017,**15**, 5025-5032.

[120] D. Kim, K. Ham, S. Hong, *Org. Biomol. Chem.* 2012,**10**, 7305-7312.

[121] Zhou L, Saksena NK. HIV associated neurocognitive disorder. *Infect Dis Rep*. 2013; 5 (suppl 1): e8. www.ncbi.nlm.nih.gov/pmc/articles/PMC3892625/pdf/idr-2013-s1-e8.pdf.

[122] Global HIV & AIDS statistics — 2019 fact sheet - https://www.unaids.org/en/resources/fact-sheet

[123] F. Barre-Sinoussi, J. Chermann, F. Rey, M. Nugeyre, S. Chamaret, J. Gruest, C. Dauguet, C. Axler-Blin, F. Vezinet-Brun, C. Rouzioux, W. Rozenbaum, L. Montagnier, *Science.* 1983**, 220**, 868-871.

[124] T. Shors, *Understanding Viruses.* 2013, **2e**, 484-523.

[125] M. LeBreton, O. Yang, U. Tamoufe, E. Mpoudi-Ngole, J. N. Torimiro, C. F. Djoko, J. K. Carr, A. Tassy Prosser, A. W. Rimoin, D. L. Birx, D. S. Burke, N. D. Wolfe, *Emerging infectious diseases.* 2007**, 13**, 1579-1582.

[126] T. Huet, R. Cheynier, A. Meyerhans, G. Roelants, S. Wain-Hobson, *Nature.* 1990**, 345**, 356-359.

[127] L. Li, H. Li, C. Pauza, *Cell Res.* 2005, **15,** 923–934.

[128] H. Deng, R. Liu, W. Ellmeier, S. Choe, D. Unutmaz, M. Burkhart, P. Di Marzio, S. Marmon, R. E. Sutton, C. M. Hill, C. B. Davis, S. C. Peiper, T. J. Schall, D. R. Littman, N. R. Landau, *Nature.* 1996**, 381**, 661-666.

[129] Y. Feng, C. C. Broder, P. E. Kennedy, E. A. Berger, *Science.* 1996**, 272**, 872-877.

[130] C. A. Derdeyn, E. Hunter, *Curr. Opin. HIV AIDS.* 2008**, 3**, 16-21.

[131] C. Gomez, T. J. Hope, *Cellular Microbiology.* 2005, **7**, 621-626.

[132] S. Sierra, B. Kupfer, R. Kaiser, *J. Clin. Virol.* 2005, **34**, 233-44.

[133] S. R. King, *Annals of Emergency Medicine.* 1994**, 24**, 443-449.

[134] J. Stebbing, B. Gazzard, D. C. Douek, *New England Journal of Medicine* 2004**, 350**, 1872-1880.

[135] M. Siegel, H. Masur, J. Kovacs, *Semin. Respir. Crit. Care Med.* 2016, **37**, 243-256.

[136] Y. S. Su, J. J. Lu, C. L. Perng, F. Y. Chang, *J. Microbiol. Immunol. Infect.* 2008**, 41**, 478-482.

[137] M. A. Smith, D. J. Brennessel, *Infect. Dis. Clin. North Am.* 1994, **8**, 427-438.

[138] C. R. Horsburgh Jr., *J. Infect. Dis.* 1999, **179** (Supplement_3), S461-S465.

[139] G. V. Quinnan Jr., H. Masur, A. H. Rook, G. Armstrong, W. R. Frederick, J. Epstein, J. F. Manischewitz, A. M. Macher, L. Jackson, J. Ames, *JAMA.* 1984**, 252**, 72-77.

[140] A. S. Fauci, H. D. Marston, *N. Engl. J. Med*. 2015, **373**, 2197-2199.

[141] I. L. Tan, J. C. McArthur, *CNS Drugs*. 2012, **26**, 123-134.

[142] B. A. Navia, E. S. Cho, C. K. Petito, R. W. Price, *Ann. Neurol*. 1986, **19**, 525-535.

[143] S. I. Letendre, J. A. McCutchan, M. E. Childers, S. P. Woods, D. Lazzaretto, R. K. Heaton, I. Grant, R. J. Ellis, *Ann. Neurol*. 2004, **56**, 416-423.

[144] N. Lohse, A. B. Hansen, J. Gerstoft, N. Obel, *J. Antimicrob. Chemother*. 2007, **60**, 461-463.

[145] K. A. Nagashima, D. A. Thompson, S. I. Rosenfield, P. J. Maddon, T. Dragic, W. C. Olson, *J. Infect. Dis.* 2001, **183**, 1121-1125.

[146] C. L. Tremblay, C. Kollmann, F. Giguel, T. C. Chou, M. S. Hirsch, *J. Acquir. Immune Defic. Syndr.* 2000, **25**, 99-102.

[147] National Institute of Allergy and Infectious Diseases. FDA-approved HIV medicines.

[148] M. Baba, O. Nishimura, N. Kanzaki, M. Okamoto, H. Sawada, Y. Iizawa, M. Shiraishi, Y. Aramaki, K. Okonogi, Y. Ogawa, K. Meguro, M. Fujino, *Proc. Natl. Acad. Sci. U S A.* 1999, **96**, 5698-5703.

[149] M. M. Rosenkilde, L.-O. Gerlach, J. S. Jakobsen, R. T. Skerlj, G. J. Bridger, T. W. Schwartz, *Journal of Biological Chemistry.* 2004, **279,** 3033-3041.

[150] B. Emu, J. Fessel, S. Schrader, P. Kumar, G. Richmond, S. Win, S. Weinheimer, C. Marsolais, S. Lewis, *New England Journal of Medicine.* 2018, **379**, 645-654.

[151] D. Hazuda, M. Iwamoto, L. Wenning, *Annual Review of Pharmacology and Toxicology.* 2009, **49**, 377-394.

[152] A. S. Espeseth, P. Felock, A. Wolfe, M. Witmer, J. Grobler, N. Anthony, M. Egbertson, J. Y. Melamed, S. Young, T. Hamill, J. L. Cole, D. J. Hazuda, *Proc. Natl. Acad. Sci. U S A.* 2000, **97**, 11244-11249.

[153] T. Cihlar, A. S. Ray, *Antiviral Research.* 2010, **85**, 39-58.

[154] P. A. Furman, J. Fyfe, M. H. Stclair, K. Weinhold, J. L. Rideout, G. A. Freeman, S. N. Lehrman, D. P. Bolognesi, S. Broder, H. Mitsuya, D. W. Barry, *Proc. Natl. Acad. Sci. U S A.* 1986, **83**, 8333-8337.

[155] S. G. Sarafianos, A. D. Clark, K. Das, S. Tuske, J. J. Birktoft, P. Ilankumaran, A. R. Ramesha, J. M. Sayer, D. M. Jerina, P. L. Boyer, S. H. Hughes, E. Arnold, *Embo Journal.* 2002, **21**, 6614-6624.

[156] T. A. Steitz, *Scientist.* 1993, **7**, 16-16.

[157] N. Sluis-Cremer, G. Tachedjian, *Virus Research.* 2008, **134**, 147-156.

[158] J. Adams, N. Patel, N. Mankaryous, M. Tadros, C. D. Miller, *Annals of Pharmacotherapy.* 2010, **44,** 157-165.

[159] V. Namasivayam, M. Vanangamudi, V. G. Kramer, S. Kurup, P. Zhan, X. Liu, J. Kongsted, S. N. Byrareddy, *Journal of Medicinal Chemistry.* 2018.

[160] J. Tozser, S. Oroszlan, *Current Pharmaceutical Design.* 2003, **9**, 1803-1815.

[161] H. Tzoupis, G. Leonis, G. Megariotis, C. T. Supuran, T. Mavromoustakos, M. G. Papadopoulos, *J. Med. Chem.* 2012, **55**, 5784-5796.

[162] A. H. Robbins, R. M. Coman, E. Bracho-Sanchez, M. A. Fernandez, C. T. Gilliland, M. Li, M. Agbandje-McKenna, A. Wlodawer, B. M. Dunn, R. McKenna, *Acta crystallographica. Section D, Biological crystallography.* 2010, **66,** 233-242.

[163] A. Brik, C.-H. Wong, *Organic & Biomolecular Chemistry.* 2003, **1**, 5-14.

[164] A. Krohn, S. Redshaw, J. C. Ritchie, B. J. Graves, M. H. Hatada, *Journal of Medicinal Chemistry.* 1991, **34**, 3340-3342.

[165] Y. Tie, A. Y. Kovalevsky, P. Boross, Y.-F. Wang, A. K. Ghosh, J. Tozser, R. Harrison, I. T. Weber, *Proteins: Structure, Function, and Bioinformatics.* 2007, **67**, 232-242.

[166] D. J. Kempf, K. C. Marsh, J. F. Denissen, E. McDonald, S. Vasavanonda, C. A. Flentge, B. E. Green, L. Fino, C. H. Park, X. P. Kong, *Proceedings of the National Academy of Sciences.* 1995, **92**, 2484-2488.

[167] G. N. Kumar, A. D. Rodrigues, A. M. Buko, J. F. Denissen, *Journal of Pharmacology and Experimental Therapeutics.* 1996, **277**, 423-431.

[168] J. P. Vacca, B. D. Dorsey, W. A. Schleif, R. B. Levin, S. L. McDaniel, P. L. Darke, J. Zugay, J. C. Quintero, O. M. Blahy, E. Roth, *Proceedings of the National Academy of Sciences.* 1994, **91**, 4096-4100.

[169] S. W. Kaldor, V. J. Kalish, J. F. Davies, B. V. Shetty, J. E. Fritz, K. Appelt, J. A. Burgess, K. M. Campanale, N. Y. Chirgadze, D. K. Clawson, B. A. Dressman, S. D. Hatch, D. A. Khalil, M. B. Kosa, P. P. Lubbehusen, M. A. Muesing, A. K. Patick, S. H. Reich, K. S. Su, J. H. Tatlock, *Journal of Medicinal Chemistry.* 1997, **40**, 3979-3985.

[170] E. E. Kim, C. T. Baker, M. D. Dwyer, M. A. Murcko, B. G. Rao, R. D. Tung, M. Navia, *Journal of the American Chemical Society.* 1995, **117**, 1181-1182.

[171] H. L. Sham, D. J. Kempf, A. Molla, K. C. Marsh, G. N. Kumar, C.-M. Chen, W. Kati, K. Stewart, R. Lal, A. Hsu, D. Betebenner, M. Korneyeva, S. Vasavanonda, E. McDonald, A. Saldivar, N. Wideburg, X. Chen, P. Niu, C. Park, V. Jayanti, B. Grabowski, G. R. Granneman, E. Sun, A. J. Japour, J. M. Leonard, J. J. Plattner, D. W. Norbeck, *Antimicrobial agents and chemotherapy.* 1998, **42**, 3218-3224.

[172] B. S. Robinson, K. A. Riccardi, Y-f. Gong, Q. Guo, D. A. Stock, W. S. Blair, B. J. Terry, C. A. Deminie, F. Djang, R. J. Colonno, P.-f. Lin, *Antimicrobial agents and chemotherapy.* 2000, **44**, 2093-2099.

[173] L. Doyon, S. Tremblay, L. Bourgon, E. Wardrop, M. G. Cordingley, *Antiviral Research.* 2005, **68**, 27-35.

[174] A. K. Ghosh, J. F. Kincaid, W. Cho, D. E. Walters, K. Krishnan, K. A. Hussain, Y. Koo, H. Cho, C. Rudall, L. Holland, J. Buthod, *Bioorg. Med. Chem. Lett.* 1998, **8**, 687-690.

[175] A. K. Ghosh, P. R. Sridhar, N. Kumaragurubaran, Y. Koh, I. T. Weber, H. Mitsuya, C*hemMedChem*. 2006, **1**, 939-950.

[176] A. K. Ghosh, Z. L. Dawson, H. Mitsuya, *Bioorg. Med. Chem*. 2007, **15**, 7576-7580.

[177] A. K. Ghosh, B. D. Chapsal, "Design of the anti-HIV-1 protease inhibitor darunavir," Chapter 13 in: Introduction to Drug Research and development, 2013, Elsevier, Ltd.

[178] A. K. Ghosh, D. D. Anderson, I. T. Weber, H. Mitsuya, *Angewandte Chemie International Edition.* 2012, **51**, 1778-1802.

[179] A. K. Ghosh, B. D. Chapsal, I. T. Weber, H. Mitsuya, *Accounts of Chemical Research.* 2008, **41**, 78-86.

[180] A. K. Ghosh, W. Cho, D. E. Walters, K. Krishnan, K. A. Hussain, Y. Koo, H. Cho, C. Rudall, L. Holland, J. Buthod, *Bioorg. Med. Chem. Lett*. 1998, **8**, 979–982.

[181] M. V. Toth, G. R. Marshall, *Int. J. Pept. Protein Res*. 1990, **36**, 544-550.

VITA

Hannah M. Simpson was born in March of 1994 in Fort Collins, CO. She graduated high school from Lee's Summit North High School in Lee's Summit, MO in 2012 and received a diploma from the International Baccalaureate Program. She then attended Rochester Institute of Technology in Rochester, NY, for her undergraduate education. Here, she discovered an interest in organic and medicinal chemistry, and was first introduced to organic chemistry and biochemistry research techniques. In 2016, she earned her Bachelor of Science in Chemistry where she moved to West Lafayette, IN to start her graduate work at Purdue University. She joined the research group of Professor Arun K. Ghosh and focused on developing concise total syntheses of biologically active compounds.

Organic & Biomolecular Chemistry

PAPER

View Article Online
View Journal | View Issue

Cite this: *Org. Biomol. Chem.*, 2018, **16**, 5979

Enantioselective total synthesis of decytospolide A and decytospolide B using an Achmatowicz reaction†

Arun K. Ghosh, * Hannah M. Simpson and Anne M. Veitschegger

Received 28th June 2018,
Accepted 30th July 2018

DOI: 10.1039/c8ob01529e

rsc.li/obc

Enantioselective syntheses of decytospolide A and decytospolide B are described here. The current synthesis highlights an Achmatowicz rearrangement of an optically active furanyl alcohol followed by reduction of the resulting dihydropyranone hemiacetal with $BF_3{\cdot}OEt_2$ and Et_3SiH to provide the saturated tetrahydropyranyl alcohol directly. This reduction was investigated with a variety of other Lewis acids. The synthesis also features Noyori asymmetric transfer hydrogenation and Friedel–Crafts acylation. Overall, the synthesis provides ready access to the natural products and may be useful in the preparation of bioactive derivatives.

Introduction

Functionalized tetrahydropyrans are important structural features present in many bioactive natural products.[1,2] Over the years, several methods have been developed for the synthesis of substituted tetrahydropyran rings.[3–5] However, there are limitations with respect to readily available starting materials, stereo- and regiochemical issues and lack of potential for incorporation of multiple substitutions within the tetrahydropyran ring system. Additionally, many of these transformations rely on transition metals such as a Pd-catalyzed decarboxylative allylation and an indium catalysed Prins cyclization.[6,7] The Achmatowicz reaction, an oxidative ring enlargement of a furanyl alcohol, has been developed into a very practical reaction with immense potential.[8,9] In recent years, the Achmatowicz reaction has been utilized in the synthesis of a variety of natural products.[10,11] We have utilized this reaction in the synthesis of a number of bioactive natural products containing functionalized tetrahydropyran rings.[10,12,13] In particular, the Achmatowicz reaction of furanyl alcohol **1** (Fig. 1) provides dihydropyranone hemiacetal **2** which upon reduction, typically with triethylsilane in the presence of trifluoroacetic acid (TFA) provided a variety of 2,6-disubstituted dihydropyranone derivatives **3**.[10,11] Such enones have been utilized in the synthesis of bioactive natural products, including the potent anticancer agent, herboxidiene **4**.[10,13]

Thus far, dihydropyranone hemiacetal reduction provides access to a range of enones under a variety of reaction conditions.[10,11] However, the potential for reduction of an Achmatowicz reaction product enone hemiacetal to a saturated tetrahydropyran derivative and further reduction to the alcohol functionality has been scarcely explored. For further development of the Achmatowicz reaction as well as its application, we sought to synthesize 2,6-disubstituted tetrahydropyranyl alcohols as exemplified by alcohol **5** using a silane in the presence

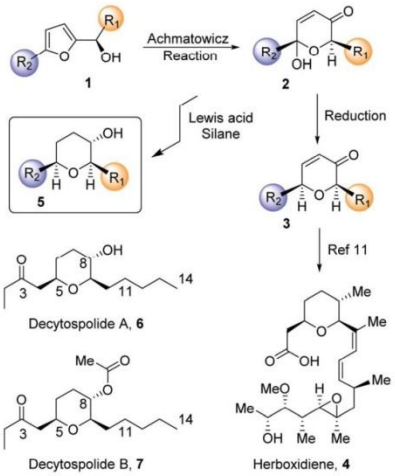

Fig. 1 Achmatowicz reaction and structures of the decytospolides.

Department of Chemistry and Department of Medicinal Chemistry, Purdue University, 560 Oval Drive, West Lafayette, Indiana 47907, USA. E-mail: akghosh@purdue.edu

†Electronic supplementary information (ESI) available: ^{1}H- and ^{13}C-NMR spectra of new compounds. See DOI: 10.1039/c8ob01529e

of a Lewis acid. There have been limited studies for this transformation.[14] This transformation would provide easy access to natural products containing substituted tetrahydropyran rings with three contiguous chiral centers. Such functionalized tetrahydropyran rings are imbedded in a variety of bioactive molecules, including decytospolides A (**6**) and B (**7**) and their derivatives.

The decytospolides contain three asymmetric centers surrounding a central tetrahydropyran ring flanked by two alkyl chains. Both natural products were recently isolated by Zhang and co-workers from the endophytic fungus, *Cytospora* sp. No ZW02, from *Ilex canariensis*, an evergreen shrub from the Canary Islands.[15] The chemical structure of both decytospolides was determined by extensive NMR studies and HRMS analysis. The absolute configuration was established through Mosher ester analysis.[15,16] Decytospolide B exhibited moderate cytotoxicity in A549 and QGY cancer cell lines with IC_{50} values of 14.8 and 46.8 μg mL^{-1}, respectively. Since decytospolide A did not show appreciable cytotoxicity, the acyl group in decytospolide B may be responsible for its moderate anticancer activity. There is potential for further improvement through modification of this acyl group. Several syntheses of these natural products have been reported.[6,7,17–19] We, however, planned to assemble the functionalized tetrahydropyran ring using the Achmatowicz reaction as the key step. Herein, we report our synthesis of decytospolides A and B using the Achmatowicz, Noyori reduction, and Friedel–Crafts reactions as the key steps. We particularly sought to synthesize 2,5,6-trisubstituted tetrahydropyran derivatives in a highly stereoselective manner in optically active form in a one-pot operation directly from the Achmatowicz product, the dihydropyranone hemiacetal.

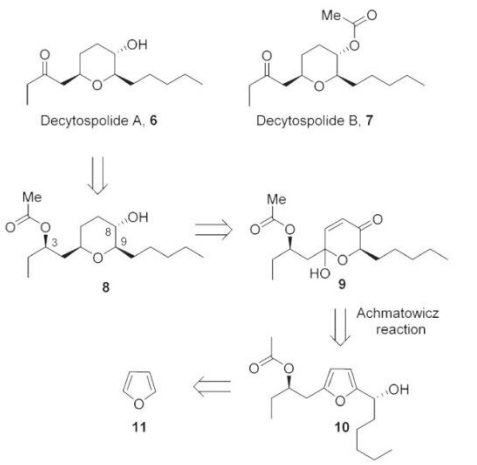

Scheme 1 Retrosynthetic analysis of the decytospolides.

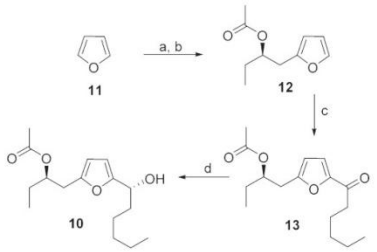

Scheme 2 Synthesis of alcohol **10**. Reagents and conditions: (a) (*R*)-1,2-Epoxybutane, *n*-BuLi, THF, 0 °C to 23 °C; (b) Ac_2O, Et_3N, DMAP, CH_2Cl_2, (84%, 2-steps); (c) $C_5H_{11}COCl$, $SnCl_4$, CH_2Cl_2, 0 °C (75%); (d) RuCl(mesitylene)[(*R*,*R*)-Ts-DPEN], (1 mol%), HCO_2H, Et_3N, CH_2Cl_2, 55° C (93%).

Results and discussion

Our synthetic strategies to decytospolides A and B is shown in Scheme 1. We planned to synthesize trisubstituted tetrahydropyran alcohol **8** in an optically active manner by reduction of dihydropyran hemiacetal **9** which would be obtained directly from furanyl alcohol **10** using an Achmatowicz rearrangement. We particularly planned to synthesize alcohol **8** stereoselectively from dihydropyran hemiacetal **9**.[10,11] Furan derivative **10** would be synthesized from furan **11** by a Friedel–Crafts acylation followed by asymmetric reduction.[20]

The synthesis of furanyl alcohol **10** in optically active form is shown in Scheme 2. Deprotonation of furan **11** with *n*-BuLi in THF at 0 °C to 23 °C followed by addition of commercially available (*R*)-butylene oxide furnished the corresponding alcohol through epoxide opening. The resulting alcohol was acetylated with acetic anhydride in the presence of Et_3N and DMAP to afford furan derivative **12** in 84% yield over two steps. We specifically planned to install the C3-acetoxy group with defined stereochemistry to avoid forming a mixture of diastereomers and provide easy access to C3 stereo-defined derivatives for biological evaluation. Furan derivative **12** underwent a Friedel–Crafts acylation by reaction with hexanoyl chloride in the presence of $SnCl_4$ at 0 °C for 30 min to provide ketone derivative **13** in 75% yield.[21] For enantioselective reduction of the ketone, we planned an asymmetric transfer hydrogenation reaction developed by Noyori and co-workers.[22,23] Therefore, reaction of **13** with a catalytic (1 mol%) amount of Noyori's catalyst, (*R*,*R*) RuCl(mesitylene)-Ts-DPEN, in the presence of Et_3N and formic acid in CH_2Cl_2 at 55 °C for 12 h, furnished alcohol **10** in 93% yield. The asymmetric reduction proceeded with high diastereoselectivity as alcohol **10** was isolated as the single product by ^{1}H- and ^{13}C-NMR analysis (diastereoselectivity >20 : 1).

The synthesis of the decytospolides is shown in Scheme 3. Initially, the Achmatowicz reaction of **10** was carried out with a catalytic amount of $VO(acac)_2$ and ^{t}BuOOH; however, the reaction was sluggish.[24,25] Achmatowicz reaction with oxone in the

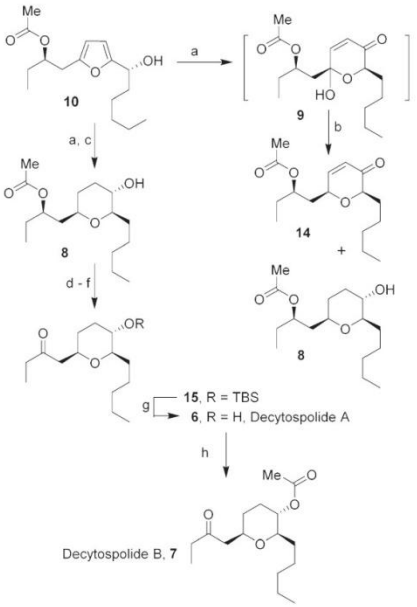

Scheme 3 Synthesis of the decytospolides. Reagents and conditions: (a) Oxone, KBr, $NaHCO_3$, THF/H_2O (4 : 1); (b) Et_3SiH, TFA, CH_2Cl_2, −45 °C to rt, (40%, **14**); (c) Et_3SiH, TFA, $BF_3{\cdot}OEt_2$, CH_2Cl_2, −45 °C (47%, **8**); (d) TBSOTf, 2,6-lutidine, CH_2Cl_2, 0 °C to 23 °C; (e) K_2CO_3, MeOH; (f) DMP, $NaHCO_3$, CH_2Cl_2, 0 °C to 23 °C, (89%, 3-steps); (g) TBAF, THF, 23 °C (99%); (h) Ac_2O, pyr, DMAP, 23 °C, CH_2Cl_2 (99%).

presence of $NaHCO_3$ in a mixture (4 : 1) of THF and water at 23 °C for 30 min smoothly converted **10** to the corresponding dihydropyranone hemiacetal (**9**).[26] The resulting hemiacetal was initially subjected to reduction with Et_3SiH and TFA at −45 °C for 3 h. This resulted in a mixture of dihydropyranone **14** and a small amount of alcohol **8**. Further optimization of the reaction with an excess of $BF_3{\cdot}OEt_2$ at −45 °C for 3 h provided alcohol **8** as the exclusive product in 47% yield over 2-steps. The stereochemistry at C8 was determined by ^{1}H NMR coupling with the proton at C9, which has two J values (2.4 and 9 Hz). Having J = 9 Hz indicates a *trans* relationship between the protons at C8 and C9 and since the stereocenter at C9 was set by the Noyori reduction, the stereochemistry at C8 was assigned based on that. We then, investigated silane reduction of the dihydropyranone hemiacetal **9** in the presence of a number of other Lewis acids. The results are shown in Table 1. As can be seen, the use of $BF_3{\cdot}OEt_2$ and $SnCl_4$ as the Lewis acids provided alcohol **8** exclusively in 56% and 82% yield, respectively (entries 3 and 4). Reductions with Lewis acids $Sc(OTf)_3$ and $Cu(OTf)_2$ yielded only trace amounts of dihydropyranone **14**, while using $TiCl_4$ as the Lewis acid gave 14% of **14**.

Table 1 Reduction of the dihydropyranone hemiacetal **9** with various Lewis acids[a]

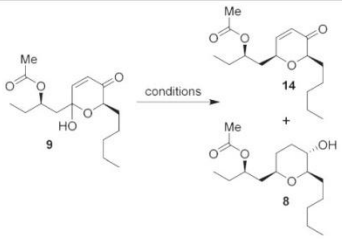

Entry	Lewis acid (equiv.)	Et_3SiH (equiv.)	Time	Yield for enone **14**	Yield for THP **8**
1	TFA [15]	5	24 h	40%	Trace
2	TFA [15] $BF_3{\cdot}OEt_2$ [3]	5, then 5 more	4 h	None	47%
3	$BF_3{\cdot}OEt_2$ [6]	10	6 h	None	56%
4	$SnCl_4$ [6]	10	4 h	None	82%
5	$Cu(OTf)_2$ [6]	10	18 h	Trace	None
6	$TiCl_4$ [6]	10	18 h	14%	None
7	$Sc(OTf)_3$ [6]	10	18 h	Trace	None

[a] All reactions were carried out in CH_2Cl_2 at −45 °C.

To complete the synthesis of the decytospolides, alcohol **8** was protected as a TBS-ether with TBSOTf in the presence of 2,6-lutidine in CH_2Cl_2 at 0 °C to 23 °C for 12 h. The acetate was hydrolyzed with K_2CO_3 in MeOH at 23 °C to provide the corresponding alcohol. Oxidation of the resulting alcohol with Dess–Martin periodinane (DMP) in the presence of $NaHCO_3$ in CH_2Cl_2 furnished ketone **15** in 89% yield over 3-steps. Removal of the silyl ether was carried out with tetrabutylammonium fluoride (TBAF) in THF at 23 °C for 12 h to provide decytospolide A (**6**) {$[\alpha]_D^{23}$ +18.4 (*c* 0.45, $CHCl_3$)} in quantitative yield. Treatment of decytospolide A (**6**) with acetic anhydride in the presence of pyridine and DMAP in CH_2Cl_2 at 23 °C for 1.5 h furnished decytospolide B (**7**) {$[\alpha]_D^{23}$ +28.4 (*c* 0.75, $CHCl_3$)} in quantitative yield. The ^{1}H- and ^{13}C-NMR spectra of synthetic decytospolides are in complete agreement with the spectra reported for the natural decytospolide A {$[\alpha]_D^{20}$ +6.1 (*c* 0.08, $CHCl_3$)} and decytospolide B {$[\alpha]_D^{20}$ +26.6 (*c* 0.02, $CHCl_3$)}.[14]

We also investigated an alternative route to the decytospolides in an effort to synthesize the saturated tetrahydropyranol directly following the Achmatowicz reaction. As shown in Scheme 4, commercially available furfural, was converted to furanyl methyl acetate **17** by a one-carbon homologation using a Jocic reaction as developed by Snowden and co-workers.[27,28] Methyl ester **17** is also commercially available. Methyl ester **17** was reacted with hexanoyl chloride in the presence of $SnCl_4$ as described above to provide furanyl-ketone **18** in 57% yield. Reduction of ketone **18** using Noyori's catalyst RuCl(mesitylene)[(*R*,*R*)-Ts-DPEN] (1 mol%) in the presence of Et_3N and formic acid at 50 °C for 12 h afforded optically active furanyl alcohol **19** in 83% yield and 99% *ee* determined by chiral

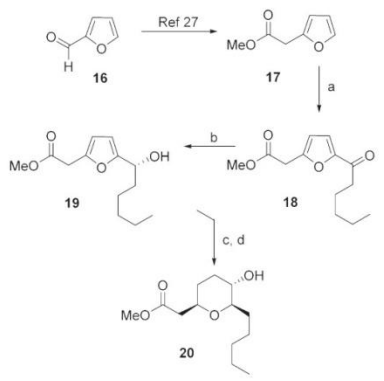

Scheme 4 Synthesis of alcohol **20**. Reagents and conditions: (a) $C_5H_{11}COCl$, $SnCl_4$, CH_2Cl_2, 0 °C (57%); (b) RuCl(mesitylene)[(*R*,*R*)-Ts-DPEN], (1 mol%), Et_3N, HCO_2H, CH_2Cl_2, 50 °C, 12 h (83%, 99% *ee*); (c) KBr, $NaHCO_3$, oxone, THF/H_2O (4 : 1), 0 °C to 23 °C, 3 h; (d) $BF_3{\cdot}OEt_2$, Et_3SiH, CH_2Cl_2, −40 °C, 16 h (58%, over 2-steps).

HPLC analysis (please see Experimental section for details).[20,21] Achmatowicz reaction of **19** with oxone at 23 °C for 30 min furnished the corresponding dihydropyranone hemiacetal which was subjected to reduction with excess Et_3SiH in the presence of $BF_3{\cdot}OEt_2$ at −40 °C for 16 h to provide saturated tetrahydropyranol derivative **20** as a single product by ^{1}H-NMR analysis. Presumably, the reduction of enone first provided the ketone which was reduced by Lewis acid chelation followed by axial delivery of hydride.

Tetrahydropyranol derivative **20** was readily converted to the decytospolides as shown in Scheme 5. Reaction of methyl ester **20** with NH(OMe)Me·HCl in the presence of *i*-PrMgCl in THF at −30 °C for 5 h provided Weinreb amide derivative **21**. Treatment of Weinreb amide **21** with EtMgBr in THF at 0 °C to 23 °C for 5 h afforded decytospolide A, **6** in 97% yield $\{[\alpha]_D^{23}$ +7.8 (*c*, 1.33, $CHCl_3$)$\}$. Acylation of **6** with acetic anhydride in the presence of pyridine and DMAP furnished decytospolide B, **7** $\{[\alpha]_D^{23}$ +22.8 (*c*, 1.96, $CHCl_3$)$\}$ in 86% yield. The ^{1}H-NMR and ^{13}C-NMR spectra of these synthetic decytospolides are in complete agreement with reported spectra for the natural products.[14]

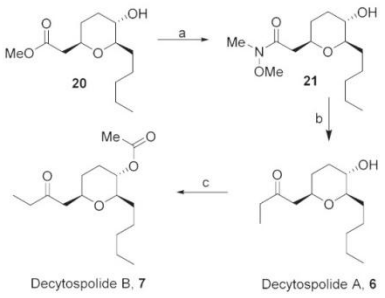

Scheme 5 Synthesis of decytospolides. Reagents and conditions: (a) NH(OMe)Me·HCl, *i*-PrMgCl, THF, −30 °C, 5 h (93%); (b) EtMgBr, THF, 0 °C to rt, 5 h (97%); (c) Ac_2O, pyridine, DMAP, CH_2Cl_2, 0 °C to 23 °C, 3 h (86%).

Conclusions

In summary, we have accomplished an enantioselective total synthesis of decytospolides A and B. The synthesis features an Achmatowicz rearrangement of an optically active furanyl alcohol which was obtained conveniently by use of the Friedel–Crafts reaction followed by a Noyori asymmetric transfer hydrogenation reaction as the key steps. The synthesis highlights a highly stereoselective reduction of the Achmatowicz product, a dihydropyranone hemiacetal to the saturated tetrahydropyranol derivative using $BF_3{\cdot}OEt_2$ and Et_3SiH. Reduction presumably proceeds through Lewis Acid chelation followed by delivery of an axial hydride. The current work will provide access to structural variants of these natural products for further studies. Further studies and applications are in progress in our laboratories.

Experimental section

Chemicals and reagents were purchased from commercial suppliers and used without further purification. Anhydrous solvents were obtained as follows: dichloromethane and toluene from calcium hydride, diethyl ether and tetrahydrofuran from sodium/benzophenone, and methanol from activated magnesium. All other solvents were reagent grade. All moisture-sensitive reactions were either carried out in flame- or oven-dried (120 °C) glassware under an argon atmosphere. TLC analysis was conducted using glass-backed thin-layer silica gel chromatography plates (60 Å, 250 μm thickness, F254 indicator). Column chromatography was performed using Silicycle 230–400 mesh, 60 Å pore diameter silica gel. ^{1}H and ^{13}C NMR spectra were recorded on either Bruker ARX400, Bruker DRX-500, Bruker AV500HD, or Bruker Avance-III-800 spectrometers. Chemical shift (δ values) are reported in parts per million and are referenced to the residual solvent signal ($CDCl_3$ ^{1}H singlet = 7.26, ^{13}C triplet = 77.16). Characteristic splitting patterns due to spin–spin coupling are identified as follows: s = singlet, d = doublet, t = triplet, q = quartet, quint = quintet, sep = septet, m = multiplet, dd = doublet of doublets, ddd = doublet of doublet of doublets, td = triplet of doublets, dq = doublet of quartets, brs = broad singlet, app = apparent. All coupling constants are measured in hertz (Hz). Optical rotations were recorded by a PerkinElmer 341 polarimeter. IR spectra were recorded on a PerkinElmer Spectrum Two FT-IR Spectrometer. LRMS and HRMS spectra were recorded at the Purdue University Department of Chemistry Mass Spectrometry Center. HPLC data was obtained on an Agilent 1290 Infinity II.

(*R*)-1-(Furan-2-yl)butan-2-yl acetate (12)

To furan (2.02 mL, 27.74 mmol) dissolved in THF (23 mL) at 0 °C was added *n*-BuLi (15.6 mL, 24.97 mmol) dropwise upon which a bright yellow color developed. After stirring for 1 h at this temperature, (*R*)-(+)-butylene oxide (1.21 mL, 13.87 mmol) was added and the reaction was slowly warmed to room temperature. After stirring for 12 h, the deep red solution was quenched with saturated NH_4Cl, extracted with EtOAc, washed with brine and dried over Na_2SO_4. Purification by column chromatography (10% EtOAc/hexanes) gave 1.69 g (87% yield) of the resulting furan alcohol as a yellow oil.

To (*R*)-furan alcohol (868 mg, 6.19 mmol) dissolved in CH_2Cl_2 (21 mL) at 0 °C was added acetic anhydride (1.2 mL, 12.4 mmol), Et_3N (1.3 mL, 9.3 mmol) and a few crystals of DMAP. The reaction was allowed to warm to room temperature. After 6 h, the reaction was quenched with saturated $NaHCO_3$, extracted with CH_2Cl_2, washed with brine and dried over Na_2SO_4. Purification by column chromatography (5% to 10% EtOAc/hexanes) afforded 1.1 g (97% yield) of acetate **12** as a clear oil $[\alpha]_D^{20}$ +19.6 (*c* 0.73, $CHCl_3$); ^{1}H NMR (500 MHz, $CDCl_3$) δ: 7.31 (dd, J = 1.9, 0.9 Hz, 1H), 6.28 (dd, J = 3.2, 1.9 Hz, 1H), 6.05 (dd, J = 3.2, 0.9 Hz, 1H), 5.04 (m, 1H), 2.87 (d, J = 6.3 Hz, 2H), 2.02 (s, 3H), 1.65–1.55 (m, 2H), 0.92 (t, J = 7.5 Hz, 3H); ^{13}C NMR (125 MHz, $CDCl_3$) δ: 170.7, 151.9, 141.5, 110.4, 107.0, 73.8, 32.5, 26.7, 21.3, 9.7; FT-IR (neat) ν_{max} = 2965, 2925, 2852, 1738, 1507, 1461, 1436, 1376, 1239, 1012, 739 cm^{-1}.

(*R*)-1-(5-Hexanoylfuran-2-yl)butan-2-yl acetate (13)

Hexanoic acid (604 mg, 5.20 mmol) in an excess of thionyl chloride was refluxed overnight. The thionyl chloride was removed by distillation, strictly keeping the system under argon. The remaining hexanoyl chloride was used immediately for the subsequent reaction. To hexanoyl chloride (699 mg, 5.2 mmol) in CH_2Cl_2 (15 mL) at 0 °C was added $SnCl_4$ (8.7 mL, 8.7 mmol, 1 M in CH_2Cl_2) dropwise. After stirring for 1 h at this temperature, acetate **12** (789 mg, 4.33 mmol) dissolved in CH_2Cl_2 (5 mL) was added to the reaction mixture *via* cannula and remained stirring at 0 °C. After 30 min, the red-brown solution was quenched with ice, extracted with CH_2Cl_2, washed with brine and dried over Na_2SO_4. Purification by column chromatography (10% to 20% EtOAc/hexanes) gave 909 mg (75% yield) of furan derivative **13** as a clear oil; $[\alpha]_D^{20}$ +16.2 (*c* 0.86, $CHCl_3$); ^{1}H NMR (500 MHz, $CDCl_3$) δ: 7.07 (d, J = 3.5 Hz, 1H), 6.21 (d, J = 3.5 Hz, 1H), 5.07 (quint, J = 6.4 Hz, 1H), 2.99–2.91 (m, 2H), 2.74 (t, J = 7.9 Hz, 2H), 2.02 (s, 3H), 1.72–1.66 (m, 2H), 1.65–1.59 (m, 2H), 1.34–1.31 (m, 4H), 0.92 (t, J = 7.4 Hz, 3H), 0.89 (t, J = 6.5 Hz, 3H); ^{13}C NMR (125 MHz, $CDCl_3$) δ: 189.4, 170.6, 157.0, 152.1, 118.3, 109.9, 73.2, 38.4, 32.8, 31.6, 26.9, 24.3, 22.6, 21.2, 14.0, 9.7; FT-IR (neat) ν_{max} = 2961, 2931, 2866, 1741, 1674, 1588, 1516, 1374, 1238, 1023 cm^{-1}.

(*R*)-1-(5-((*R*)-1-Hydroxyhexyl)furan-2-yl)butan-2-yl acetate (10)

To furan derivative **13** (280 mg, 1 mmol) in CH_2Cl_2 (5 mL) was sequentially added Et_3N (1.0 mL, 7.5 mmol), formic acid (0.28 mL, 7.5 mmol) and Noyori catalyst, (*R*,*R*) RuCl(mesitylene)-Ts-DPEN (6.2 mg, 0.01 mmol), and the reaction was set to reflux at 55 °C. After refluxing for 12 h, the orange solution was diluted with water, extracted with CH_2Cl_2, washed with brine and dried over Na_2SO_4. Purification by column chromatography (10% to 20% EtOAc/hexanes) provided 261 mg (93% yield) of alcohol **10** as a clear oil. This alcohol was obtained as a single diastereomer by ^{1}H NMR (ratio >20 : 1) $[\alpha]_D^{20}$ +13.5 (*c* 0.84, $CHCl_3$); ^{1}H NMR (500 MHz, $CDCl_3$) δ: 6.10 (d, J = 3.1 Hz, 1H), 5.97 (d, J = 3.1 Hz, 1H), 5.04 (m, 1H), 4.59 (q, J = 6.8 Hz, 1H), 2.88–2.80 (m, 2H), 2.01 (s, 3H), 1.92 (d, J = 5.2 Hz, 1H), 1.83–1.79 (m, 2H), 1.65–1.55 (m, 2H), 1.42 (m, 1H), 1.31–1.30 (m, 5H), 0.93–0.86 (m, 6H); ^{13}C NMR (125 MHz, $CDCl_3$) δ: 170.7, 155.9, 151.3, 107.6, 106.7, 73.8, 68.0, 35.6, 32.6, 31.7, 26.8, 25.4, 22.7, 21.3, 14.2, 9.7; FT-IR (neat) ν_{max} = 3447, 2958, 2933, 2859, 1739, 1559, 1464, 1433, 1373, 1242, 1021, 964, 792 cm^{-1}; LRMS-ESI (+) *m*/*z* 305.1 $[M + Na]^+$.

(*R*)-1-((2*R*,5*S*,6*R*)-5-Hydroxy-6-pentyltetrahydro-2*H*-pyran-2-yl) butan-2-yl acetate (8)

To furanyl alcohol **10** (317 mg, 1.12 mmol) dissolved in THF (8 mL) and H_2O (2 mL) at 0 °C was added KBr (6.7 mg, 0.06 mmol), $NaHCO_3$ (47 mg, 0.56 mmol) and oxone (826 mg, 1.34 mmol) after which a light yellow color developed. After stirring at 0 °C for 30 min, the reaction was quenched with saturated $NaHCO_3$, extracted with EtOAc, washed with brine and dried over Na_2SO_4. The resulting crude hemiacetal **9** was used directly for the subsequent reaction.

To crude hemiacetal dissolved in CH_2Cl_2 (10 mL) at −45 °C was added Et_3SiH (0.89 mL, 5.6 mmol) and TFA (1.3 mL, 16.8 mmol) dropwise upon which a yellow color developed. The reaction was stirred at this temperature for 3 h, then was allowed to warm to room temperature. After stirring for 30 min at 23 °C, the reaction was cooled to 0 °C and additional Et_3SiH (0.895 mL, 5.6 mmol) was added followed by $BF_3{\cdot}OEt_2$ (0.415 mL, 3.36 mmol). After stirring for 30 min at 0 °C, the reaction was quenched slowly with satd. $NaHCO_3$ until the effervescence ceased. The reaction was extracted with CH_2Cl_2, washed with brine and dried over Na_2SO_4. Purification by column chromatography (10% to 30% EtOAc/hexanes) provided 151 mg (47% yield over two steps) of tetrahydropyran derivative **8** as a clear oil. It was obtained as a single diastereomer by ^{1}H NMR analysis (>20 : 1) $[\alpha]_D^{20}$ +2.7 (*c* 0.49, $CHCl_3$); ^{1}H NMR (500 MHz, $CDCl_3$) δ: 5.01 (m, 1H), 3.30–3.22 (m, 2H), 2.95 (td, J = 9.0, 2.4 Hz, 1H), 2.06 (m, 1H), 2.03 (s, 3H), 1.79 (m, 1H), 1.65–1.53 (m, 6H), 1.43–1.24 (m, 9H), 0.90–0.85 (m, 6H); ^{13}C NMR (125 MHz, $CDCl_3$) δ: 170.7, 82.2, 74.1, 72.9, 70.9, 40.0, 33.3, 32.2, 32.1, 32.0, 31.8, 27.8, 25.0, 22.7, 21.3, 14.2, 9.5; FT-IR (neat) ν_{max} = 3451, 2929, 2859, 1739, 1718, 1461, 1436, 1373, 1242, 1080, 1056, 1024, 954 cm^{-1}; LRMS-ESI (+) *m*/*z* 287.1 $[M + H]^+$.

1-((2*R*,5*S*,6*R*)-5-((*tert*-Butyldimethylsilyl)oxy)-6-pentyltetrahydro-2*H*-pyran-2-yl)butan-2-one (15)

To tetrahydropyran derivative **8** (141 mg, 0.49 mmol) dissolved in CH_2Cl_2 (5 mL) at 0 °C was added 2,6-lutidine (0.23 mL, 1.97 mmol) and TBSOTf (0.34 mL, 1.48 mmol) and the reac-

tion was warmed to 23 °C. After stirring for 12 h, the reaction was quenched with saturated $NaHCO_3$, extracted with CH_2Cl_2, washed with brine and dried over Na_2SO_4. Purification by column chromatography (5% to 10% EtOAc/hexanes) gave 200 mg (quantitative) of the resulting silyl ether as a clear oil.

To the silyl ether (186 mg, 0.46 mmol) in MeOH (3 mL) at 0 °C was added K_2CO_3 (6.4 mg, 0.05 mmol) upon which a yellow color developed. The reaction was warmed to room temperature. After 12 h, the reaction was diluted with H_2O and EtOAc, extracted with EtOAc, washed with brine and dried over Na_2SO_4. Purification by column chromatography (5% to 20% EtOAc/hexanes) gave 155 mg (93% yield) of the resulting alcohol as a clear oil.

To the above alcohol (144 mg, 0.40 mmol) dissolved in CH_2Cl_2 (4 mL) at 0 °C was added $NaHCO_3$ (202 mg, 2.41 mmol) followed by DMP (341 mg, 0.8 mmol) and the reaction was warmed to room temperature. After 12 h, the reaction was quenched with a 1 : 1 mixture of saturated sodium thiosulfate and saturated $NaHCO_3$. The mixture was extracted with CH_2Cl_2, washed with brine and dried over Na_2SO_4. Purification by column chromatography (5% to 10% EtOAc/hexanes) gave 138 mg (96% yield) of ketone **15** as a clear oil $[\alpha]_D^{23}$ +32.0 (*c* 0.58, $CHCl_3$); ^{1}H NMR (500 MHz, $CDCl_3$) δ: 3.71 (m, 1H), 3.21 (m, 1H), 3.02 (m, 1H), 2.62 (dd, J = 14.9, 8.2 Hz, 1H), 2.53–2.41 (m, 2H), 2.36 (dd, J = 14.9, 4.7 Hz, 1H), 1.94 (m, 1H), 1.78–1.69 (m, 2H), 1.52–1.22 (m, 9H), 1.03 (t, J = 7.3 Hz, 3H), 0.86 (s, 12H), 0.04 (s, 6H); ^{13}C NMR (125 MHz, $CDCl_3$) δ: 210.3, 82.5, 74.3, 71.4, 48.7, 37.2, 33.6, 32.2, 31.9, 31.5, 25.9, 25.1, 22.7, 18.1, 14.2, 7.6, −3.9, −4.6; FT-IR (neat) ν_{max} = 2954, 2929, 2855, 1721, 1464, 1376, 1253, 1105, 887, 837, 774 cm^{-1}; LRMS-ESI (+) m/z 357.3 $[M + H]^+$.

Decytospolide A (6)

To ketone **15** (126 mg, 0.35 mmol) dissolved in THF (4 mL) at 0 °C was added TBAF (0.71 mL, 0.71 mmol, 1 M in THF) and the reaction was warmed to 23 °C. After 12 h, the reaction was concentrated and purification by column chromatography (30% to 50% EtOAc/hexanes) provided 82 mg (96% yield) of decytospolide A (**6**) as a clear oil $[\alpha]_D^{23}$ +18.4 (*c* 0.45, $CHCl_3$); ^{1}H NMR (500 MHz, $CDCl_3$) δ: 3.72 (m, 1H), 3.24 (td, J = 9.8, 4.5 Hz, 1H), 3.01 (m, 1H), 2.64 (dd, J = 15.0, 8.1 Hz, 1H), 2.53–2.41 (m, 2H), 2.37 (dd, J = 15.0, 4.8 Hz, 1H), 2.06 (m, 1H), 1.81–1.69 (m, 2H), 1.54 (brs, 1H), 1.47–1.24 (m, 9H), 1.03 (t, J = 7.3 Hz, 3H), 0.86 (t, J = 6.7 Hz, 3H); ^{13}C NMR (125 MHz, $CDCl_3$) δ: 210.2, 82.3, 74.2, 70.6, 48.5, 37.2, 33.1, 32.1, 31.9, 31.4, 25.1, 22.7, 14.2, 7.6; FT-IR (neat) ν_{max} = 3447, 2929, 2859, 1714, 1457, 1376, 1077 cm^{-1}; LRMS-ESI (+) m/z 243.1 $[M + H]^+$; HRMS-ESI (+) m/z calc'd for $C_{14}H_{27}O_3$ $[M + H]^+$: 243.1955, found 243.1958.

Decytospolide B (7)

To decytospolide A (**6**) (73 mg, 0.30 mmol) dissolved in CH_2Cl_2 (3 mL) at 0 °C was added pyridine (73 μL, 0.9 mmol), acetic anhydride (85 μL, 0.9 mmol) and a few crystals of DMAP and the reaction was warmed to 23 °C. After 1.5 h, the reaction was diluted with H_2O, extracted with CH_2Cl_2, washed with brine and dried over Na_2SO_4. Purification by column chromatography (10% to 20% EtOAc/hexanes) provided 77 mg (89% yield) of decytospolide B (**7**) as a clear oil $[\alpha]_D^{20}$ +28.1 (*c* 0.75, $CHCl_3$); ^{1}H NMR (500 MHz, $CDCl_3$) δ: 4.43 (td, J = 10.0, 4.6 Hz, 1H), 3.75 (m, 1H), 3.21 (td, J = 9.1, 2.4 Hz, 1H), 2.66 (dd, J = 15.2, 8.0 Hz, 1H), 2.52–2.40 (m, 2H), 2.36 (dd, J = 15.3, 4.9 Hz, 1H), 2.12 (m, 1H), 2.02 (s, 3H), 1.73 (m, 1H), 1.53–1.35 (m, 4H), 1.29–1.20 (m, 6H), 1.02 (t, J = 7.3 Hz, 3H), 0.85 (t, J = 6.9 Hz, 3H); ^{13}C NMR (125 MHz, $CDCl_3$) δ: 209.9, 170.4, 79.4, 74.3, 72.2, 48.3, 37.3, 32.0, 31.8, 30.9, 29.5, 24.9, 22.7, 21.3, 14.1, 7.6; FT-IR (neat) ν_{max} = 2933, 2859, 1739, 1714, 1457, 1373, 1235, 1080, 1042 cm^{-1}; LRMS-ESI (+) m/z 285.1 $[M + H]^+$; HRMS-ESI (+) m/z calc'd for $C_{16}H_{28}O_4Na$ $[M + Na]^+$: 307.1880, found 307.1884.

Methyl 2-(5-hexanoylfuran-2-yl)acetate (18)

Hexanoic acid (94 μL, 0.75 mmol) was dissolved in thionyl chloride (6 mL) and refluxed for 3 h. The excess thionyl chloride was distilled off to give the resulting hexanoyl chloride as a dark yellow oil. It was then dissolved in CH_2Cl_2 (6 mL) and cooled to 0 °C. $SnCl_4$ (1.13 mL, 1 M in CH_2Cl_2, 1.13 mmol) was then added slowly dropwise and the resulting solution stirred at 0 °C for 45 min. Methyl ester **17** (105.3 mg, 0.75 mmol) was dissolved in CH_2Cl_2 (2 mL) and the resulting solution was added slowly to the reaction over 10 min. The reaction was then stirred at 0 °C for 45 min before being quenched with ice. The biphasic mixture was separated and the aqueous layer extracted with CH_2Cl_2. The combined organic layers were washed with brine, dried over Na_2SO_4 and concentrated under reduced pressure. The crude residue was purified by column chromatography (10% to 20% EtOAc/hexanes) to give ketone **18** (102 mg, 57%) as yellow oil. ^{1}H NMR (400 MHz, $CDCl_3$) δ: 7.12 (d, J = 3.5 Hz, 1H), 6.41 (d, J = 3.5 Hz, 1H), 3.77 (s, 2H), 3.74 (s, 3H), 2.84–2.66 (m, 2H), 1.70 (t, J = 7.4 Hz, 2H), 1.34 (h, J = 3.6 Hz, 4H), 0.90 (td, J = 7.1, 5.9, 3.4 Hz, 3H); ^{13}C NMR (100 MHz, $CDCl_3$) δ: 189.3, 168.7, 152.1, 129.0 118.1, 110.7, 77.2, 76.9, 76.6, 52.4, 38.2, 34.0, 31.4, 24.1, 22.3, 13.8; ESI-API MS: $[M + H]$ = 239.1; HRMS-ESI (+) m/z calc'd for $C_{13}H_{10}O_4$ $[M + H]^+$: 239.1280, found 239.1282.

Methyl (*R*)-2-(5-(1-hydroxyhexyl)furan-2-yl)acetate (19)

Ketone **18** (60.5 mg, 0.25 mmol) was dissolved in CH_2Cl_2 (7 mL) and Et_3N (0.5 mL, 3.81 mmol) was added followed by HCO_2H (143 μL, 3.81 mmol). RuCl[(*R*,*R*)-TsDPEN](mesitylene) (3.9 mg, 0.006 mmol) was dissolved in CH_2Cl_2 (0.5 mL) and then added to the reaction. The reaction was then set to stir at 50 °C for 12 h before being quenched with H_2O. It was then extracted with CH_2Cl_2 and the combined organic layers washed with brine, dried over Na_2SO_4 and concentrated under reduced pressure. The crude residue was purified by column chromatography (10% to 30% EtOAc/hexanes) to give optically active alcohol **19** (50.3 mg, 83%) as a clear oil. $[\alpha]_D^{23}$ +2.9 (*c* 2.4, $CHCl_3$), $[\alpha]_D^{23}$ +7.9 (*c* 2.97, MeOH) ^{1}H-NMR (400 MHz, $CDCl_3$) δ 6.15 (d, J = 0.9 Hz, 2H), 4.62 (t, J = 6.8 Hz, 1H), 3.71 (s, 3H), 3.66 (s, 2H), 1.98 (s, 1H), 1.88–1.74 (m, 2H), 1.43 (tdd, J = 10.0, 8.1, 7.5, 4.1 Hz, 1H), 1.36–1.22 (m, 5H), 0.88 (q, J = 4.9, 4.1 Hz,

3H); ^{13}C NMR (100 MHz, $CDCl_3$) δ 169.8, 156.5, 146.8, 108.5, 106.6, 67.7, 52.2, 35.3, 33.8, 31.5, 25.1, 22.4, 13.9; ESI-API MS: [M + Na] = 263.1; HRMS-ESI (+) *m*/*z* calc'd for $C_{13}H_{20}O_4Na$ $[M + H]^+$: 263.1254, found 263.1256; 99% ee, determined by HPLC using Chiralpak IA3 and gradient of 0–10% isopropanol/hexanes (t_{major} = 25.7 min, t_{minor} = 24.8 min).

Methyl 2-((2*R*,5*S*,6*R*)-5-hydroxy-6-pentyltetrahydro-2*H*-pyran-2-yl)acetate (20)

Furanyl alcohol **19** (16.9 mg, 0.07 mmol) was dissolved in THF (2 mL) and H_2O (0.5 mL) and cooled to 0 °C. KBr (0.4 mg, 0.003 mmol), $NaHCO_3$ (2.9 mg, 0.03 mmol) and oxone (51.9 mg, 0.08 mmol) were then added and the reaction slowly warmed to 23 °C. After 3 h, it was quenched with saturated $NaHCO_3$ and extracted with EtOAc. The combined organic layers were washed with brine, dried over Na_2SO_4 and concentrated under reduced pressure. The crude residue was used immediately for the next reaction.

The crude oil was dissolved in CH_2Cl_2 (3 mL) and Et_3SiH (112 μL, 0.7 mmol) was added. The reaction was then cooled to −40 °C and $BF_3{\cdot}OEt_2$ (52 μL, 0.42 mmol) was added slowly dropwise. The reaction was then stirred at −40 °C for 16 h before being warmed to 23 °C and stirred for an additional 1 h. It was then quenched with saturated NH_4Cl and extracted with CH_2Cl_2. The combined organic layers were washed with brine, dried over Na_2SO_4 and concentrated under reduced pressure. The crude residue was purified by column chromatography (20% to 30% EtOAc/hexanes) give tetrahydropyran derivative **20** (10.0 mg, 58%) as a clear oil. $[\alpha]_D^{23}$ +27.5 (*c* 2.57, $CHCl_3$) ^{1}H NMR (400 MHz, $CDCl_3$) δ: 3.80–3.69 (m, 1H), 3.67 (s, 3H), 3.27 (ddd, *J* = 10.4, 8.9, 4.6 Hz, 1H), 3.04 (td, *J* = 9.0, 2.4 Hz, 1H), 2.53 (dd, *J* = 14.9, 8.0 Hz, 1H), 2.40 (dd, *J* = 14.9, 5.4 Hz, 1H), 2.13–2.01 (m, 1H), 1.85–1.72 (m, 2H), 1.54–1.29 (m, 3H), 1.32–1.22 (m, 6H), 0.87 (t, *J* = 6.8 Hz, 3H); ^{13}C NMR (100 MHz, $CDCl_3$) δ 171.7, 82.1, 73.8, 70.4, 51.5, 40.8, 32.7, 31.7, 31.6, 30.8, 24.8, 22.6, 13.9; ESI-API MS: [M + H] = 245.1, [M + Na] = 267.1; HRMS-ESI (+) *m*/*z* calc'd for $C_{13}H_{25}O_4$ $[M + H]^+$: 245.1747, found 245.1750.

2-((2*R*,5*S*,6*R*)-5-Hydroxy-6-pentyltetrahydro-2*H*-pyran-2-yl)-*N*-methoxy-*N*-methylacetamide (21)

To a solution of NH(OMe)Me·HCl (16.0 mg, 0.16 mmol) in dry THF (3 mL) and cooled to −30 °C, *i*-PrMgCl (450 μL, 0.45 mmol) was added slowly dropwise and the reaction stirred at −30 °C for 1 h. Methyl ester **20** (10 mg, 0.04 mmol) was dissolved in dry THF and then added slowly, dropwise to the reaction which was stirred at −30 °C for an additional 4 h before being quenched with saturated NH_4Cl. It was extracted with EtOAc and the combined organic layers were washed with brine, dried over Na_2SO_4 and concentrated under reduced pressure. The crude residue was purified by column chromatography (50% to 80% EtOAc/hexanes) to give Weinreb amide **21** (10.4 mg, 93%) as a clear oil. $[\alpha]_D^{23}$ +7.8 (*c* 1.33, $CHCl_3$); ^{1}H NMR (800 MHz, $CDCl_3$) δ 3.85–3.80 (m, 1H), 3.71 (d, *J* = 2.2 Hz, 3H), 3.32–3.27 (m, 1H), 3.20 (s, 3H), 3.09 (ddd, *J* = 8.9, 6.5, 2.5 Hz, 1H), 2.85 (d, *J* = 13.4 Hz, 1H), 2.43 (dd, *J* = 15.1, 6.3 Hz, 1H), 2.13–2.08 (m, 1H), 1.90–1.79 (m, 2H), 1.55–1.44 (m, 2H), 1.46–1.39 (m, 1H), 1.41–1.31 (m, 1H), 1.33–1.27 (m, 5H), 0.90 (td, *J* = 7.0, 2.3 Hz, 3H); ^{13}C NMR (100 MHz, $CDCl_3$) δ 172.0, 82.2, 74.1, 70.6, 61.3, 37.9, 33.0, 32.0, 31.9, 31.2, 29.7, 25.0, 22.6, 14.1; ESI-API MS: [M + H] = 274.0, [M + Na] = 296.1.

Decytospolide A (6) *via* Weinreb amide 21

Weinreb amide **21** (10.4 mg, 0.038 mmol) was dissolved in dry THF (2 mL) and cooled to 0 °C. EtMgBr in THF solution (305 μL, 0.3 mmol) was added slowly dropwise and the reaction slowly warmed to 23 °C. It was stirred for 5 h, then quenched with saturated NH_4Cl and extracted with EtOAc. The combined organic layers were then washed with brine and dried over Na_2SO_4. The crude residue was purified by column chromatography (20% to 50% EtOAc/hexanes) to give decytospolide A, **6** (8.9 mg, 97%) as a clear oil. $[\alpha]_D^{23}$ = +7.8 (*c* 1.33, $CHCl_3$); ^{1}H NMR (400 MHz, $CDCl_3$) δ 3.73 (dddd, *J* = 10.2, 8.0, 4.8, 2.0 Hz, 1H), 3.25 (ddd, *J* = 10.6, 9.0, 4.6 Hz, 1H), 3.02 (td, *J* = 8.9, 2.5 Hz, 1H), 2.65 (dd, *J* = 15.0, 8.1 Hz, 1H), 2.58–2.29 (m, 3H), 2.07 (ddd, *J* = 12.0, 5.5, 2.8 Hz, 1H), 1.85–1.70 (m, 2H), 1.53–1.41 (m, 1H), 1.46 (s, 2H), 1.44–1.33 (m, 1H), 1.37–1.24 (m, 5H), 1.03 (t, *J* = 7.3 Hz, 3H), 0.93–0.83 (m, 3H); ^{13}C NMR (100 MHz, $CDCl_3$) δ 209.9, 82.0, 74.0, 70.4, 48.2, 36.9, 32.8, 31.8, 31.7, 31.1, 24.9, 22.5, 13.9, 7.4; ESI-API MS: [M + H] = 243.1, [M + Na] = 265.1; HRMS-ESI (+) *m*/*z* calc'd for $C_{14}H_{27}O_3$ $[M + H]^+$: 243.1955, found 243.1958.

Decytospolide B (7) *via* Weinreb amide 21

Above synthetic decytospolide A (9.7 mg, 0.04 mmol) was dissolved in CH_2Cl_2 (3 mL) and cooled to 0 °C. Pyridine (10 μL, 0.12 mmol), Ac_2O (4 μL, 0.04 mmol) and a few crystals of DMAP were added and the reaction warmed to 23 °C. The reaction was stirred for 3 h before being quenched with water. It was extracted with CH_2Cl_2 and the combined organic layers washed with brine and dried over Na_2SO_4. The crude residue was purified by column chromatography (10 to 30% EtOAc/hexanes) to give **7** (9.8 mg, 86%) as a clear oil. $[\alpha]_D^{20}$ = +22.8 in $CHCl_3$ (*c* 1.96); ^{1}H NMR (400 MHz, $CDCl_3$) δ 4.44 (td, *J* = 10.0, 4.7 Hz, 1H), 3.76 (ddd, *J* = 10.9, 7.8, 4.9 Hz, 1H), 3.22 (td, *J* = 9.0, 2.6 Hz, 1H), 2.67 (dd, *J* = 15.2, 8.0 Hz, 1H), 2.58–2.33 (m, 3H), 2.13 (ddd, *J* = 11.3, 5.6, 3.3 Hz, 1H), 2.03 (s, 3H), 1.79–1.70 (m, 1H), 1.58–1.36 (m, 3H), 1.40–1.17 (m, 7H), 1.03 (t, *J* = 7.3 Hz, 3H), 0.86 (t, *J* = 6.9 Hz, 3H); ^{13}C NMR (100 MHz, $CDCl_3$) δ 209.8, 170.2, 79.2, 74.1, 71.9, 48.1, 37.1, 31.8, 31.6, 30.7, 29.2, 24.7, 22.5, 21.1, 13.9, 7.4; ESI-API MS: [M + H] = 285.1, [M + Na] = 307.2; HRMS-ESI (+) *m*/*z* calc'd for $C_{16}H_{28}O_4Na$ $[M + Na]^+$: 307.1880, found 307.1884.

Conflicts of interest

There are no conflicts to declare.

Acknowledgements

Financial support of this work was provided by the National Institutes of Health and Purdue University.

Notes and references

1 E. J. Kang and E. Lee, *Chem. Rev.*, 2005, **105**, 4348–4378.
2 K. S. Yeung and I. Paterson, *Chem. Rev.*, 2005, **105**, 4237–4313.
3 H. Fuwa, *Mar. Drugs*, 2016, **14**, 65.
4 N. M. Nasir, K. Ermanis and P. A. Clarke, *Org. Biomol. Chem.*, 2014, **12**, 3323–3335.
5 M. A. Brimble, K. P. Kaliappan, A. J. Moreno-Vargas, K. Palanichamy, M. A. Perry, J. D. Rainier, S. D. Rychnovsky, N. Sizemore, L. A. Stubbing and P. Vogel, *Synthesis of saturated oxygenated heterocycles. I, 5- and 6-membered rings*, Springer, Berlin, 2014.
6 E. Arundale and L. A. Mikeska, *Chem. Rev.*, 1952, **51**, 505–555.
7 J. Zeng, Y. J. Tan, J. Ma, M. L. Leow, D. Tirtorahardjo and X.-W. Liu, *Chem. – Eur. J.*, 2014, **20**, 405–409.
8 O. Achmatowicz, P. Bukowski, B. Szechner, Z. Zwierzchowska and A. Zamojski, *Tetrahedron*, 1971, **27**, 1973–1996.
9 O. Achmatowicz, G. Grynkiewicz and B. Szechner, *Tetrahedron*, 1976, **32**, 1051–1054.
10 A. K. Ghosh and M. Brindisi, *RSC Adv.*, 2016, **6**, 111564–111598.
11 J. Deska, D. Thiel and E. Gianolio, *Synthesis*, 2015, **47**, 3435–3450.
12 A. K. Ghosh, Z.-H. Chen, K. A. Effenberger and M. S. Jurica, *J. Org. Chem.*, 2014, **79**, 5697–5709.
13 A. K. Ghosh and J. Li, *Org. Lett.*, 2011, **13**, 66–69.
14 P.-F. Koh and T.-P. Loh, *Green Chem.*, 2015, **17**, 3746–3450.
15 S. Lu, P. Sun, T. Li, T. Kurtán, A. Mándi, S. Antus, K. Krohn, S. Draeger, B. Schulz, Y. Yi, L. Li and W. Zhang, *J. Org. Chem.*, 2011, **76**, 9699–9710.
16 J. A. Dale and H. S. Mosher, *J. Am. Chem. Soc.*, 1973, **95**, 512–519.
17 P. R. Krishna, R. Nomula and D. V. Ramana, *Tetrahedron Lett.*, 2012, **53**, 3612–3614.
18 D. Clarisse and F. Fache, *Tetrahedron Lett.*, 2014, **55**, 2221–2222.
19 K. Yahata, M. Minami, K. Watanabe and H. Fujioka, *Org. Lett.*, 2014, **16**, 3680–3683.
20 P. H. Gore, *Chem. Rev.*, 1955, **55**, 229–281.
21 M. Tofi, K. Koltsida and G. Vassilikogiannakis, *Org. Lett.*, 2009, **11**, 313–316.
22 S. Hashiguchi, A. Fujii, J. Takehara, T. Ikariya and R. Noyori, *J. Am. Chem. Soc.*, 1995, **117**, 7562–7563.
23 A. Fujii, S. Hashiguchi, N. Uematsu, T. Ikariya and R. Noyori, *J. Am. Chem. Soc.*, 1996, **118**, 2521–2522.
24 A. K. Ghosh and Z.-H. Chen, *Org. Lett.*, 2013, **15**, 5088–5091.
25 M.-P. Georgiadis, K. F. Albizati and T. M. Georgiadis, *Org. Prep. Proced. Int.*, 1992, **24**, 95–118.
26 Z. Li and R. Tong, *J. Org. Chem.*, 2016, **81**, 4847–4855.
27 L. R. Cafiero and T. S. Snowden, *Org. Lett.*, 2008, **10**, 3853–3856.
28 J. L. Shamshina and T. S. Snowden, *Org. Lett.*, 2006, **8**, 5881–5884.

Journal of Medicinal Chemistry

Article

Cite This: J. Med. Chem. 2018, 61, 9722−9737

pubs.acs.org/jmc

Design and Synthesis of Potent HIV-1 Protease Inhibitors Containing Bicyclic Oxazolidinone Scaffold as the P2 Ligands: Structure−Activity Studies and Biological and X-ray Structural Studies

Arun K. Ghosh,*[,†] Jacqueline N. Williams,[†] Rachel Y. Ho,[†] Hannah M. Simpson,[†] Shin-ichiro Hattori,[§] Hironori Hayashi,[§] Johnson Agniswamy,[‡] Yuan-Fang Wang,[‡] Irene T. Weber,[‡] and Hiroaki Mitsuya[§,∥,⊥]

[†]Department of Chemistry and Department of Medicinal Chemistry, Purdue University, 560 Oval Drive, West Lafayette, Indiana 47907, United States

[‡]Department of Biology, Molecular Basis of Disease, Georgia State University, Atlanta, Georgia 30303, United States

[§]Department of Refractory Viral Infections, National Center for Global Health and Medicine Research Institute, Tokyo 162-8655, Japan

[∥]Departments of Infectious Diseases and Hematology, Kumamoto University Graduate School of Biomedical Sciences, Kumamoto 860-8556, Japan

[⊥]Experimental Retrovirology Section, HIV and AIDS Malignancy Branch, National Cancer Institute, National Institutes of Health, Bethesda, Maryland 20892, United States

Supporting Information

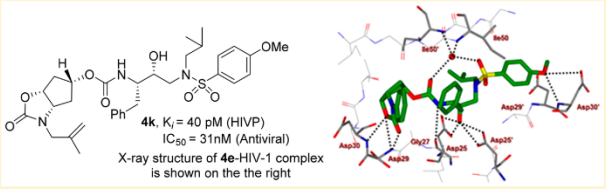

ABSTRACT: We have designed, synthesized, and evaluated a new class of potent HIV-1 protease inhibitors with novel bicyclic oxazolidinone derivatives as the P2 ligand. We have developed an enantioselective synthesis of these bicyclic oxazolidinones utilizing a key *o*-iodoxybenzoic acid mediated cyclization. Several inhibitors displayed good to excellent activity toward HIV-1 protease and significant antiviral activity in MT-4 cells. Compound **4k** has shown an enzyme K_i of 40 pM and antiviral IC_{50} of 31 nM. Inhibitors **4k** and **4l** were evaluated against a panel of highly resistant multidrug-resistant HIV-1 variants, and their fold-changes in antiviral activity were similar to those observed with darunavir. Additionally, two X-ray crystal structures of the related inhibitors **4a** and **4e** bound to HIV-1 protease were determined at 1.22 and 1.30 Å resolution, respectively, and revealed important interactions in the active site that have not yet been explored.

INTRODUCTION

The development of combined antiretroviral therapy (cART) has dramatically improved the treatment of human immunodeficiency virus type 1 (HIV-1) infections and acquired immunity deficiency syndrome (AIDS).[1,2] HIV-1 protease inhibitors (PIs) are a critically important class of antiretroviral medications in cART.[3,4] HIV-1 protease plays an essential role in the HIV life cycle and is a primary target for HIV/AIDS treatment.[5,6] PIs block the ability of HIV-1 protease to cleave polyproteins and prevent the formation of mature virions.[7,8] While cART drastically improved the course of HIV management and reduced the mortality and morbidity rates of HIV-1 infected individuals, the early FDA-approved PIs suffer from the traditional problems of peptide-like drugs including poor absorption, metabolic instability, and a number of other debilitating side effects.[9,10] Perhaps the most alarming problem is the emergence of drug resistance which renders these therapies ineffective.[11,12] Darunavir (DRV) is the latest FDA-approved PI and is the only PI-drug recommended as a first-line therapy.[13,14] DRV exhibits a high genetic barrier to resistance and is used for both treatment-experienced and treatment-naive patients with HIV-1 infection and AIDS.[15,16] DRV exhibits a dual mechanism of action as (1) an inhibitor of

Received: August 3, 2018
Published: October 24, 2018

DOI: 10.1021/acs.jmedchem.8b01227
J. Med. Chem. 2018, 61, 9722−9737

catalytically important dimeric HIV-1 protease and (2) an inhibitor of the dimerization of protease monomers.[17,18] The present first-line cART with boosted PI-based drugs and integrase-inhibitor bound regimens are effective against developing multidrug-resistant HIV-1 variants over an extended period of time. However, there are limitations with regard to drug related side effects, toxicity, and rapid emergence of drug-resistant variants for some patient groups. Therefore, potent and more effective HIV-1 protease inhibitors are necessary for the long-term success of cART.

DRV incorporates a privileged P2 ligand, 3(*R*),3a(*S*),6a(*R*)-bis-tetrahydrofuranylurethane (bis-THF), on an (*R*)-(hydroxyethylamino)sulfonamide isostere (**1**, Figure 1).[19,20]

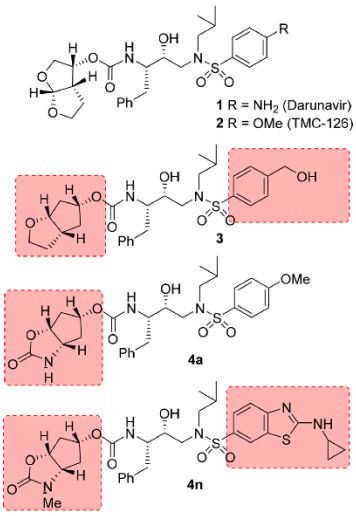

Figure 1. Structures of HIV-1 protease inhibitors **1**–**4**.

The X-ray structural studies of DRV-bound HIV-1 protease revealed a network of hydrogen bonds with backbone atoms like a molecular crab throughout the S2 and S2′ subsites.[21,22] In particular, both oxygens on the bis-THF P2 ligand formed a pair of strong hydrogen bonds with the backbone amide NHs of Asp30 and Asp29. Furthermore, the 4-aminobenzene-sulfonamide P2′ ligand also formed a strong hydrogen bond with the Asp30 backbone amide NH. These ligand-binding site interactions are responsible for DRV's superb antiviral and drug-resistance properties. Further modulation of ligand-binding site interactions in the active site of HIV-1 protease led us to develop a range of very potent PIs effective against multidrug-resistant HIV-1 variants.[23,24] In particular, we have designed inhibitor **3** containing a cyclopentanyltetrahydrofuran (Cp-THF) as the P2 ligand. Upon the basis of the X-ray structure of DRV-bound HIV-1 protease, we now speculate that a bicyclic oxazolidinone derivative can mimic the hydrogen-bonding interactions as well as the van der Waals interactions of the bis-THF and Cp-THF ligands in PIs **1**–**3** in the S2 subsite. We describe here the design and synthesis of a new class of HIV-1 protease inhibitors that incorporate stereochemically defined bicyclic oxazolidinone scaffolds as the P2 ligands.

CHEMISTRY

For initial investigation, we planned to synthesize an unsubstituted oxazolidinone ligand as represented in inhibitor **4a**. The synthesis of the requisite bicyclic oxazolidinone ligand in inhibitor **4a** in the optically active form is shown in Scheme 1. Multigram quantities of optically active (1*R*,4*S*)-*cis*-4-acetoxy-2-cyclopenten-1-ol (−)-**5** were prepared from cyclopentadiene using procedures described previously.[25,26] We utilized a 2-iodoxybenzoic acid (IBX) mediated cyclization protocol developed by Nicolaou and Baran for the synthesis of the bicyclic oxazolidine ligand.[27] Thus, monoacetate **5** was treated with phenyl isocyanate or 4-methoxyphenyl isocyanate and a catalytic amount (10 mol %) of DBU in CH_2Cl_2 at 23 °C for 4 h to provide carbamate derivatives **6a** and **6b**, respectively, in 81% yield. Treatment of these aryl carbamates with IBX in a mixture (10:1) of THF and DMSO at 90 °C for 24 h afforded oxazolidinones **7a** and **7b**, respectively, in 37–65% yields. Both *N*-aryl oxazolidinones were obtained as a single isomer (by ^{1}H NMR analysis). The cleavage of the *p*-methoxyphenyl group on **7b** was accomplished by treatment with ceric ammonium nitrate (CAN) in a mixture (5:1) of acetonitrile and water at 23 °C for 1 h to afford the acetate derivative **8** in 71% yield. Removal of the acetate group in **8** with K_2CO_3 in methanol provided the optically active 5-hydroxyhexahydro-2*H*-cyclopenta[*d*]oxazol-2-one **9** in near quantitative yield. To investigate the stereochemical effect on the ligand-binding site interactions, we have also prepared the corresponding enantiomeric oxazolidinone, *ent*-**9**. This was prepared from the known optically active (1*S*,4*R*)-*cis*-4-acetoxy-2-cyclopen-1-ol, *ent*-**5** using the steps as described for compound **9**.

Scheme 1. Synthesis of Bicyclic Oxazolidinone Ligands 9

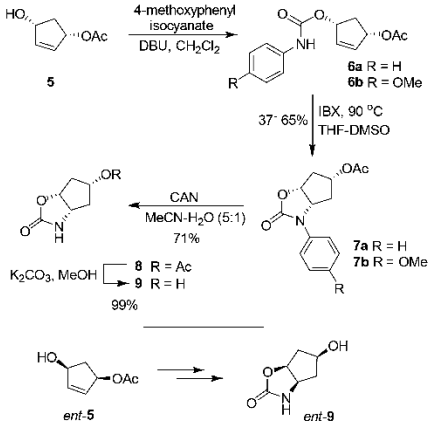

For the structure–activity relationship studies, we have prepared a number of substituted oxazolidinone derivatives. Upon the basis of our initial X-ray structure of DRV-bound HIV-1 protease-based models, it appeared that (3a*S*,5*R*,6a*R*)-5-hydroxyhexahydro-2*H*-cyclopenta[*d*]oxazol-2-one stereochemistry would be well-accommodated by the HIV-1 protease active site.[21] Our preliminary studies of the unsubstituted oxazolidinone-derived inhibitors revealed the preference for the (3a*S*,5*R*,6a*R*)-oxazolidinone stereochemistry as in inhibitor

DOI: 10.1021/acs.jmedchem.8b01227
J. Med. Chem. 2018, 61, 9722–9737

4a over the enantiomeric ligand in compound 4b. The synthesis of various substituted oxazolidinone derivatives is shown in Scheme 2. For the synthesis of *N*-phenyl and

Scheme 2. Synthesis of Substituted Oxazolidinone Ligand Alcohols

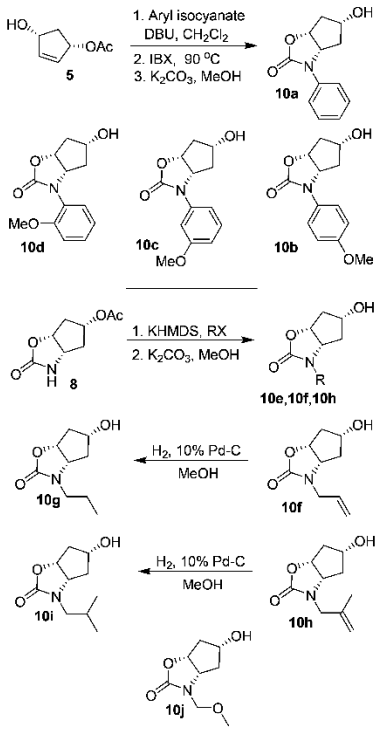

substituted phenyl oxazolidinones, optically active (1*R*,4*S*)-*cis*-4-acetoxy-2-cyclopenten-1-ol **5** was reacted with various aryl isocyanates in the presence of DBU to provide the respective carbamates. IBX-mediated cyclization of these carbamates at 90 °C in a mixture (10:1) of THF and DMSO provided the corresponding bicyclic oxazolidinone derivatives.[27] Removal of the acetate group by exposure to K_2CO_3 in methanol at 23 °C afforded the phenyl-substituted oxazolidinone ligand alcohols **10a**−**d**. For the synthesis of various aliphatic *N*-alkyl derivatives, acetoxy oxazolidinone derivative **8** was alkylated with various alkyl halides. As shown, oxazolidinone **8** was reacted with KHMDS in CH_3CN at 0 °C and the resulting anion was treated with MeI and the reaction mixture was warmed to 23 °C for 1 h to provide the *N*-Me derivative **10e** in 80% isolated yield. Saponification of the resulting ester afforded *N*-Me ligand alcohol **10e** in near quantitative yield. The corresponding enantiomeric *N*-Me derivative *ent*-**10** was prepared from *ent*-**9**. Similarly, *N*-alkylation with allyl iodide followed by removal of the acetate group furnished *N*-allyl derivative **10f** in 60% yield over two steps. Catalytic hydrogenation of **10f** in the presence of catalytic amount of 10% Pd−C in methanol under a hydrogen-filled balloon furnished the *N*-propyl derivative **10g** in 86% yield. Similarly, alkylation of **8** with 3-bromo-2-methylpropene followed by removal of the acetate provided ligand alcohol **10h** in 84% yield. Catalytic hydrogenation of **10h** furnished saturated ligand alcohol **10i** in 92% yield. For the introduction of the methoxymethyl side chain in ligand alcohol, oxazolidinone **8** was alkylated with KHMDS and chloromethyl methyl ether in THF at 0−23 °C for 1 h, providing the corresponding alkylated product. Removal of acetate group gave ligand alcohol **10j** in 33% yield over two steps.

The diverse optically active ligand alcohols **9**, *ent*-**9**, **10a**−**j**, and *ent*-**10e** were converted to the corresponding activated mixed carbonates.[28] As shown in Scheme 3, treatment of ligand alcohols with 4-nitrophenyl chloroformate and 4-methylmorpholine in CH_2Cl_2 at 0 °C for 12 h provided carbonates **11a**−**m** in good to excellent yields (30−97%).

Scheme 3. Synthesis of Actived Carbonates of Oxazolidinone Ligands

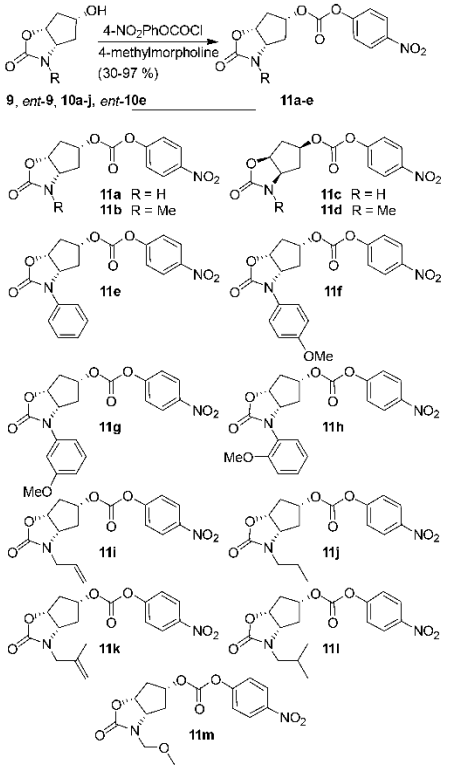

The syntheses of various inhibitors containing hydroxyethylaminesulfonamide isosteres with 4-methoxysulfonamide as the P2′ ligands are shown in Scheme 4. Reaction of known amine **12**[28] with activated carbonate **11a** provided inhibitor **4a** in good yield. Similarly, reaction of carbonates **11b**−**m** and amine **12** provided inhibitors **4b**−**m**. Inhibitor **4n**

DOI: 10.1021/acs.jmedchem.8b01227
J. Med. Chem. 2018, 61, 9722−9737

Scheme 4. Synthesis of HIV-1 Protease Inhibitors 4a−n

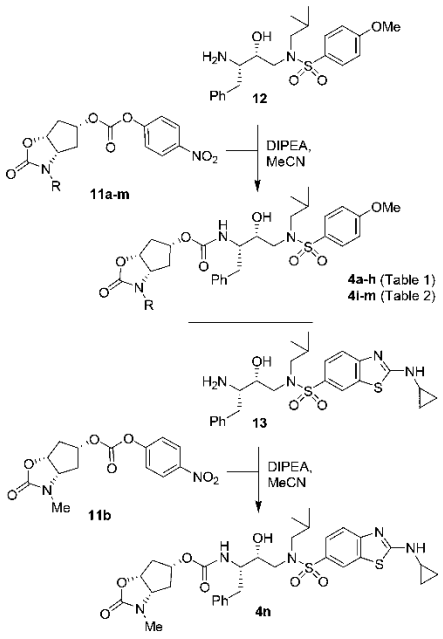

was prepared by reaction of known amine **13**[29] and carbonate **11b** as described above.

RESULTS AND DISCUSSION

We first evaluated all new inhibitors in an HIV-1 protease inhibitory assay according to the protocol described by Toth and Marshall.[30] Inhibitors that displayed potent K_i values (<1 nM), were then selected for further evaluation in an antiviral assay in MT-4 human T-lymphocytes exposed to HIV-1_{NL4-3}, and the antiviral assay was carried out as described previously.[15] Inhibitor structures and biological results are shown in Tables 1 and 2. As can be seen in Table 1, inhibitor **4a** with (3a*S*,5*R*,6a*R*)-2-oxohexahydro-2*H*-cyclopenta[*d*]-5-oxazolyl urethane as the P2 ligand exhibited very potent enzyme inhibitory and antiviral activity. The corresponding enantiomeric ligand in inhibitor **4b** showed an over 1000-fold reduction of enzyme inhibitory activity. Also, this inhibitor did not exhibit any appreciable antiviral activity. We then examined the effect of an *N*-alkyl group and stereochemical effects on potency. Inhibitor **4c** containing (3a*S*,5*R*,6a*R*)-oxazolidinone with an *N*-Me group showed an enzyme inhibitory K_i of 0.03 nM. This inhibitor showed slight improvement of antiviral activity (36 nM, entry 3). Inhibitor **4d**, containing the enantiomeric *N*-Me oxazolidinone derivative, displayed substantial reduction of enzyme inhibitory as well as antiviral activity. This result is consistent with activity observed for the unsubstituted ligand in inhibitor **4b** (entry 2). The stereochemical preference for (3a*S*,5*R*,6a*R*)-oxazolidinone is also consistent with our preliminary models. All further SAR studies were carried out with (3a*S*,5*R*,6a*R*)-oxazolidinone derived compounds. We then examined the effect of steric

Table 1. HIV-1 Protease Inhibitory and Antiviral Activity of PIs 4a−h

Entry	Inhibitor	K_i(nM)[a]	IC_{50}(nM)[b]
1.	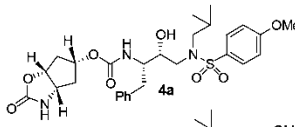 **4a**	0.0012	48.3
2.	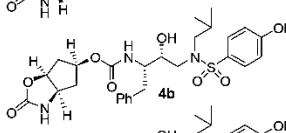 **4b**	1.33	>1000
3.	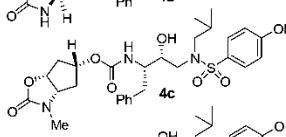 **4c**	0.03	36
4.	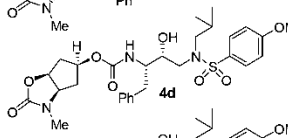 **4d**	0.16	436
5.	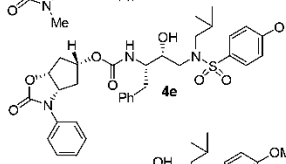 **4e**	0.33	>1000
6.	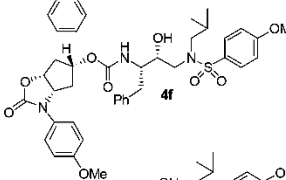 **4f**	0.63	>1000
7.	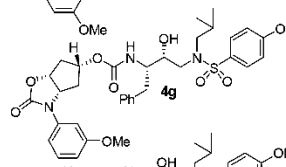 **4g**	92.8	>1000
8.	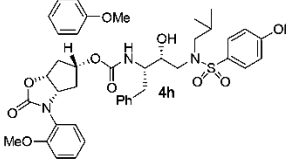 **4h**	0.08	251

[a]K_i values represents at least four data points. Standard error in all cases was less than 7%. Darunavir exhibited K_i = 16 pM. [b]Values are the mean of at least three experiments. Standard error in all cases was less than 5%. Darunavir exhibited antiviral IC_{50} = 3.2 nM, saquinavir IC_{50} = 21 nM.

bulk on the oxazolidinone nitrogen. Incorporation of an *N*-phenyl derivative in inhibitor **4e** (entry 5) resulted in significant loss of enzyme inhibitory activity. This inhibitor also displayed no appreciable antiviral activity. To promote hydrogen bonding interactions in the S2 subsite of HIV-1 protease, we incorporated a methoxy substituent on the *N*-phenyl ring. As shown, both *p*-methoxy and *m*-methoxy derivatives show reduction of enzymatic K_i values, particularly

DOI: 10.1021/acs.jmedchem.8b01227
J. Med. Chem. 2018, 61, 9722−9737

Table 2. HIV-1 Protease Inhibitory and Antiviral Activity of PIs 4i–n

Entry	Inhibitor	K_i (nM)[a]	IC_{50} (nM)[b]
1.	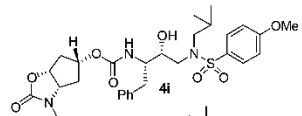 4i	0.016	369
2.	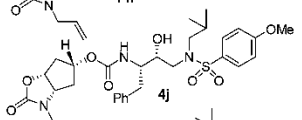 4j	0.14	447
3.	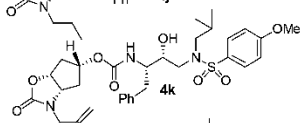 4k	0.04	31
4.	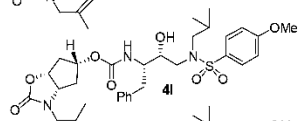 4l	0.16	41
5.	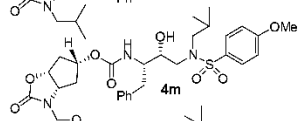 4m	0.016	84
6.	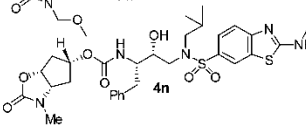 4n	0.19	28

[a] K_i values represents at least four data points. Standard error in all cases was less than 7%. Darunavir exhibited K_i = 16 pM. [b] Values are the mean of at least three experiments. Standard error in all cases was less than 5%. Darunavir exhibited antiviral IC_{50} = 3.2 nM, saquinavir IC_{50} = 21 nM.

for inhibitor **4g** (entry 7). Inhibitor **4h** with a 2-methoxy substituent on the *N*-phenyl ring, showed an improvement in enzyme inhibitory and antiviral activity (entry 8).

We then investigated the effect of a sterically demanding alkyl chain on the oxazolidinone ring. The results are shown in Table 2. Inhibitor **4i** with an *N*-allyl oxazolidinone as the P2 ligand showed a comparable enzyme inhibitory K_i as the *N*-methyl derivative **4c** (entry 3). However, there is a 10-fold reduction of antiviral activity compared to the corresponding *N*-methyl derivative **4c**. The corresponding inhibitor **4j** with *N*-propyl side chain showed a 10-fold reduction of HIV-1 protease inhibitory activity compared to *N*-allyl derivative **4i**. There was a slight reduction of antiviral activity as well. Incorporation of a sterically demanding branched chain *N*-methylallyl group in inhibitor **4k** resulted in good enzyme inhibitory activity as well as antiviral activity with an IC_{50} value of 31 nM (entry 3). Inhibitor **4l** with a saturated isobutyl side chain resulted in slight reduction of both enzyme K_i and antiviral activity compared to inhibitor 4k (entry 4). We have introduced an *N*-methoxymethyl side chain in an effort to promote hydrogen bonding with the methoxyl oxygen in the S2 subsite. Inhibitor **4m** showed very potent enzyme inhibitory activity. We recently demonstrated the potency enhancing effect of the cyclopropylaminobenzothiazole group as a P2′ ligand as it forms additional hydrogen bonding and van der Waals interactions in the S2′ subsite. We, therefore, synthesized inhibitor **4n** with a *N*-methyloxazolidinone as the P2 ligand and cyclopropylaminobenzothiazole as the P2′ ligand. However, there was no significant change in potency for this inhibitor compared to inhibitor **4c** (entry 3, Table 1) with a 4-methoxyphenylsulfonamide as the P2′ ligand.

PIs continue to be an important in current ART regimens, and in particular, they are extensively used for the treatment of naive and experienced HIV/AIDS patients. However, heavily ART regimen-experienced HIV/AIDS patients show drug failure with current PIs including DRV.[31,32] Therefore, one of the main design objectives is to develop new PIs that maintain potency against a variety of existing multi-PI-resistant HIV-1 variants. In preliminary studies, we examined the activity of two potent oxazolidinone containing PIs **4k** and 4l against a panel of HIV-1 variants that had been selected in vitro with three widely used FDA-approved PIs, ATV, LPV, and APV. Each of these HIV-1 variants was selected in vitro by propagating HIV-1_{NL4-3} in the presence of increasing concentrations of each PI (up to 5 μM) in MT-4 cells as described by us previously.[31,33]

The viruses used in the present work were obtained, propagated, and titrated as described by us previously.[34] Also, the IC_{50} values were determined as previously described and the names of HIV-1 strains used are described in the very left

Table 3. Comparison of the Antiviral Activity of 4k and 4l and Other PIs against Highly PI-Resistant HIV-1 Variants

	mean IC_{50} ± SD (nM)[b]					
virus[a]	LPV	APV	ATV	DRV	4k	4l
HIV-1_{NL4-3}	6.0 ± 0.09	431 ± 3	0.89 ± 0.02	3.5 ± 0.09	23 ± 0.1	40 ± 1
HIV-$1_{ATV}{}^{R}{}_{5\mu M}$	311 ± 6	>1000	>1000	19 ± 2 (5)	36 ± 2 (1)	33 ± 2 (1)
HIV-$1_{LPV}{}^{R}{}_{5\mu M}$	>1000	>1000	293 ± 4	301 ± 0.2 (86)	>1000	615 ± 8 (15)
HIV-$1_{APV}{}^{R}{}_{5\mu M}$	218 ± 1	>1000	2.0 ± 0.08	129 ± 3 (37)	261 ± 15 (11)	309 ± 4 (7)
HIV-$1_{DRV}{}^{R}{}_{P20}$	>1000	>1000	>1000	169 ± 15	>1000	>1000
HIV-$1_{DRV}{}^{R}{}_{P30}$	>1000	>1000	>1000	426 ± 26	>1000	>1000
HIV-$1_{DRV}{}^{R}{}_{P51}$	>1000	>1000	>1000	>1000	>1000	>1000

[a] The amino acid substitutions identified in the protease-encoding region compared to the wild-type HIV-1_{NL4-3} were L23I, E34Q, K43I, M46I, I50L, G51A, L63P, A71V, V82A, T91A in HIV-$1_{ATV}{}^{R}{}_{5\mu M}$; L10F, M46I, I54V, V82A in HIV-$1_{LPV}{}^{R}{}_{5\mu M}$; or L10F, M46I, I50V, I85V in HIV-$1_{APV}{}^{R}{}_{5\mu M}$. [b] The IC_{50} (50% effective concentration) values were determined by using MT-4 cells as target cells. MT-4 cells (10^5/mL) were exposed to 100 $TCID_{50}$ values of each HIV-1, and the inhibition of p24 Gag protein production by each drug was used as an end point. All assays were conducted in duplicate, and the data shown represent mean values (±SD) derived from the results of two independent experiments.

DOI: 10.1021/acs.jmedchem.8b01227
J. Med. Chem. 2018, 61, 9722–9737

column of Table 3.[34] The results are shown in Table 3. As can be seen, PI APV lost significant activity against all multidrug-resistant HIV-1 variants. LPV also lost activity against the three HIV-1 variants. DRV showed relatively better results; however, it too failed to block replication of each of these three variants very effectively. DRV exhibited an IC_{50} value fold-change ranging from 5- to 86-fold. While both oxazolidinone-based new PIs **4k** and **4l** are significantly less potent than DRV, both PIs maintained good activity against all three HIV-1 variants compared to wild-type HIV_{NL4-3}. Inhibitor **4l** showed antiviral activity with IC_{50} values ranging from 33 nM to 615 nM. In particular, its fold-changes in activity are better than any other PIs examined. Both PIs **4k** and **4l** maintained full antiviral activity against highly ATV-resistant HIV-1 variants. While DRV was relatively less potent against HIV-$1_{DRV^{R}P20}$ with an IC_{50} value of 169 nM, both oxazolidinone-derived inhibitors **4k** and **4l** failed to block the replication of a highly DRV-resistant HIV-1 variants. In general, oxazolidinone-derived inhibitors showed low cytotoxicity (CC_{50}) values in MT-4 cells. The CC_{50} values were determined as previously described.[34] The selectivity index of selected inhibitors is shown in Table 4. In general, our detailed X-ray crystallographic studies of structurally related inhibitor **4e**-bound HIV-1 protease provided molecular insight into the binding features responsible for its properties.[35]

Table 4. Selectivity Index for Selected Inhibitors[a]

inhibitor	CC_{50} (μM)	selectivity index[a]
4a	>100	>2070
4c	>100	>2778
4d	>100	>229
4k	>100	>3226
4l	>100	>2439
4n	43	1536

[a]Each selectivity index denotes a ratio of CC_{50} to IC_{50}.

The X-ray structures of wild-type HIV-1 protease cocrystallized with inhibitors **4a** (GRL-034-17A) and **4e** (GRL-042-17A) were refined to resolutions of 1.22 and 1.30 Å resolution with R/R_{free} of 15.5/18.8 and 15.0/18.2%, respectively. The protease dimer complexed with **4a** bound two alternative orientations of inhibitor in the active site cavity with 0.7/0.3 relative occupancy, while the other protease structure contained a single conformation of the inhibitor **4e**. The overall backbones of the two protease dimers were very similar to that of the PR/DRV complex with a RMSD of 0.20 and 0.24 Å for 198 equivalent Cα atoms in the complexes with **4a** and **4e**, respectively.[21,36] The **4a**-bound protease showed the largest shift of approximately 1.0 Å for flap residue Phe53, which may result from the hydrogen bond between the urethane nitrogen of P2 ligand and the carbonyl oxygen of Gly48 in the adjacent β strand of the flap. In contrast, the largest disparity of approximately 0.8 Å at Gly48 in the **4e**-bound protease is likely caused by steric hindrance of the additional phenyl group of P2. The key interactions of inhibitors **4a** and **4e** with HIV-1 protease are highlighted in a stereoview of the active sites in Figures 2 and 3, respectively. Both inhibitors form a water-mediated tetracoordinated hydrogen bonding interaction involving the inhibitor carbonyl oxygen and one of the oxygens of the sulfonamide functionality with amides of Ile50 and Ile50′ in the flaps. Such interactions have been observed for many other HIV-1 protease inhibitors.[3,21,22] With the exception of the P2 ligand, the inhibitors retain the majority of hydrogen bonds observed between DRV and the main chain atoms of the protease. The oxazolidin-2-one P2 group of both inhibitors is embedded between the amide of Asp29 and the carbonyl oxygen of Gly48. The two oxygens of the oxazolidinone group form good hydrogen bond interactions with the amide NH of Asp29 at 3.1−3.2 Å and 2.8−2.9 Å distances for the ring oxygen and the carbonyl oxygen, respectively. The P2 urethane NH of the major conformation of inhibitor **4a** forms a good hydrogen bond with the main chain carbonyl oxygen of Gly48 with distance of 3.0 Å, although the distance lengthened to 3.5 Å, for the minor conformation.

The larger P2 group of **4e** exhibits hydrophobic, C−H···π, and hydrogen bond interactions with the protease (Figure 4). The phenyl group is sandwiched between the carbonyl oxygen atom of Gly48 and the guanidinium group of Arg8′ and forms several C−H···π interactions with shortest interatomic distances of 2.8 and 3.5 Å with Gly48 and Arg8′, respectively. These short hydrophobic interactions of **4e** are associated with a shift of Gly48 and may be responsible for the higher K_i of this inhibitor compared to that of **4a**. The cyclopentaloxazol group of both inhibitors has van der Waals contacts with Val32, Ile47, Ile50′, and Ile84 similar to those seen for the bis-THF P2 ligand of DRV.[21,22] A comparison of the ligand binding

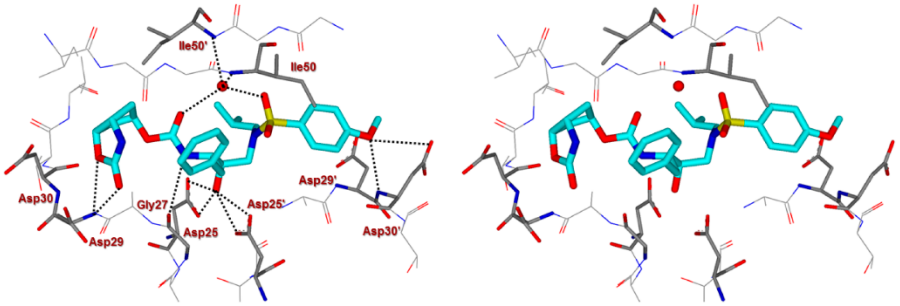

Figure 2. Stereoview of the X-ray crystal structure of inhibitor **4a** (turquoise) in the active site of HIV-1 protease (PDB code 6E9A). The oxazolidinone P2 ligand makes hydrogen-bonding and van der Waals interactions in the S2 subsite. All key hydrogen bonds are shown as black dotted lines.

DOI: 10.1021/acs.jmedchem.8b01227
J. Med. Chem. 2018, 61, 9722−9737

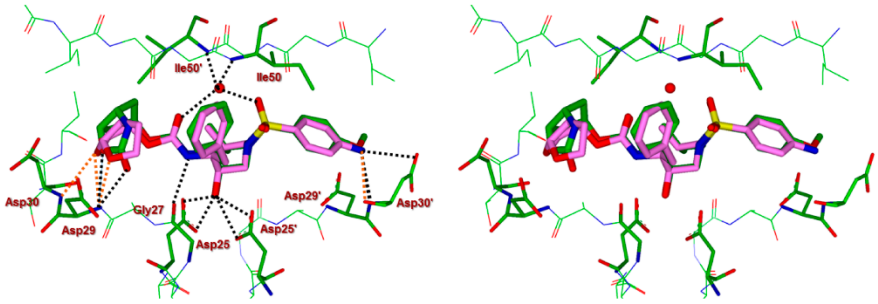

Figure 3. Stereoview of the overlay of X-ray crystal structures of inhibitor **4a** (green) and DRV (magenta) in the active site of HIV-1 protease (PDB code 6E9A for **4a** and PDB code 2IEN for DRV). Both P2 and P2′ ligands make strong hydrogen bonds in the S2 subsite. All key hydrogen bonds are shown as black dotted lines for **4a** and orange dotted lines for DRV.

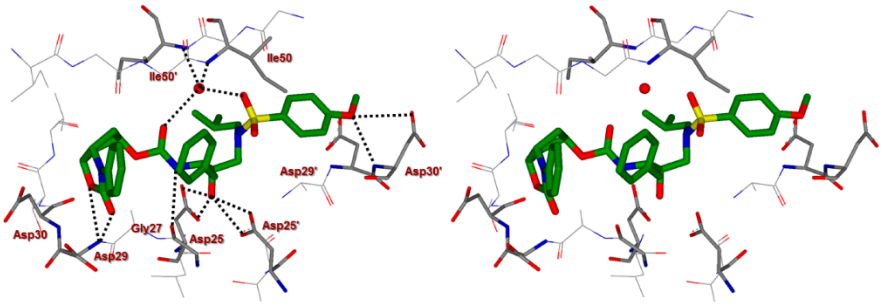

Figure 4. Stereoview of the X-ray crystal structure of inhibitor **4e** (green) in the active site of HIV-1 protease (PDB code 6E7J). The oxazolinone P2 ligand makes hydrogen-bonding and van der Waals interactions in the S2 subsite. All key hydrogen bonds are shown as black dotted lines.

interactions of the bis-THF ligand of darunavir and the oxazolidinone ligand of inhibitor **4a** in the HIV-1 protease active site is shown in the stereoview of Figure 3. The figure was created based upon the X-ray structures of DRV-bound and **4a**-bound HIV-1 protease. It appears that the bis-THF ligand in DRV makes additional hydrogen bonding interactions with the backbone amide NH of Asp30. However, van der Waals interactions of both bicyclic scaffolds are comparable. The bicyclic oxazolidinone moiety for both inhibitors **4a** and **4e** make similar hydrogen bonding interactions in the active site. These interactions contribute to the high enzyme affinity and antiviral activity of the majority of the oxazolidinone-derived inhibitors in our current studies.

■ CONCLUSION

In summary, we have designed and synthesized a new class of HIV-1 protease inhibitors incorporating bicyclic oxazolidinone as the P2 ligand. We demonstrated that the ligand stereochemistry is very important for potency. Inhibitor **4a** with (3a*S*,5*R*,6a*R*)-oxazolidinone stereochemistry is significantly more potent than the corresponding inhibitor with the enantiomeric ligand. We have examined various *N*-aryl and *N*-alkyl oxazolidinone derivatives to improve potency. It turns out that *N*-alkyl oxazolidinones with small aliphatic alkyl groups can be accommodated by the active site. The *N*-methyl, *N*-isobutenyl, and *N*-isobutyl derivatives **4c**, **4k**, and **4l**, respectively, have shown excellent enzyme inhibitory and antiviral activity. Inhibitors **4k** and **4l** were evaluated against a panel of multidrug-resistant HIV-1 variants. While both compounds are less potent than darunavir, its fold-changes in activity were similar to those observed with other approved PIs. Both inhibitors **4k** and **4l** maintained near full antiviral potency against ATV-resistant HIV-1 variants. However, these PIs failed to block the replication of highly DRV-resistant HIV-1 variants. The bicyclic oxazolidinones contain three asymmetric centers, and various ligands were synthesized efficiently from readily available, optically active *cis*-4-acetoxycyclopenten-1-ol by formation of the aryl carbamate followed by an IBX-mediated cyclization reaction developed by Nicolaou and Baran. Our X-ray structural studies of inhibitor **4a**- and **4e**-bound HIV-1 protease provided molecular insight into their ligand-binding site interactions. As it turns out, the oxazolidinone oxygen forms a strong hydrogen bonding interaction with Asp29 backbone amide NH. The bicyclic scaffold and the *N*-phenyl ring form van der Waals interactions with residues in the S2 site. The preliminary results of these oxazolidinone-derived inhibitors are very encouraging, and we plan to carry out optimization of ligand-binding site interactions and improve inhibitor potency. Further structural modifications are in progress in our laboratories.

■ EXPERIMENTAL METHODS

All moisture-sensitive reactions were carried out in oven-dried glassware under an argon atmosphere unless otherwise stated. Anhydrous solvents were obtained as follows: Tetrahydrofuran was

DOI: 10.1021/acs.jmedchem.8b01227
J. Med. Chem. 2018, 61, 9722−9737

distilled from sodium metal/benzophenone under argon. Dichloromethane was distilled from calcium hydride under argon. All other solvents were reagent grade. Column chromatography was performed using Silicycle SiliaFlash F60 230−400 mesh silica gel. Thin layer chromatography was carried out using EMD Millipore TLC silica gel 60 F254 plates. ^{1}H NMR and ^{13}C NMR spectra were recorded on a Bruker AV-III-400, Bruker DRX500, or Bruker AV-III-800. Low-resolution mass spectra were collected on an LCMS. High-resolution mass spectra were collected by the Purdue University Campus-Wide Mass Spectrometry Center. HPLC analysis and purification were done an on Agilent 1100 series instrument using a YMC Pack ODS-A column of 4.6 mm i.d. for analysis and either 10 mm i.d. or 20 mm i.d. for purification. The purity of all test compounds was determined by HPLC analysis to be ≥95% pure.

(3a*S*,5*R*,6a*R*)-2-Oxohexahydro-2*H*-cyclopenta[*d*]oxazol-5-yl ((2*S*,3*R*)-3-Hydroxy-4-((*N*-isobutyl-4-methoxyphenyl)-sulfonamido)-1-phenylbutan-2-yl)carbamate (4a). To a stirred solution of activated carbonate **11a** (16 mg, 0.05 mmol) in dry acetonitrile (1.5 mL) were added *N*,*N*-diisopropylethylamine (56 μL, 0.3 mmol) and isostere amine **12** (23 mg, 0.06 mmol) at 23 °C under argon atmosphere. The reaction mixture was stirred for 48 h. Upon completion, solvent was removed under reduced pressure. The crude product was purified by silica gel column chromatography (80% EtOAc in hexane) to afford **4a** (13 mg, 44%): ^{1}H NMR (500 MHz, CD_3OD) δ 7.77 (d, *J* = 8.8 Hz, 2H), 7.24 (dd, *J* = 8.9, 6.1 Hz, 4H), 7.19−7.14 (m, 1H), 7.08 (d, *J* = 8.9 Hz, 2H), 5.12 (t, *J* = 6.7 Hz, 1H), 5.03−4.96 (m, 1H), 4.33−4.27 (m, 1H), 3.87 (s, 3H), 3.78−3.68 (m, 2H), 3.48−3.37 (m, 1H), 3.03 (ddd, *J* = 20.0, 13.1, 9.7 Hz, 3H), 2.98−2.83 (m, 2H), 2.57 (dd, *J* = 13.7, 10.4 Hz, 1H), 2.09−1.94 (m, 3H), 1.90−1.82 (m, 2H), 1.16 (dd, *J* = 10.7, 6.3 Hz, 1H), 0.95−0.80 (m, 7H). ^{13}C NMR (201 MHz, $CDCl_3$) δ 162.9, 158.8, 155.5, 138.4, 137.5, 129.6, 128.4, 126.3, 114.3, 81.4, 81.2, 72.8, 58.6, 57.9, 55.6, 54.8, 52.2, 40.0, 39.2, 36.4, 35.9, 29.7, 27.2, 27.1, 20.2, 19.9. LRMS (ESI) *m*/*z*: [M + H]$^+$ 576.2. HRMS (ESI) *m*/*z*: [M + Na]$^+$ calcd $C_{28}H_{37}N_3O_8SNa$ 598.2194; found 598.2185.

(3a*R*,5*S*,6a*S*)-2-Oxohexahydro-2*H*-cyclopenta[*d*]oxazol-5-yl ((2*S*,3*R*)-3-Hydroxy-4-((*N*-isobutyl-4-methoxyphenyl)-sulfonamido)-1-phenylbutan-2-yl)carbamate (4b). Compound **11c** (4.8 mg, 0.02 mmol) was treated with isostere amine **12** (7 mg, 0.02 mmol) by following the same procedure outlined for inhibitor **4a** to give inhibitor **4b** (5.3 mg, 60%): ^{1}H NMR (800 MHz, CD_3OD) δ 7.77 (d, *J* = 8.9 Hz, 2H), 7.29−7.21 (m, 4H), 7.16 (tt, *J* = 7.0, 1.7 Hz, 1H), 7.08 (d, *J* = 8.9 Hz, 2H), 5.16−5.11 (m, 1H), 4.99 (t, *J* = 4.5 Hz, 1H), 4.35 (t, *J* = 7.1 Hz, 1H), 3.87 (s, 3H), 3.80−3.72 (m, 1H), 3.65 (ddd, *J* = 10.5, 6.8, 3.6 Hz, 1H), 3.44 (dd, *J* = 15.0, 3.0 Hz, 1H), 3.34 (d, *J* = 10.8 Hz, 1H), 3.10−3.02 (m, 2H), 2.93 (dd, *J* = 15.0, 8.6 Hz, 1H), 2.87 (dd, *J* = 13.6, 7.1 Hz, 1H), 2.55 (dd, *J* = 13.7, 10.6 Hz, 1H), 2.09−1.96 (m, 3H), 1.96−1.88 (m, 2H), 1.29 (s, 2H), 0.91 (d, *J* = 6.5 Hz, 3H), 0.87 (d, *J* = 6.6 Hz, 3H). ^{13}C NMR (201 MHz, CD_3OD) δ 163.1, 160.7, 156.3, 138.7, 130.8, 129.4, 129.3, 129.2, 128.0, 125.6, 114.0, 82.1, 76.4, 72.6, 57.3, 56.6, 56.2, 54.8, 52.3, 39.3, 39.1, 35.8, 26.6, 19.1, 19.0. LRMS (ESI) *m*/*z*: [M + H]$^+$ 576.2. HRMS (ESI) *m*/*z*: [M + Na]$^+$ calcd $C_{28}H_{37}N_3O_8SNa$ 598.2194; found 598.2189.

(3a*S*,5*R*,6a*R*)-3-Methyl-2-oxohexahydro-2*H*-cyclopenta[*d*]-oxazol-5-yl ((2*S*,3*R*)-3-Hydroxy-4-((*N*-isobutyl-4-methoxyphenyl)sulfonamido)-1-phenylbutan-2-yl)carbamate (4c). Compound **11b** (7.5 mg, 0.02 mmol) was treated with isostere amine **12** (10.4 mg, 0.03 mmol) by following the same procedure outlined for inhibitor **4a** to give inhibitor **4c** (3.5 mg, 88%): ^{1}H NMR (800 MHz, $CDCl_3$) δ 7.80−7.74 (m, 2H), 7.35−7.24 (m, 4H), 7.23−7.16 (m, 1H), 7.04−6.95 (m, 2H), 5.04 (t, *J* = 4.3 Hz, 1H), 4.95 (q, *J* = 9.3, 6.9 Hz, 1H), 4.20−4.12 (m, 1H), 3.96 (dq, *J* = 9.8, 4.4 Hz, 1H), 3.89 (s, 3H), 3.79 (q, *J* = 17.3, 10.2 Hz, 1H), 3.22 (dd, *J* = 14.4, 4.2 Hz, 1H), 3.14 (dd, *J* = 14.9, 8.3 Hz, 2H), 3.00 (dd, *J* = 13.5, 8.0 Hz, 1H), 2.94 (dd, *J* = 13.5, 7.1 Hz, 1H), 2.75 (dd, *J* = 14.2, 10.1 Hz, 2H), 2.57 (s, 3H), 2.39−2.32 (m, 1H), 2.18 (dd, *J* = 15.1, 3.0 Hz, 1H), 1.97 (p, *J* = 6.7 Hz, 1H), 1.90 (dt, *J* = 15.7, 5.5 Hz, 1H), 1.63 (ddd, *J* = 15.5, 6.6, 4.0 Hz, 1H), 0.92 (t, *J* = 6.9 Hz, 6H). ^{13}C NMR (201 MHz, $CDCl_3$) δ 162.8, 157.6, 155.3, 138.0, 130.5, 129.5, 129.4, 128.4, 126.2, 114.3, 77.7, 75.7, 71.9, 61.3, 58.3, 55.6, 54.7, 54.6, 53.1, 39.4, 35.4, 34.9, 29.7, 28.8, 27.2, 20.2, 19.9. LRMS (ESI) *m*/*z*: [M + H]$^+$ 590.3. HRMS (ESI) *m*/*z*: [M + H]$^+$ calcd $C_{29}H_{40}N_3O_8S$ 590.2531; found 590.2525.

(3a*R*,5*S*,6a*S*)-3-Methyl-2-oxohexahydro-2*H*-cyclopenta[*d*]-oxazol-5-yl ((2*S*,3*R*)-3-Hydroxy-4-((*N*-isobutyl-4-methoxyphenyl)sulfonamido)-1-phenylbutan-2-yl)carbamate (4d). Compound **11d** (4.9 mg, 0.02 mmol) was treated with isostere amine **12** (6.8 mg, 0.02 mmol) by following the same procedure outlined for inhibitor **4a** to give inhibitor **4d** (6.1 mg, 68%): ^{1}H NMR (800 MHz, $CDCl_3$) δ 7.76 (d, *J* = 8.4 Hz, 2H), 7.35−7.19 (m, 5H), 7.01 (d, *J* = 8.8 Hz, 2H), 5.08 (s, 1H), 4.99 (t, *J* = 6.7 Hz, 1H), 4.89 (d, *J* = 8.8 Hz, 1H), 4.23−4.18 (m, 1H), 3.90 (s, 3H), 3.82 (d, *J* = 19.1 Hz, 1H), 3.64 (s, 1H), 3.38 (s, 1H), 3.16 (dd, *J* = 15.0, 9.1 Hz, 1H), 3.05−2.96 (m, 2H), 2.82 (dd, *J* = 13.6, 7.6 Hz, 1H), 2.79 (s, 3H), 2.30 (d, *J* = 15.4 Hz, 1H), 2.19 (d, *J* = 15.9 Hz, 1H), 1.91 (dd, *J* = 15.5, 5.4 Hz, 1H), 1.88−1.82 (m, 1H), 1.74−1.69 (m, 1H), 1.67 (s, 2H), 0.92 (dd, *J* = 35.7, 6.6 Hz, 6H). ^{13}C NMR (201 MHz, $CDCl_3$) δ 163.0, 157.4, 155.4, 137.7, 130.1, 129.6, 129.5, 128.6, 128.3, 126.4, 114.3, 77.6, 75.8, 72.1, 61.4, 58.6, 56.0, 55.6, 55.6, 53.4, 39.8, 35.8, 35.3, 29.7, 29.2, 29.0, 27.3, 27.0, 20.2, 19.9. LRMS (ESI) *m*/*z*: [M + H]$^+$ 590.6. HRMS (ESI) *m*/*z*: [M + Na]$^+$ calcd $C_{29}H_{39}N_3O_8SNa$ 612.2350; found 612.2358.

(3a*S*,5*R*,6a*R*)-2-Oxo-3-phenylhexahydro-2*H*-cyclopenta[*d*]-oxazol-5-yl ((2*S*,3*R*)-3-Hydroxy-4-((*N*-isobutyl-4-methoxyphenyl)sulfonamido)-1-phenylbutan-2-yl)carbamate (4e). Compound **11e** (8 mg, 0.02 mmol) was treated with isostere amine **12** (9.3 mg, 0.02 mmol) by following the same procedure outlined for inhibitor **4a** to give inhibitor **4e** (6.1 mg, 45%): ^{1}H NMR (800 MHz, $CDCl_3$) δ 7.74 (d, *J* = 8.4 Hz, 2H), 7.54−7.46 (m, 2H), 7.44−7.35 (m, 2H), 7.15 (dt, *J* = 16.1, 5.6 Hz, 6H), 6.99 (d, *J* = 8.4 Hz, 2H), 5.12 (q, *J* = 3.5 Hz, 1H), 5.09 (t, *J* = 6.7 Hz, 1H), 4.91−4.82 (m, 2H), 3.87 (s, 3H), 3.78 (s, 2H), 3.70 (s, 1H), 3.14 (dd, *J* = 14.9, 8.1 Hz, 1H), 3.06−3.00 (m, 1H), 2.97 (dd, *J* = 14.4, 6.8 Hz, 2H), 2.82 (dd, *J* = 13.4, 6.8 Hz, 1H), 2.77 (dd, *J* = 13.9, 8.2 Hz, 1H), 2.48−2.41 (m, 1H), 2.21−2.14 (m, 1H), 1.99 (d, *J* = 15.8 Hz, 1H), 1.63 (s, 2H), 0.89 (dd, *J* = 29.2, 6.4 Hz, 6H). ^{13}C NMR (201 MHz, $CDCl_3$) δ 162.9, 155.3, 154.6, 137.5, 137.3, 130.3, 129.5, 129.4, 129.3, 128.4, 126.4, 124.5, 120.3, 119.8, 114.3, 75.6, 72.0, 60.7, 58.5, 55.6, 55.3, 53.3, 39.7, 37.5, 35.8, 29.7, 27.2, 20.2, 19.9. LRMS (ESI) *m*/*z*: [M + Na]$^+$ 674.2. HRMS (ESI) *m*/*z*: [M + Na]$^+$ calcd $C_{34}H_{41}N_3O_8SNa$ 674.2507; found 674.2497.

(3a*S*,5*R*,6a*R*)-3-(4-Methoxyphenyl)-2-oxohexahydro-2*H*-cyclopenta[*d*]oxazol-5-yl ((2*S*,3*R*)-3-Hydroxy-4-((*N*-isobutyl-4-methoxyphenyl)sulfonamido)-1-phenylbutan-2-yl)carbamate (4f). Compound **11f** (3.9 mg, 0.01 mmol) was treated with isostere amine **12** (4.2 mg, 0.01 mmol) by following the same procedure outlined for inhibitor **4a** to give inhibitor **4f** (2.7 mg, 47%): ^{1}H NMR (800 MHz, $CDCl_3$) δ 7.72 (dd, *J* = 33.8, 8.5 Hz, 2H), 7.34 (d, *J* = 9.2 Hz, 2H), 7.20 (dd, *J* = 24.4, 7.4 Hz, 4H), 6.97 (dd, *J* = 22.4, 8.5 Hz, 3H), 6.90 (t, *J* = 7.9 Hz, 2H), 5.12 (s, 1H), 5.11−5.06 (m, 2H), 4.97 (d, *J* = 9.2 Hz, 1H), 4.76 (t, *J* = 7.5 Hz, 1H), 3.87 (s, 3H), 3.81 (s, 3H), 3.15 (dd, *J* = 15.0, 8.7 Hz, 1H), 3.06 (d, *J* = 15.0 Hz, 1H), 3.02−2.88 (m, 2H), 2.82 (ddd, *J* = 34.6, 16.1, 8.6 Hz, 2H), 2.43 (d, *J* = 15.9 Hz, 1H), 2.22 (s, 1H), 2.16 (d, *J* = 15.3 Hz, 1H), 1.96 (tt, *J* = 15.8, 4.6 Hz, 2H), 1.91−1.78 (m, 2H), 0.95−0.85 (m, 6H). ^{13}C NMR (201 MHz, $CDCl_3$) δ 162.9, 157.1, 155.2, 137.6, 130.3, 130.1, 129.5, 129.4, 128.5, 126.5, 123.0, 114.6, 114.3, 77.4, 77.2, 77.0, 76.9, 75.8, 72.0, 61.5, 58.5, 55.6, 55.5, 55.2, 53.3, 39.8, 37.2, 35.8, 27.2, 20.2, 19.9. LRMS (ESI) *m*/*z*: [M + H]$^+$ 682.2. HRMS (ESI) *m*/*z*: [M + H]$^+$ calcd $C_{35}H_{44}N_3O_9SNa$ 682.2793; found 682.2800.

(3a*S*,5*R*,6a*R*)-3-(3-Methoxyphenyl)-2-oxohexahydro-2*H*-cyclopenta[*d*]oxazol-5-yl ((2*S*,3*R*)-3-Hydroxy-4-((*N*-isobutyl-4-methoxyphenyl)sulfonamido)-1-phenylbutan-2-yl)carbamate (4g). Compound **11g** (13.6 mg, 0.03 mmol) was treated with isostere amine **12** (14.7 mg, 0.04 mmol) by following the same procedure outlined for inhibitor **4a** to give inhibitor **4g** (13.1 mg, 58%): ^{1}H NMR (800 MHz, CD_3OD) δ 7.77 (d, *J* = 7.9 Hz, 2H), 7.35 (t, *J* = 7.7 Hz, 1H), 7.26 (dd, *J* = 14.5, 7.2 Hz, 4H), 7.16 (dd, *J* = 22.0, 7.2 Hz, 2H), 7.09 (t, *J* = 7.2 Hz, 3H), 6.91 (s, 1H), 5.23−5.17 (m, 1H), 5.10 (s, 1H), 4.85−4.80 (m, 1H), 3.89−3.85 (m, 6H), 3.84 (s, 1H), 3.82−3.75 (m, 2H), 3.38 (d, *J* = 15.2 Hz, 1H), 3.12 (d, *J* = 14.3 Hz, 1H),

DOI: 10.1021/acs.jmedchem.8b01227
J. Med. Chem. 2018, 61, 9722−9737

3.04 (dt, J = 13.1, 7.2 Hz, 2H), 2.91 (dd, J = 13.4, 7.0 Hz, 1H), 2.72−2.65 (m, 1H), 2.26 (d, J = 15.8 Hz, 1H), 2.10 (d, J = 15.9 Hz, 1H), 2.05−1.96 (m, 1H), 1.89 (d, J = 15.3 Hz, 1H), 1.74 (dd, J = 13.9, 7.0 Hz, 1H), 0.89 (dd, J = 21.6, 6.2 Hz, 6H). ^{13}C NMR (201 MHz, CD_3OD) δ 163.1, 157.8, 156.3, 155.4, 138.7, 130.8, 130.0, 129.3, 129.0, 128.0, 125.9, 124.3, 120.5, 114.0, 111.9, 79.5, 76.2, 72.2, 61.8, 57.3, 55.9, 54.8, 54.8, 52.3, 39.5, 36.2, 35.4, 26.6, 19.1, 19.1. LRMS (ESI) m/z: [M + H]$^+$ 682.2. HRMS (ESI) m/z: [M + H]$^+$ calcd $C_{35}H_{44}N_3O_9SNa$ 682.2793; found 682.2787.

(3a*S*,5*R*,6a*R*)-3-(2-Methoxyphenyl)-2-oxohexahydro-2*H*-cyclopenta[*d*]oxazol-5-yl ((2*S*,3*R*)-3-Hydroxy-4-((*N*-isobutyl-4-methoxyphenyl)sulfonamido)-1-phenylbutan-2-yl)carbamate (4h). Compound **11h** (14.5 mg, 0.03 mmol) was treated with isostere amine **12** (15.6 mg, 0.04 mmol) by following the same procedure outlined for inhibitor **4a** to give inhibitor **4h** (12.2 mg, 51%): ^{1}H NMR (400 MHz, $CDCl_3$) δ 7.72 (d, J = 8.5 Hz, 2H), 7.37−7.08 (m, 7H), 7.08−6.92 (m, 3H), 6.70 (d, J = 8.2 Hz, 1H), 5.18−5.02 (m, 2H), 4.83 (dd, J = 15.7, 5.4 Hz, 2H), 3.86 (s, 3H), 3.78 (dt, J = 13.8, 3.5 Hz, 5H), 3.68 (s, 1H), 3.14 (dd, J = 15.1, 8.7 Hz, 1H), 3.06−2.90 (m, 3H), 2.78 (ddd, J = 22.2, 13.4, 7.2 Hz, 2H), 2.43 (d, J = 15.9 Hz, 1H), 2.19 (d, J = 15.5 Hz, 1H), 2.02−1.79 (m, 3H), 0.88 (d, J = 6.8 Hz, 6H). ^{13}C NMR (201 MHz, CD_3OD) δ 163.1, 160.5, 156.1, 155.8, 138.6, 130.8, 129.6, 129.3, 128.9, 127.8, 125.6, 114.0, 112.2, 109.5, 106.6, 78.7, 75.9, 72.1, 61.2, 57.4, 56.1, 54.8, 54.5, 52.4, 39.1, 37.2, 35.7, 26.7, 19.1, 19.0. LRMS (ESI) m/z: [M + H]$^+$ 682.2. HRMS (ESI) m/z: [M + Na]$^+$ calcd $C_{35}H_{43}N_3O_9SNa$ 704.2612; found 704.2602.

(3a*S*,5*R*,6a*R*)-3-Allyl-2-oxohexahydro-2*H*-cyclopenta[*d*]-oxazol-5-yl ((2*S*,3*R*)-3-Hydroxy-4-((*N*-isobutyl-4-methoxyphenyl)sulfonamido)-1-phenylbutan-2-yl)carbamate (4i). Compound **11i** (17 mg, 0.05 mmol) was treated with isostere amine **12** (22 mg, 0.06 mmol) by following the same procedure outlined for inhibitor **4a** to give inhibitor **4i** (23 mg, 76%): ^{1}H NMR (400 MHz, $CDCl_3$) δ 7.75 (d, J = 8.9 Hz, 2H), 7.39−7.22 (m, 4H), 7.22−7.11 (m, 1H), 7.04−6.86 (m, 2H), 5.68−5.52 (m, 1H), 5.46 (d, J = 8.8 Hz, 1H), 5.20−5.09 (m, 2H), 4.97 (d, J = 4.1 Hz, 1H), 4.92 (t, J = 6.8 Hz, 1H), 4.16 (t, J = 7.0 Hz, 1H), 4.02−3.89 (m, 2H), 3.86 (s, 3H), 3.83−3.70 (m, 2H), 3.29 (dd, J = 14.8, 5.1 Hz, 1H), 3.22−2.87 (m, 5H), 2.71 (dd, J = 14.2, 10.1 Hz, 1H), 2.32 (d, J = 15.9 Hz, 1H), 2.15 (d, J = 15.3 Hz, 1H), 2.02−1.93 (m, 1H), 1.85 (dd, J = 15.0, 9.7 Hz, 1H), 1.54 (ddd, J = 15.4, 6.7, 4.1 Hz, 1H), 0.88 (dd, J = 16.0, 6.6 Hz, 6H). ^{13}C NMR (201 MHz, $CDCl_3$) δ 162.8, 157.4, 155.2, 138.2, 131.9, 130.6, 129.5, 129.4, 128.4, 126.2, 118.6, 114.3, 78.1, 75.6, 71.6, 58.8, 58.2, 55.6, 54.6, 54.5, 52.9, 44.7, 39.4, 35.6, 34.5, 29.7, 27.1, 20.2, 20.0. LRMS (ESI) m/z: [M + H]$^+$ 616.2. HRMS (ESI) m/z: [M + Na]$^+$ calcd $C_{31}H_{41}N_3O_8SNa$ 638.2507; found 638.2498.

(3a*S*,5*R*,6a*R*)-2-Oxo-3-propylhexahydro-2*H*-cyclopenta[*d*]-oxazol-5-yl ((2*S*,3*R*)-3-Hydroxy-4-((*N*-isobutyl-4-methoxyphenyl)sulfonamido)-1-phenylbutan-2-yl)carbamate (4j). Compound **11j** (3.7 mg, 0.01 mmol) was treated with isostere amine **12** (4.7 mg, 0.01 mmol) by following the same procedure outlined for inhibitor **4a** to give inhibitor **4j** (4 mg, 62%): ^{1}H NMR (800 MHz, $CDCl_3$) δ 7.78−7.70 (m, 2H), 7.33−7.22 (m, 4H), 7.20 (s, 1H), 7.02−6.93 (m, 2H), 5.08−5.02 (m, 1H), 4.98 (s, 1H), 4.94 (s, 1H), 4.22 (d, J = 7.7 Hz, 1H), 3.87 (d, J = 2.7 Hz, 3H), 3.79 (s, 1H), 3.74 (s, 1H), 3.33−3.25 (m, 1H), 3.14 (ddd, J = 17.8, 8.9, 4.7 Hz, 2H), 3.07 (d, J = 14.3 Hz, 1H), 2.97 (dd, J = 13.6, 8.2 Hz, 1H), 2.93−2.86 (m, 1H), 2.75 (t, J = 12.2 Hz, 1H), 2.67 (d, J = 8.7 Hz, 1H), 2.33 (d, J = 16.0 Hz, 1H), 2.13 (d, J = 15.2 Hz, 1H), 1.89 (dt, J = 13.2, 6.2 Hz, 2H), 1.60−1.50 (m, 3H), 1.48 (d, J = 7.2 Hz, 1H), 1.02−0.76 (m, 9H). ^{13}C NMR (201 MHz, $CDCl_3$) δ 162.9, 157.5, 155.4, 137.8, 130.4, 129.5, 129.4, 128.5, 126.4, 114.3, 77.7, 75.7, 72.1, 59.0, 58.4, 55.6, 54.9, 53.2, 43.7, 39.6, 35.8, 35.4, 29.7, 27.2, 20.3, 20.2, 19.9, 11.2. LRMS (ESI) m/z: [M + H]$^+$ 618.2. HRMS (ESI) m/z: [M + Na]$^+$ calcd $C_{31}H_{43}N_3O_8SNa$ 640.2663; found 640.2669.

(3a*S*,5*R*,6a*R*)-3-(2-Methylallyl)-2-oxohexahydro-2*H*-cyclopenta[*d*]oxazol-5-yl ((2*S*,3*R*)-3-Hydroxy-4-((*N*-isobutyl-4-methoxyphenyl)sulfonamido)-1-phenylbutan-2-yl)carbamate (4k). Compound **11k** (6.1 mg, 0.02 mmol) was treated with isostere amine **12** (7.5 mg, 0.02 mmol) by following the same procedure outlined for inhibitor **4a** to give inhibitor **4k** (8 mg, 75%): ^{1}H NMR (800 MHz, $CDCl_3$) δ 7.77 (d, J = 8.8 Hz, 2H), 7.36−7.25 (m, 4H), 7.24−7.15 (m, 1H), 7.00 (d, J = 8.9 Hz, 2H), 5.19 (s, 1H), 5.03 (s, 1H), 4.96 (t, J = 6.9 Hz, 1H), 4.92 (s, 1H), 4.82 (s, 1H), 4.12 (t, J = 7.1 Hz, 1H), 4.01−3.95 (m, 1H), 3.93−3.87 (m, 4H), 3.85−3.76 (m, 2H), 3.24 (dd, J = 15.1, 4.5 Hz, 1H), 3.14 (dd, J = 14.8, 8.4 Hz, 2H), 3.06 (d, J = 15.4 Hz, 1H), 3.01 (dd, J = 13.6, 8.0 Hz, 1H), 2.96 (dd, J = 13.6, 7.2 Hz, 1H), 2.76 (dd, J = 14.3, 10.1 Hz, 1H), 2.36 (d, J = 15.6 Hz, 1H), 2.16 (d, J = 15.1 Hz, 1H), 1.98 (dt, J = 13.1, 6.5 Hz, 1H), 1.90 (dt, J = 15.4, 4.8 Hz, 1H), 1.68 (s, 3H), 1.59 (ddd, J = 15.3, 6.7, 4.2 Hz, 1H), 0.92 (dd, J = 13.5, 6.6 Hz, 6H). ^{13}C NMR (201 MHz, $CDCl_3$) δ 162.9, 157.6, 155.3, 139.4, 138.1, 130.6, 129.5, 129.4, 128.5, 126.3, 114.3, 114.0, 78.0, 75.7, 71.8, 58.6, 58.3, 55.6, 54.7, 53.1, 48.1, 39.5, 35.5, 34.8, 29.7, 27.2, 20.3, 20.0, 19.9. LRMS (ESI) m/z: [M + H]$^+$ 630.6. HRMS (ESI) m/z: [M + Na]$^+$ calcd $C_{32}H_{43}N_3O_8SNa$ 652.2663; found 652.2666.

(3a*S*,5*R*,6a*R*)-3-Isobutyl-2-oxohexahydro-2*H*-cyclopenta[*d*]-oxazol-5-yl ((2*S*,3*R*)-3-Hydroxy-4-((*N*-isobutyl-4-methoxyphenyl)sulfonamido)-1-phenylbutan-2-yl)carbamate (4l). Compound **11l** (9 mg, 0.02 mmol) was treated with isostere amine **12** (11 mg, 0.03 mmol) by following the same procedure outlined for inhibitor **4a** to give inhibitor **4l** (10 mg, 65%): ^{1}H NMR (800 MHz, $CDCl_3$) δ 7.80−7.75 (m, 2H), 7.30 (d, J = 23.2 Hz, 4H), 7.21 (t, J = 7.3 Hz, 1H), 7.00 (d, J = 8.8 Hz, 2H), 5.17−5.11 (m, 1H), 5.04 (t, J = 4.2 Hz, 1H), 4.97 (t, J = 6.8 Hz, 1H), 4.23 (t, J = 6.9 Hz, 1H), 3.98−3.92 (m, 1H), 3.89 (s, 4H), 3.82 (s, 1H), 3.23 (d, J = 12.5 Hz, 1H), 3.19−3.04 (m, 3H), 3.04−2.91 (m, 2H), 2.81−2.73 (m, 1H), 2.52 (d, J = 13.9 Hz, 1H), 2.37 (d, J = 15.6 Hz, 1H), 2.18 (d, J = 15.0 Hz, 1H), 2.01−1.94 (m, 1H), 1.94−1.82 (m, 2H), 1.71 (s, 1H), 1.64 (d, J = 14.7 Hz, 1H), 0.92 (dq, J = 19.3, 6.4 Hz, 12H). ^{13}C NMR (201 MHz, $CDCl_3$) δ 162.9, 157.8, 155.3, 138.0, 130.6, 129.5, 129.4, 128.5, 126.3, 114.3, 77.8, 75.7, 71.8, 59.3, 58.3, 55.6, 54.8, 53.1, 49.4, 39.5, 35.6, 34.9, 29.7, 27.2, 26.2, 20.3, 20.0, 19.8. LRMS (ESI) m/z: [M + H]$^+$ 630.6. HRMS (ESI) m/z: [M + Na]$^+$ calcd $C_{32}H_{45}N_3O_8SNa$ 654.2820; found 654.2815.

(3a*S*,5*R*,6a*R*)-3-(Methoxymethyl)-2-oxohexahydro-2*H*-cyclopenta[*d*]oxazol-5-yl ((2*S*,3*R*)-3-Hydroxy-4-((*N*-isobutyl-4-methoxyphenyl)sulfonamido)-1-phenylbutan-2-yl)carbamate (4m). Compound **11m** (3.2 mg, 0.01 mmol) was treated with isostere amine **12** (4.1 mg, 0.01 mmol) by following the same procedure outlined for inhibitor **4a** to give inhibitor **4m** (3.4 mg, 60%): ^{1}H NMR (800 MHz, CD_3OD) δ 7.76 (d, J = 8.8 Hz, 2H), 7.28−7.19 (m, 4H), 7.19−7.15 (m, 1H), 7.10−7.05 (m, 2H), 5.12 (s, 1H), 5.06 (t, J = 6.9 Hz, 1H), 5.02 (t, J = 4.6 Hz, 1H), 4.58 (d, J = 11.0 Hz, 1H), 4.40−4.33 (m, 2H), 3.88 (s, 3H), 3.75 (ddd, J = 14.9, 10.4, 5.1 Hz, 1H), 3.40−3.32 (m, 4H), 3.22 (s, 2H), 3.18 (s, 1H), 3.09 (dd, J = 14.2, 3.5 Hz, 1H), 3.05 (dd, J = 13.6, 7.9 Hz, 1H), 2.99 (dd, J = 14.9, 8.1 Hz, 1H), 2.89 (dd, J = 13.6, 7.0 Hz, 1H), 2.57 (dd, J = 14.2, 10.2 Hz, 1H), 2.26−2.17 (m, 1H), 2.10 (dd, J = 15.2, 2.8 Hz, 1H), 2.08−2.02 (m, 1H), 1.82 (ddd, J = 15.4, 6.9, 4.7 Hz, 1H), 0.97−0.82 (m, 6H). ^{13}C NMR (201 MHz, CD_3OD) δ 163.1, 158.6, 156.2, 138.7, 130.8, 129.3, 128.9, 127.9, 125.8, 114.0, 79.5, 76.9, 76.2, 74.7, 72.5, 59.0, 57.3, 55.5, 54.8, 52.4, 38.9, 36.3, 35.2, 31.6, 29.3, 29.0, 26.6, 19.0. LRMS (ESI) m/z: [M + H]$^+$ 620.2. HRMS (ESI) m/z: [M + Na]$^+$ calcd $C_{30}H_{41}N_3O_9SNa$ 642.2456; found 642.2454.

(3a*S*,5*R*,6a*R*)-3-Methyl-2-oxohexahydro-2*H*-cyclopenta[*d*]-oxazol-5-yl ((2*S*,3*R*)-4-((2-(Cyclopropylamino)-*N*-isobutylbenzo[*d*]thiazole)-6-sulfonamido)-3-hydroxy-1-phenylbutan-2-yl)carbamate (4n). Compound **11b** (7.1 mg, 0.02 mmol) was treated with isostere amine **13** (12 mg, 0.02 mmol) by following the same procedure outlined for inhibitor **4a** to give inhibitor **4n** (10 mg, 69%): ^{1}H NMR (400 MHz, $CDCl_3$) δ 8.17−8.07 (m, 1H), 7.72 (dd, J = 8.5, 1.9 Hz, 1H), 7.53 (d, J = 8.6 Hz, 1H), 7.26 (d, J = 2.8 Hz, 5H), 7.19 (dd, J = 6.7, 2.3 Hz, 1H), 5.10 (d, J = 10.3 Hz, 1H), 5.02 (s, 1H), 4.91 (t, J = 6.9 Hz, 1H), 3.89 (dd, J = 34.2, 5.3 Hz, 3H), 3.34 (s, 1H), 3.28−3.07 (m, 3H), 3.07−2.88 (m, 2H), 2.74 (td, J = 9.7, 6.4 Hz, 3H), 2.57 (s, 3H), 2.30 (d, J = 15.8 Hz, 1H), 2.15 (dd, J = 15.2, 2.9 Hz, 1H), 2.00−1.80 (m, 2H), 1.60 (ddd, J = 15.3, 6.5, 4.1 Hz, 1H), 0.91 (dd, J = 13.9, 5.7 Hz, 9H), 0.78 (t, J = 1.8 Hz, 2H). ^{13}C NMR (201 MHz, CD_3OD) δ 158.6, 156.3, 155.4, 138.8, 131.4, 130.8, 129.6, 129.0, 127.9, 127.7, 125.7, 125.3, 121.0, 120.7, 117.5, 78.9, 76.0, 72.5, 61.7, 57.4, 55.6, 52.5, 39.2, 35.3, 34.9,

DOI: 10.1021/acs.jmedchem.8b01227
J. Med. Chem. 2018, 61, 9722−9737

27.9, 26.7, 25.9, 19.1, 19.1, 19.1, 6.5. LRMS (ESI) *m/z*: $[M + H]^+$ 672.3. HRMS (ESI) *m/z*: $[M + Na]^+$ calcd $C_{32}H_{42}N_5O_7S_2Na$ 672.2520; found 672.2512.

(1*S*,4*R*)-4-(((4-Methoxyphenyl)carbamoyl)oxy)cyclopent-2-en-1-yl Acetate (6a). To a stirring solution of (1*R*,4*S*)-*cis*-4-acetoxy-2-cyclopenten-1-ol **5** (49 mg, 0.34 mmol) in dry dichloromethane were added phenyl isocyanate (45 mg, 0.38 mmol) and 1,8-diazabicyclo[5.4.0]undec-7-ene (5.3 mg, 0.03 mmol) all under an argon atmosphere. Reaction was stirred at 23 °C for 1 h. After this period, the reaction was quenched with in saturated solution of $NaHCO_3$ and the aqueous phase was extracted with EtOAc. The organic extracts were dried with Na_2SO_4, and the solvent was removed under reduced pressure. The crude product was purified by silica gel column chromatography (20% EtOAc in hexane) to afford the known[27] carbamate derivative **6a** (73 mg, 81%).

(1*S*,4*R*)-4-(((4-Methoxyphenyl)carbamoyl)oxy)cyclopent-2-en-1-yl Acetate (6b). To a stirring solution of (1*R*,4*S*)-*cis*-4-acetoxy-2-cyclopenten-1-ol **5** (0.6 g, 4.2 mmol) in dry dichloromethane were added 4-methoxyphenyl isocyanate (0.7 g, 4.6 mmol) and 1,8-diazabicyclo[5.4.0]undec-7-ene (64 mg, 0.42 mmol) all under an argon atmosphere. Reaction was stirred at 23 °C for 1 h. Upon completion, the residue was taken up in saturated solution of $NaHCO_3$ and the aqueous phase was extracted with EtOAc. The organic extracts were dried with Na_2SO_4, and the solvent was removed under reduced pressure. The crude product was purified by silica gel column chromatography (20% EtOAc in hexane) to afford **6b** (1 g, 81%): ^{1}H NMR (400 MHz, $CDCl_3$) δ 7.33−7.22 (m, 2H), 6.84 (d, J = 9.0 Hz, 2H), 6.57 (s, 1H), 6.12 (dddd,J = 20.7, 5.6, 2.1, 1.1 Hz, 2H), 5.58 (qd, J = 6.1, 3.5, 2.1 Hz, 2H), 3.77 (s, 3H), 2.90 (qt, J = 15.1, 7.5 Hz, 1H), 2.06 (s, 3H), 1.80 (dt, J = 15.0, 3.7 Hz, 1H). ^{13}C NMR (101 MHz, $CDCl_3$) δ 170.6, 156.0, 153.3, 134.9, 134.5, 130.7, 120.6, 114.2, 77.3, 77.0, 76.6, 55.4, 37.2, 21.0. LRMS (ESI) *m/z*: $[M + Na]^+$ 314.0.

(3a*S*,5*R*,6a*R*)-2-Oxo-3-phenylhexahydro-2*H*-cyclopenta[*d*]oxazol-5-yl Acetate (7a). In a sealed tube, phenyl carbamate **6a** (60 mg, 0.2 mmol) was dissolved in dry tetrahydrofuran (8.4 mL) followed by the addition of freshly distilled dimethyl sulfoxide (0.84 mL). Freshly made 2-iodoxybenzoic acid (0.13 g, 0.46 mmol) was added all at once. The reaction vessel was heated for 8 h at 90 °C. Another portion of 2-iodoxybenzoic acid (0.13 g, 0.5 mmol) was added, and the reaction was heated for an additional 8 h. Upon completion, the residue was taken up in 5% saturated solution of $NaHCO_3$ and the aqueous phase was extracted with EtOAc. The organic extracts were dried with Na_2SO_4, and the solvent was removed under reduced pressure. The crude product was purified by silica gel column chromatography (60% EtOAc in hexane) to afford **7a** (23 mg, 37%): ^{1}H NMR (800 MHz, $CDCl_3$) δ 7.54 (d, J = 7.7 Hz, 2H), 7.42−7.38 (m, 2H), 7.18 (t, J = 7.4 Hz, 1H), 5.30 (t, J = 4.5 Hz, 1H), 5.18 (t, J = 7.0 Hz, 1H), 4.95 (t, J = 7.2 Hz, 1H), 2.53 (dd, J = 16.0, 3.1 Hz, 1H), 2.30 (dd, J = 15.5, 3.0 Hz, 1H), 2.12 (ddd, J = 16.0, 6.5, 4.5 Hz, 1H), 2.03 (s, 3H), 1.98 (ddd, J = 15.4, 6.8, 4.5 Hz, 1H). ^{13}C NMR (201 MHz, $CDCl_3$) δ 170.6, 154.6, 137.3, 129.3, 124.6, 120.2, 77.4, 77.2, 77.1, 76.9, 75.0, 60.7, 42.7, 39.9, 37.0, 21.2. LRMS (ESI) *m/z*: $[M + H]^+$ 262.1.

(3a*S*,5*R*,6a*R*)-3-(4-Methoxyphenyl)-2-oxohexahydro-2*H*-cyclopenta[*d*]oxazol-5-yl Acetate (7b). In a sealed tube, *p*-methoxyphenyl carbamate **6b** (0.8 g, 2.5 mmol) was dissolved in dry tetrahydrofuran (46 mL) followed by the addition of freshly distilled dimethyl sulfoxide (4.6 mL). Freshly made 2-iodoxybenzoic acid (1.4 g, 5 mmol) was added all at once. The reaction vessel was heated for 8 h at 90 °C. Another portion of 2-iodoxybenzoic acid (1.4 g, 5 mmol) was added, and the reaction was heated for an additional 8 h. Upon completion, the residue was taken up in 5% saturated solution of $NaHCO_3$ and the aqueous phase was extracted with EtOAc. The organic extracts were dried with Na_2SO_4, and the solvent was removed under reduced pressure. The crude product was purified by silica gel column chromatography (60% EtOAc in hexane) to afford **7b** (0.48 g, 65%): ^{1}H NMR (400 MHz, $CDCl_3$) δ 7.40−7.34 (m, 2H), 6.94−6.88 (m, 2H), 5.27 (t, J = 4.5 Hz, 1H), 5.14 (t, J = 7.2, 6.7 Hz, 1H), 4.84 (t, J = 7.0 Hz, 1H), 3.80 (s, 3H), 2.49 (dd, J = 15.9, 2.5 Hz, 1H), 2.24 (dd, J = 15.4, 3.0 Hz, 1H), 2.08 (ddd, J = 15.9, 6.4, 4.6 Hz, 1H), 2.03 (s, 3H), 1.88 (ddd, J = 15.4, 6.6, 4.6 Hz, 1H). ^{13}C NMR (101 MHz, $CDCl_3$) δ 170.4, 156.8, 154.8, 130.0, 122.8, 114.5, 77.2, 76.9, 76.6, 74.9, 61.3, 55.4, 39.9, 36.7, 21.1. LRMS (ESI) *m/z*: $[M + H]^+$ 292.0.

(3a*S*,5*R*,6a*R*)-3-(3-Methoxyphenyl)-2-oxohexahydro-2*H*-cyclopenta[*d*]oxazol-5-yl Acetate (7c). In a sealed tube, *m*-methoxyphenyl carbamate **6c** (57 mg, 0.2 mmol) was dissolved in dry tetrahydrofuran (7.1 mL) followed by the addition of freshly distilled dimethyl sulfoxide (0.7 mL). Freshly made 2-iodoxybenzoic acid (0.11 g, 0.4 mmol) was added all at once. The reaction vessel was heated for 8 h at 90 °C. Another portion of 2-iodoxybenzoic acid (0.11 g, 0.4 mmol) was added, and the reaction was heated for an additional 8 h. Upon completion, the residue was taken up in 5% saturated solution of $NaHCO_3$ and the aqueous phase was extracted with EtOAc. The organic extracts were dried with Na_2SO_4, and the solvent was removed under reduced pressure. The crude product was purified by silica gel column chromatography (60% EtOAc in hexane) to afford **7c** (24 mg, 42%): ^{1}H NMR (400 MHz, $CDCl_3$) δ 7.30−7.23 (m, 1H), 7.21 (t, J = 2.3 Hz, 1H), 7.03 (ddd, J = 8.2, 2.1, 0.9 Hz, 1H), 6.70 (ddd, J = 8.3, 2.5, 0.8 Hz, 1H), 5.27 (t, J = 4.5 Hz, 1H), 5.14 (t, J = 7.1, 6.6 Hz, 1H), 4.88 (t, J = 7.1 Hz, 1H), 3.81 (s, 3H), 2.50 (dd, J = 15.9, 2.6 Hz, 1H), 2.31 (dd, J = 15.4, 3.0 Hz, 1H), 2.09 (ddd, J = 15.9, 6.2, 4.6 Hz, 1H), 2.00 (s, 3H), 1.99−1.90 (m, 1H). ^{13}C NMR (101 MHz, $CDCl_3$) δ 170.4, 160.2, 154.3, 138.4, 129.8, 112.0, 109.6, 106.3, 77.3, 77.2, 76.9, 76.6, 74.8, 60.6, 55.3, 39.7, 37.0, 21.1. LRMS (ESI) *m/z*: $[M + H]^+$ 292.0.

(3a*S*,5*R*,6a*R*)-3-(2-Methoxyphenyl)-2-oxohexahydro-2*H*-cyclopenta[*d*]oxazol-5-yl Acetate (7d). In a sealed tube, *o*-methoxyphenyl carbamate **6d** (17 mg, 0.06 mmol) was dissolved in dry tetrahydrofuran (2.1 mL) followed by the addition of freshly distilled dimethyl sulfoxide (0.2 mL). Freshly made 2-iodoxybenzoic acid (33 mg, 0.1 mmol) was added all at once. The reaction vessel was heated for 8 h at 90 °C. Another portion of 2-iodoxybenzoic acid (33 mg, 0.1 mmol) was added, and the reaction was heated for an additional 8 h. Upon completion, the residue was taken up in 5% saturated solution of $NaHCO_3$ and the aqueous phase was extracted with EtOAc. The organic extracts were dried with Na_2SO_4, and the solvent was removed under reduced pressure. The crude product was purified by silica gel column chromatography (60% EtOAc in hexane) to afford **7d** (11 mg, 65%): ^{1}H NMR (400 MHz, $CDCl_3$) δ 7.34−7.26 (m, 2H), 7.03−6.93 (m, 2H), 5.28 (t, J = 4.5 Hz, 1H), 5.19 (t, J = 7.4, 5.7 Hz, 1H), 4.96 (t, J = 7.2 Hz, 1H), 3.86 (s, 3H), 2.49 (dd, J = 16.0, 2.6 Hz, 1H), 2.13 (s, 3H), 2.11−2.01 (m, 2H), 1.78−1.63 (m, 1H). ^{13}C NMR (101 MHz, $CDCl_3$) δ 170.5, 156.2, 154.8, 129.6, 128.8, 124.7, 120.9, 111.9, 78.2, 77.2, 76.9, 76.6, 75.3, 61.0, 55.5, 42.6, 39.9, 36.6, 21.3. LRMS (ESI) *m/z*: $[M + H]^+$ 292.0.

(3a*S*,5*R*,6a*R*)-2-Oxohexahydro-2*H*-cyclopenta[*d*]oxazol-5-yl Acetate (8). To a stirring solution of cyclic *p*-methoxyphenyl carbamate **7b** (0.14 g, 0.5 mmol) in acetonitrile (4.7 mL) and water (0.9 mL) was added cerium ammonium nitrate (1.3 g, 2.4 mmol) at 0 °C. Reaction was stirred for 30 min. Upon completion, the residue was taken up in 5% saturated solution of $NaHCO_3$ and the aqueous phase was extracted with EtOAc. The organic extracts were dried with Na_2SO_4, and the solvent was removed under reduced pressure. The crude product was purified by silica gel column chromatography (80% EtOAc in hexane) to afford **8** (62 mg, 71%): ^{1}H NMR (400 MHz, $CDCl_3$) δ 5.53 (s, 1H), 5.28 (t, J = 4.5 Hz, 1H), 5.17 (t, J = 7.0 Hz, 1H), 4.39 (t, J = 7.0 Hz, 1H), 2.44 (dd, J = 15.9, 2.9 Hz, 1H), 2.12 (dd, J = 15.4, 2.9 Hz, 1H), 2.03 (s, 3H), 1.95 (tdd, J = 15.8, 6.5, 4.6 Hz, 2H). ^{13}C NMR (101 MHz, $CDCl_3$) δ 170.6, 158.7, 81.3, 77.2, 77.12, 76.9, 76.6, 75.3, 55.9, 40.1, 39.3, 21.1. LRMS (ESI) *m/z*: $[M + H]^+$ 186.1.

(3a*R*,5*S*,6a*S*)-2-Oxohexahydro-2*H*-cyclopenta[*d*]oxazol-5-yl Acetate (*ent*-8). To a stirring solution of of cyclic *p*-methoxyphenyl carbamate ent-**7b** (20 mg, 0.07 mmol) in acetonitrile (0.7 mL) and water (0.2 mL) was added cerium ammonium nitrate (0.2 g, 0.3 mmol) at 0 °C. Reaction was stirred for 30 min. Upon completion, the residue was taken up in 5% saturated solution of $NaHCO_3$ and the aqueous phase was extracted with EtOAc. The organic extracts were

DOI: 10.1021/acs.jmedchem.8b01227
J. Med. Chem. 2018, 61, 9722−9737

dried with Na_2SO_4, and the solvent was removed under reduced pressure. The crude product was purified by silica gel column chromatography (80% EtOAc in hexane) to afford *ent*-**8** (7.7 mg, 61%): ^{1}H NMR (800 MHz, $CDCl_3$) δ 5.36 (s, 1H), 5.31 (t, J = 4.2 Hz, 1H), 5.20 (t, J = 6.8 Hz, 1H), 4.41 (t, J = 6.9 Hz, 1H), 2.47 (dd, J = 15.9, 2.2 Hz, 1H), 2.15 (dd, J = 15.3, 2.9 Hz, 1H), 2.07 (s, 3H), 1.99 (dddd, J = 30.4, 15.3, 6.6, 4.5 Hz, 2H). ^{13}C NMR (201 MHz, $CDCl_3$) δ 170.8, 158.7, 81.4, 77.2, 77.0, 76.9, 75.4, 56.0, 40.3, 39.4, 21.2. LRMS (ESI) m/z: $[M + H]^+$ 185.9.

(3a*S*,5*R*,6a*R*)-5-Hydroxyhexahydro-2*H*-cyclopenta[*d*]oxazol-2-one (9). To a stirring solution of protected oxazolidinone **8** (6 mg, 0.03 mmol) in methanol (1 mL) was added potassium carbonate (5.5 mg, 0.04 mmol). Reaction was stirred at 23 °C for 4 h. Upon completion, the residue solvent was removed under reduced pressure. The crude product was purified by silica gel column chromatography (80% EtOAc in hexane) to afford **9** (4.6 mg, 99%). $[\alpha]_D^{20}$ +20.0 (c 1.0, MeOH). ^{1}H NMR (800 MHz, CD_3OD) δ 5.14 (t, J = 7.0 Hz, 1H), 4.41 (t, J = 4.4 Hz, 1H), 4.33 (t, J = 7.3 Hz, 1H), 2.18 (d, J = 15.2 Hz, 1H), 1.99−1.94 (m, 2H), 1.88 (ddd, J = 14.5, 6.9, 4.4 Hz, 1H). ^{13}C NMR (201 MHz, CD_3OD) δ 160.5, 82.4, 72.1, 56.6, 47.9, 47.8, 47.7, 47.6, 47.5, 47.4, 47.3, 41.6, 41.2. LRMS (ESI) m/z: $[M + H]^+$ 144.1. HRMS (ESI) m/z: $[M + H]^+$ calcd $C_6H_{10}NO_3$ 144.0655; found 144.0653.

(3a*R*,5*S*,6a*S*)-5-Hydroxyhexahydro-2*H*-cyclopenta[*d*]oxazol-2-one (*ent*-9). To a stirring solution of protected oxazolidinone *ent*-**8** (8 mg, 0.04 mmol) in methanol (1.4 mL) was added potassium carbonate (7.2 mg, 0.05 mmol). Reaction was stirred at 23 °C for 4 h. Upon completion, the residue solvent was removed under reduced pressure. The crude product was purified by silica gel column chromatography (80% EtOAc in hexane) to afford *ent*-**9** (5.9 mg, 95%). $[\alpha]_D^{20}$ −7.65 (c 1.35, MeOH). ^{1}H NMR (800 MHz, CD_3OD) δ 5.14 (t, J = 7.0 Hz, 1H), 4.41 (t, J = 4.3 Hz, 1H), 4.33 (t, J = 7.2 Hz, 1H), 2.18 (d, J = 15.2 Hz, 1H), 1.99−1.94 (m, 2H), 1.88 (ddd, J = 14.5, 6.9, 4.5 Hz, 1H). ^{13}C NMR (201 MHz, CD_3OD) δ 160.5, 82.4, 72.1, 56.6, 47.9, 47.8, 47.7, 47.6, 47.5, 47.4, 47.3, 41.6, 41.2. LRMS (ESI) m/z: $[M + H]^+$ 144.1. HRMS (ESI) m/z: $[M + H]^+$ calcd $C_6H_{10}NO_3$ 144.0655; found 144.0653.

(3a*S*,5*R*,6a*R*)-5-Hydroxy-3-phenylhexahydro-2*H*-cyclopenta[*d*]oxazol-2-one (10a). To a stirring solution of cyclic phenyl carbamate **7a** (22 mg, 0.08 mmol) in methanol (2.8 mL) was added potassium carbonate (14 mg, 0.1 mmol). Reaction was stirred at 23 °C for 12 h. Upon completion, the residue solvent was removed under reduced pressure. The crude product was purified by silica gel column chromatography (60% EtOAc in hexane) to afford **10a** (14 mg, 73%). $[\alpha]_D^{20}$ +87.6 (c 1.90, MeOH). ^{1}H NMR (800 MHz, $CDCl_3$) δ 7.56 (dt, J = 8.6, 1.2 Hz, 2H), 7.39 (ddt, J = 8.7, 7.3, 1.7 Hz, 2H), 7.16 (td, J = 7.3, 1.3 Hz, 1H), 5.15 (t, J = 7.0 Hz, 1H), 4.88 (t, J = 7.3 Hz, 1H), 4.53 (t, J = 4.4 Hz, 1H), 2.41 (dd, J = 15.6, 3.0 Hz, 1H), 2.20 (ddd, J = 14.9, 3.0, 1.5 Hz, 1H), 2.06 (ddd, J = 15.5, 6.3, 4.3 Hz, 1H), 1.90 (ddd, J = 15.0, 7.0, 4.4 Hz, 1H), 1.84 (s, 1H). ^{13}C NMR (201 MHz, $CDCl_3$) δ 154.9, 137.6, 129.2, 124.4, 120.4, 78.0, 77.2, 77.0, 76.9, 72.6, 61.1, 42.6, 39.5. LRMS (ESI) m/z: $[M + H]^+$ 220.1. HRMS (ESI) m/z: $[M + Na]^+$ calcd $C_{12}H_{13}NO_3Na$ 242.0788; found 242.0786.

(3a*S*,5*R*,6a*R*)-5-Hydroxy-3-(4-methoxyphenyl)hexahydro-2*H*-cyclopenta[*d*]oxazol-2-one (10b). To a stirring solution of cyclic *p*-methoxyphenyl carbamate **7b** (46 mg, 0.2 mmol) in methanol (6 mL) was added potassium carbonate (26 mg, 0.2 mmol). Reaction was stirred at 23 °C for 12 h. Upon completion, the residue solvent was removed under reduced pressure. The crude product was purified by silica gel column chromatography (60% EtOAc in hexane) to afford **10b** (38 mg, 96%). $[\alpha]_D^{20}$ +75.5 (c 2.00, MeOH). ^{1}H NMR (400 MHz, $CDCl_3$) δ 7.45−7.36 (m, 2H), 6.95−6.87 (m, 2H), 5.13 (dd, J = 7.8, 5.2 Hz, 1H), 4.78 (t, J = 7.2 Hz, 1H), 4.54−4.46 (m, 1H), 3.80 (s, 3H), 2.41−2.31 (m, 1H), 2.14 (ddt, J = 14.9, 2.8, 1.2 Hz, 1H), 2.03 (ddd, J = 15.4, 6.4, 4.2 Hz, 1H), 1.78 (ddd, J = 14.9, 6.9, 4.3 Hz, 1H), 1.71 (d, J = 2.4 Hz, 1H). ^{13}C NMR (101 MHz, $CDCl_3$) δ 156.8, 155.2, 130.3, 123.3, 114.4, 77.9, 77.2, 76.9, 76.6, 72.6, 61.7, 55.4, 42.7, 39.0. LRMS (ESI) m/z: $[M + H]^+$ 250.0. HRMS (ESI) m/z: $[M + Na]^+$ calcd $C_{13}H_{15}NO_4Na$ 272.0893; found 272.0895.

(3a*S*,5*R*,6a*R*)-5-Hydroxy-3-(3-methoxyphenyl)hexahydro-2*H*-cyclopenta[*d*]oxazol-2-one (10c). To a stirring solution of cyclic *m*-methoxyphenyl carbamate **7c** (24 mg, 0.08 mmol) in methanol (6.7 mL) was added potassium carbonate (17 mg, 0.1 mmol). Reaction was stirred at 23 °C for 12 h. Upon completion, the residue solvent was removed under reduced pressure. The crude product was purified by silica gel column chromatography (60% EtOAc in hexane) to afford **10c** (20 mg, 97%). $[\alpha]_D^{20}$ +98.2 (c 2, MeOH). ^{1}H NMR (800 MHz, $CDCl_3$) δ 7.32−7.26 (m, 2H), 7.07 (ddd, J = 8.2, 2.1, 0.9 Hz, 1H), 6.71 (ddd, J = 8.3, 2.5, 0.8 Hz, 1H), 5.14 (t, J = 7.0 Hz, 1H), 4.85 (t, J = 7.3 Hz, 1H), 4.54 (t, J = 4.3 Hz, 1H), 3.84 (s, 3H), 2.40 (dd, J = 15.5, 2.2 Hz, 1H), 2.23 (dd, J = 14.9, 2.9 Hz, 1H), 2.10−2.02 (m, 1H), 1.92 (dddd, J = 15.0, 7.1, 4.4, 0.6 Hz, 1H), 1.71 (s, 1H). ^{13}C NMR (201 MHz, $CDCl_3$) δ 160.3, 154.7, 138.8, 129.8, 112.2, 109.8, 106.3, 77.9, 77.2, 77.0, 76.9, 72.6, 61.1, 55.4, 42.5, 39.7. LRMS (ESI) m/z: $[M + H]^+$ 250.1. HRMS (ESI) m/z: $[M + Na]^+$ calcd $C_{13}H_{15}NO_4Na$ 272.0893; found 272.0895.

(3a*S*,5*R*,6a*R*)-5-Hydroxy-3-(2-methoxyphenyl)hexahydro-2*H*-cyclopenta[*d*]oxazol-2-one (10d). To a stirring solution of cyclic *o*-methoxyphenyl carbamate **7d** (20 mg, 0.1 mmol) in methanol (5.5 mL) was added potassium carbonate (17 mg, 0.1 mmol). Reaction was stirred at 23 °C for 12 h. Upon completion, the residue solvent was removed under reduced pressure. The crude product was purified by silica gel column chromatography (60% EtOAc in hexane) to afford **10d** (17 mg, 96%) $[\alpha]_D^{20}$ +71.2 (c 2.67, MeOH). ^{1}H NMR (400 MHz, $CDCl_3$) δ 7.38 (dd, J = 7.7, 1.7 Hz, 1H), 7.30 (ddd, J = 8.3, 7.5, 1.7 Hz, 1H), 7.05−6.96 (m, 2H), 5.19 (t, J = 7.2 Hz, 1H), 4.82 (t, J = 7.3 Hz, 1H), 4.47 (t, J = 4.4 Hz, 1H), 3.87 (s, 3H), 2.39 (ddd, J = 15.5, 3.1, 0.9 Hz, 2H), 2.10−1.87 (m, 3H), 1.63 (dddd, J = 15.1, 6.7, 4.5, 0.6 Hz, 2H). ^{13}C NMR (101 MHz, $CDCl_3$) δ 156.1, 155.1, 129.8, 129.0, 125.0, 121.3, 112.1, 79.0, 77.2, 77.1, 76.9, 76.6, 72.7, 62.1, 55.7, 43.0, 38.8, 29.6. LRMS (ESI) m/z: $[M + H]^+$ 250.0. HRMS (ESI) m/z: $[M + H]^+$ calcd $C_{13}H_{16}NO_4$ 250.1074; found 250.1072.

(3a*S*,5*R*,6a*R*)-5-Hydroxy-3-methylhexahydro-2*H*-cyclopenta[*d*]oxazol-2-one (10e). Protected oxazolidinone **8** (21 mg, 0.1 mmol) was dissolved with dry acetonitrile (1.4 mL) and was placed under an argon atmosphere. Reaction mixture was cooled to 0 °C, and potassium bis(trimethylsilyl)amide (0.5 M solution) (0.25 mL, 0.1 mmol) was added dropwise. The reaction stirred for 30 min. Iodomethane (18 mg, 0.1 mmol) was then added dropwise, and the reaction mixture was allowed to warm up to 23 °C for 1 h. Upon completion, the residue was taken up in DI water and the aqueous phase was extracted with EtOAc. The organic extracts were dried with Na_2SO_4, and the solvent was removed under reduced pressure. The crude product was taken up in methanol (3 mL) and followed the addition of potassium carbonate (19 mg, 0.14 mmol). The reaction was stirred at 23 °C for 12 h. Upon completion, the residue solvent was removed under reduced pressure. The crude product was purified by silica gel column chromatography (60% EtOAc in hexane) to afford **10e** (14 mg, 80%). $[\alpha]_D^{20}$ +31.2 (c 2.20, MeOH). ^{1}H NMR (400 MHz, $CDCl_3$) δ 4.98 (t, J = 7.0 Hz, 1H), 4.48 (t, J = 4.2 Hz, 1H), 4.17 (t, J = 7.2 Hz, 1H), 2.85 (s, 3H), 2.38 (s, 1H), 2.23 (ddd, J = 34.7, 15.9, 1.9 Hz, 2H), 1.94 (dddd, J = 15.4, 6.6, 4.3, 0.6 Hz, 1H), 1.66 (dddd, J = 14.8, 6.8, 4.3, 0.6 Hz, 1H). ^{13}C NMR (101 MHz, $CDCl_3$) δ 157.6, 78.4, 77.3, 76.9, 76.6, 72.4, 61.9, 42.4, 37.6, 29.2. LRMS (ESI) m/z: $[M + H]^+$ 158.0. HRMS (ESI) m/z: $[M + Na]^+$ calcd $C_7H_{11}NO_3Na$ 180.0631; found 180.0630.

(3a*R*,5*S*,6a*S*)-5-Hydroxy-3-methylhexahydro-2*H*-cyclopenta[*d*]oxazol-2-one (*ent*-10e). Protected oxazolidinone *ent*-**8** (20 mg, 0.1 mmol) was dissolved with freshly distilled dimethylformamide (2.1 mL) and was placed under an argon atmosphere. Reaction mixture was cooled to 0 °C, and sodium hydride (0.1 mmol) was added all at once. Reaction stirred for 20 min, and then iodomethane (21 mg, 0.2 mmol) was added dropwise. Reaction was allowed to warm up to 23 °C for 1 h. Upon completion, the residue was taken up in water and the aqueous phase was extracted with EtOAc. The organic extracts were dried with Na_2SO_4,

DOI: 10.1021/acs.jmedchem.8b01227
J. Med. Chem. 2018, 61, 9722−9737

and the solvent was removed under reduced pressure. The crude product was taken up in methanol (2.1 mL) and followed the addition of potassium carbonate (17 mg, 0.1 mmol). Reaction was stirred at 23 °C for 12 h. Upon completion, the residue solvent was removed under reduced pressure. The crude product was purified by silica gel column chromatography (60% EtOAc in hexane) to afford *ent*-**10e** (10 mg, 60%). $[\alpha]_D^{20}$ −16.0 (*c* 1.00, MeOH). ^{1}H NMR (800 MHz, CD_3OD) δ 5.04 (t, *J* = 8.0, 7.0 Hz, 1H), 4.40 (t, *J* = 4.3 Hz, 1H), 4.27 (t, *J* = 7.2 Hz, 1H), 2.85 (s, 3H), 2.20−2.13 (m, 2H), 2.03−1.96 (m, 2H), 1.77−1.71 (m, 2H). ^{13}C NMR (201 MHz, CD_3OD) δ 158.6, 79.2, 71.8, 62.1, 47.9, 47.9, 47.8, 47.7, 47.6, 47.5, 47.4, 47.3, 41.3, 36.9, 27.9. LRMS (ESI) *m*/*z*: $[M + H]^+$ 158.0. HRMS (ESI) *m*/*z*: $[M + H]^+$ calcd $C_7H_{12}NO_3$ 158.0812; found 158.0810.

(3a*S*,5*R*,6a*R*)-3-Allyl-5-hydroxyhexahydro-2*H*-cyclopenta-[*d*]oxazol-2-one (10f). Protected oxazolidinone **8** (17 mg, 0.1 mmol) was dissolved with dry acetonitrile (4 mL) and was placed under an argon atmosphere. Reaction mixture was cooled to 0 °C, and potassium bis(trimethylsilyl)amide (0.5 M solution, 0.2 mL, 0.1 mmol) was added dropwise. The reaction stirred for 30 min. Allyl iodide (17 mg, 0.1 mmol) was then added dropwise, and the reaction mixture was allowed to warm up to 23 °C for 1 h. Upon completion, the residue was taken up in DI water and the aqueous phase was extracted with EtOAc. The organic extracts were dried with Na_2SO_4, and the solvent was removed under reduced pressure. The crude product was taken up in methanol (2 mL) and followed the addition of potassium carbonate (15 mg, 0.11 mmol). Reaction was stirred at 23 °C for 12 h. Upon completion, the residue solvent was removed under reduced pressure. The crude product was purified by silica gel column chromatography (80% EtOAc in hexane) to afford **10f** (10 mg, 60%). $[\alpha]_D^{20}$ +19 (*c* 2.0, MeOH). ^{1}H NMR (800 MHz, CD_3OD) δ 5.76 (dddd, *J* = 17.2, 10.2, 7.1, 4.9 Hz, 1H), 5.22 (dq, *J* = 17.1, 1.5 Hz, 1H), 5.16 (dq, *J* = 10.2, 1.4 Hz, 1H), 4.96 (t, *J* = 7.1 Hz, 1H), 4.31 (dq, *J* = 4.3, 2.1, 1.6 Hz, 1H), 4.24 (t, *J* = 7.3 Hz, 1H), 4.04 (ddt, *J* = 15.8, 5.0, 1.7 Hz, 1H), 3.58 (ddt, *J* = 15.8, 7.1, 1.3 Hz, 1H), 2.07 (dd, *J* = 28.0, 15.3 Hz, 2H), 1.92 (ddd, *J* = 15.1, 6.5, 4.3 Hz, 1H), 1.63 (ddd, *J* = 14.7, 6.9, 4.3 Hz, 1H). ^{13}C NMR (201 MHz, CD_3OD) δ 159.7, 133.7, 118.5, 80.9, 73.2, 61.1, 49.1, 49.0, 48.9, 46.1, 42.7, 38.7. LRMS (ESI) *m*/*z*: $[M + H]^+$ 183.9. HRMS (ESI) *m*/*z*: $[M + H]^+$ calcd $C_9H_{14}NO_3$ 184.0968; found 184.0967.

(3a*S*,5*R*,6a*R*)-5-Hydroxy-3-propylhexahydro-2*H*-cyclopenta-[*d*]oxazol-2-one (10g). To a stirred reaction of alcohol **10f** (4.5 mg, 0.02 mmol) in dry methanol (1 mL) under an argon atmosphere were added Pd/C (10 wt %) and a hydrogen balloon. Reaction mixture was stirred at 23 °C for 12 h. Upon completion, the residue was filtered over Celite and rinsed with dichloromethane. The solvent collected was removed under reduced pressure. The crude product was purified by silica gel column chromatography (60% EtOAc in hexane) to afford **10g** (3.9 mg, 86%). $[\alpha]_D^{20}$ +14.3 (*c* 0.77, MeOH). ^{1}H NMR (800 MHz, $CDCl_3$) δ 5.02 (t, *J* = 7.0 Hz, 1H), 4.51 (t, *J* = 4.4 Hz, 1H), 4.28 (t, *J* = 7.2 Hz, 1H), 3.51 (ddd, *J* = 14.1, 8.7, 7.3 Hz, 1H), 3.04 (ddd, *J* = 13.9, 8.6, 5.2 Hz, 1H), 2.30−2.26 (m, 1H), 2.20−2.16 (m, 1H), 2.03 (ddd, *J* = 15.5, 6.5, 4.4 Hz, 1H), 1.75 (ddd, *J* = 14.9, 6.9, 4.5 Hz, 1H), 1.69−1.64 (m, 1H), 1.61 (ddd, *J* = 13.5, 8.0, 6.6 Hz, 1H), 0.97 (t, *J* = 7.4 Hz, 3H). ^{13}C NMR (201 MHz, $CDCl_3$) δ 157.3, 78.3, 77.2, 77.0, 76.9, 72.8, 59.5, 44.2, 42.7, 38.3, 29.7, 20.5, 11.2. LRMS (ESI) *m*/*z*: $[M + H]^+$ 186.0. HRMS (ESI) *m*/*z*: $[M + Na]^+$ calcd $C_9H_{15}NO_3Na$ 208.0944; found 208.0942.

(3a*S*,5*R*,6a*R*)-5-Hydroxy-3-(2-methylallyl)hexahydro-2*H*-cyclopenta[*d*]oxazol-2-one (10h). Protected oxazolidinone **8** (10 mg, 0.06 mmol) was dissolved with dry acetonitrile (1 mL) and was placed under an argon atmosphere. Reaction mixture was cooled to 0 °C, and potassium bis(trimethylsilyl)amide (0.5 M solution, 0.13 mL, 0.07 mmol) was added dropwise. The reaction stirred for 30 min. 3-Bromo-2-methylprop-1-ene (8.8 mg, 0.06 mmol) was then added dropwise, and the reaction mixture was allowed to warm up to 23 °C for 1 h. Upon completion, the residue was taken up in DI water and the aqueous phase was extracted with EtOAc. The organic extracts were dried with Na_2SO_4 and the solvent was removed under reduced pressure. The crude product was taken up in methanol (0.6 mL) and followed the addition of potassium carbonate (4.6 mg, 0.02 mmol). Reaction was stirred at 23 °C for 12 h. Upon completion, the residue solvent was removed under reduced pressure. The crude product was purified by silica gel column chromatography (80% EtOAc in hexane) to afford **10h** (3.2 mg, 84%). $[\alpha]_D^{20}$ +22.9 (*c* 0.67, MeOH). ^{1}H NMR (800 MHz, $CDCl_3$) δ 5.03 (t, *J* = 7.0 Hz, 1H), 4.95 (d, *J* = 20.5 Hz, 2H), 4.51 (s, 1H), 4.19 (t, *J* = 7.3 Hz, 1H), 4.15 (d, *J* = 15.2 Hz, 1H), 3.58 (d, *J* = 15.3 Hz, 1H), 2.30 (dd, *J* = 15.5, 2.9 Hz, 1H), 2.19 (dt, *J* = 14.8, 1.8 Hz, 1H), 2.01 (ddd, *J* = 15.4, 6.4, 4.3 Hz, 1H), 1.77 (s, 2H), 1.69 (ddt, *J* = 19.2, 7.0, 3.7 Hz, 2H). ^{13}C NMR (201 MHz, $CDCl_3$) δ 157.5, 140.1, 113.8, 78.5, 77.2, 77.0, 76.9, 72.7, 59.3, 48.9, 42.7, 38.0, 19.9. LRMS (ESI) *m*/*z*: $[M + H]^+$ 198.0 HRMS (ESI) *m*/*z*: $[M + H]^+$ calcd $C_{10}H_{14}NO_3$ 198.1125; found 198.1126.

(3a*S*,5*R*,6a*R*)-5-Hydroxy-3-isobutylhexahydro-2*H*-cyclopenta[*d*]oxazol-2-one (10i). To a stirred reaction of alcohol **10h** (16 mg, 0.07 mmol) in dry methanol (2.2 mL) under an argon atmosphere were added of Pd/C (10 wt %) and a hydrogen balloon. Reaction mixture was stirred at 23 °C for 12 h. Upon completion, the residue was filtered over Celite and rinsed with dichloromethane. The solvent collected was removed under reduced pressure. The crude product was purified by silica gel column chromatography (60% EtOAc in hexane) to afford **10i** (15 mg, 92%). $[\alpha]_D^{20}$ +65.2 (*c* 2.00, MeOH). ^{1}H NMR (800 MHz, $CDCl_3$) δ 5.02 (t, *J* = 6.9 Hz, 1H), 4.51 (s, 1H), 4.26 (t, *J* = 7.4 Hz, 1H), 3.33 (t, *J* = 12.5, 11.0 Hz, 1H), 2.89 (ddd, *J* = 14.1, 6.2, 2.3 Hz, 1H), 2.29 (d, *J* = 15.4 Hz, 1H), 2.19 (d, *J* = 14.7 Hz, 1H), 2.05−1.91 (m, 2H), 1.78−1.67 (m, 2H), 0.99 (d, *J* = 6.5 Hz, 3H), 0.94 (d, *J* = 6.5 Hz, 3H). ^{13}C NMR (201 MHz, $CDCl_3$) δ 157.7, 78.38, 77.2, 77.0, 76.9, 72.7, 59.9, 50.0, 42.7, 38.0, 26.4, 20.2, 19.8. LRMS (ESI) *m*/*z*: $[M + H]^+$ 200.1. HRMS (ESI) *m*/*z*: $[M + H]^+$ calcd $C_{10}H_{18}NO_3$ 200.1281; found 200.1280.

(3a*S*,5*R*,6a*R*)-5-Hydroxy-3-(methoxymethyl)hexahydro-2*H*-cyclopenta[*d*]oxazol-2-one (10j). Protected oxazolidinone **8** (8 mg, 0.04 mmol) was dissolved with dry tetrahydrofuran (2.7 mL) and was placed under an argon atmosphere. Reaction mixture was cooled to 0 °C, and potassium bis(trimethylsilyl)amide (0.5 M solution, 0.13 mL, 0.07 mmol) was added dropwise. The reaction stirred for 30 min. Chloromethyl methyl ether (5.7 mg, 0.07 mmol) was then added dropwise, and the reaction mixture was allowed to warm up to 23 °C for 1 h. Upon completion, the residue was taken up in DI water, and the aqueous phase was extracted with EtOAc. The organic extracts were dried with Na_2SO_4, and the solvent was removed under reduced pressure. The crude product was taken up in methanol (1 mL) and followed the addition of potassium carbonate (8 mg, 0.06 mmol). Reaction was stirred at 23 °C for 12 h. Upon completion, the residue solvent was removed under reduced pressure. The crude product was purified by silica gel column chromatography (60% EtOAc in hexane) to afford **10j** (2.7 mg, 33%). $[\alpha]_D^{20}$ +9.87 (*c* 2.60, MeOH). ^{1}H NMR (800 MHz, CD_3OD) δ 5.09 (t, *J* = 7.1 Hz, 1H), 4.77 (d, *J* = 11.0 Hz, 1H), 4.68 (d, *J* = 11.1 Hz, 1H), 4.45−4.40 (m, 2H), 3.35 (s, 3H), 2.20 (dd, *J* = 14.9, 1.4 Hz, 2H), 2.04−1.98 (m, 1H), 1.83−1.76 (m, 1H). ^{13}C NMR (201 MHz, CD_3OD) δ 158.7, 79.9, 74.8, 71.9, 59.4, 54.8, 47.9, 47.9, 47.8, 47.7, 47.6, 47.5, 47.4, 47.3, 41.1, 38.3. LRMS (ESI) *m*/*z*: $[M + Na]^+$ 209.9. HRMS (ESI) *m*/*z*: $[M + Na]^+$ calcd $C_{18}H_{13}NO_3Na$ 210.0737; found 210.0736.

4-Nitrophenyl ((3a*S*,5*R*,6a*R*)-2-Oxohexahydro-2*H*-cyclopenta[*d*]oxazol-5-yl)carbonate (11a). To a stirred solution of alcohol **9** (10 mg, 0.07 mmol) in dry dichloromethane (2 mL) were added 4-methylmorpholine (23 μL, 0.2 mmol) and 4-nitrophenyl chloroformate (42 mg, 0.2 mmol) at 0 °C under an argon atmosphere. The reaction mixture was warmed to 23 °C and stirred for 12 h. Upon completion, solvent was removed under reduced pressure. The crude product was purified by silica gel column chromatography (80% EtOAc in hexane) to afford **11a** (18 mg, 83%): ^{1}H NMR (800 MHz, $CDCl_3$) δ 8.29 (d, *J* = 9.1 Hz, 2H), 7.40 (d, *J* = 9.1 Hz, 2H), 5.36 (t, *J* = 4.6 Hz, 1H), 5.29 (s, 1H), 5.26 (t, *J* = 6.9 Hz, 1H), 4.49 (t, *J* = 7.2 Hz, 1H), 2.67 (dd, *J* = 16.3, 3.0 Hz, 1H), 2.34 (dd, *J* = 15.6, 3.0 Hz, 1H), 2.16 (ddd, *J* = 16.2, 6.4, 4.6 Hz, 1H), 2.10 (ddd, *J* = 15.6, 6.8, 4.7 Hz, 1H). ^{13}C NMR (201 MHz, $CDCl_3$) δ 158.1, 155.4, 151.9, 145.5, 125.3, 121.9, 81.0, 80.7, 77.2, 77.0, 76.9, 55.9, 40.2, 39.5, 29.7. LRMS (ESI) *m*/*z*: $[M + H]^+$ 309.0.

DOI: 10.1021/acs.jmedchem.8b01227
J. Med. Chem. 2018, 61, 9722−9737

(3a*S*,5*R*,6a*R*)-3-Methyl-2-oxohexahydro-2*H*-cyclopenta[*d*]-oxazol-5-yl (4-Nitrophenyl) Carbonate (11b). Alcohol **10e** (13 mg, 0.08 mmol) was treated with 4-methylmorpholine (27 μL, 0.3 mmol) and 4-nitrophenyl chloroformate (50 mg, 0.3 mmol) by following the procedure outline for activated alcohol **11a** to afford **11b** (15 mg, 56%): ^{1}H NMR (500 MHz, $CDCl_3$) δ 8.26 (d, *J* = 9.2 Hz, 2H), 7.35 (d, *J* = 9.2 Hz, 2H), 5.32−5.28 (m, 1H), 5.07 (t, *J* = 7.1 Hz, 1H), 4.28 (t, *J* = 7.1 Hz, 1H), 2.89 (s, 3H), 2.59 (dd, *J* = 16.3, 2.7 Hz, 1H), 2.44 (dd, *J* = 15.7, 3.1 Hz, 1H), 2.21−2.13 (m, 1H), 1.98−1.88 (m, 1H). ^{13}C NMR (126 MHz, $CDCl_3$) δ 156.9, 155.3, 151.9, 145.5, 125.3, 121.9, 80.5, 77.3, 77.0, 76.8, 61.5, 39.7, 35.6, 29.3. LRMS (ESI) *m*/*z*: $[M + H]^+$ 323.0

4-Nitrophenyl ((3a*R*,5*S*,6a*S*)-2-Oxohexahydro-2*H*-cyclopenta[*d*]oxazol-5-yl)carbonate (11c). Alcohol *ent*-**9** (6.3 mg, 0.04 mmol) was treated with 4-methylmorpholine (15 μL, 0.1 mmol) and 4-nitrophenyl chloroformate (27 mg, 0.1 mmol) by following the procedure outline for activated alcohol **11a** to afford **11c** (4.8 mg, 35%): ^{1}H NMR (800 MHz, $CDCl_3$) δ 8.29 (d, *J* = 8.5 Hz, 2H), 7.40 (d, *J* = 8.7 Hz, 2H), 5.36 (t, *J* = 4.8 Hz, 1H), 5.26 (t, *J* = 7.0 Hz, 1H), 5.19 (s, 1H), 4.49 (t, *J* = 7.2 Hz, 1H), 2.67 (d, *J* = 15.9 Hz, 1H), 2.34 (d, *J* = 15.5 Hz, 1H), 2.15 (dt, *J* = 16.3, 5.5 Hz, 1H), 2.10 (dt, *J* = 15.6, 5.8 Hz, 1H). ^{13}C NMR (201 MHz, $CDCl_3$) δ 158.1, 155.4, 151.9, 145.5, 125.3, 121.9, 81.0, 80.7, 77.2, 77.0, 76.9, 55.9, 40.2, 39.5. LRMS (ESI) *m*/*z*: $[M + H]^+$ 309.0.

4-Nitrophenyl ((3a*R*,5*S*,6a*S*)-2-Oxohexahydro-2*H*-cyclopenta[*d*]oxazol-5-yl)carbonate (11d). Alcohol *ent*-**10e** (5.7 mg, 0.04 mmol) was treated with 4-methylmorpholine (12 μL, 0.1 mmol) and 4-nitrophenyl chloroformate (22 mg, 0.1 mmol) by following the procedure outline for activated alcohol **11a** to afford **11d** (11 mg, 94%): ^{1}H NMR (500 MHz, $CDCl_3$) δ 8.27 (d, *J* = 9.2 Hz, 2H), 7.36 (d, *J* = 9.2 Hz, 2H), 5.30 (t, *J* = 4.6 Hz, 1H), 5.07 (t, *J* = 7.0 Hz, 1H), 4.28 (t, *J* = 7.1 Hz, 1H), 2.89 (s, 3H), 2.45 (dd, *J* = 15.6, 3.0 Hz, 1H), 2.20−2.13 (m, 1H), 1.96−1.89 (m, 1H). ^{13}C NMR (126 MHz, $CDCl_3$) δ 156.9, 155.3, 151.9, 145.5, 125.3, 121.9, 80.5, 77.3, 77.2, 77.0, 76.8, 61.5, 39.7, 35.6, 29.3. LRMS (ESI) *m*/*z*: $[M + H]^+$ 323.0.

4-Nitrophenyl ((3a*R*,5*S*,6a*S*)-2-Oxohexahydro-2*H*-cyclopenta[*d*]oxazol-5-yl)carbonate (11e). Alcohol **10a** (14 mg, 0.06 mmol) was treated with 4-methylmorpholine (20 μL, 0.2 mmol) and 4-nitrophenyl chloroformate (37 mg, 0.2 mmol) by following the procedure outline for activated alcohol **11a** to afford **11e** (19 mg, 78%): ^{1}H NMR (800 MHz, $CDCl_3$) δ 8.27 (dd, *J* = 9.0, 1.8 Hz, 2H), 7.54 (d, *J* = 7.9 Hz, 2H), 7.44−7.38 (m, 2H), 7.33−7.26 (m, 3H), 7.21 (t, *J* = 7.4 Hz, 1H), 5.33 (t, *J* = 4.6 Hz, 1H), 5.25 (t, *J* = 7.0 Hz, 1H), 5.02 (t, *J* = 7.1 Hz, 1H), 2.72 (dd, *J* = 16.3, 3.2 Hz, 1H), 2.49 (dd, *J* = 15.7, 3.2 Hz, 1H), 2.27 (dddd, *J* = 16.2, 6.4, 4.5, 1.6 Hz, 1H), 2.09 (dddd, *J* = 15.8, 6.5, 4.4, 1.5 Hz, 1H). ^{13}C NMR (201 MHz, $CDCl_3$) δ 155.3, 154.3, 151.8, 145.5, 137.0, 129.3, 125.3, 124.9, 121.9, 120.7, 80.4, 77.2, 77.0, 76.9, 60.6, 39.9, 36.9. LRMS (ESI) *m*/*z*: $[M + H]^+$ 385.0.

(3a*S*,5*R*,6a*R*)-3-(4-Methoxyphenyl)-2-oxohexahydro-2*H*-cyclopenta[*d*]oxazol-5-yl (4-Nitrophenyl) Carbonate (11f). Alcohol **10b** (6.8 mg, 0.03 mmol) was treated with 4-methylmorpholine (9.0 μL, 0.08 mmol) and 4-nitrophenyl chloroformate (17 mg, 0.08 mmol) by following the procedure outline for activated alcohol **11a** to afford **11f** (11 mg, 97%): ^{1}H NMR (500 MHz, $CDCl_3$) δ 8.27 (d, *J* = 9.2 Hz, 2H), 7.38 (d, *J* = 9.1 Hz, 2H), 7.32 (d, *J* = 9.2 Hz, 2H), 6.92 (d, *J* = 9.1 Hz, 2H), 5.31 (t, *J* = 4.5 Hz, 1H), 5.22 (t, *J* = 7.1 Hz, 1H), 4.92 (t, *J* = 7.0 Hz, 1H), 3.81 (s, 3H), 2.69 (dd, *J* = 16.3, 2.8 Hz, 1H), 2.43 (dd, *J* = 15.7, 3.1 Hz, 1H), 2.27−2.19 (m, 1H), 2.03−1.95 (m, 1H). ^{13}C NMR (126 MHz, $CDCl_3$) δ 157.2, 155.3, 154.7, 151.9, 145.5, 129.8, 125.3, 123.5, 121.9, 114.6, 80.5, 77.3, 77.0, 76.8, 61.3, 55.6, 40.0, 36.7. LRMS (ESI) *m*/*z*: $[M + H]^+$ 415.0.

(3a*S*,5*R*,6a*R*)-3-(3-Methoxyphenyl)-2-oxohexahydro-2*H*-cyclopenta[*d*]oxazol-5-yl (4-Nitrophenyl) Carbonate (11g). Alcohol **10c** (20 mg, 0.08 mmol) was treated with 4-methylmorpholine (26 μL, 0.2 mmol) and 4-nitrophenyl chloroformate (48 mg, 0.2 mmol) by following the procedure outline for activated alcohol **11a** to afford **11g** (13 mg, 60%): ^{1}H NMR (800 MHz, $CDCl_3$) δ 8.27 (d, *J* = 9.2 Hz, 2H), 7.32−7.29 (m, 3H), 7.22 (t, *J* = 2.3 Hz, 1H), 7.05 (dd, *J* = 8.0, 1.7 Hz, 1H), 6.75 (dd, *J* = 8.3, 2.3 Hz, 1H), 5.32 (t, *J* = 4.5 Hz, 1H), 5.24 (t, *J* = 7.0 Hz, 1H), 4.98 (t, *J* = 7.1 Hz, 1H), 3.81 (s, 3H), 2.71 (dd, *J* = 16.2, 3.1 Hz, 1H), 2.52 (dd, *J* = 15.8, 3.1 Hz, 1H), 2.26 (ddd, *J* = 16.2, 6.6, 4.6 Hz, 1H), 2.09 (ddd, *J* = 15.8, 6.8, 4.5 Hz, 1H). ^{13}C NMR (201 MHz, $CDCl_3$) δ 160.4, 155.3, 154.1, 151.8, 145.5, 138.2, 130.0, 125.3, 121.9, 112.6, 109.9, 107.3, 80.4, 77.2, 77.0, 76.9, 60.6, 55.4, 39.9, 37.0. LRMS (ESI) *m*/*z*: $[M + H]^+$ 415.0.

(3a*S*,5*R*,6a*R*)-3-(2-Methoxyphenyl)-2-oxohexahydro-2*H*-cyclopenta[*d*]oxazol-5-yl (4-Nitrophenyl) Carbonate (11h). Alcohol **10d** (21 mg, 0.08 mmol) was treated with 4-methylmorpholine (28 μL, 0.3 mmol) and 4-nitrophenyl chloroformate (51 mg, 0.3 mmol) by following the procedure outline for activated alcohol **11a** to afford **11h** (15 mg, 42%): ^{1}H NMR (800 MHz, $CDCl_3$) δ 8.32 (d, *J* = 9.0 Hz, 2H), 7.42 (t, *J* = 8.0 Hz, 3H), 7.33 (t, *J* = 7.8 Hz, 2H), 7.00 (d, *J* = 8.0 Hz, 2H), 5.33 (t, *J* = 4.3 Hz, 1H), 5.28 (t, *J* = 7.2 Hz, 1H), 5.09 (t, *J* = 7.2 Hz, 1H), 3.90 (s, 3H), 2.71 (dd, *J* = 16.2, 3.1 Hz, 2H), 2.28−2.21 (m, 3H), 1.85 (ddd, *J* = 15.8, 6.8, 4.6 Hz, 2H). ^{13}C NMR (201 MHz, $CDCl_3$) δ 156.0, 155.4, 154.9, 152.0, 145.5, 129.8, 129.0, 125.4, 124.6, 121.9, 121.1, 112.0, 80.8, 77.9, 77.2, 77.0, 76.9, 60.8, 55.7, 40.1, 36.7. LRMS (ESI) *m*/*z*: $[M + H]^+$ 415.1.

(3a*S*,5*R*,6a*R*)-3-Allyl-2-oxohexahydro-2*H*-cyclopenta[*d*]-oxazol-5-yl (4-Nitrophenyl) Carbonate (11i). Alcohol **10f** (14 mg, 0.08 mmol) was treated with 4-methylmorpholine (25 μL, 0.2 mmol) and 4-nitrophenyl chloroformate (46 mg, 0.2 mmol) by following the procedure outline for activated alcohol **11a** to afford **11i** (17 mg, 66%): ^{1}H NMR (800 MHz, $CDCl_3$) δ 8.30 (d, *J* = 9.2 Hz, 2H), 7.39 (d, *J* = 9.2 Hz, 2H), 5.83 (dddd, *J* = 17.2, 10.1, 7.1, 5.4 Hz, 1H), 5.34−5.27 (m, 3H), 5.10 (t, *J* = 7.1 Hz, 1H), 4.37 (t, *J* = 7.2 Hz, 1H), 4.20 (ddt, *J* = 15.5, 5.4, 1.6 Hz, 1H), 3.69 (ddt, *J* = 15.5, 7.1, 1.2 Hz, 1H), 2.63 (dd, *J* = 16.2, 2.5 Hz, 1H), 2.48 (dd, *J* = 15.7, 3.0 Hz, 1H), 2.18 (dddd, *J* = 16.2, 6.6, 4.6, 0.7 Hz, 1H), 1.92 (dddd, *J* = 15.6, 6.8, 4.7, 0.7 Hz, 1H). ^{13}C NMR (201 MHz, $CDCl_3$) δ 156.6, 155.3, 151.9, 145.5, 132.3, 125.3, 121.9, 118.9, 80.5, 77.6, 77.2, 77.2, 77.0, 76.9, 59.3, 45.6, 39.7, 36.0. LRMS (ESI) *m*/*z*: $[M + H]^+$ 349.0.

4-Nitrophenyl ((3a*S*,5*R*,6a*R*)-2-oxo-3-propylhexahydro-2*H*-cyclopenta[*d*]oxazol-5-yl)carbonate (11j). Alcohol **10g** (7 mg, 0.04 mmol) was treated with 4-methylmorpholine (12 μL, 0.1 mmol) and 4-nitrophenyl chloroformate (23 mg, 0.1 mmol) by following the procedure outline for activated alcohol **11a** to afford **11j** (4 mg, 30%): ^{1}H NMR (500 MHz, $CDCl_3$) δ 8.27 (d, *J* = 9.2 Hz, 2H), 7.36 (d, *J* = 9.2 Hz, 2H), 5.29 (t, *J* = 4.6 Hz, 1H), 5.07 (t, *J* = 7.0 Hz, 1H), 4.35 (t, *J* = 7.2 Hz, 1H), 3.47 (ddd, *J* = 14.0, 8.8, 7.1 Hz, 1H), 3.02 (ddd, *J* = 14.0, 8.6, 5.2 Hz, 1H), 2.60 (ddd, *J* = 16.3, 3.0, 1.0 Hz, 1H), 2.43 (dd, *J* = 15.7, 3.0 Hz, 1H), 2.16 (dddd, *J* = 16.1, 6.5, 4.7, 0.7 Hz, 1H), 1.94 (dddd, *J* = 15.6, 6.8, 4.7, 0.7 Hz, 1H), 1.73−1.57 (m, 2H), 0.95 (t, *J* = 7.4 Hz, 3H). ^{13}C NMR (126 MHz, $CDCl_3$) δ 156.9, 155.3, 151.9, 145.5, 125.3, 121.9, 80.5, 77.3, 77.0, 76.8, 59.4, 44.3, 39.7, 36.2, 29.7, 20.7, 11.2. LRMS (ESI) *m*/*z*: $[M + H]^+$ 351.0.

(3a*S*,5*R*,6a*R*)-3-(2-Methylallyl)-2-oxohexahydro-2*H*-cyclopenta[*d*]oxazol-5-yl (4-Nitrophenyl) Carbonate (11k). Alcohol **10h** (6 mg, 0.03 mmol) was treated with 4-methylmorpholine (10 μL, 0.09 mmol) and 4-nitrophenyl chloroformate (19 mg, 0.09 mmol) by following the procedure outline for activated alcohol **11a** to afford **11k** (7.2 mg, 66%): ^{1}H NMR (500 MHz, $CDCl_3$) δ 8.27 (d, *J* = 9.3 Hz, 2H), 7.36 (d, *J* = 9.2 Hz, 2H), 5.30 (t, *J* = 4.6 Hz, 1H), 5.08 (t, *J* = 7.0 Hz, 1H), 4.95 (d, *J* = 17.9 Hz, 2H), 4.26 (t, *J* = 7.2 Hz, 1H), 4.09 (d, *J* = 15.2 Hz, 1H), 3.59 (d, *J* = 15.2 Hz, 1H), 2.61 (dd, *J* = 16.4, 2.7 Hz, 1H), 2.43 (dd, *J* = 15.7, 3.0 Hz, 1H), 2.15 (dddd, *J* = 16.2, 6.5, 4.6, 0.7 Hz, 1H), 1.89 (dddd, *J* = 15.8, 7.0, 4.8, 0.7 Hz, 1H), 1.76 (t, *J* = 0.8 Hz, 3H). ^{13}C NMR (126 MHz, $CDCl_3$) δ 157.0, 155.3, 151.9, 145.5, 139.9, 125.3, 121.9, 114.2, 80.5, 77.6, 77.3, 77.0, 76.8, 59.3, 49.2, 39.7, 35.9, 19.9. LRMS (ESI) *m*/*z*: $[M + H]^+$ 363.0.

(3a*S*,5*R*,6a*R*)-3-Isobutyl-2-oxohexahydro-2*H*-cyclopenta[*d*]-oxazol-5-yl (4-Nitrophenyl) Carbonate (11l). Alcohol **10i** (11 mg, 0.05 mmol) was treated with 4-methylmorpholine (18 μL, 0.2 mmol) and 4-nitrophenyl chloroformate (33 mg, 0.2 mmol) by following the procedure outline for activated alcohol **11a** to afford **11l** (15 mg, 77%): ^{1}H NMR (800 MHz, $CDCl_3$) δ 8.29 (d, *J* = 9.2 Hz, 2H), 7.38 (d, *J* = 9.2 Hz, 2H), 5.32 (t, *J* = 4.7 Hz, 1H), 5.10 (t, *J* = 7.0 Hz, 1H), 4.36 (t, *J* = 7.2 Hz, 1H), 3.33 (dd, *J* = 14.0, 8.9 Hz, 1H),

DOI: 10.1021/acs.jmedchem.8b01227
J. Med. Chem. 2018, 61, 9722−9737

2.88 (dd, J = 14.0, 6.3 Hz, 1H), 2.63 (dd, J = 16.2, 2.6 Hz, 1H), 2.45 (dd, J = 15.7, 3.0 Hz, 1H), 2.20−2.15 (m, 1H), 2.01−1.93 (m, 2H), 1.00 (d, J = 6.7 Hz, 3H), 0.96 (d, J = 6.7 Hz, 3H). ^{13}C NMR (201 MHz, $CDCl_3$) δ 157.2, 155.3, 151.9, 145.5, 125.3, 121.9, 80.5, 77.4, 77.2, 77.0, 76.9, 59.7, 50.2, 39.7., 36.0, 26.5, 20.2, 19.8. LRMS (ESI) m/z: $[M + H]^+$ 365.0.

(3a*S*,5*R*,6a*R*)-3-(Methoxymethyl)-2-oxohexahydro-2*H*-cyclopenta[*d*]oxazol-5-yl (4-Nitrophenyl) Carbonate (11m). Alcohol **10j** (5 mg, 0.03 mmol) was treated with 4-methylmorpholine (9.0 μL, 0.08 mmol) and 4-nitrophenyl chloroformate (16 mg, 0.08 mmol) by following the procedure outline for activated alcohol **11a** to afford **11m** (7 mg, 74%): ^{1}H NMR (800 MHz, $CDCl_3$) δ 8.29 (d, J = 9.2 Hz, 2H), 7.38 (d, J = 9.2 Hz, 2H), 5.35 (t, J = 4.6 Hz, 1H), 5.14 (t, J = 7.1 Hz, 1H), 4.79 (d, J = 0.6 Hz, 2H), 4.48 (t, J = 7.1 Hz, 1H), 3.41 (s, 3H), 2.70−2.59 (m, 2H), 2.18 (dddd, J = 16.2, 6.6, 4.6, 0.7 Hz, 1H), 2.02 (dddd, J = 15.7, 6.9, 4.7, 0.7 Hz, 1H). ^{13}C NMR (201 MHz, $CDCl_3$) δ 157.1, 155.3, 151.9, 145.5, 125.3, 121.8, 80.6, 78.0, 77.2, 77.2, 77.0, 76.9, 75.8, 59.4, 56.2, 39.5, 37.4. LRMS (ESI) m/z: $[M + Na]^+$ 375.0.

Determination of X-ray Structures of HIV-1 Protease−Inhibitor Complexes. HIV-1 protease was expressed and purified as described.[37] The protease complexes with inhibitors **4a** and **4e** were crystallized using the hanging drop vapor diffusion method with well solutions of 1.0 M NaCl, 0.1 M sodium acetate, pH 4.8 for **4a**, and 1.4 M NaCl, 0.1 M sodium acetate, pH 5.5 for **4e**. X-ray diffraction data were collected on a single crystal cooled to 90 K at SER-CAT (22-ID beamline), Advanced Photon Source, Argonne National Lab (Chicago, IL, USA) with X-ray wavelength of 1.0 Å. X-ray data were processed by HKL-2000[38] to give R_{merge} values of 9.9% for **4a**-bound protease and 8.2% for **4e**-bound protease. The crystal structures were solved by PHASER[39] in CCP4i Suite[40−42] using one of the previously reported isomorphous structures[43] as the initial model, and refined using both SHELX-2014[44,45] and Refmac5[46] with X-ray data at 1.22 and 1.30 Å resolution for **4a** and **4e** complexes, respectively. PRODRG-2[48] was used to construct the inhibitors and geometric restraints for refinement. COOT[47,49]was used for modification of the models. Alternative conformations were modeled, and isotropic atomic displacement parameters (B factors) were applied for all atoms including solvent molecules. The final refined solvent structure comprised two Na^+ ions, two Cl^- ions, one formic acid, and 190 waters for **4a**-bound protease and two Na^+ ions, four Cl^- ions, and 155 water molecules for the **4e**-bound protease structure. The crystallographic data collection and refinement statistics are listed in Table 1 of Supporting Information. The coordinates and structure factors of the HIV-1 protease structures have been deposited in the Protein Data Bank[49] with accession code of 6E9A for **4a**-bound protease and 6E7J for **4e**-bound protease.

■ ASSOCIATED CONTENT

Supporting Information

The Supporting Information is available free of charge on the ACS Publications website at DOI: 10.1021/acs.jmedchem.8b01227.

Full NMR spectroscopic data for all final compounds and X-ray structural data for inhibitors **4a** and **4e**-bound HIV-1 protease (PDF)

Molecular formula strings and some data (CSV)

Accession Codes

The PDB accession codes for inhibitor **4a**-bound HIV-1 protease and inhibitor **4e**-bound HIV-1 protease X-ray structures are 6E9A and 6E7J. Authors will release the atomic coordinates and experimental data upon article publication.

■ AUTHOR INFORMATION

Corresponding Author

*Phone: (765) 494-5323. Fax: (765) 496-1612. E-mail: akghosh@purdue.edu.

ORCID

Arun K. Ghosh: 0000-0003-2472-1841

Irene T. Weber: 0000-0003-4876-7393

Notes

The authors declare no competing financial interest.

■ ACKNOWLEDGMENTS

This research was supported by the National Institutes of Health (Grant GM53386, A.K.G., and Grant GM62920, I.T.W.). X-ray data were collected at the Southeast Regional Collaborative Access Team (SER-CAT) beamline 22ID at the Advanced Photon Source, Argonne National Laboratory. Use of the Advanced Photon Source was supported by the U.S. Department of Energy, Basic Energy Sciences, Office of Science, under Contract W-31-109-Eng-38. This work was also supported by the Intramural Research Program of the Center for Cancer Research, National Cancer Institute, National Institutes of Health, and in part by a Grant-in-Aid for Scientific Research (Priority Areas) from the Ministry of Education, Culture, Sports, Science, and Technology of Japan (Monbu Kagakusho), a Grant for Promotion of AIDS Research from the Ministry of Health, Welfare, and Labor of Japan, and the Grant to the Cooperative Research Project on Clinical and Epidemiological Studies of Emerging and Reemerging Infectious Diseases (Renkei Jigyo) of Monbu-Kagakusho. The authors thank the Purdue University Center for Cancer Research, which supports the shared NMR and mass spectrometry facilities.

■ ABBREVIATIONS USED

APV,amprenavir; ART,antiretroviral therapy; ATV,atazanavir; bis-THF,bis-tetrahydrofuran; DIPEA,*N*,*N*-diisopropylethylamine; DRV,darunavir; LPV,lopinavir; PI,protease inhibitor; TFA,trifluoroacetic acid; Cp-THF,cyclopentanyltetrahydrofuran; IBX,*O*-iodoxybenzoic acid

■ REFERENCES

(1) Naggie, S.; Hicks, C. Protease Inhibitor-Based Antiretroviral Therapy in Treatment-Naive HIV-1-Infected Patients: The Evidence Behind the Options. *J. Antimicrob. Chemother.* **2010**, *65*, 1094−1099.

(2) Broder, S. The Development of Antiretroviral Therapy and Its Impact on the HIV-1/AIDS Pandemic. *Antiviral Res.* **2010**, *85*, 1−18.

(3) Montaner, J. S. G.; Lima, V. D.; Barrios, R.; Yip, B.; Wood, E.; Kerr, T.; Shannon, K.; Harrigan, P. R.; Hogg, R. S.; Daly, P.; Kendall, P. Association of Highly Active Antiretroviral Therapy Coverage, Population Viral Load, and Yearly New HIV Diagnoses in British Columbia, Canada: a Population-based Study. *Lancet* **2010**, *376*, 532−539.

(4) Lohse, N.; Hansen, A. B.; Gerstoft, J.; Obel, N. Improved Survival in HIV-Infected Persons: Consequences and Perspectives. *J. Antimicrob. Chemother.* **2007**, *60*, 461−463.

(5) Brik, A.; Wong, C.-H. HIV-1 Protease: Mechanism and Drug Discovery. *Org. Biomol. Chem.* **2003**, *1*, 5−14.

(6) Pettit, S. C.; Everitt, L. E.; Choudhury, S.; Dunn, B. M.; Kaplan, A. H. Initial Cleavage of the Human Immunodeficiency Virus Type 1 GagPol Precursor by Its Activated Protease Occurs by an Intramolecular Mechanism. *J. Virol.* **2004**, *78*, 8477−8485.

(7) Kohl, N. E.; Emini, E. A.; Schleif, W. A.; Davis, L. J.; Heimbach, J. C.; Dixon, R. A.; Scolnick, E. M.; Sigal, I. S. Active Human Immunodeficiency Virus Protease is Required for Viral Infectivity. *Proc. Natl. Acad. Sci. U. S. A.* **1988**, *85*, 4686−4690.

(8) Smith, R.; Brereton, I. M.; Chai, R. Y.; Kent, S. B. H. Ionization States of the Catalytic Residues in HIV-1 Protease. *Nat. Struct. Biol.* **1996**, *3*, 946−950.

(9) Wlodawer, A.; Vondrasek, J. Inhibitors of HIV-1 Protease: A Major Success of Structure-Assisted Drug Design. *Annu. Rev. Biophys. Biomol. Struct.* **1998**, *27*, 249−284.
(10) Ghosh, A. K.; Osswald, H. L.; Prato, G. Recent Progress in the Development of HIV-1 Protease Inhibitors for the Treatment of HIV/AIDS. *J. Med. Chem.* **2016**, *59*, 5172−5208.
(11) Edmonds, A.; Yotebieng, M.; Lusiama, J.; Matumona, Y.; Kitetele, F.; Napravnik, S.; Cole, S. R.; Van Rie, A.; Behets, F. The Effect of Highly Active Antiretroviral Therapy on the Survival of HIV-Infected Children in a Resource-Deprived Setting: A Cohort Study. *PLoS Med.* **2011**, *8*, e1001044.
(12) Hue, S.; Gifford, R. J.; Dunn, D.; Fernhill, E.; Pillay, D. Demonstration of Sustained Drug-Resistant Human Immunodeficiency Virus Type 1 Lineages Circulating among Treatment-Naïve Individuals. *J. Virol.* **2009**, *83*, 2645−2654.
(13) Ghosh, A. K.; Chapsal, B. D. Design of the Anti-HIV-1 Protease Inhibitor Darunavir. In *Introduction to Biological and Small Molecule Drug Research and Development: Theory and Case Studies*; Ganellin, C. R., Jefferis, R., Roberts, S., Eds.; Elsevier: London, 2013; pp 355−384.
(14) Ghosh, A. K.; Dawson, Z. L.; Mitsuya, H. Darunavir, a Conceptually New HIV-1 Protease Inhibitor for the Treatment of Drug-Resistant HIV. *Bioorg. Med. Chem.* **2007**, *15*, 7576−7580.
(15) Koh, Y.; Nakata, H.; Maeda, K.; Ogata, H.; Bilcer, G.; Devasamudram, T.; Kincaid, J. F.; Boross, P.; Wang, Y. F.; Tie, Y.; Volarath, P.; Gaddis, L.; Harrison, R. W.; Weber, I. T.; Ghosh, A. K.; Mitsuya, H. Novel *bis*-Tetrahydrofuranylurethane-Containing Nonpeptidic Protease Inhibitor (PI) UIC-94017 (TMC114) with Potent Activity Against Multi-PI-Resistant Human Immunodeficiency Virus In Vitro. *Antimicrob. Agents Chemother.* **2003**, *47*, 3123−3129.
(16) De Meyer, S.; Azijn, H.; Surleraux, D.; Jochmans, D.; Tahri, A.; Pauwels, R.; Wigerinck, P.; de Béthune, M. P. TMC114, a Novel Human Immunodeficiency Virus Type 1 Protease Inhibitor Active Against Protease Inhibitor-Resistant Viruses, Including a Broad Range of Clinical Isolates. *Antimicrob. Agents Chemother.* **2005**, *49*, 2314−2321.
(17) Koh, Y.; Matsumi, S.; Das, D.; Amano, M.; Davis, D. A.; Li, J.; Leschenko, S.; Baldridge, A.; Shioda, T.; Yarchoan, R.; Ghosh, A. K.; Mitsuya, H. Potent Inhibition of HIV-1 Replication by Novel Nonpeptidyl Small Molecule Inhibitors of Protease Dimerization. *J. Biol. Chem.* **2007**, *282*, 28709−28720.
(18) Hayashi, H.; Takamune, N.; Nirasawa, T.; Aoki, M.; Morishita, Y.; Das, D.; Koh, Y.; Ghosh, A. K.; Misumi, S.; Mitsuya, H. Dimerization of HIV-1 Protease Occurs Through Two Steps Relating to the Mechanism of Protease Dimerization Inhibition by Darunavir. *Proc. Natl. Acad. Sci. U. S. A.* **2014**, *111*, 12234−12239.
(19) Ghosh, A. K.; Sridhar, P. R.; Kumaragurubaran, N.; Koh, Y.; Weber, I. T.; Mitsuya, H. Bis-Tetrahydrofuran: a Privileged Ligand for Darunavir and a New Generation of HIV Protease Inhibitors That Combat Drug Resistance. *ChemMedChem* **2006**, *1*, 939−950.
(20) de Béthune, M. P.; Sekar, V.; Spinosa-Guzman, S.; Vanstockem, M.; De Meyer, S.; Wigerinck, P.; Lefebvre, E. Darunavir (Prezista, TMC114): From bench to clinic, improving treatment options for HIV-infected patients. In *Antiviral Drugs: From Basic Discovery through Clinical Trials*; Kazmierski, W. M., Ed.; John Wiley & Sons, Inc.: Hoboken, NJ, 2011; pp 31−45, DOI: 10.1002/9780470929353.ch3.
(21) Tie, Y.; Boross, P. I.; Wang, Y.-F.; Gaddis, L.; Hussain, A. K.; Leshchenko, S.; Ghosh, A. K.; Louis, J. M.; Harrison, R. W.; Weber, I. T. High Resolution Crystal Structures of HIV-1 Protease with a Potent Non-peptide Inhibitor (UIC-94017) Active Against Multi-Drug-Resistant Clinical Strains. *J. Mol. Biol.* **2004**, *338*, 341−352.
(22) Kovalevsky, A. Y.; Liu, F.; Leshchenko, S.; Ghosh, A. K.; Louis, J. M.; Harrison, R. W.; Weber, I. T. Ultra-High Resolution Crystal Structure of HIV-1 Protease Mutant Reveals Two Binding Sites for Clinical Inhibitor TMC114. *J. Mol. Biol.* **2006**, *363*, 161−173.
(23) Ghosh, A. K.; Chapsal, B. D.; Weber, I. T.; Mitsuya, H. Design of HIV Protease Inhibitors Targeting Protein Backbone: An Effective Strategy for Combating Drug Resistance. *Acc. Chem. Res.* **2008**, *41*, 78−86.
(24) Ghosh, A. K.; Anderson, D. D.; Weber, I. T.; Mitsuya, H. Enhancing Protein Backbone Binding—A Fruitful Concept for Combating Drug-Resistant HIV. *Angew. Chem., Int. Ed.* **2012**, *51*, 1778−1802.
(25) Deardorff, D. R.; Windham, C. Q.; Carnney, C. L. Enantioselective Hydrolysis of *cis*-3,5-Diacetoxycyclopentene: (1*R*,4*S*)-(+)-4-Hydroxy-2-Cyclopentenyl Acetate. *Org. Synth., Collect. Vol.* **1998**, *9*, 487.
(26) Ghosh, A. K.; Chapsal, B. D.; Baldridge, A.; Ide, K.; Koh, Y.; Mitsuya, H. Design and Synthesis of Stereochemically Defined Novel Spirocyclic P2-Ligands for HIV-1 Protease Inhibitors. *Org. Lett.* **2008**, *10*, 5135−5138.
(27) Nicolaou, K. C.; Baran, P. S.; Zhong, Y.-L.; Barluenga, S.; Hunt, K. W.; Kranich, R.; Vega, J. A. Iodine(V) Reagents in Organic Synthesis. Part 3. New Routes to Heterocyclic Compounds via o-Iodoxybenzoic Acid-Mediated Cyclizations: Generality, Scope, and Mechanism. *J. Am. Chem. Soc.* **2002**, *124*, 2233−2244.
(28) Ghosh, A. K.; Chapsal, B. D.; Baldridge, A.; Steffey, M. P.; Walters, D. E.; Koh, Y.; Amano, M.; Mitsuya, H. Design and Synthesis of Potent HIV-1 Protease Inhibitors Incorporating Hexahydrofuropyranol-Derived High Affinity P_2 Ligands: Structure − Activity Studies and Biological Evaluation. *J. Med. Chem.* **2011**, *54*, 622−634.
(29) Ghosh, A. K.; Rao, K. V.; Nyalapatla, P. R.; Osswald, H. L.; Martyr, C. D.; Aoki, M.; Hayashi, H.; Agniswamy, J.; Wang, Y.-F.; Bulut, H.; Das, D.; Weber, I. T.; Mitsuya, H. Design and Development of Highly Potent HIV-1 Protease Inhibitors with a Crown-like Oxotricyclic Core as the P2-Ligand to Combat Multidrug-Resistant HIV Variants. *J. Med. Chem.* **2017**, *60*, 4267−4278.
(30) Toth, M. V.; Marshall, G. R. A Simple, Continuous Fluorometric Assay for HIV Protease. *Int. J. Pept. Protein Res.* **1990**, *36*, 544−550.
(31) Koh, Y.; Amano, M.; Towata, T.; Danish, M.; Leshchenko-Yashchuk, S.; Das, D.; Nakayama, M.; Tojo, Y.; Ghosh, A. K.; Mitsuya, H. *In Vitro* Selection of Highly Darunavir-Resistant and Replication-Competent HIV-1 Variants by Using a Mixture of Clinical HIV-1 Isolates Resistant to Multiple Conventional Protease Inhibitors. *J. Virol.* **2010**, *84*, 11961−11969.
(32) Hughes, P. J.; Cretton-Scott, E.; Teague, A.; Wensel, T. M. Protease Inhibitors for Patients with HIV-1 Infection: A Comparitive Overview. *Pharm. Ther.* **2011**, *36*, 332−345.
(33) Aoki, M.; Danish, M. L.; Aoki-Ogata, H.; Amano, M.; Ide, K.; Das, D.; Koh, Y.; Mitsuya, H. Loss of the Protease Dimerization Inhibition Activity of Tipranavir (TPV) and Its Association with the Acquisition of Resistance to TPV by HIV-1. *J. Virol.* **2012**, *86*, 13384−13396.
(34) Amano, M.; Tojo, Y.; Salcedo-Gómez, P. M.; Campbell, J. R.; Das, D.; Aoki, M.; Xu, C.-X.; Rao, K. V.; Ghosh, A. K.; Mitsuya, H. GRL-0519, a Novel Oxatricyclic Ligand-Containing Nonpeptidic HIV-1 Protease Inhibitor (PI), Potently Suppresses Replication of a Wide Spectrum of Multi-PI-Resistant HIV-1 Variants *In Vitro*. *Antimicrob. Agents Chemother.* **2013**, *57*, 2036−2046.
(35) For details of X-ray studies, see Supporting Information.
(36) Mahalingam, B.; Louis, J. M.; Hung, J.; Harrison, R. W.; Weber, I. T. Structural Implications of Drug-Resistant Mutants of HIV-1 Protease: High-Resolution Crystal Structures of the Mutant Protease/Substrate Analogue Complexes. *Proteins: Struct., Funct., Genet.* **2001**, *43*, 455−464.
(37) Otwinowski, Z.; Minor, W. Processing of X-ray Diffraction Data Collected in Oscillation Mode. *Methods in Enzymology, 276: Macromolecular Crystallography, Part A*; Carter, C. W., Jr., Sweet, R. M., Eds.; Academic Press: New York, 1997; pp 307−326.
(38) McCoy, A. J.; Grosse-Kunstleve, R. W.; Adams, P. D.; Winn, M. D.; Storoni, L. C.; Read, R. J. Phaser Crystallographic Software. *J. Appl. Crystallogr.* **2007**, *40*, 658−674.
(39) Winn, M. D.; Ballard, C. C.; Cowtan, K. D.; Dodson, E. J.; Emsley, P.; Evans, P. R.; Keegan, R. M.; Krissinel, E. B.; Leslie, A. G. W.; McCoy, A.; McNicholas, S. J.; Murshudov, G. N.; Pannu, N. S.; Potterton, E. A.; Powell, H. R.; Read, R. J.; Vagin, A.; Wilson, K. S.

DOI: 10.1021/acs.jmedchem.8b01227
J. Med. Chem. 2018, 61, 9722−9737

Overview of the CCP4 Suite and Current Developments. *Acta Crystallogr., Sect. D: Biol. Crystallogr.* **2011**, *67*, 235−242.
(40) Collaborative Computational Project, Number 4.. The CCP4 Suite: Programs for Protein Crystallography. *Acta Crystallogr., Sect. D: Biol. Crystallogr.* **1994**, *50*, 760−763.
(41) Potterton, E.; Briggs, P.; Turkenburg, M.; Dodson, E. A Graphical User Interface to the CCP4 Program Suite. *Acta Crystallogr., Sect. D: Biol. Crystallogr.* **2003**, *59*, 1131−1137.
(42) Shen, C.-H.; Wang, Y.-F.; Kovalevsky, A. Y.; Harrison, R. W.; Weber, I. T. Amprenavir Complexes with HIV-1 Protease and its Drug-Resistant Mutants Altering Hydrophobic Clusters. *FEBS J.* **2010**, *277*, 3699−3714.
(43) Sheldrick, G. M. A Short History of SHELX. *Acta Crystallogr., Sect. A: Found. Crystallogr.* **2008**, *64*, 112−122.
(44) Sheldrick, G. M.; Schneider, T. R. SHELXL: High-Resolution Refinement. *Methods Enzymol.* **1997**, *277*, 319−343.
(45) Murshudov, G. N.; Vagin, A. A.; Dodson, E. J. Refinement of Macromolecular Structures by the Maximum-Likelihood Method. *Acta Crystallogr., Sect. D: Biol. Crystallogr.* **1997**, *53*, 240−255.
(46) Schuettelkopf, A. W.; van Aalten, D. M. F. PRODRG: a Tool for High-Throughput Crystallography of Protein−Ligand Complexes. *Acta Crystallogr., Sect. D: Biol. Crystallogr.* **2004**, *60*, 1355−1363.
(47) Emsley, P.; Lohkamp, B.; Scott, W. G.; Cowtan, K. Features and Development of Coot. *Acta Crystallogr., Sect. D: Biol. Crystallogr.* **2010**, *66*, 486−501.
(48) Emsley, P.; Cowtan, K. Coot: Model-Building Tools for Molecular Graphics. *Acta Crystallogr., Sect. D: Biol. Crystallogr.* **2004**, *60*, 2126−2132.
(49) Berman, H. M.; Westbrook, J.; Feng, Z.; Gilliland, G.; Bhat, T. N.; Weissig, H.; Shindyalov, I. N.; Bourne, P. E. The Protein Data Bank. *Nucleic Acids Res.* **2000**, *28*, 235−242.

DOI: 10.1021/acs.jmedchem.8b01227
J. Med. Chem. 2018, 61, 9722−9737

European Journal of Medicinal Chemistry 160 (2018) 171–182

Contents lists available at ScienceDirect

European Journal of Medicinal Chemistry

journal homepage: http://www.elsevier.com/locate/ejmech

Research paper

Design, synthesis, and X-ray studies of potent HIV-1 protease inhibitors incorporating aminothiochromane and aminotetrahydronaphthalene carboxamide derivatives as the P2 ligands

Arun K. Ghosh [a, *], Ravindra D. Jadhav [a], Hannah Simpson [a], Satish Kovela [a], Heather Osswald [a], Johnson Agniswamy [b], Yuan-Fang Wang [b], Shin-ichiro Hattori [c], Irene T. Weber [b], Hiroaki Mitsuya [c, d, e]

[a] Department of Chemistry and Department of Medicinal Chemistry, Purdue University, West Lafayette, IN, 47907, United States
[b] Department of Biology, Molecular Basis of Disease, Georgia State University, Atlanta, GA, 30303, United States
[c] Department of Refractory Viral Infections, National Center for Global Health & Medicine Research Institute, Tokyo, 162-8655, Japan
[d] Departments of Hematology and Infectious Diseases, Kumamoto University Graduate School of Medical and Pharmaceutical Sciences, Kumamoto, 860-8556, Japan
[e] Experimental Retrovirology Section, HIV and AIDS Malignancy Branch, National Cancer Institute, National Institutes of Health, Bethesda, MD, 20892, United States

ARTICLE INFO

Article history:
Received 25 June 2018
Received in revised form
13 September 2018
Accepted 14 September 2018
Available online 18 September 2018

Keywords:
HIV-1 protease inhibitors
P2 ligand
Drug resistance
Design and synthesis
X-ray crystal structure

ABSTRACT

We describe the design, synthesis, and biological evaluation of a series of novel HIV-1 protease inhibitors with carboxamide derivatives as the P2 ligands. We have specifically designed aminothiochromane and aminotetrahydronaphthalene-based carboxamide ligands to promote hydrogen bonding and van der Waals interactions in the active site of HIV-1 protease. Inhibitors **4e** and **4j** have shown potent enzyme inhibitory and antiviral activity. High resolution X-ray crystal structures of **4d-** and **4k-**bound HIV-1 protease revealed molecular insights into the ligand-binding site interactions.

1. Introduction

Design and development of HIV-1 protease inhibitors and their introduction in combination therapy represent a major innovation for the treatment of HIV-1 infection and AIDS [1,2]. These combination antiretroviral therapies (ART) significantly improve the life expectancy of HIV-1 infected patients [3,4]. The mortality rates for HIV/AIDS patients who are treated with ART, have become close to those of the general population [5,6]. However, the majority of approved protease inhibitors in ART have limitations due to rapid occurrence of resistant strains, high pill burdens and other side effects [7,8]. The last FDA approved protease inhibitor, darunavir (**1**, Fig. 1), has significantly improved properties [9,10]. Darunavir has been shown to maintain excellent potency against a broad-spectrum of highly multidrug-resistant HIV-1 variants [11,12]. Darunavir and related derivative TMC126 (**2**) were specifically designed to promote extensive hydrogen-bonding interactions with HIV-1 protease backbone atoms [13,14]. Indeed, the X-ray structure of darunavir-bound HIV-1 protease revealed these critical ligand-binding site interactions which are now further utilized in our molecular design [15,16]. The design of protease inhibitors (PIs) continues to be an important area of research. There are recent reports of novel PIs incorporating P2/P2′ ligands [17–20]. PIs were also designed with new P1 and P2′ ligands [21,22]. Recently, a new class of piperazine derived non-peptide inhibitors have been reported [23,24].

In our continuing studies towards the design and synthesis of

* Corresponding author.
E-mail address: akghosh@purdue.edu (A.K. Ghosh).

https://doi.org/10.1016/j.ejmech.2018.09.046
0223-5234/

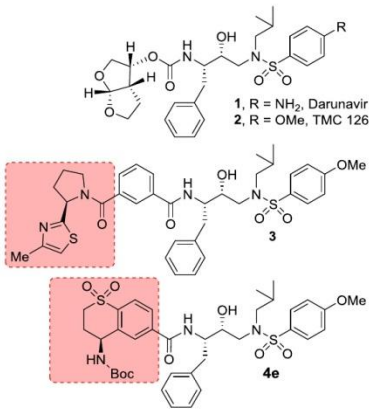

Fig. 1. Structure of protease inhibitors **1**–**3, 4e**.

new class of PIs, we have structure-based designed a range of exceptionally potent PIs with intriguing molecular features including, GRL-6579, GRL-02031, GRL-0519, and more recently GRL-0142 [14,25–28]. These inhibitors exhibit broad-spectrum antiviral activity against highly multidrug-resistant HIV-1 mutant strains and also show high genetic barrier to resistance [27,29]. In these inhibitors, we incorporated a variety of cyclic ether-derived templates as the P2-ligand attached to the hydroxyethylamine sulfonamide isostere with a urethane functionality [30]. The major design concept behind these PIs is to promote extensive hydrogen bonding with the HIV-1 protease active site backbone atoms like a molecular crab [13,14]. Recently, we and others reported a variety of protease inhibitors with benzoic acid amide derivatives as the P2-ligands [31–34]. These inhibitors were designed based upon the X-ray structures of FDA approved inhibitors darunavir and nelfinavir-bound to HIV-1 protease [15,16,35]. Our efforts led to very potent inhibitors with picomolar enzyme inhibitory activity and low nanomolar antiviral activity. The X-ray structural studies of a number of these inhibitors provided structural insights into the ligand and HIV-1 protease interactions, particularly in the active site of the enzyme [15,35]. We have now further explored these molecular insights and we report the design, synthesis, biological evaluation, and X-ray structural studies of a new series of protease inhibitors incorporating stereochemically defined amino-thiochromane and aminotetrahydronaphthalene carboxamide derivatives as the P2 ligands.

2. Results and discussion

2.1. Chemistry

Based upon the X-ray structures of darunavir-bound HIV-1 protease and nelfinavir-bound HIV-1 protease, we designed 4-aminothiochromane and 4-aminotetrahydronaphthalene carboxamide derivatives as the P2 ligand. The synthesis of 4-aminothiochromane-6-carboxylic acid in optically active form is shown in Scheme 1. Reaction of 4-mercaptobenzoic acid methyl ester **5** with 3-bromopropionic acid in the presence of pyridine at 80 °C for 1 h provided the corresponding alkylated product. The resulting acid was reacted with polyphosphoric acid (PPA) at 65 °C

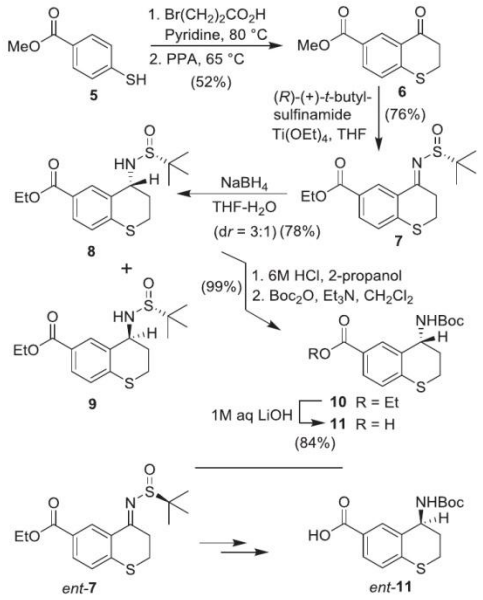

Scheme 1. 4-Aminothiochromane-6-carboxylic acid.

for 6 h to afford 4-oxothiochromane derivative **6** [36]. Reaction of ketone **6** with commercially available (*R*)-(+)-t-butyl sulfinamide in the presence of $Ti(OEt)_4$ in THF at 70 °C furnished sulfinyl imins **7** [37,38]. Imine derivative **7** was reduced with $NaBH_4$ in a mixture of THF and water at −50 °C to afford a mixture (3:1) of diastereomeric sulfonamides **8** and **9** in 78% combined yield. The diastereomers were separated by silica gel chromatography to provide *R*-sulfinyl inamide **8** as the major product. Sulfinamide **8** was treated with HCl (6 M solution in isopropanol) in methanol at 23 °C for 1 h to provide the corresponding amine hydrochloride salt. Reaction of this amine salt in CH_2Cl_2 with Boc_2O in the presence of triethylamine afforded Boc-protected amine derivative **10**. Saponification of the ethyl ester with aqueous LiOH provided carboxylic acid **11**. For the synthesis of the enantiomeric amine derivative ***ent*-11** (enantiomer of compound **11**), 4-oxochromane derivative **6** was reacted with commercially available (*S*)-(-)-t-butyl sulfinamide to obtain the corresponding imine which was reduced with $NaBH_4$ to provide mixture of diastereomers. Separation of diastereomers followed by reaction of the major isomers with 6 M HCl, and protection of amine as a *Boc*-derivative, and aqueous LiOH hydrolysis as described above resulted in enantiomeric acid ***ent*-11**.

The synthesis of optically active amino-hydroxytetrahydronaphthalene carboxylic acids is shown in Scheme 2. Commercially available bromotetralone **12** was reacted with (*R*)-(+)-t-butyl- sulfinamide in the presence of $Ti(OEt)_4$ in THF at 66 °C for 10 h to provide sulfinyl imine **13** in 87% yield. Reduction of **13** with $NaBH_4$ in a mixture of (98:2) THF and water at −50 °C to 23 °C for 3 h provided **14** and **15** in 2:1 ratio in 94% combined yield. The diastereomeric sulfinamides were separated by silica gel chromatography using 30% ethyl acetate in hexanes as the eluent. Reduction of **13** with L-selectride at 0 °C–23 °C for 3 h afforded only disatereomer **15** in 96% yield.

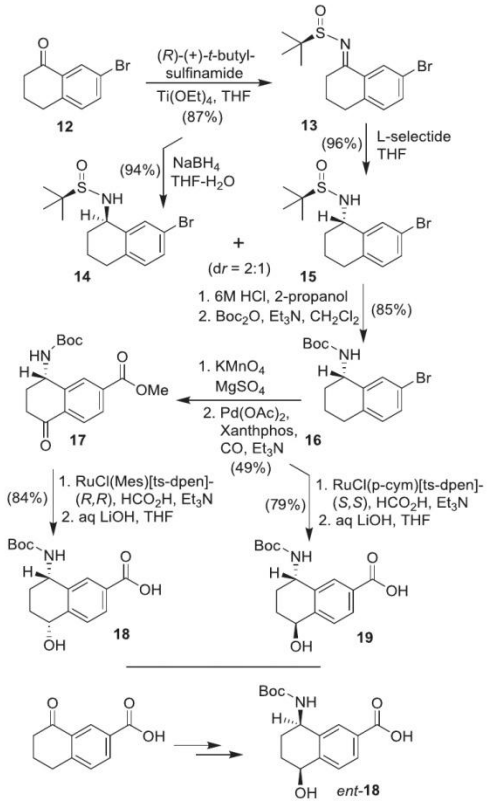

Scheme 2. Synthesis of 8-amino-5-hydroxy-tetrahydronaphthalene-2-carboxylic acid.

Treatment of sulfinamide **15** with HCl (6M solution in isopropanol) in methanol at 23 °C for 2.5 h afforded the corresponding amine which was reacted with Boc_2O in the presence of Et_3N in CH_2Cl_2 at 0 °C–23 °C for 12 h to provide optically active Boc-derivative **16** in 85% yield over two-steps. For introduction of the 5-hydroxyl group, Boc-amine derivative **16** was oxidized using $KMnO_4$ in the presence of $MgSO_4$ in acetone at 0 °C–23 °C for 8 h to furnish the corresponding bromoketone derivative in 61% yield. Treatment of the resulting bromoketone in methanol in the presence of catalytic amount $Pd(OAc)_2$ (2 mol%), xantphos (4 mol%) and excess of Et_3N under a CO-filled balloon at 70 °C for 3.5 h provided methyl ester derivative **17** in 80% yield [39]. Ketoester **17** was converted to the corresponding Boc-aminoalcohol derivative by a catalytic transfer hydrogenation reaction using the Noyori catalyst RuCl(*Mes*)[*R,R*-ts-dpen] in DMF in the presence of formic acid and Et_3N at 60 °C for 12 h to afford the corresponding alcohol as a single diastereomer in 94% yield [40,41]. Saponification of the resulting methyl ester with 1N aqueous LiOH in THF in the presence of a few drops of MeOH at 23 °C for 12 h afforded carboxylic acid **18** in 89% yield. Furthermore, reduction of ketoester **17** with RuCl(*p*-Cym)[*S,S*-ts-dpen] under the same reaction conditions mentioned above, provided the diastereomeric alcohol as a single diastereomer in 93% yield. Basic ester hydrolysis furnished ligand acid **19**. The synthesis of enantiomeric ligand carboxylic acid *ent*-**18** was carried out from commercially available methyl 8-oxo-5,6,7,8-tetrahydronaphthalene-2-carboxylate and (*S*)-*t*-butyl sulfinamide to provide imine which was reduced with $NaBH_4$ to obtain a mixture (2:1) of diastereomers. The major diastereomer was treated with 6 M HCl to provide the corresponding amine. Protection of the resulting amine as Boc-derivative. This was converted to carboxylic acid *ent*-**18** by following the same sequence of reactions as described above.

The synthesis of various inhibitors containing the (*R*)-hydroxyethylaminesulfonamide isostere and various thiochromane derivatives as the P2-ligand is shown in Scheme 3. Optically active thiochromane carboxylic acid **11** with the known aminoalcohol **20** [25,26] was reacted with EDC and HOBt in the presence of diisopropyl-ethylamine (DIPEA) in THF at 23 °C for 8 h to furnish inhibitor **4a** in 63% yield. Oxidation of thiochromane derivative **4a** with mCPBA in CH_2Cl_2 at 0 °C–23 °C for 6 h afforded sulfone derivative **4b** in 92% yield. Treatment of **4b** with trifluoroacetic acid (TFA) in CH_2Cl_2 at 23 °C for 3 h furnished the amine derivative **4c** in 83% yield. Enantiomeric ligand acid *ent*-**11** was converted to inhibitors **4d-f** as described above. The full structures of these inhibitors are shown in Table 1.

The synthesis of various aminotetrahydronapthalene derivatives as the P2 ligands is shown in Scheme 4. Coupling of acid containing Boc-aminoalcohol derivative **18** with amine **20** using EDCI and HOBt in the presence of DIPEA in THF to provide inhibitor **4g**. Removal of Boc-group by exposure to TFA in CH_2Cl_2 at 23 °C for 3 h provided inhibitor **4h** with aminoalcohol functionalities. Coupling of diastereomeric ligand acid **19** with amine **20** under similar coupling conditions afforded inhibitor **4i**. Removal of the Boc group with TFA provided inhibitor **4j**. The corresponding enantiomeric ligand *ent*-**19** was then converted to inhibitors **4k** and

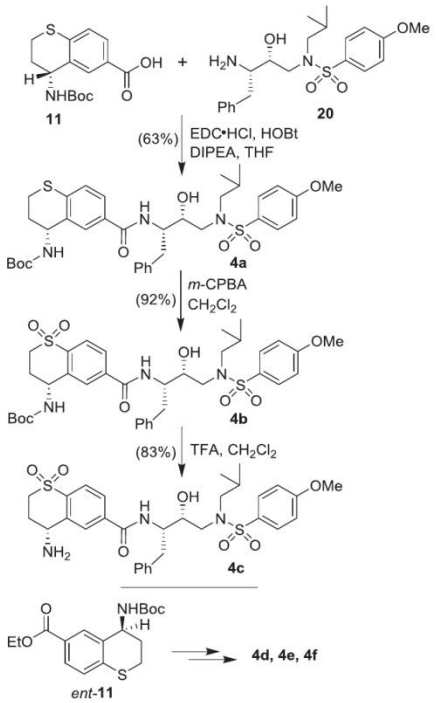

Scheme 3. Synthesis of protease inhibitors **4a-f**.

Table 1
Structures and potency of inhibitors **4a-f**.[a,b]

Entry	Inhibitor Structure	K_i (nM)	IC_{50} (nM)
1	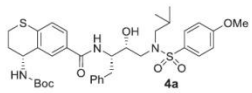 **4a**	26.7	>1000
2	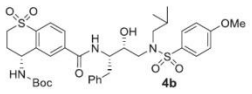 **4b**	0.10	476
3	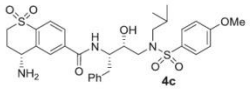 **4c**	18	>1000
4	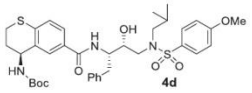 **4d**	0.38	>1000
5	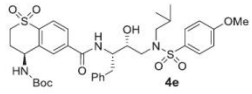 **4e**	0.008	47
6	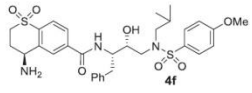 **4f**	15.8	>1000

[a] All antiviral assays were performed using MT-4 cells and HIV_{NL4-3} (subtype B). Values are the mean value of at least two experiments.
[b] The IC_{50} values of amprenavir (APV), saquinavir (SQV), indinavir (IDV), and darunavir (DRV) were 0.03, 0.015, 0.03, and 0.003 μM, respectively.

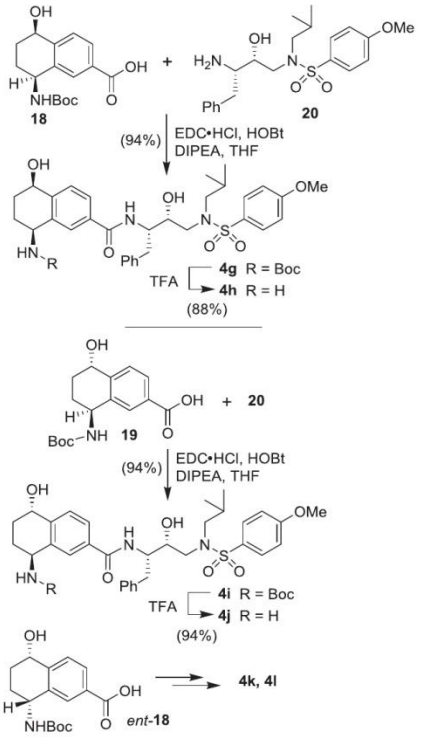

Scheme 4. Synthesis of protease inhibitors **4g-e**.

4l as described above. The full structures of these inhibitors are shown in Table 2.

2.2. HIV-1 protease inhibitory and antiviral activity

Our preliminary model of inhibitor **4a** that we created in the Nelfinavir-bound HIV-1 protease active site [35], indicated that the thiochroman heterocycle with (*S*)-Boc-amine functionality can interact with Asp29 and Asp30 backbone NHs in the S2 subsite, while the thiochroman moiety would fill the hydrophobic pocket. The results of HIV-1 protease inhibitory K_i and antiviral IC_{50} values are shown in Table 1. The assay protocol for HIV-1 protease activity is similar to the report of Toth and Marshall [42]. Antiviral activity was determined in MT-4 human T-lymphoid cells exposed to $HIV\text{-}1_{NL4\text{-}3}$ (subtype B) as described by us previously [11]. We chose to utilize a hydroxyethylaminesulfonamide isostere with 4-methoxybenzene sulfonamide as the P2′ ligand as in inhibitor **2**. As can be seen, inhibitor **4a** with 4-(*R*)-aminothiochroman carboxamide as the P2 ligand, showed a HIV-1 protease inhibitory K_i of 26.7 nM, but did not show any appreciable antiviral activity ($IC_{50} > 1$ μM). Since sulfone oxygens are known [43,44] to form strong bonding interactions, we oxidized the ring sulfur to its sulfone derivative. The resulting inhibitor **4b** showed improvement of potency, exhibiting an enzyme K_i of 0.1 nM. It also exhibited improvement of antiviral activity with an IC_{50} value of 476 nM (entry 2). The removal of the Boc-group provided 4-amine derivative **4c** which displayed significant loss of activity (entry 3). We then examined stereochemical effect and inhibitor **4d** with a 4-(*S*)-aminothiochroman carboxamide as the P2 ligand showed potent enzyme inhibitory activity with a K_i of 0.38 nM. However, inhibitor **4d** did not exhibit appreciable antiviral activity ($IC_{50} > 1$ μM). We oxidized the ring sulfur to its sulfone derivative **4e**. This led to significant improvement of enzyme inhibitory activity with a K_i of 8 pM (entry 5). Inhibitor **4e** also showed very good antiviral activity ($IC_{50} = 47$ nM). We presume that the improvement of activity is due to formation of a hydrogen bond through one of the sulfone oxygens of the P2 ligand. Removal of the Boc-group provided inhibitor **4f**, which showed substantial loss of enzyme inhibitory and antiviral activity similar to inhibitor **4c** (entries 3 and 6). In general, this series of inhibitors showed low cytotoxicity (CC_{50}) values in MT4 cells. The selectivity index of selected inhibitors are shown in Table 3.

Since both sulfone derivatives **4b** and **4e** are significantly more potent than the corresponding sulfides **4a** and **4d**, we speculated that one of the sulfone oxygens may have formed hydrogen bonding interactions with a residue in the active site. We, therefore, designed tetrahydronapthalene carboxamide derivatives with aminoalcohol substitution on the ring to mimic the interactions of Boc-amine and sulfone functionalities of inhibitor **4e**. The results are shown in Table 2. Inhibitor **4g** with a (*R*)-hydroxy derivative as the P2 ligand showed good enzyme activity, but antiviral activity was >1 μM. The corresponding amine derivative **4h** is significantly less potent (entry 2). The 4(*S*)-hydroxy derivative **4i** showed improvement of both enzyme inhibitory and antiviral activity with an IC_{50} value of 254 nM. The corresponding aminoalcohol derivative **4j** exhibited 1-fold improvement in enzyme activity, but

Table 2
Structures and potency of inhibitors **4g-l**.[a,b]

Entry	Inhibitor Structure	K_i (nM)	IC_{50} (nM)
1	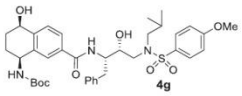 **4g**	0.3	>1000
2	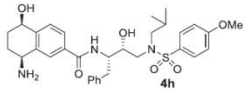 **4h**	17	>1000
3	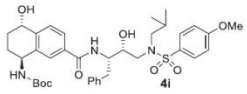 **4i**	0.14	254
4	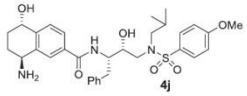 **4j**	0.06	232
5	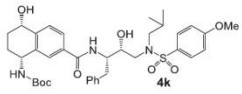 **4k**	1.63	>1000
6	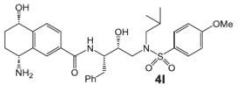 **4l**	1.10	>1000

[a] All antiviral assays were performed using MT-4 cells and HIV_{NL4-3} (subtype B).
[b] The IC_{50} values of amprenavir (APV), saquinavir (SQV), indinavir (IDV), and darunavir (DRV) were 0.03, 0.015, 0.03, and 0.003 μM, respectively.

Table 3
Selectivity Index for selected inhibitors.[a]

Inhibitor	CC_{50} (μM)	Selectivity Index[a]
4b	>100	>210
4e	>100	>2128
4i	33.3	131
4j	35.1	151

[a] Each selectivity index denotes a ratio of CC_{50} to IC_{50}.

showed comparable antiviral activity to its Boc-derivative **4i**. We also examined the stereochemical effect of the Boc derivative **4k** and the corresponding amine derivative **4l**. Both compounds were less potent.

2.3. X-ray crystal structure of inhibitor-bound HIV-1 protease

To obtain molecular insight into the ligand-binding site interactions, we set up co-crystallization experiments with several inhibitors and HIV-1 protease [45]. The X-ray structures were obtained for the wild-type HIV-1 protease co-crystallized independently with inhibitors **4d** (GRL-02815A) and **4k** (GRL-04315A) and were refined to a resolution of 1.20 Å and 1.14 Å, respectively. The protease dimer structures were very similar to the darunavir-bound HIV-1 protease complex [15] with a RMSD of 0.15 Å for 198 equivalent Cα atoms, and the largest disparity of around 0.4–0.6 Å. In both structures, the active site of the protease dimer was occupied by two alternate conformations of inhibitor related by 180° rotation with a relative occupancy of 0.60/0.40. The two inhibitor conformations show similar interactions with the protease, hence details are given for the major conformation. With the exception of the P2 ligand, both inhibitors retain the hydrogen bonds observed between darunavir and the main chain atoms of the protease. These inhibitors have distinctly different P2 ligands from the bis-tetrahydrofuran in darunavir. Inhibitor **4d** contains a thiochroman heterocycle with (*S*)-Boc-amine functionality as the P2 ligand and a stereoview of the active site interactions is shown in Fig. 2. Inhibitor **4k**, on the other hand, contains a tetrahydronaphthalene carboxamide with (*R*)-Boc-amine and (*S*)-hydroxyl functionalities as the P2 ligand and a stereoview of the active site interactions is shown in Fig. 3.

In inhibitor **4d**-bound HIV-1 protease structure, the bulky sulfur atom in the thiochroman group provides hydrophobic interactions with the side chains of Asp29, Asp30 and Ile47. The amide of the carbamate group forms a hydrogen bond of 2.6 Å length with the carbonyl oxygen atom of Gly48 in the flap, and carbonyl oxygen forms a hydrogen bond of 3.4 Å with NH_2 moiety of guanidinium side chain of Arg8'. As can be seen from the X-ray structure of **4d**, the significant improvement of enzyme inhibitory and antiviral activity of the corresponding sulfone derivative **4e** could be due to formation of hydrogen bonding interactions of the sulfone oxygens with the backbone NH's of Asp29 and Asp30 located in the S2 subsite. The *t*-butyl group forms van der Waals interactions with the hydrophobic side chains of Pro81, Val82 and Phe53. In the inhibitor **4k**-HIV-1 protease complex, the hydroxyl oxygen on the cyclohexane ring is in an equivalent location to the methoxy oxygen of the P2′ ligand and forms similar hydrogen bonds with the main chain amides of Asp29 and Asp30 with bond lengths of 3.5 Å and 3.1 Å, respectively, and a 2.8 Å-long hydrogen bond with the carboxylate oxygen of the Asp30 side chain (not shown in Fig. 3). The different chiral orientation relative to inhibitor **4d** shifts the carbamate away from the flap residue Gly48. The carbamate amide and carbonyl oxygen can only form hydrogen bonds via one or two water intermediates to the amide atom of Asp29 and main chain oxygen and amide of Gly49, respectively. The terminal *t*-butyl group embeds between the side chains of Arg8′, Pro81 and Val82, forming a C-H...π interaction with the guanidinium group of Arg8′ and van der Waals interactions with Pro81 and Val82. These differences in the P2 group may contribute to the inhibitor potency against HIV-1 protease.

3. Conclusion

In summary, we have reported the structure-based design and synthesis of a series of HIV-1 protease inhibitors incorporating stereochemically defined amino-thiochroman and amino-tetrahydronaphthalene carboxamide derivatives as the P2 ligands. We have investigated various stereoisomers in order to promote effective hydrogen bonding interactions with backbone atoms in the S2 subsite. These functionalized ligands were synthesized stereoselectively in optically active form by reduction of chiral sulfinamide derivatives. Also, Noyori transfer hydrogenation using chiral ruthenium catalyst provided selective reduction of the 8-amino-5-tetralone derivatives to the corresponding 5-hydroxynaphthalene derivatives. Amide derivatives of these ligands on a hydroxyethylamine sulfonamide isostere provided potent inhibitors. Inhibitors **4e** and **4j** exhibited very potent enzyme inhibitory activity in the picomolar range. These inhibitors have also shown very good antiviral activity. To obtain molecular insights into the ligand-binding site interactions, we determined high resolution X-ray crystal structures of related inhibitors **4d** and **4k**-bound HIV-1 protease. The structures show key interactions of

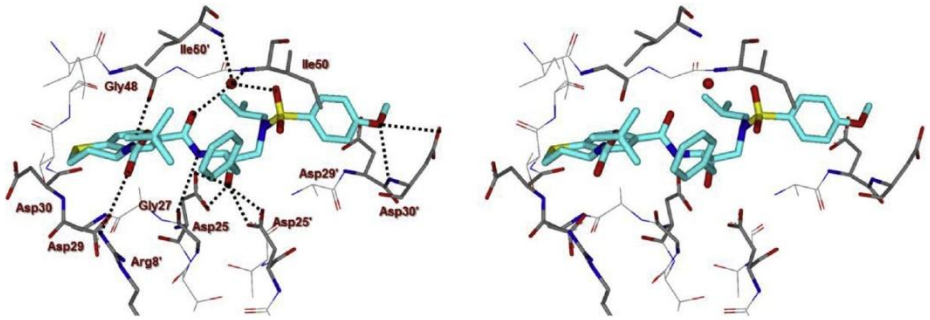

Fig. 2. Stereoview of the X-ray structure of inhibitor **4d** (turquoise)-bound HIV-1 protease (PDB code: 6DV0). All strong active site hydrogen bonding interactions of inhibitor **4d** with HIV-1 protease are shown as dotted lines.

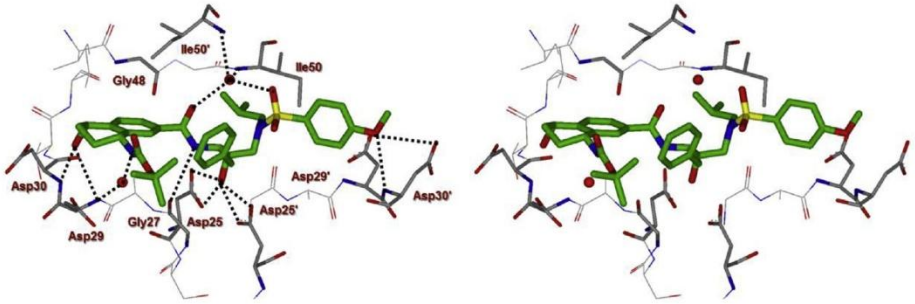

Fig. 3. Stereoview of the X-ray structure of inhibitor **4k** (green)-bound HIV-1 protease (PDB code: 6DV4). All strong active site hydrogen bonding interactions of inhibitor **4k** with HIV-1 protease are shown as dotted lines. (For interpretation of the references to colour in this figure legend, the reader is referred to the Web version of this article.)

amino-thiochroman and amino-tetrahydronaphthalene ligands in the S2 subsite. Amine functionality of inhibitor **4k** formed strong hydrogen bonds with the Asp30 backbone NH. This may explain the high enzyme inhibitory activity of these inhibitors. Further design and ligand optimization using X-ray structural insights are currently underway in our laboratories.

4. Experimental section

4.1. General experimental conditions

All moisture-sensitive reactions were carried out in oven-dried glassware under an argon atmosphere unless otherwise stated. Anhydrous solvents were obtained as follows: Diethyl ether and tetrahydrofuran were distilled from sodium metal/benzophenone under argon. Toluene and dichloromethane were distilled from calcium hydride under argon. All other solvents were reagent grade. Column chromatography was performed using Silicycle SiliaFlash F60 230–400 mesh silica gel. Thin-layer chromatography was carried out using EMD Millipore TLC silica gel 60 F_{254} plates. ^{1}H NMR and ^{13}C NMR spectra were recorded on a Varian INOVA300, Bruker ARX400, Bruker DRX500, or Bruker AV-III-500-HD. Low-resolution mass spectra were collected on a Waters 600 LCMS or by the Purdue University Campus-Wide Mass Spectrometry Center. High-resolution mass spectra were collected by the Purdue University Campus-Wide Mass Spectrometry Center. HPLC analysis and purification was done an on Agilent 1100 series instrument using a YMC Pack ODS-A column of 4.6 mm ID for analysis and either 10 mm ID or 20 mm ID for purification. The purity of all test compounds was determined by HPLC analysis to be $\geq$ 95% pure.

4.2. Synthesis of inhibitors

4.2.1. Methyl 4-oxothiochromane-6-carboxylate (6)

A mixture of 3-bromopropionic acid (0.91 g, 5.95 mmol) and *p*-(carbomethoxy)thio-phenol (1 g, 5.95 mmol) was placed in a round-bottom flask. The flask was heated slowly with the aid of an oil bath. When the mixture melted, giving a homogeneous solution, pyridine (0.96 mL, 11.90 mmol) was added and the reaction was allowed to proceed under an atmosphere of nitrogen at 80 °C for 1 h. After this period, the product was dissolved in ethyl acetate and extracted repeatedly with aqueous bicarbonate. Acidification of the bicarbonate layer afforded 3-((4-(methoxycarbonyl)phenyl)thio) propanoic acid (982 mg, 69%) as an amorphous crystals. LRMS-ESI (*m/z*): 241 $[M+H]^+$.

To the above 3-((4-(methoxycarbonyl)phenyl)-thio)propanoic acid (200 mg, 0.832 mmol), 1.5 g of polyphosphoric acid was added and the resulting mixture was stirred at 65 °C for 6 h. After this period, the reaction mixture was allowed to cool to room temperature and quenched by the addition of cold water and extracted with ethyl acetate (3×25 mL). The organic layer was washed with saturated aq. $NaHCO_3$ solution, water, saturated aq. NaCl solution, and dried over anhydrous Na_2SO_4. The solvent was removed under reduced pressure to give **6** (141 mg, 76%) as a yellow solid. $R_f = 0.4$ (30% EtOAc/hexanes). LRMS-ESI (*m/z*): 223 $[M+H]^+$.

*4.2.2. Ethyl (S,E)-4-((tert-butylsulfinyl)imino)thiochromane-6-carboxylate **(7)***

To a stirred solution of **6** (435 mg, 1.92 mmol) in THF (18 mL) was added $Ti(OEt)_4$ (1.0 mL, 4.805 mmol). The solution was stirred at ambient temperature for 5 min before addition of (*R*)-(+)-2-methyl-2-propanesulfinamide (291 mg, 2.4 mmol). Then reaction mixture refluxed for 12 h. The reaction mixture was cooled to room temperature and concentrated in *vacuo*, diluted with EtOAc (35 mL). Saturated $NaHCO_3$ (17 mL) was added under vigourous stirring and the slurry was filtered through a pad of celite. The organic phase was separated, dried over Na_2SO_4 and concentrated in *vacuo*. The crude residue was purified by silica gel column chromatography (30% EtOAc/hexanes) to furnish **7** (500 mg, 76%). R_f = 0.3 (30% EtOAc/hexanes); ^{1}H NMR (400 MHz, $CDCl_3$) δ 8.81 (d, *J* = 2.0 Hz, 1H), 7.91 (dt, *J* = 8.3, 2.0 Hz, 1H), 7.28 (s, 1H), 4.36 (q, *J* = 7.1 Hz, 2H), 3.77–3.61 (m, 1H), 3.50 (ddd, *J* = 16.9, 6.7, 5.5 Hz, 1H), 3.14 (dd, *J* = 7.1, 5.6 Hz, 2H), 1.38 (t, *J* = 7.3 Hz, 3H), 1.35 (s, 9H); LRMS-ESI *(m/z)*: 340 $[M+H]^+$.

*4.2.3. Ethyl (R)-4-(((R)-tert-butylsulfinyl)amino)thiochromane-6-carboxylate (8) and Ethyl (S)-4-(((R)-tert-butylsulfinyl)amino) thiochromane-6-carboxylate **(9)***

To a srirred solution of **7** (400 mg, 1.22 mmol) in THF/H_2O (4 mL, 98:2) was added $NaBH_4$ (139 mg, 3.68 mmol) at −50 °C. The resulting solution was warmed to room temperature over 3 h. The solvent was then removed in *vacuo* and the resulting residue was triturated with CH_2Cl_2. The solution was dried over anhydrous Na_2SO_4, filtered, and concentrated in *vacuo* to furnish a crude product. The crude product was purified by flash column chromatography over silica gel (30% ethyl acetate/hexanes) to furnish **8** (250 mg, 60%) and **9** (76 mg, 18%).

*4.2.4. Compound **8***

R_f = 0.4 (50% EtOAc/hexanes); $[\alpha]_D^{23} = -14.4$ (*c* 0.83, $CHCl_3$); ^{1}H NMR (400 MHz, $CDCl_3$) δ 8.05 (d, *J* = 1.9 Hz, 1H), 7.77 (dd, *J* = 8.3, 2.0 Hz, 1H), 7.16 (d, *J* = 8.3 Hz, 1H), 4.56 (dt, *J* = 10.2, 5.5 Hz, 1H), 4.34 (q, *J* = 7.1 Hz, 2H), 3.49 (d, *J* = 9.2 Hz, 1H), 3.21–3.06 (m, 2H), 2.43 (qd, *J* = 6.2, 5.4, 2.7 Hz, 2H), 1.37 (t, *J* = 7.1 Hz, 3H), 1.27 (s, 9H); LRMS-ESI *(m/z)*: 342 $[M+H]^+$.

*4.2.5. Compound **9***

R_f = 0.3 (50% EtOAc/hexanes); $[\alpha]_D^{23} = +32.2$ (c 0.75, $CHCl_3$); ^{1}H NMR (400 MHz, $CDCl_3$) δ 7.95 (d, *J* = 1.9 Hz, 1H), 7.81 (dd, *J* = 8.3, 1.9 Hz, 1H), 7.19 (d, *J* = 8.3 Hz, 1H), 4.69 (d, *J* = 4.7 Hz, 1H), 4.35 (q, *J* = 7.1 Hz, 2H), 3.34 (td, *J* = 12.7, 3.0 Hz, 1H), 3.17 (s, 1H), 2.85 (dt, *J* = 12.4, 4.0 Hz, 1H), 2.58 (dq, *J* = 14.5, 3.9 Hz, 1H), 2.07–1.93 (m, 2H), 1.38 (t, *J* = 7.1 Hz, 3H), 1.23 (s, 9H). LRMS-ESI *(m/z)*: 342 $[M+H]^+$.

*4.2.6. Ethyl (R)-4-((tert-butoxycarbonyl)amino)thiochromane-6-carboxylate **(10)***

To a solution of **8** (350 mg, 1.02 mmol) in MeOH (10 mL) was added 6 M HCl in Isopropanol (4 mL) at 23 °C under argon atmosphere. The reaction mixture was stirred at 23 °C for 1 h. After this period, the solvent was removed under reduced pressure to afford the desired amine salt. Thus obtained amine salt and Et_3N (0.46 mL, 3.20 mmol) were dissolved in CH_2Cl_2 (5 mL), cooled to 0 °C and di-*tert*-butyldicarbonate (349 mg, 1.60 mmol) was added and allowed to warm to 23 °C. After stirring for 12 h, the reaction was diluted with CH_2Cl_2 and washed with water, brine solution, dried over Na_2SO_4 and concentrated under reduced pressure. The crude product was purified by silica gel column chromatography (10% EtOAc/hexanes) to afford **10** (347 mg, 99% over two steps). R_f = 0.3 (10% EtOAc/hexanes); $[\alpha]_D^{23} = +36.5$ (*c* 1.0, $CHCl_3$); ^{1}H NMR (400 MHz, $CDCl_3$) δ 7.96 (d, *J* = 1.9 Hz, 1H), 7.77 (dd, *J* = 8.3, 2.0 Hz, 1H), 7.15 (d, *J* = 8.3 Hz, 1H), 4.89 (s, 1H), 4.75 (s, 1H), 4.35 (qd, *J* = 7.1, 1.4 Hz, 2H), 3.13 (td, *J* = 11.8, 10.6, 3.1 Hz, 1H), 3.07–2.98 (m, 1H), 2.39 (s, 1H), 2.09 (td, *J* = 10.5, 3.5 Hz, 1H), 1.49 (s, 10H), 1.38 (t, *J* = 7.1 Hz, 3H). LRMS-ESI *(m/z)*: 355 $[M+NH_4]^+$.

*4.2.7. (R)-4-((tert-Butoxycarbonyl)amino)thiochromane-6-carboxylic acid **(11)***

A solution of **10** (364 mg, 1.08 mmol) in THF: MeOH (6 mL, 2:1) was treated with 1N LiOH solution (1.62 mL, 1.62 mmol). The resulting mixture was stirred for 12 h, and then concentrated under reduced pressure. The residue was dissolved in water and acidified with citric acid then extracted with ethyl acetate (3×20 mL). The combined ethyl acetate layer was dried over Na_2SO_4, filtered, and concentrated to give carboxylic acid **11** (280 mg, 84%). R_f = 0.5 (10% MeOH/CH_2Cl_2); $[\alpha]_D^{23} = +33.2$ (*c* 0.8, $CHCl_3$); ^{1}H NMR (400 MHz, $CDCl_3$) δ 8.03 (s, 1H), 7.82 (dd, *J* = 8.3, 1.9 Hz, 1H), 7.19 (d, *J* = 8.3 Hz, 1H), 4.91 (s, 1H), 4.78 (s, 1H), 3.14 (t, *J* = 11.5 Hz, 1H), 3.04 (ddd, *J* = 12.7, 6.5, 3.6 Hz, 1H), 2.39 (s, 1H), 2.18–2.06 (m, 1H), 1.49 (s, 9H). LRMS-ESI *(m/z)*: 332 $[M+Na]^+$.

*4.2.8. Ethyl (S)-4-((tert-butoxycarbonyl)amino)thiochromane-6-carboxylate **(ent-10)***

Compound *ent*-**10** (50 mg, 68%) was synthesized from *ent*-**8** (75 mg, 0.21 mmol) by following the procedure outlined for compound **10**. R_f = 0.2 (10% EtOAc/hexanes); $[\alpha]_D^{23} = -37.5$ (*c* 1.0, $CHCl_3$); ^{1}H NMR (400 MHz, $CDCl_3$) δ 7.96 (d, *J* = 1.9 Hz, 1H), 7.77 (dd, *J* = 8.3, 2.0 Hz, 1H), 7.15 (d, *J* = 8.3 Hz, 1H), 4.89 (s, 1H), 4.75 (s, 1H), 4.35 (q, *J* = 7.1, 1.4 Hz, 2H), 3.12 (td, *J* = 11.8, 10.6, 3.2 Hz, 1H), 3.06–2.97 (m, 1H), 2.38 (s, 1H), 2.18–2.03 (m, 1H), 1.48 (s, 9H), 1.38 (t, *J* = 7.1 Hz, 3H). LRMS-ESI *(m/z)*: 360 $[M+Na]^+$.

*4.2.9. (S)-4-((tert-Butoxycarbonyl)amino)thiochromane-6-carboxylic acid **(ent-11)***

Compound *ent*-**10** (120 mg, 0.37 mmol) was treated with 1N LiOH (0.55 mL, 0.55 mmol) by following the procedure outlined for compound **11** to give compound *ent*-**11** (75 mg, 66%). R_f = 0.5 (10% MeOH/CH_2Cl_2); $[\alpha]_D^{23} = -36.6$ (*c* 0.12, $CHCl_3$); ^{1}H NMR (400 MHz, $CDCl_3$) δ 8.03 (s, 1H), 7.81 (dd, *J* = 8.3, 1.9 Hz, 1H), 7.19 (d, *J* = 8.3 Hz, 1H), 4.91 (s, 1H), 4.77 (s, 1H), 3.12 (d, *J* = 11.2 Hz, 1H), 3.07–2.98 (m, 1H), 2.39 (s, 1H), 2.18–2.06 (m, 1H), 1.49 (s, 9H); LRMS-ESI *(m/z)*: 332 $[M+Na]^+$.

*4.2.10. tert-Butyl ((R)-6-(((2S,3R)-3-hydroxy-4-((N-isobutyl-4-methoxyphenyl)sulfonamido)-1-phenylbutan-2-yl)carbamoyl) thiochroman-4-yl)carbamate **(4a)***

To a solution of **11** (85 mg, 0.27 mmol) and HOBt (56 mg, 0.41 mmol) in anhydrous THF (5 mL) at 0 °C was added EDC.HCl (58 mg, 0.30 mmol) and stirred at 23 °C for 1 h. An isostere amine **20** (112 mg, 0.27 mmol) and DIPEA (0.1 mL, 0.54 mmol) in THF (3 mL) was added and resulting mixture was stirred for 8 h at 23 °C. The reaction mixture was extracted with ethyl acetate and successively washed with 5% citric acid, sat $NaHCO_3$, brine solution, dried over Na_2SO_4 and concentrated. The crude product was purified by column chromatography over silica gel (30% EtOAc/hexanes) to afford inhibitor **4a** (120 mg, 63%). R_f = 0.3 (30% EtOAc/hexanes); $[\alpha]_D^{23} = +22.0$ (*c* 0.85, $CHCl_3$); ^{1}H NMR (400 MHz, $CDCl_3$) δ 7.66 (t, *J* = 6.7 Hz, 2H), 7.57 (d, *J* = 5.4 Hz, 1H), 7.29 (m, 4H), 7.21 (m, 1H), 7.10–7.05 (m, 1H), 6.93 (t, *J* = 7.5 Hz, 2H), 6.48 (d, *J* = 8.6 Hz, 1H), 4.79 (m, 2H), 4.40–4.17 (m, 2H), 3.98 (s, 1H), 3.85 (s, 3H), 3.24–2.90 (m, 6H), 2.89–2.73 (m, 2H), 2.35 (d, *J* = 9.5 Hz, 1H), 2.04 (d, *J* = 12.3 Hz, 1H), 1.91–1.67 (m, 2H), 1.51–1.34 (m, 9H), 0.85 (t, *J* = 6.2 Hz, 6H); ^{13}C NMR (100 MHz, $CDCl_3$) δ 167.5, 163.1, 154.9, 139.0, 138.0, 133.1, 129.9, 129.5, 129.0, 128.8, 126.9, 126.8, 126.1, 114.5, 80.1, 73.0, 58.9, 55.7, 54.9, 53.6, 48.1, 35.1, 28.5, 28.2, 27.3, 23.0, 20.2, 20.1; HRMS-ESI (*m/z*): $[M+H]^+$ calcd for $C_{36}H_{48}N_3O_7S_2$, 698.2928; found 698.2925.

*4.2.11. tert-Butyl ((R)-6-(((2S,3R)-3-hydroxy-4-((N-isobutyl-4-methoxyphenyl)sulfonamido)-1-phenylbutan-2-yl)carbamoyl)-1,1-dioxidothiochroman-4-yl)carbamate **(4b)***

To a solution of inhibitor **4a** (50 mg, 0.07 mmol) in dichloromethane (1 mL), 3- chloroperbenzoic acid (26 mg, 0.15 mmol) was added slowly at 0 °C under argon atmosphere. The reaction was stirred for 6 h at 23 °C. The reaction mixture was diluted with dichloromethane and washed with sat. Na_2CO_3 solution and brine. The organic layers were dried over Na_2SO_4, filtered and concentrated in *vacuo*. The crude residue was purified by flash column chromatography over silica gel to afford inhibitor **4b** (48 mg, 92%). R_f = 0.3 (60% EtOAc/hexanes); $[\alpha]_D^{23} = -11.0$ (*c* 0.2, $CHCl_3$); ^{1}H NMR (400 MHz, $CDCl_3$) δ 7.78–7.70 (m, 2H), 7.70–7.62 (m, 2H), 7.54 (d, *J* = 8.1 Hz, 1H), 7.29–7.26 (m, 4H), 7.20 (m, 1H), 7.00–6.91 (m, 3H), 5.20 (d, *J* = 8.5 Hz, 1H), 4.98 (s, 1H), 4.42 (s, 1H), 4.06 (dt, *J* = 12.0, 4.8 Hz, 1H), 3.86 (s, 3H), 3.50 (t, *J* = 11.5 Hz, 1H), 3.37 (t, *J* = 10.9 Hz, 1H), 3.11 (dt, *J* = 21.0, 7.4 Hz, 4H), 2.87 (dt, *J* = 10.1, 5.2 Hz, 2H), 2.70–2.47 (m, 2H), 1.87 (m, 1H), 1.47 (s, 9H), 0.86 (dd, *J* = 6.7, 3.5 Hz, 6H); ^{13}C NMR (100 MHz, $CDCl_3$) δ 166.26, 163.24, 155.10, 138.40, 137.88, 137.05, 130.25, 129.84, 129.54, 129.42, 128.79, 128.27, 127.44, 126.86, 124.18, 114.54, 80.64, 72.86, 60.54, 58.92, 55.79, 54.92, 53.42, 48.15, 47.72, 35.03, 28.46, 27.84, 27.33, 21.19, 20.24, 20.13, 14.32; HRMS-ESI (*m/z*): $[M+H]^+$ calcd for $C_{36}H_{48}N_3O_9S_2$, 730.2827; found 730.2824.

*4.2.12. (S)-4-Amino-N-((2S,3R)-3-hydroxy-4-((N-isobutyl-4-methoxyphenyl)sulfonamido)-1-phenylbutan-2-yl)thiochromane-6-carboxamide 1,1-dioxide **(4c)***

To a stirred solution of inhibitor **4b** (25 mg, 0.034 mmol) in dichloromethane (1.0 mL) was added TFA (0.1 mL) at 0 °C under argon atmosphere. The reaction mixture was warmed to 23 °C and stirred at for 3 h. Upon completion, solvent was removed under reduced pressure. The residue was extracted with dichloromethane and washed with sat. NaHCO3 solution, brine, dried over Na_2SO_4 and concentrated in *vacuo*. The crude residue was purified by column chromatography over silica gel to give inhibitor **4c** (18 mg, 83%) as an amorphous solid. R_f = 0.2 (5% MeOH/CH_2Cl_2); $[\alpha]_D^{23} = -13.6$ (*c* 0.6, $CHCl_3$); ^{1}H NMR (400 MHz, $CDCl_3$) δ 7.82–7.74 (m, 2H), 7.69–7.63 (m, 2H), 7.56 (dd, *J* = 8.2, 1.7 Hz, 1H), 7.29–7.23 (m, 4H), 7.19 (m, 1H), 6.95 (dd, *J* = 8.4, 5.4 Hz, 3H), 4.40 (tt, *J* = 9.4, 5.0 Hz, 1H), 4.15 (dd, *J* = 7.1, 4.3 Hz, 1H), 4.05 (dt, *J* = 8.3, 4.3 Hz, 1H), 3.85 (s, 3H), 3.67 (ddd, *J* = 13.4, 9.8, 3.0 Hz, 1H), 3.37–3.24 (m, 1H), 3.22–2.99 (m, 4H), 2.87 (d, *J* = 7.5 Hz, 2H), 2.65 (dt, *J* = 20.3, 6.8 Hz, 1H), 2.38–2.26 (m, 2H), 1.87 (m, 1H), 0.85 (d, *J* = 6.6 Hz, 6H); ^{13}C NMR (100 MHz, $CDCl_3$) δ 166.71, 163.13, 142.56, 138.11, 137.26, 130.04, 129.54, 129.47, 128.68, 126.71, 114.46, 72.90, 60.51, 58.73, 55.75, 54.95, 53.48, 48.12, 44.11, 34.91, 28.56, 28.47, 27.28, 22.25, 21.73, 20.24, 20.13; HRMS-ESI (*m/z*): $[M+H]^+$ calcd for $C_{31}H_{40}N_3O_7S_2$, 630.2302; found 630.2298.

*4.2.13. tert-Butyl ((S)-6-(((2S,3R)-3-hydroxy-4-((N-isobutyl-4-methoxyphenyl)sulfonamido)-1-phenylbutan-2-yl)carbamoyl) thiochroman-4-yl)**carbamate (4d)***

Compound *ent*-**11** (65 mg, 0.21 mmol) was treated with isostere amine **20** (85 mg, 0.21 mmol) by following the procedure outlined for inhibitor **4a** to give inhibitor **4d** (117 mg, 80%) as an amorphous solid. R_f = 0.2 (30% EtOAc/hexanes); $[\alpha]_D^{23} = -6.5$ (*c* 0.49, $CHCl_3$); ^{1}H NMR (400 MHz, $CDCl_3$) δ 7.66 (d, *J* = 8.5 Hz, 2H), 7.54 (s, 1H), 7.27 (d, *J* = 4.6 Hz, 3H), 7.24 (s, 1H), 7.19 (m, 1H), 7.06 (d, *J* = 8.3 Hz, 1H), 6.92 (d, *J* = 8.6 Hz, 2H), 6.43 (d, *J* = 8.4 Hz, 1H), 4.78 (s, 2H), 4.32 (m, 1H), 3.96 (s, 1H), 3.84 (s, 3H), 3.22–2.91 (m, 6H), 2.85 (d, *J* = 7.5 Hz, 1H), 2.33 (s, 1H), 2.03 (d, *J* = 9.7 Hz, 1H), 1.83 (m, 1H), 1.72 (m, 1H), 1.45 (s, 9H), 0.84 (t, *J* = 5.7 Hz, 6H); ^{13}C NMR (100 MHz, $CDCl_3$) δ 167.80, 163.44, 155.25, 139.27, 138.28, 133.42, 130.32, 129.88, 129.10, 127.21, 127.13, 126.50, 114.78, 80.51, 73.21, 59.24, 56.08, 55.04, 53.96, 48.40, 35.43, 28.87, 28.53, 27.67, 23.27, 20.56, 20.44; HRMS-ESI (*m/z*): $[M+H]^+$ calcd for $C_{36}H_{48}N_3O_7S_2$, 698.2928; found 698.2920.

*4.2.14. tert-Butyl ((S)-6-(((2S,3R)-3-hydroxy-4-((N-isobutyl-4-methoxyphenyl)sulfonamido)-1-phenylbutan-2-yl)carbamoyl)-1,1-dioxidothiochroman-4-yl)carbamate **(4e)***

Inhibitor **4d** (25 mg, 0.035 mmol) was treated with *m*CPBA (13 mg, 0.075 mmol) by following the procedure outlined for compound **4b** to give compound inhibitor **4e** (26 mg, 96%) as an amorphous solid. R_f = 0.2 (60% EtOAc/hexanes); $[\alpha]_D^{23} = -8.0$ (*c* 0.1, $CHCl_3$); ^{1}H NMR (400 MHz, $CDCl_3$) δ 7.70 (s, 1H), 7.67 (d, *J* = 8.8 Hz, 2H), 7.58 (dd, *J* = 15.8, 8.3 Hz, 1H), 7.44–7.36 (m, 1H), 7.30–7.26 (m, 4H), 7.19 (m, 1H), 7.07 (d, *J* = 8.6 Hz, 1H), 6.94 (d, *J* = 8.8 Hz, 2H), 5.34 (s, 1H), 4.97 (s, 1H), 4.40 (dq, *J* = 9.6, 4.8 Hz, 1H), 4.06 (dt, *J* = 8.3, 4.6 Hz, 1H), 3.85 (s, 3H), 3.53 (ddd, *J* = 12.5, 8.8, 3.2 Hz, 1H), 3.36 (dd, *J* = 13.3, 8.0 Hz, 1H), 3.18–3.01 (m, 4H), 2.89 (dd, *J* = 7.7, 2.1 Hz, 2H), 2.70–2.49 (m, 3H), 1.88 (m, 1H), 1.49 (d, *J* = 5.0 Hz, 9H), 0.86 (d, *J* = 6.6 Hz, 6H); ^{13}C NMR (100 MHz, $CDCl_3$) δ 166.24, 163.21, 155.40, 141.03, 138.30, 137.96, 137.02, 133.68, 129.95, 129.56, 129.50, 128.75, 128.29, 127.45, 126.90, 124.00, 114.52, 80.96, 77.43 72.86, 58.84, 55.79, 54.85, 53.49, 48.04, 47.58, 34.94, 28.51, 27.32, 20.26, 20.11; HRMS-ESI (*m/z*): $[M+H]^+$ calcd for $C_{36}H_{48}N_3O_9S_2$, 730.2827; found 730.2822.

*4.2.15. (S)-4-Amino-N-((2S,3R)-3-hydroxy-4-((N-isobutyl-4-methoxyphenyl)sulfonamido)-1-phenylbutan-2-yl)thiochromane-6-carboxamide 1,1-**dioxide (4f)***

Inhibitor **4f** (20 mg, 0.027 mmol) was treated with TFA (0.1 mL) by following the procedure outlined for inbitor **4c** to give inhibitor **4f** (16 mg, 93%) as an amorphous solid; R_f = 0.1 (5% MeOH/CH_2Cl_2); $[\alpha]_D^{23} = +13.7$ (*c* 0.35, $CHCl_3$); ^{1}H NMR (400 MHz, $CDCl_3$) δ 7.80 (d, *J* = 8.1 Hz, 2H), 7.71–7.63 (m, 2H), 7.56 (d, *J* = 8.2 Hz, 1H), 7.27 (d, *J* = 4.4 Hz, 4H), 7.20 (m, 1H), 6.99–6.91 (m, 2H), 6.88 (d, *J* = 8.5 Hz, 1H), 4.46–4.33 (m, 1H), 4.16 (s, 1H), 4.05 (dt, *J* = 8.4, 4.2 Hz, 1H), 3.86 (s, 3H), 3.68 (ddd, *J* = 13.5, 9.6, 3.0 Hz, 1H), 3.38–3.24 (m, 1H), 3.13 (m, 4H), 2.88 (d, *J* = 7.5 Hz, 2H), 2.65 (t, *J* = 12.8 Hz, 1H), 2.41–2.28 (m, 1H), 1.87 (m, 2H), 0.86 (d, *J* = 6.6 Hz, 6H); ^{13}C NMR (100 MHz, $CDCl_3$) δ 166.45, 163.24, 140.49, 138.15, 137.92, 129.84, 129.56, 129.49, 128.79, 128.09, 126.93, 126.85, 124.19, 114.54, 77.41, 72.81, 58.89, 55.80, 54.84, 53.51, 48.12, 47.53, 35.00, 30.58, 27.31, 20.24, 20.15; HRMS-ESI (*m/z*): $[M+H]^+$ calcd for $C_{31}H_{40}N_3O_7S_2$, 630.2302; found 630.2294.

*4.2.16. (R,E)-N-(7-Bromo-3,4-dihydronaphthalen-1(2H)-ylidene)-2-methylpropane-2-sulfinamide **(13)***

A mixture of 5-bromo-1-tetralone **12** (1.5 g, 6.66 mmol), (*R*)-(+)-2-methyl-2 propanesulfinamide (1.21 g, 9.99 mmol) and titanium (IV) ethoxide (3.01 g, 13.32 mmol) were dissolved in anhydrous THF (15 mL) and stirred at 66 °C for 10 h under argon atmosphere. The reaction mixture was cooled to 23 °C and ethyl acetate and aq sodium bicarbonate was added. The mixture was filtered through a pad of celite and the aqueous layer was extracted with ethyl acetate. The combined organic phase were dried over Na_2SO_4 and concentrated under reduced pressure. The crude residue was purified by column chromatography over silica gel (5% EtOAc/hexanes) to afford **13** (1.9 g, 87%). R_f = 0.5 (40% EtOAc/hexanes); ^{1}H NMR (400 MHz, $CDCl_3$) δ 8.24 (d, *J* = 2.2 Hz, 1H), 7.48 (dd, *J* = 8.2, 2.2 Hz, 1H), 7.07 (d, *J* = 8.2 Hz, 1H), 3.27 (ddd, *J* = 17.6, 9.3, 4.8 Hz, 1H), 3.05 (ddd, *J* = 17.6, 7.5, 4.5 Hz, 1H), 2.81 (t, *J* = 6.2 Hz, 2H), 1.99–1.87 (m, 2H), 1.33 (d, *J* = 2.3 Hz, 9H).

*4.2.17. (R)-N-((R)-7-Bromo-1,2,3,4-tetrahydronaphthalen-1-yl)-2-methylpropane-2-sulfinamide **(14)***

Compound **13** (175 mg, 0.53 mmol) was dissolved in THF/H_2O (2 mL, 98:2) and cooled to −50 °C. To the mixture was then added

$NaBH_4$ (61 mg, 1.59 mmol), and the resulting solution was warmed to 23 °C over a period of 3 h. The solvent was then removed in *vacuo*, and the resulting residue was triturated with dichloromethane, dried over Na_2SO_4, filtered, and concentrated under reduced pressure.The crude product was purified by column chromatography over silica gel (30% EtOAc/hexanes) to afford **14** (110 mg, 63%) and **15** (55 mg, 31%). R_f = 0.4 (30% EtOAc/hexanes); ^{1}H NMR (400 MHz, $CDCl_3$) δ 7.60 (d, *J* = 2.1 Hz, 1H), 7.30 (dd, *J* = 8.2, 2.1 Hz, 1H), 6.98 (d, *J* = 8.2 Hz, 1H), 4.52 (q, *J* = 4.2 Hz, 1H), 3.21 (d, *J* = 3.7 Hz, 1H), 2.76 (dt, *J* = 17.0, 5.2 Hz, 1H), 2.70–2.57 (m, 1H), 2.08–1.97 (m, 1H), 1.96–1.81 (m, 2H), 1.79–1.70 (m, 1H), 1.22 (s, 9H).

*4.2.18. (R)-N-((S)-7-Bromo-1,2,3,4-tetrahydronaphthalen-1-yl)-2-methylpropane-2-sulfinamide **(15)***

Compound **13** (275 mg, 0.83 mmol) was dissolved in anhydrous THF (3 mL) and cooled to 0 °C. To this solution was then added L-Selectride (2.5 mL, 1.0 M in THF, 2.51 mmol) and the resulting solution was allowed to warm to 23 °C over period of 3 h. The solution was then concentrated under *vacuo* to furnish crude product. The crude residue was purified by column chromatography over silica gel (30% EtOAc/hexanes) to give **15** (265 mg, 96%). R_f = 0.3 (30% EtOAc/hexanes); ^{1}H NMR (400 MHz, $CDCl_3$) δ 7.54 (d, *J* = 2.1 Hz, 1H), 7.28 (dd, *J* = 8.1, 2.1 Hz, 1H), 6.96 (d, *J* = 8.2 Hz, 1H), 4.42 (q, *J* = 8.0, 7.4 Hz, 1H), 3.36 (d, *J* = 10.1 Hz, 1H), 2.80–2.56 (m, 2H), 2.40–2.24 (m, 1H), 1.96–1.73 (m, 3H), 1.28 (s, 9H).

*4.2.19. tert-Butyl (S)-(7-bromo-1,2,3,4-tetrahydronaphthalen-1-yl) carbamate **(16)***

A solution of **15** (1.2 g, 3.63 mmol) in MeOH (20 mL) was treated with 6 N HCl in isopropanol (5 mL). After 2.5 h, solvent was removed in *vacuo*, and the residue was co-evaporated with ethyl acetate. The residue obtained was dried under high vacuum to provide (*S*)-7-bromo-1,2,3,4-tetrahydronaphthalen-1-amine hydrochloride (0.94 g).

To a stirred solution of above amine hydrochloride (0.94 g, 3.6 mmol) in CH_2Cl_2 (30 mL) was consecutively added triethylamine (1.5 mL, 10.89 mmol) and di-*tert*-butyl-dicarbonate (1.17 g, 5.44 mmol) at 0 °C. The reaction mixture was stirred at 23 °C for 12 h. The reaction mixture was then diluted with CH_2Cl_2 and washed with water and brine solution, dried over Na_2SO_4 and concentrated. The crude product was purified by column chromatography over silica gel (20% EtOAc/hexanes) to give **16** (1.0 g, 85% over two steps) as an amorphous solid. R_f = 0.7 (20% EtOAc/hexanes); $[\alpha]_D^{23} = -9.32$ (*c* 1.0, $CHCl_3$); ^{1}H NMR (400 MHz, $CDCl_3$) δ 7.54–7.39 (m, 1H), 7.33–7.09 (m, 1H), 6.94 (d, *J* = 8.1 Hz, 1H), 4.78 (q, *J* = 10.6, 8.8 Hz, 2H), 2.88–2.50 (m, 2H), 2.02 (td, *J* = 10.9, 9.9, 4.9 Hz, 1H), 1.78 (ddp, *J* = 23.3, 11.4, 4.2 Hz, 3H), 1.49 (s, 9H); ^{13}C NMR (100 MHz, $CDCl_3$) δ 155.55, 139.66, 136.43, 131.38, 130.84, 130.31, 119.73, 79.77, 48.67, 30.45, 28.89, 28.57, 20.05.

*4.2.20. Methyl (S)-8-((tert-butoxycarbonyl)amino)-5-oxo-5,6,7,8-tetrahydronaphthalene-2-carboxylate **(17)***

Boc-amine derivative **16** (950 mg, 2.91 mmol) was dissolved in acetone (55 mL) and cooled to 0 °C. $MgSO_4$ (837 mg, 6.99 mmol) and water (23 mL) were added to the solution. $KMnO_4$ (2.38 g, 15.15 mmol) was added to this mixture in small portions over 1 h and stirred for 8 h at 23 °C. The solid was filtered off and the filtrate was treated with a saturated solution of sodium sulfite. The resulting mixture was filtered and the acetone was removed from the filtrate in *vacuo*. The remaining aqueous residue was extracted with dichloromethane. The combined organic phases were washed with water, brine, dried over anhydrous Na_2SO_4 and concentrated under reduced pressure. The crude residue was purified by column chromatography over silica gel (20% EtOAc/hexanes) to afford bromo ketone derivative (600 mg, 61%) as an amorphous solid. ^{1}H NMR (400 MHz, $CDCl_3$) δ 7.88 (d, *J* = 8.4 Hz, 1H), 7.62 (s, 1H), 7.53 (dd, *J* = 8.4, 2.0 Hz, 1H), 5.03 (s, 1H), 4.82 (d, *J* = 9.0 Hz, 1H), 2.81 (dt, *J* = 17.4, 5.3 Hz, 1H), 2.66 (ddd, *J* = 17.1, 11.5, 4.7 Hz, 1H), 2.49–2.32 (m, 1H), 2.18–1.99 (m, 2H), 1.51 (s, 9H).

A solution of above bromo ketone (600 mg, 1.76 mmol) in triethylamine (5.3 mL) and methanol (1 mL) was degassed with argon and palladium (II) acetate (8.0 mg, 0.035 mmol) and Xantphos (41 mg, 0.070 mmol) were added. The solution was degassed again and CO gas was bubbled through the solution for approximately 2 min. The reaction flask was fitted with a condenser and a CO balloon and the reaction mixture was heated at 70 °C for 3.5 h. The reaction mixture was cooled to 23 °C, diluted with EtOAc and filtered through a pad of celite. The filtrate was evaporated and the residue was purified by silica gel column chromatography (20% EtOAc/hexanes) to afford titled compound **17** (450 mg, 80%). R_f = 0.3 (20% EtOAc/hexanes); $[\alpha]_D^{23} = -10.7$ (*c* 1.28, $CHCl_3$); ^{1}H NMR (400 MHz, $CDCl_3$) δ 8.15 (s, 1H), 8.09 (d, *J* = 8.1 Hz, 1H), 8.03 (d, *J* = 8.1 Hz, 1H), 5.09 (s, 1H), 4.83 (s, 1H), 3.95 (s, 3H), 2.87 (dt, *J* = 17.4, 5.0 Hz, 1H), 2.71 (ddd, *J* = 16.9, 11.4, 4.7 Hz, 1H), 2.50–2.32 (m, 1H), 2.22–2.03 (m, 1H), 1.52 (s, 9H); LRMS-ESI *(m/z)*: 342 $[M+Na]^+$.

*4.2.21. (5R,8S)-8-((tert-Butoxycarbonyl)amino)-5-hydroxy-5,6,7,8-tetrahydronaphthalene-2-carboxylic acid **(18)***

Argon was bubbled through a solution of **17** (150 mg, 0.46 mmol) and RuCl[(*R,R*)-TsDPEN](mesitylene) (9.0 mg, 0.014 mmol) in dry DMF (2 mL) for 10 min. A premixed combination of formic acid (35 μL, 0.938 mmol) and Et_3N (135 μL, 0.938 mmol) was added and the mixture stirred at 60 °C for 12 h. The mixture was cooled to 23 °C and diluted with CH_2Cl_2 and successively washed with water, brine and dried over anhydrous Na_2SO_4. The solvent was removed in *vacuo* to give the crude product. The crude residue was purified by column chromatography over silica gel (30% EtOAc/hexanes) to afford the desired alcohol (142 mg, 94%) as an amorphous white solid. R_f = 0.3 (30% EtOAc/hexanes); ^{1}H NMR (400 MHz, $CDCl_3$) δ 8.04 (s, 1H), 7.92 (d, *J* = 7.9 Hz, 1H), 7.51 (d, *J* = 8.0 Hz, 1H), 4.85 (s, 1H), 4.77 (m, 2H), 3.91 (s, 3H), 2.09–1.93 (m, 5H), 1.49 (s, 9H); LRMS-ESI *(m/z)*: 643 $[2M+H]^+$.

To a solution of above methyl ester (80 mg, 0.248 mmol) in THF: MeOH (1.5 mL, (2:1) was added 1N LiOH (0.37 mL, 0.373 mmol) at 23 °C. The reaction mixture was stirred at 23 °C for 12 h. Solvent was removed under reduced pressure, acidified with aq. saturated citric acid to pH 3–4 and the product was extracted with ethyl acetate, dried over Na_2SO_4 and concentrated to afford **18** (68 mg, 89%) as an amorphous solid. R_f = 0.3 (10% MeOH/CH_2Cl_2); $[\alpha]_D^{23} = -38.6$ (*c* 0.29, CH_3OH); ^{1}H NMR (400 MHz, $CDCl_3$) δ 7.98 (s, 1H), 7.89 (dd, *J* = 8.0, 1.9 Hz, 1H), 7.52 (d, *J* = 8.1 Hz, 1H), 7.08 (d, *J* = 9.1 Hz, 1H), 4.71 (s, 2H), 2.05–1.89 (m, 4H), 1.50 (d, *J* = 4.7 Hz, 9H); LRMS-ESI *(m/z)*: 615 $[2M+H]^+$.

*4.2.22. (5S,8S)-8-((tert-Butoxycarbonyl)amino)-5-hydroxy-5,6,7,8-tetrahydronaphthalene-2-carboxylic acid **(19)***

Argon was bubbled through a solution of **17** (150 mg, 0.469 mmol) and RuCl(p-cymene)[(*S,S*)-Ts-DPEN] (9.0 mg, 0.014 mmol) in dry DMF (1.5 mL) for 10 min. A premixed combination of formic acid (35 μL, 0.938 mmol) and Et_3N (135 μL, 0.938 mmol) was added and the mixture was stirred at 60 °C for 12 h. The mixture was cooled to 23 °C and diluted with CH_2Cl_2 and successively washed with water, brine and dried over anhydrous Na_2SO_4. The solvent was removed in *vacuo* to give the crude product. The crude product was purified by column chromatography over silica gel (30% EtOAc/hexanes) to give the desired alcohol (140 mg, 93%) as an amorphous white solid. R_f = 0.3 (30% EtOAc/hexanes); ^{1}H NMR (400 MHz, $CDCl_3$) δ 8.01 (s, 1H), 7.94–7.88 (m, 1H), 7.57 (d, *J* = 8.1 Hz, 1H), 4.88 (s, 1H), 4.83–4.59 (m, 2H), 3.90

(s, 3H), 2.38–2.16 (m, 2H), 2.07–1.94 (m, 1H), 1.89–1.66 (m, 2H), 1.49 (s, 9H); LRMS-ESI *(m/z)*: 643 $[2M+H]^+$.

Above methyl ester (75 mg, 0.233 mmol) was treated with 1N LiOH (0.46 mL, 0.466 mmol) by following the procedure outlined for **18** to give the titled compound **19** (60 mg, 85%) as an amorphous solid; $R_f = 0.3$ (10% MeOH/CH_2Cl_2); $[\alpha]_D^{23} = -6.0$ (*c* 0.5, CH_3OH); ^1H NMR (400 MHz, $CDCl_3$) δ 7.94 (s, 1H), 7.85 (dd, *J* = 8.2, 1.8 Hz, 1H), 7.56 (d, *J* = 8.1 Hz, 1H), 4.79–4.67 (m, 2H), 2.24–2.11 (m, 3H), 1.74 (td, *J* = 12.1, 8.8 Hz, 2H), 1.46 (s, 9H); LRMS-ESI *(m/z)*: 615 $[2M+H]^+$.

4.2.23. (5S,8R)-8-((tert-Butoxycarbonyl)amino)-5-hydroxy-5,6,7,8-tetrahydronaphthalene-2-carboxylic acid (ent-18)

Argon was bubbled through a solution of ethyl (*R*)-8-((*tert*-butoxycarbonyl)amino)-5-oxo-5,6,7,8-tetrahydronaphthalene-2-carboxylate (100 mg, 0.299 mmol) and RuCl(p-cymene)[(*S,S*)-Ts-DPEN] (6.0 mg, 0.0089 mmol) in dry DMF (1.0 mL) for 10 min. A premixed combination of formic acid (22 μL, 0.598 mmol) and Et_3N (83 μL, 0.598 mmol) was added and the mixture stirred at 60 °C for 12 h. The mixture was cooled to room temperature and diluted with CH_2Cl_2 and successively washed with water, brine and dried over anhydrous Na_2SO_4. The solvent was removed in *vacuo* to give the crude product. The crude product was purified by column chromatography over silica gel (30% EtOAc/hexanes) to give desired alcohol (87 mg, 86%) as an amorphous white solid. $R_f = 0.3$ (30% EtOAc/hexanes); ^1H NMR (400 MHz, $CDCl_3$) δ 8.03 (s, 1H), 7.94 (d, *J* = 7.9 Hz, 1H), 7.57 (d, *J* = 8.1 Hz, 1H), 4.90 (s, 1H), 4.84–4.67 (m, 2H), 4.37 (q, *J* = 7.1 Hz, 2H), 2.46–2.12 (m, 2H), 1.90–1.67 (m, 3H), 1.50 (s, 9H), 1.39 (t, *J* = 7.2 Hz, 3H). LRMS-ESI *(m/z)*: 353 $[M+NH_4]^+$.

Above ethyl ester (47 mg, 0.11 mmol) was treated with 1N LiOH (0.2 mL, 0.21 mmol) by following the procedure outlined for **18** to give the titled compound *ent*-**18** (40 mg, 89%) as an amorphous solid. $R_f = 0.3$ (10% MeOH/CH_2Cl_2); LRMS-ESI *(m/z)*: 615 $[2M+H]^+$.

4.2.24. tert-Butyl ((1S,4R)-4-hydroxy-7-(((2S,3R)-3-hydroxy-4-((N-isobutyl-4-methoxyphenyl)sulfonamido)-1-phenylbutan-2-yl)carbamoyl)-1,2,3,4-tetrahydronaphthalen-1-yl)carbamate (4g)

Carboxylic acid **18** (40 mg, 0.130 mmol) was treated with isostere amine **20** (68 mg, 0.130 mmol) by following the procedure outlined for inhibitor **4a** to give inhibitor **4g** (85 mg, 94%) as an amorphous white solid. $R_f = 0.5$ (80% EtOAc/hexanes); $[\alpha]_D^{23} = -3.2$ (*c* 0.62, $CHCl_3$); ^1H NMR (400 MHz, $CDCl_3$) δ 7.65 (d, *J* = 8.5 Hz, 2H), 7.57 (d, *J* = 17.2 Hz, 1H), 7.40 (m, 1H), 7.31–7.18 (m, 4H), 7.18–7.07 (m, 2H), 6.952 (d, *J* = 8.8 Hz, 2H), 6.86 (d, *J* = 8.5 Hz, 1H), 5.35–5.24 (m, 1H), 4.66 (m, 1H), 4.56 (m, 1H), 4.35 (m, 2H), 4.10 (q, *J* = 7.1 Hz, 1H), 3.97 (s, 1H), 3.83 (s, 3H), 3.27–2.93 (m, 5H), 2.85 (d, *J* = 7.6 Hz, 2H), 1.89 (m, 2H), 1.46 (s, 9H), 0.84 (m, 6H); ^{13}C NMR (100 MHz, $CDCl_3$) δ 167.75, 163.09, 155.79, 142.78, 138.07, 137.74, 133.70, 129.94, 129.52, 128.86, 128.65, 126.90, 126.65, 126.10, 114.44, 79.83, 73.00, 67.38, 58.70, 55.73, 54.57, 53.53, 48.80, 35.08, 29.79, 29.20, 28.56, 27.24, 25.96, 20.21, 20.06; HRMS-ESI (*m/z*): $[M+Na]^+$ calcd for $C_{37}H_{49}N_3O_8SNa$, 718.3133; found 718.3124.

4.2.25. (5R,8S)-8-Amino-5-hydroxy-N-((2S,3R)-3-hydroxy-4-((N-isobutyl-4-methoxyphenyl)sulfonamido)-1-phenylbutan-2-yl)-5,6,7,8-tetrahydronaphthalene-2-carboxamide (4h)

To a solution of **4g** (80 mg, 0.114 mmol) in CH_2Cl_2 (1 mL) was added TFA (0.3 mL) and resulting solution was stirred at 23 °C for 3 h. Then reaction mixture concentrated under *vacuo* and extracted with ethyl acetate and washed with sat. $NaHCO_3$, water, brine, dried over Na_2SO_4, filtered and evaporated under reduced pressure. The crude residue was purified by column chromatography over silica gel (10% MeOH/NH_3 in CH_2Cl_2) to give inhibitor **4h** (60 mg, 88%) as an amorphous white solid. $R_f = 0.15$ (10% MeOH/CH_2Cl_2); $[\alpha]_D^{23} = +12.2$ (*c* 0.63, $CHCl_3$); ^1H NMR (400 MHz, $CDCl_3$) δ 7.66 (dd, *J* = 9.1, 2.8 Hz, 2H), 7.58–7.53 (m, 1H), 7.36–7.29 (m, 1H), 7.29–7.24 (m, 3H), 7.21 (t, *J* = 7.4 Hz, 2H), 7.17–7.07 (m, 2H), 6.91 (dd, *J* = 9.5, 2.6 Hz, 2H), 4.54 (d, *J* = 5.3 Hz, 1H), 4.38 (dp, *J* = 9.2, 4.8 Hz, 2H), 4.03 (dt, *J* = 8.4, 4.2 Hz, 2H), 3.86 (d, *J* = 6.0 Hz, 1H), 3.82 (s, 3H), 3.23 (dd, *J* = 15.1, 4.0 Hz, 1H), 3.15–2.96 (m, 4H), 2.88 (td, *J* = 13.9, 6.9 Hz, 3H), 1.97–1.61 (m, 6H), 0.83 (t, *J* = 5.6 Hz, 6H); ^{13}C NMR (100 MHz, $CDCl_3$) δ 168.11, 163.05, 143.02, 140.41, 138.27, 133.62, 130.06, 129.51, 128.60, 128.46, 126.94, 126.56, 125.91, 114.41, 77.48, 72.92, 67.88, 58.60, 55.71, 54.61, 53.42, 49.18, 34.97, 28.64, 28.50, 27.18, 20.20, 20.11; HRMS-ESI (*m/z*): $[M+H]^+$ calcd for $C_{32}H_{42}N_3O_6S$, 596.2789; found 596.2785.

4.2.26. tert-Butyl ((1S,4S)-4-hydroxy-7-(((2S,3R)-3-hydroxy-4-((N-isobutyl-4-methoxyphenyl)sulfonamido)-1-phenylbutan-2-yl)carbamoyl)-1,2,3,4-tetrahydronaphthalen-1-yl)carbamate (4i)

Carboxylic acid **19** (40 mg, 0.13 mmol) was treated with isostere amine **20** (68 mg, 0.13 mmol) by following the procedure outlined for inhibitor **4a** to give inhibitor **4i** (85 mg, 94%) as an amorphous solid. $R_f = 0.5$ (80% EtOAc/hexanes); $[\alpha]_D^{23} = +15.0$ (*c* 0.22, $CHCl_3$); ^1H NMR (400 MHz, $CDCl_3$) δ 7.64 (d, *J* = 8.9 Hz, 2H), 7.53 (s, 1H), 7.46–7.43 (m, 1H), 7.41 (d, *J* = 8.1 Hz, 1H), 7.25–7.20 (m, 4H), 7.15 (td, *J* = 6.2, 2.9 Hz, 2H), 6.90 (d, *J* = 8.9 Hz, 2H), 5.03 (d, *J* = 8.9 Hz, 1H), 4.68 (dd, *J* = 16.6, 10.3 Hz, 2H), 4.28 (d, *J* = 20.1 Hz, 1H), 3.96 (dt, *J* = 8.6, 4.3 Hz, 1H), 3.82 (s, 3H), 3.22–2.92 (m, 4H), 2.84 (h, *J* = 7.6, 6.8 Hz, 2H), 2.22 (m, 6H), 1.86 (dt, *J* = 13.6, 6.7 Hz, 1H), 1.77–1.55 (m, 2H), 1.46 (s, 9H), 0.83 (d, *J* = 6.6 Hz, 6H); ^{13}C NMR (100 MHz, $CDCl_3$) δ 168.13, 163.05, 156.10, 143.27, 138.26, 137.31, 133.64, 129.93, 129.49, 128.58, 128.46, 126.57, 114.40, 80.15, 72.86, 67.63, 58.61, 55.70, 54.74, 53.42, 49.80, 49.58, 49.37, 49.03, 34.94, 30.22, 28.49, 27.73, 27.18, 20.11, 20.03; HRMS-ESI (*m/z*): $[M+H]^+$ calcd for $C_{37}H_{50}F_2N_3O_8S$, 696.3313; found 696.3305.

4.2.27. (5S,8S)-8-Amino-5-hydroxy-N-((2S,3R)-3-hydroxy-4-((N-isobutyl-4-methoxyphnyl)sulfonamido)-1-phenylbutan-2-yl)-5,6,7,8-tetrahydronaphthalene-2-carboxamide (4j)

Inhibitor **4i** (50 mg, 0.071 mmol) was treated with TFA (0.2 mL) by following the procedure outlined for inbitor **4h** to give compound inhibitor **4j** (40 mg, 94%) as an amorphous solid. $R_f = 0.15$ (10% MeOH/CH_2Cl_2); $[\alpha]_D^{23} = +35.6$ (*c* 0.8, $CHCl_3$); ^1H NMR (400 MHz, $CDCl_3$) δ 7.67 (d, *J* = 8.8 Hz, 2H), 7.62 (s, 1H), 7.38–7.31 (m, 2H), 7.30–7.24 (m, 4H), 7.22–7.14 (m, 1H), 6.98–6.86 (m, 2H), 6.83 (d, *J* = 8.3 Hz, 1H), 4.68 (dd, *J* = 7.6, 4.3 Hz, 1H), 4.37 (dd, *J* = 9.4, 4.9 Hz, 1H), 4.04 (m, 1H), 3.84 (s, 3H), 3.23 (dd, *J* = 15.0, 4.2 Hz, 1H), 3.16–2.97 (m, 4H), 2.87 (m 3H), 2.26–2.10 (m, 2H), 1.87 (dq, *J* = 13.8, 6.8 Hz, 2H), 1.69 (q, *J* = 9.6, 8.2 Hz, 2H), 1.52 (q, *J* = 11.3, 9.9 Hz, 1H), 0.84 (dd, *J* = 6.6, 2.5 Hz, 6H); ^{13}C NMR (100 MHz, $CDCl_3$) δ 168.10, 163.09, 142.51, 140.87, 138.30, 133.51, 130.08, 129.55, 128.68, 128.33, 126.68, 125.50, 114.44, 72.92, 68.03, 58.72, 55.74, 54.77, 53.50, 49.34, 35.00, 31.05, 30.20, 29.89, 27.22, 20.22, 20.14; HRMS-ESI (*m/z*): $[M+H]^+$ calcd for $C_{32}H_{42}N_3O_6S$, 596.2789; found 596.2784.

4.2.28. tert-Butyl ((1R,4S)-4-hydroxy-7-(((2S,3R)-3-hydroxy-4-((N-isobutyl-4-methoxyphenyl)sulfonamido)-1-phenylbutan-2-yl)carbamoyl)-1,2,3,4-tetrahydronaphthalen-1-yl)carbamate (4k)

Carboxylic acid *ent*-**18** (41 mg, 0.10 mmol) was treated with isostere amine **20** (52 mg, 0.10 mmol) by following the procedure outlined for compound **4a** to give compound inhibitor **4k** (75 mg, 94%) as an amorphous solid. $R_f = 0.5$ (80% EtOAc/hexanes); $[\alpha]_D^{23} = +5.9$ (*c* 0.57, $CHCl_3$); ^1H NMR (400 MHz, $CDCl_3$) δ 7.65 (dd, *J* = 8.5, 6.4 Hz, 3H), 7.34 (d, *J* = 7.7 Hz, 1H), 7.28 (m, 4H), 7.23–7.15 (m, 1H), 6.99–6.87 (m, 2H), 6.70 (d, *J* = 8.7 Hz, 1H), 5.06 (d, *J* = 8.9 Hz, 1H), 4.71 (m, 1H), 4.64 (m, 1H), 4.47–4.27 (m, 2H), 3.99 (s, 1H), 3.85 (s, 3H), 3.21–2.99 (m, 4H), 2.85 (d, *J* = 7.5 Hz, 2H), 2.62 (s, 1H), 1.97 (m, 3H), 1.86 (m, 3H), 1.47 (s, 9H), 0.85 (dd, *J* = 6.6, 3.3 Hz, 6H); ^{13}C NMR (100 MHz, $CDCl_3$) δ 167.89, 163.15, 155.72, 142.88, 138.06, 137.88, 133.87, 129.95, 129.55, 128.96, 128.76, 127.01, 126.75,

126.08, 114.47, 79.93, 73.04, 67.50, 58.87, 55.76, 54.87, 53.62, 48.89, 35.02, 29.83, 29.33, 28.57, 27.34, 26.07, 20.24, 20.13; HRMS-ESI (*m/z*): $[M+H]^+$ calcd for $C_{37}H_{50}N_3O_8S$, 696.3313; found 696.3310.

*4.2.29. (5S,8R)-8-Amino-5-hydroxy-N-((2S,3R)-3-hydroxy-4-((N-isobutyl-4-methoxyphenyl)sulfonamido)-1-phenylbutan-2-yl)-5,6,7,8-tetrahydronaphthalene-2-carboxamide (**4l**)*

Inhibitor **4k** (30 mg, 0.043 mmol) was treated with TFA (0.1 mL) by following the procedure outlined for inbitor **4h** to give inhibitor **4l** (23 mg, 89%) as an amorphous solid. $R_f = 0.15$ (10% MeOH/CH_2Cl_2); $[\alpha]_D^{23} = -9.5$ (*c* 0.2, $CHCl_3$); ^1H NMR (400 MHz, $CDCl_3$) δ 7.73–7.59 (m, 3H), 7.48–7.40 (m, 1H), 7.38–7.25 (m, 4H), 7.19 (t, *J* = 7.0 Hz, 1H), 6.93 (d, *J* = 8.6 Hz, 2H), 6.81 (d, *J* = 8.3 Hz, 1H), 4.66 (t, *J* = 4.7 Hz, 1H), 4.38 (d, *J* = 8.7 Hz, 1H), 4.01 (dt, *J* = 10.4, 4.5 Hz, 2H), 3.85 (s, 3H), 3.22 (dd, *J* = 15.0, 4.3 Hz, 1H), 3.14–3.01 (m, 4H), 2.85 (dt, *J* = 13.5, 7.4 Hz, 2H), 1.96–1.76 (m, 6H), 0.85 (d, *J* = 6.7 Hz, 6H); ^{13}C NMR (100 MHz, $CDCl_3$) δ 168.03, 163.12, 143.32, 140.01, 138.25, 133.71, 130.09, 130.08, 129.56, 128.69, 126.82, 126.68, 126.30, 114.45, 73.02, 68.02, 58.67, 55.75, 54.85, 53.40, 49.38, 35.05, 29.83, 28.66, 28.09, 27.24, 20.23, 20.15; HRMS-ESI (*m/z*): $[M+H]^+$ calcd for $C_{32}H_{42}N_3O_6S$, 596.2789; found 596.2786.

4.3. Determination of X-ray structure of HIV-1 protease inhibitor complexes

For X-ray crystallographic studies, HIV-1 protease was expressed and purified as described [45]. The protease-inhibitor complex was crystallized by the hanging drop vapor diffusion method with well solutions of 0.9M NaCl, 0.1M Sodium Cacodylate, pH 6.4 for PR/GRL-02815A (**4d**) complex, and 0.95M NaCl, 0.1M Sodium Acetate, pH 5.5 for PR/GRL-043-15A (**4k**) complex. Diffraction data were collected on a single crystal cooled to 90 K at SER-CAT (22-ID beamline), Advanced Photon Source, Argonne National Lab (Chicago, USA) with X-ray wavelength of 1.0 Å. X-ray data were processed by HKL-2000 [46] to give Rmerge values of 8.5% and 7.8% for inhibitors 4d- and 4k-bound HIV-1 protease complexes, respectively. The crystal structures were solved by PHASER [47] in CCP4i Suite [48–50] using one of the previously reported isomorphous structures [51] as the initial model, and refined by SHELX-2014 [52,53] with X-ray data at 1.20 Å resolution for inhibitor **4d** and HIV-1 protease complex and 1.14 Å for inhibitor **4k** and HIV-1 protease complex. PRODRG-2 [54] was used to construct the inhibitor and geometric restraints for refinement. COOT [55,56] was used for modification of the model. Alternative conformations were modeled, and isotropic atomic displacement parameters (B factors) were applied for all atoms including solvent molecules. The final refined solvent structure comprised one Na^+ ion, two Cl^- ions, one glycerol molecules and 209 water molecules for inhibitor **4d** and HIV-1 protease complex and Na^+ ion, two Cl^- ions, one acetate ion, one glycerol molecules and 142 water molecules for inhibitor **4k** and HIV-1 protease complex. The crystallographic statistics are listed in Table 1 (Please see, supporting information). The coordinates and structure factors of the protease complexes with inhibitors **4d** and **4k** have been deposited in the Protein Data Bank [57] with accession codes of 6DV0 and 6DV4, respectively.

Acknowledgements

This research was supported by the National Institutes of Health (Grant GM53386 to A.K.G. and Grant GM62920 to I.T.W.). This work was also supported by the Intramural Research Program of the Center for Cancer Research, National Cancer Institute, National Institutes of Health; Grant-in-Aid for Scientific Research (Priority Areas), the Ministry of Education, Culture, Sports, Science, and Technology of Japan (Monbu Kagakusho); a Grant for Promotion of AIDS Research, the Ministry of Health, Welfare, and Labor of Japan; the Grant to the Cooperative Research Project on Clinical and Epidemiological Studies of Emerging and Reemerging Infectious Diseases (Renkei Jigyo) of Monbu-Kagakusho. X-ray data were collected at the Southeast Regional Collaborative Access Team (SER-CAT) beamline 22ID at the Advanced Photon Source, Argonne National Laboratory.

Appendix A. Supplementary data

Supplementary data to this article can be found online at https://doi.org/10.1016/j.ejmech.2018.09.046.

References

[1] A.K. Ghosh, H.L. Osswald, G. Prato, Recent progress in the development of HIV-1 protease inhibitors for the treatment of HIV/AIDS, J. Med. Chem. 59 (2016) 5172–5208.
[2] S. Hue, R.J. Gifford, D. Dunn, E. Fernhill, D. Pillay, Demonstration of sustained drug-resistant human immunodeficiency virus type 1 lineages circulating among treatment-naïve individuals, J. Virol. 83 (2009) 2645–2654.
[3] C.W. Diffenbach, A.S. Fauci, Thirty years of HIV and AIDS: future challenges and opportunities, Ann. Intern. Med. 154 (2011) 766–771.
[4] M.S. Cohen, Y.Q. Chen, M.N. McCauley, Prevention of HIV-1 infection with early antiretroviral therapy, Engl. J. Med. 365 (2011) 493–505.
[5] N. Lohse, A.B. Hansen, J. Gerstoft, N. Obel, Improved survival in HIV-infected persons: consequences and perspectives, J. Antimicrob. Chemother. 60 (2007) 461–463.
[6] J.S.G. Montaner, V.D. Lima, R. Barrios, B. Yip, E. Wood, T. Kerr, K. Shannon, P.R. Harrigan, R.S. Hogg, P. Daly, P. Kendall, Association of highly active antiretroviral therapy coverage, population viral load, and yearly new HIV diagnoses in british columbia, Canada: a population-based study, Lancet 376 (2010) 532–539.
[7] Guidelines for the use of antiretroviral agents in HIV-1-infected adults and adolescents https://aidsinfo.nih.gov/contentfiles/lvguidelines/adultandadolescentgl.pdf, accessed on March 31, 2018.
[8] S. Hue, R.J. Gifford, D. Dunn, E. Fernhill, D. Pillay, Demonstration of sustained drug-resistant human immunodeficiency virus type 1 lineages circulating among treatment-naïve individuals, J. Virol. 83 (2009) 2645–2654.
[9] A.K. Ghosh, Z.L. Dawson, H. Mitsuya, Darunavir, a conceptually new HIV-1 protease inhibitor for the treatment of drug-resistant HIV, Bioorg. Med. Chem. 15 (2007) 7576–7580.
[10] M.P. de Béthune, V. Sekar, S. Spinosa-Guzman, M. Vanstockem, S. De Meyer, P. Wigerinck, E. Lefebvre, Darunavir (Prezista, TMC114): from Bench to Clinic, Improving Treatment Options for HIV-infected Patients in Antiviral Drugs: from Basic Discovery through Clinical Trials, John Wiley & Sons, Inc., New Jersey, 2011, pp. 31–45.
[11] Y. Koh, H. Nakata, K. Maeda, H. Ogata, G. Bilcer, T. Devasamudram, J.F. Kincaid, P. Boross, Y.-F. Wang, Y. Tie, P. Volarath, L. Gaddis, R.W. Harrison, I.T. Weber, A.K. Ghosh, H. Mitsuya, Novel *bis*-Tetrahydrofuranylurethane-Containing Nonpeptidic Protease Inhibitor (PI) UIC-94017 (TMC114) with Potent Activity against Multi-PI-Resistant Human Immunodeficiency Virus In Vitro, Antimicrob. Agents Chemother. 47 (2003) 3123–3129.
[12] S. De Meyer, H. Azijn, D. Surleraux, D. Jochmans, A. Tahri, R. Pauwels, P. Wigerinck, M.P. de Béthune, TMC114, a novel human immunodeficiency virus type 1 protease inhibitor active against protease inhibitor-resistant viruses, including a broad range of clinical isolates, Antimicrob. Agents Chemother. 49 (2005) 2314–2321.
[13] A.K. Ghosh, B. Chapsal, I.T. Weber, H. Mitsuya, Design of HIV protease inhibitors targeting protein backbone: an effective strategy for combating drug resistance, Acc. Chem. Res. 41 (2008) 78–86.
[14] A.K. Ghosh, D.D. Anderson, I.T. Weber, H. Mitsuya, Enhancing protein backbone binding – a fruitful concept for combating drug-resistant HIV, Angew. Chem. Int. Ed. 51 (2012) 1778–1802.
[15] Y. Tie, P.I. Boross, Y.-F. Wang, L. Gaddis, A.K. Hussain, S. Leshchenko, A.K. Ghosh, J.M. Louis, R.W. Harrison, I.T. Weber, High resolution crystal structures of HIV-1 protease with a potent non-peptide inhibitor (UIC-94017) active against multi-drug-resistant clinical strains, J. Mol. Biol. 338 (2004) 341–352.
[16] A.Y. Kovalevsky, F. Liu, S. Leshchenko, A.K. Ghosh, J.M. Louis, R.W. Harrison, I.T. Weber, Ultra-high resolution crystal structure of HIV-1 protease mutant reveals two binding sites for clinical inhibitor TMC114, J. Mol. Biol. 363 (2006) 161–173.
[17] X. Bai, Z. Yang, M. Zhu, B. Dong, L. Zhou, G. Zhang, J. Wang, Y. Wang, Design and synthesis of potent HIV-1 protease inhibitors with (*S*)-Tetrahydrofuran-Tertiary amine-acetamide as P2–Ligand: structure–Activity studies and biological evaluation, Eur. J. Med. Chem. 137 (2017) 30–44.
[18] K. Hohlfeld, J.K. Wegner, B. Kesteleyn, B. Linclau, J. Unge disubstituted bis-THF moieties as new P2 ligands in nonpeptidal HIV-1 protease inhibitors (II), J. Med. Chem. 58 (2015) 4029–4038.

[19] P. Öhrngren, X. Wu, M. Persson, J.K. Ekegren, H. Wallberg, L. Vrang, A. Rosenquist, B. Samuelsson, T. Unge, M. Larhed, HIV-1 protease inhibitors with a tertiary alcohol containing transition-state mimic and various P2 and P1' substituents, MedChemComm 2 (2011) 701–709.
[20] J.K. Ekegren, J. Gising, H. Wallberg, M. Larhed, B. Samuelsson, A. Hallberg, Variations of the P2 group in HIV-1 protease inhibitors containing a tertiary alcohol in the transition-state mimicking scaffold, Org. Biomol. Chem. 4 (2006) 3040–3043.
[21] J. Yan, N. Huang, S. Li, L.M. Yang, W. Xing, Y.T. Zheng, Y. Hu, Synthesis and biological evaluation of novel amprenavir-based P1-substituted Bi-aryl derivatives as ultra-potent HIV-1 protease inhibitors, Bioorg. Med. Chem. Lett 22 (2012) 1976–1979.
[22] Z.H. Yang, X.G. Bai, L. Zhou, J.X. Wang, H.T. Liu, Y.C. Wang, Synthesis and biological evaluation of novel HIV-1 protease inhibitors using tertiary amine as P2-ligands, Bioorg. Med. Chem. Lett 25 (2015) 1880–1883.
[23] C.J. Bungard, P.D. Williams, J.E. Ballard, D.J. Bennett, C. Beaulieu, C. Bahnck-Teets, S.S. Carroll, R.K. Chang, D.C. Dubost, J.F. Fay, T.L. Diamond, T.J. Greshock, L. Hao, M.K. Holloway, P.J. Felock, J.J. Gesell, H.P. Su, J.J. Manikowski, D.J. McKay, M. Miller, X. Min, C. Molinaro, O.M. Moradei, P.G. Nantermet, C. Nadeau, R.I. Sanchez, T. Satyanarayana, W.D. Shipe, S.K. Singh, V.L. Truong, S. Vijayasaradhi, C.M. Wiscount, J.P. Vacca, S.N. Crane, J. A. McCauley discovery of MK-8718, an HIV protease inhibitor containing a novel morpholine aspartate binding group, ACS Med. Chem. Lett. 7 (2016) 702–707.
[24] C.J. Bungard, P.D. Williams, J. Schulz, C.M. Wiscount, M.K. Holloway, H.M. Loughran, J.J. Manikowski, H.P. Su, D.J. Bennett, L. Chang, X.J. Chu, A. Crespo, M.P. Dwyer, K. Keertikar, G.J. Morriello, A.W. Stamford, S.T. Waddell, B. Zhong, B. Hu, T. Ji, T.L. Diamond, C. Bahnck-Teets, S.S. Carroll, J.F. Fay, X. Min, W. Morris, J.E. Ballard, M.D. Miller, J.A. McCauley, Design and synthesis of piperazine sulfonamide cores leading to highly potent HIV-1 protease inhibitors, ACS Med. Chem. Lett. 8 (2017) 1292–1297.
[25] A.K. Ghosh, P.R. Sridhar, S. Leshchenko, A.K. Hussain, J. Li, A.Y. Kovalevsky, D.E. Walters, J.E. Wedekind, V. Grum-Tokars, D. Das, Y. Koh, K. Maeda, H. Gatanaga, I.T. Weber, H. Mitsuya, Structure-based design of novel HIV-1 protease inhibitors to combat drug resistance, J. Med. Chem. 49 (2006) 5252–5261.
[26] A.K. Ghosh, C.-X. Xu, K.V. Rao, A. Baldridge, J. Agniswamy, Y.-F. Wang, I.T. Weber, M. Aoki, S.G.P. Miguel, M. Amano, H. Mitsuya, Probing multidrug-resistance and protein–ligand interactions with oxatricyclic designed ligands in HIV-1 protease inhibitors, ChemMedChem 5 (2010) 1850–1854.
[27] A.K. Ghosh, B.D. Chapsal, Design of the anti-HIV protease inhibitor darunavir, in: C.R. Ganellin, S.M. Roberts, R. Jefferis (Eds.), From Introduction to Biological and Small Molecule Drug Research and Development, 2013, pp. 355–384.
[28] A.K. Ghosh, K.V. Rao, P.R. Nyalapatla, S. Kovela, M. Brindisi, H.L. Osswald, B.S. Reddy, J. Agniswamy, Y.-F. Wang, M. Aoki, S.-i. Hattori, I.T. Weber, H. Mitsuya, Design of highly potent, dual-acting and central-nervous-system-penetrating HIV-1 protease inhibitors with excellent potency against multi-drug-resistant HIV-1 variants, ChemMedChem 13 (2018) 803–815.
[29] M. Aoki, H. Hayashi, K.V. Rao, D. Das, N. Higashi-Kuwata, H. Bulut, H. Aoki-Ogata, Y. Takamatsu, R.S. Yedidi, D.A. Davis, S.-i. Hattori, N. Nishida, K. Hasegawa, N. Takamune, P.R. Nyalapatla, H.L. Osswald, H. Jono, H. Saito, R. Yarchoan, S. Misumi, A.K. Ghosh, H. Mitsuya, A novel central nervous system-penetrating protease inhibitor overcomes human immunodeficiency virus 1 resistance with unprecedented aM to pM potency, eLife 6 (2017), e28020.
[30] A.K. Ghosh, P.R. Sridhar, N. Kumaragurubaran, Y. Koh, I.T. Weber, H. Mitsuya, Bis-tetrahydrofuran: a privileged ligand for darunavir and a new generation of HIV protease inhibitors that combat drug resistance, ChemMedChem 1 (2006) 939–950.
[31] A.K. Ghosh, G.E. Schiltz, L.N. Rusere, H.L. Osswald, D.E. Walters, M. Amano, H. Mitsuya, Design and synthesis of potent macrocyclic HIV-1 protease inhibitors involving P1–P2 ligands, Org. Biomol. Chem. 12 (2014) 6842–6854.
[32] A.K. Ghosh, L.M. Swanson, H. Cho, K.A. Hussain, S. Leschenko, S. Kay, D.E. Walters, H. Mitsuya, Structure-based Design: synthesis and biological evaluation of a series of novel cycloamide-derived HIV-1 protease inhibitors, J. Med. Chem. 48 (2005) 3576–3585.
[33] A.K. Ghosh, M. Brindisi, P.R. Nyalapatla, J. Takayama, J.-R. Ella-Menye, S. Yashchuk, J. Agniswamy, Y.-F. Wang, M. Aoki, M. Amano, I.T. Weber, H. Mitsuya, Design of novel HIV-1 protease inhibitors incorporating isophthalamide-derived P2-P3 ligands: synthesis, biological evaluation and X-ray structural studies of inhibitor-HIV-1 protease complex, Bioorg. Med. Chem. 25 (2017) 5114–5127.
[34] R.C. Reid, L.K. Pattenden, J.D.A. Tyndall, J.L. Martin, T. Walsh, D.P. Fairlie, Countering cooperative effects in protease inhibitors using constrained β-strand-mimicking templates in focused combinatorial libraries, J. Med. Chem. 47 (2004) 1641–1651.
[35] S.W. Kaldor, V.J. Kalish, J.F. Davies, B.V. Shetty, J.E. Fritz, K. Appelt, J.A. Burgess, K.M. Campanale, N.Y. Chirgadze, D.K. Clawson, B.A. Dressman, S.D. Hatch, D.A. Khalil, M.B. Kosa, P.P. Lubbehusen, M.A. Muesing, A.K. Patick, S.H. Reich, K.S. Su, J.H. Tatlock, Viracept (nelfinavir mesylate, AG1343): a potent, orally bioavailable inhibitor of HIV-1 protease, J. Med. Chem. 40 (1997) 3979–3985.
[36] T. Moriwake, Syntheses of 3-Cyano-3-methyl-4-thiochromanone and 3-Carbomethoxy-3-methyl-4-thiochromanone, J. Med. Chem. 9 (1966) 163–164.
[37] J. Tanuwidjaja, H.M. Peltier, J.A. Ellman, One-pot asymmetric synthesis of either diastereomer of tert-Butanesulfinyl-protected amines from ketones, J. Org. Chem. 72 (2007) 626–629.
[38] J.T. Colyer, N.G. Andersen, J.S. Tedrow, T.S. Soukup, M.M. Faul, Reversal of diastereofacial selectivity in hydride reductions of N-tert-Butanesulfinyl imines, J. Org. Chem. 71 (2006) 6859–6862.
[39] J.R. Martinelli, D.A. Watson, D.M.M. Freckmann, T.E. Barder, S.L. Buchwald, Palladium-catalyzed carbonylation reactions of aryl bromides at atmospheric pressure: a general system based on xantphos, J. Org. Chem. 73 (2008) 7102–7107.
[40] R. Noyori, T. Ohkuma, Asymmetric catalysis by architectural and functional molecular engineering: practical chemo- and stereoselective hydrogenation of ketones, Angew. Chem. Int. Ed. 40 (2001) 40–73.
[41] T. Ohkuma, K. Tsutsumi, N. Utsumi, N. Arai, R. Noyori, K. Murata, Asymmetric hydrogenation of α-chloro aromatic ketones catalyzed by η6-arene/TsDPEN–Ruthenium(II) complexes, Org. Lett. 9 (2007) 255–257.
[42] M.V. Toth, G.R. Marshall, A simple continuous fluorometric assay for HIV protease, Int. J. Pept. Protein Res. 36 (1990) 544–550.
[43] A.K. Ghosh, W.J. Thompson, S.P. McKee, T.T. Duong, T.A. Lyle, J.C. Chen, P.L. Darke, J. Zugay, E.A. Emini, W.A. Schleif, J.R. Huff, P.S. Anderson, Cyclic sulfolanes as novel and high-affinity P2 ligands for HIV-1 protease inhibitors, J. Med. Chem. 36 (1993) 924–927.
[44] A.K. Ghosh, W.J. Thompson, C. Culberson, M.K. Holloway, S.P. McKee, T.T. Duong, P.M. Munson, P.L. Darke, J. Zugay, E.A. Emini, W.A. Schleif, J.R. Huff, P.S. Anderson, The development of cyclic sulfolanes as novel and high-affinity P2 ligands for HIV-1 protease inhibitors, J. Med. Chem. 37 (1994) 1177–1188.
[45] B. Mahalingam, J.M. Louis, J. Hung, R.W. Harrison, I.T. Weber, Structural implications of drug-resistant mutants of HIV-1 protease: high-resolution crystal structures of the mutant protease/substrate analogue complexes, Proteins 43 (2001) 455–464.
[46] Z. Otwinowski, W. Minor, Processing of X-ray diffraction data collected in oscillation mode, in: A. Part, C.W. Carter Jr., R.M. Sweet (Eds.), Methods in Enzymology, 276: Macromolecular Crystallography, Academic Press, New York, 1997, pp. 307–326.
[47] A.J. McCoy, R.W. Grosse-Kunstleve, P.D. Adams, M.D. Winn, L.C. Storoni, R.J. Read, Phaser crystallographic software, J. Appl. Crystallogr. 40 (2007) 658–674.
[48] M.D. Winn, C.C. Ballard, K.D. Cowtan, E.J. Dodson, P. Emsley, P.R. Evans, R.M. Keegan, E.B. Krissinel, A.G.W. Leslie, A. McCoy, S.J. McNicholas, G.N. Murshudov, N.S. Pannu, E.A. Potterton, H.R. Powell, R.J. Read, A. Vagin, K.S. Wilson, Overview of the CCP4 suite and current developments, Acta Crystallogr. Sect. D Biol. Crystallogr. 67 (2011) 235–242.
[49] Collaborative Computational Project, Number 4, the CCP4 suite: programs for protein crystallography, Acta Crystallogr. Sect. D Biol. Crystallogr. 50 (1994) 760–763.
[50] E. Potterton, P. Briggs, M. Turkenburg, E. Dodson, A graphical user interface to the CCP4 program suite, Acta Crystallogr. Sect. D Biol. Crystallogr. 59 (2003) 1131–1137.
[51] C.-H. Shen, Y.-F. Wang, A.Y. Kovalevsky, R.W. Harrison, I.T. Weber, Amprenavir complexes with HIV-1 protease and its drug-resistant mutants altering hydrophobic clusters, FEBS J. 277 (2010) 3699–3714.
[52] G.M. Sheldrick, A short history of SHELX, Acta Crystallogr. A: Found. Crystallogr. 64 (2008) 112–122.
[53] G.M. Sheldrick, T.R. Schneider, SHELXL: high-resolution refinement, Meth. Enzymol. 277 (1997) 319–343.
[54] A.W. Schuettelkopf, D.M.F. van Aalten, PRODRG: a tool for high-throughput crystallography of protein-ligand complexes, Acta Crystallogr. Sect. D Biol. Crystallogr. 60 (2004) 1355–1363.
[55] P. Emsley, B. Lohkamp, W.G. Scott, K. Cowtan, Features and development of coot, Acta Crystallogr. Sect. D Biol. Crystallogr. 66 (2010) 486–501.
[56] P. Emsley, K. Cowtan, Coot: model-building tools for molecular graphics, Acta Crystallogr. Sect. D Biol. Crystallogr. 60 (2004) 2126–2132.
[57] H.M. Berman, J. Westbrook, Z. Feng, G. Gilliland, T.N. Bhat, H. Weissig, I.N. Shindyalov, P.E. Bourne, The protein Data Bank, Nucleic Acids Res. 28 (2000) 235–242.